ASTM INTERNATIONAL
Standards Worldwide

Masonry:

OPPORTUNITIES *for the* 21st CENTURY

editors

DIANE THROOP
RICHARD E. KLINGNER

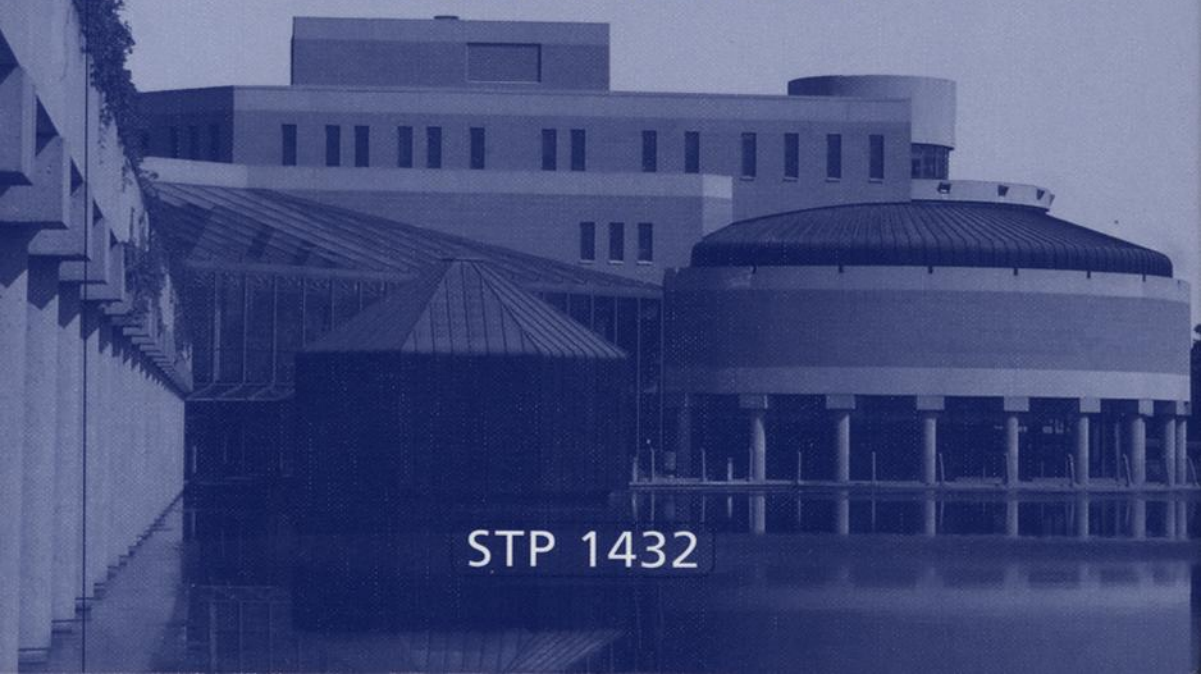

STP 1432

STP 1432

Masonry: Opportunities for the 21st Century

Diane Throop, Richard E. Klingner, editors

ASTM Stock Number: STP1432

ASTM International
100 Barr Harbor Drive
PO Box C700
West Conshohocken, PA 19428-2959

Printed in the U. S. A.

Library of Congress Cataloging-in-Publication Data

Symposium on Masonry: Opportunities for the 21st Century (10th : 2002 : Salt Lake City, Utah)
Masonry : opportunities for the 21st century / Diane Throop, Richard E. Klingner, editors.
p. cm. — (ASTM stock number : 1432)
Papers of the Tenth Symposium on Masonry: Opportunities for the 21st Century, held in Salt Lake City, Utah, June 25, 2002.
Includes bibliographical references and index.
ISBN 0-8031-3450-9
1. Masonry—Congresses. 2. Masonry—Materials—Congresses. I. Throop, Diane, 1953– II. Klingner, R. E. III. Title. IV. Series.

TA670 .S96 2002
693'.1—dc21 2002034199

Photocopy Rights

Peer Review Policy

Each paper published in this volume was evaluated by two peer reviewers and at least one editor. The authors addressed all of the reviewers' comments to the satisfaction of both the technical editor(s) and the ASTM Committee on Publications.

To make technical information available as quickly as possible, the peer-reviewed papers in this publication were prepared "camera-ready" as submitted by the authors.

The quality of the papers in this publication reflects not only the obvious efforts of the authors and the technical editor(s), but also the work of the peer reviewers. In keeping with long-standing publication practices, ASTM maintains the anonymity of the peer reviewers. The ASTM Committee on Publications acknowledges with appreciation their dedication and contribution of time and effort on behalf of ASTM.

Printed in Bridgeport, NJ
November 2002

Foreword

The Tenth Symposium on *Masonry: Opportunities for the 21st Century* was held in Salt Lake City Utah on 25 June 2002. The symposium was sponsored by ASTM Committees C-15 Manufactured Masonry Units, C-12 Mortars and Grouts for Unit Masonry, C-01 Cement and C-07 Lime. The symposium co-chairmen of this publication were Diane Throop and Richard E. Klingner.

Dedication

Dedicated to all those who went before and made these 21st Century Opportunities possible.

Contents

ASSEMBLIES

INTO THE 21ST CENTURY

Overview

These *Proceedings* are the tenth in a series of ASTM symposia on masonry that began in 1974. Sponsored jointly by ASTM Committee C-1 on Cement, C-7 on Lime, C-12 on Mortars for Unit Masonry, and C-15 on Manufactured Masonry Units, the symposia provide a forum for the exchange of ideas, information and practical experience in multiple areas related to masonry. This resulting STP includes papers presented orally at the June 25, 2002 symposium held in Salt Lake City, Utah, and two additional papers that the Joint Symposium Committee decided were deserving of publication, but which could not be presented due to time constraints.

The title, *"Masonry: Opportunities for the 21st Century,"* was chosen to reflect the forward momentum of the sponsoring masonry committees and their commitment to grasping the opportunities offered by the new millennium. It was the committees' desire to elicit presentations and papers on the historical evolution of masonry concepts that are valued today, and also on current research, new ideas, products, and applications involving masonry.

Following the theme of progress, the Symposium, and this symposium volume, addresses historical, current, and predicted masonry issues, ranging from studies of the behavior of historic masonry, through basic research into the behavior and potential application of innovative masonry materials. Papers cover state-of-the-art knowledge regarding historic structures, material testing, evaluation techniques, and new products and systems.

The papers contained in this symposium volume represent the work of 34 authors and co-authors; they were peer-reviewed by approximately 60 members of ASTM Committees C-1, C-7, C-12, and C-15. The Joint Symposium Committee was made up of representatives of the four sponsoring committees, with C-15 acting as the lead committee for the 2002 Symposium and this symposium volume. Committee members were Diane Throop and Richard Klingner—co-chairs and representatives of Committee C-15; Joseph Brisch and Bruce Kaskel, representing Committee C-12; Jim Nicholos and Paul Owen, representing Committee C-1; and Michael Tate and Robert Nelson, representing Committee C-7. Finally, many ASTM staff members aided the Joint Committee in conducting the Symposium and preparing this symposium volume. We thank the authors, reviewers, Symposium attendees, sponsoring committee members, and ASTM staff for their work to enhance the success of this Symposium and the corresponding symposium volume.

This volume was dedicated to those who have gone before and made these opportunities possible. We thank them for their work and dedication to masonry, recognizing their role in providing the foundation for much of the work presented in this volume.

Diane Throop
Diane Throop PE, LLC
Symposium Co-chair and STP Editor

Richard E. Klingner
Symposium Co-chair and STP Editor
The University of Texas at Austin

Mortars

Lauren B. Sickels-Taves,[1] Michael S. Sheehan[2]

Specifying Historic Materials: The Use of Lime

Reference: Sickels-Taves, L. B., and Sheehan, M. S., **"Specifying Historic Materials: The Use of Lime,"** *Masonry: Opportunities for the 21st Century, ASTM STP 1432*, D. Throop and R.E. Klingner, Eds., ASTM International, West Conshohocken, PA, 2002.

Abstract: Despite technological advances of the 21st century, mortars and stuccos for masonry restoration projects continue to be specified using portland cement. Without standards or codes specifically designed for historic buildings, owners and contractors often unknowingly incorporate incompatible materials into historic repairs. Using recent restoration projects in the United States and Hungary as case studies, this paper focuses on the need for mortar and stucco standards specifically oriented towards the specification of mortars and stuccos for historical structures, the practical reasoning behind this need, and the historical documentation that supports this premise. In particular, the critical importance and potential applications of lime are addressed. Past and present repairs using cement and lime, why they differ, and the effect they have had will be addressed. The structures these studies focus on predate portland cement's existence and are historical precedents for the use of lime mortars and stuccos. Finally, current ASTM specification efforts related to lime mortars are reviewed, and further development in this area is encouraged.

Keywords: lime, portland cement, historic mortar, historic stucco, standard, code, specifications, repairs, restoration, dissemination

Introduction

The 20th century saw the introduction of stainless steel, concrete blocks, and glass curtain walls—and with them, the popular rise of a companion material,

[1] Assistant Professor, Historic Preservation, Department of Geography & Geology, Eastern Michigan University, Ypsilanti, MI 48197
[2] Lecturer, Department of Geography & Geology, Eastern Michigan University, Ypsilanti, MI 48197

portland cement. Different types of portland cement were developed to allow construction to occur under hot- and cold-weather conditions, and to increase resistance to sulfate attack.

Portland cement, thought by many to be the wonder product of the 20th century, was frequently applied in historic preservation projects. In many cases, the cement repairs caused further damage that was noted only with the passage of time. Structures predating portland cement or constructed with weaker, porous building materials often suffer irreparable damage when they are repaired using portland cement [1, 2]. The dictates of historic preservation mandate "reversibility" and "replace with kind." They clearly imply that portland cement is not a cure-all, and that its use in each possible restoration scenario should be approached with thought and care. Lime mortar was once the proper material to use for many restorations. It was usually compatible in strength with a building's original materials. The key characteristics of lime mortars and stuccos are porosity and its related permeability, plasticity, and creep, enabling these mortars and stuccos to "breath," thus reducing the build-up of water vapor in the masonry and to retain sufficient flexibility to absorb movement [3, 4].

The use of lime as the binder in mortars and stuccos dates back to ancient Rome, when Vitruvius expounded on the virtues of lime in his treatise *The Ten Books of Architecture* [5]. Though lime was available in different forms, such as powder or putty, and its quality varied according to local geology, it remained the key binder for mortars and stuccos until natural and portland cements were introduced [6]. How did people lose sight of the benefits of lime in favor of portland cement? To answer this question, we need to look back with forward-thinking research.

As the 21st century dawns, preservationists and other professionals are making major strides in the physical and chemical understanding of binders such as lime. And yet, the information is not reaching the general public—especially here in the United States—despite demands. Specific standards and codes are now necessary to segue the research to that public. Tacit acknowledgment of this point is provided by the efforts of E06.24, and now C12, to produce an historic mortar standard. Furthermore, a specific need for this particular standard has been called for in two recent ASTM symposia and subsequent STPs [7–9]. James Marston Fitch, the "father" of historic preservation, stated that preservationists are curators of the built environment. It is our duty as curators to inform the public and help protect our historic buildings. Determining when lime is more appropriate than portland cement as a binder in mortars and stuccos is one important step in this protection. In this paper, the specific differences between the behavior of lime mortars and stuccos and portland cement mortars and stuccos are summarized; the probable consequences of these different behaviors are reviewed, and are supported by examples of their behavior in historical structures Finally, specific suggestions are made for deciding between lime and portland cement in the restoration of masonry structures.

Characteristics of Lime or Portland Cement

Mortars and stuccos are mixtures of binder, aggregate, and water (British Standard 6100:6.6.1:1992) [10]. Aggregate is an inert substance, leaving the binder as the active ingredient once exposed to water. Understanding the differing characteristics of lime and portland cement as binders is therefore critical to determining the appropriate mortar or stucco for use in restoration projects. "Observed behavior of both new and old mortars raises questions concerning the nature of various mortars and their abilities, in a masonry wall, to respond to various stresses and movements. [Some] evidence suggests that weaker, softer, less dense, lime-rich mortars may tolerate certain stresses and movements better that stronger, harder, more dense, cement-rich mortars" [11]. This section will briefly describe the qualities of lime and portland cement, and how these best fit the properties required to replicate traditional mortars and stuccos.

Physical Characteristics

Portland cement has been identified in literature focusing on historic masonry as "an extremely hard cement that is impermeable to water. Much too hard to be used as the only binder in mortar, particularly for old walls of soft brick and stone" [12]. Mortars with only a portland cement binder "harden faster than lime mortars and in general are stronger, less flexible, less soluble and less permeable" [13]. Lime, on the other hand, "is the binder of choice for repointing old masonry...High lime mortar is soft and porous and changes little with temperature fluctuations. Because it is slightly water soluble, it can reseal hairline cracks by combining with moisture from the air" [14].

Measurement of Characteristics

Mortars and stuccos that employ either lime or portland cement as a binder possess a variety of characteristics whose measurement can provide critical guides to the appropriate context for their use. These measures include, but are not limited to, compressive strength, shrinkage/creep, modulus of elasticity, color, texture, adhesion, and water absorption.

- *Compressive Strength* — "Compressive strength is a widely recognized mechanical property in mortar standards" [15]. By determining the strength of the existing masonry, a compatibility ratio can be established between that masonry and the proposed mortar or stucco. Table 1 aids in this process. "Mortar for historic masonry should be compatible with the stone and the existing mortar. A too-strong mortar is most often too dense and would not provide sufficient moisture migration; this would cause damage to the stone [masonry unit]" [15].
- *Shrinkage/Creep* — "Creep and shrinkage are important factors in the mechanism by which masonry walls accommodate movement without

damage" [16]. Laboratory studies have shown "that shrinkage and creep were related to the quantity of lime in a mortar mix, in the sense that the richer the mix is in lime, the higher the values for creep and the lower the values for shrinkage...The properties of a soft lime mortar appear to be such that stresses caused by thermal, moisture, and some settlement movements can be dissipated by creep. On the other hand, hard cement mortars inhibit movement to the degree that severe cracks and other damage can develop" [16]. Tables 2 and 3 illustrate these points.

- *Color* — The overall appearance of the mortar or stucco can be attributed to the type of binder used. The color of the sand is also a factor. Both can be measured with a Munsell color chart.
- *Texture* — "The term 'texture' refers to the size and arrangement of the components, the sizes and shapes of the aggregate, the amount of binder and their mutual interrelationships" [17]. This property enables comparisons to be made between the original mortar or stucco and the proposed one. Analysis is relatively simple using dilute hydrochloric acid [18] [19].
- *Water Absorption* — Given the porous nature of historic masonry (and its mortars and stuccos), water absorption can be a critical factor in evaluating its structural performance. A restoration recipe with a great absorption rate could lead to excessive water build-up. Conversely, one with a substantially lower rate could prevent adequate breathability by trapping water within the existing masonry wall. Both scenarios can lead to decay [20]. The potential for problems can be evaluated by examining the water absorption value of existing masonry units and the proposed replacement mortar or stucco.

Some of these tests, shrinkage/creep for example, require a time frame and/or the services of independent testing laboratories, either of which could unnecessarily delay a restoration project. Fortunately, the results of carefully controlled laboratory analyses have been published that have broad applicability and can be used as guides for making short term decisions, thus obviating the need for additional laboratory analyses [21].

TABLE 1—*Mortar mixes for various brick strengths.*

	Brick Stength			Mortar Mix/Strength
	psi	N/mm^2		N/mm^2
Low	1500	10.34	0:1:3H	1.07–1.46
			1:3:12	1.34–1.49
			1:2:9	2.21–2.95
Medium	3000–5000	20.69–34.48	1:6 + S	4.20–4.50
			1:1:6	5.73–6.88
			1:2:9H	5.89–7.75
High	7000–9000	48.28–62.07	1:1/4:3	Not tested
Very High	10 000+	68.97	1:0:3	25.15–28.33

TABLE 2— *Mortar mixes* [21].

	Mortar Type	Cement:lime:sand	Cement: sand with plasticizer
Increasing strength but decreasing ability to accommodate movements caused by settlement, shrinkage, etc. ↑	M or i	1:0–1/4:3	...
	S or ii	1:1:5–6	1:3–4
	N or iii	1:2:8–9	1:5–6
	O or iv	1:3:10–12	1:8–9
	K or v	1:3:10–12	1:8
	←equivalent strengths within each group→		
	←increasing frost resistance→		
	←improving bond and resistance to rain penetration→		

Application of the data obtained when using the tests noted above should focus on the compatibility of the physical properties of the original masonry and the replacement mortars and stuccos. The search for, and use of, a single "threshold" or critical value in assessing material compatibility, on a case by case basis, will not ensure the selection of an appropriate restoration mortar or stucco. When conducting the repair of historic masonry, it is imperative to match the original materials in terms of the physical properties outlined in the preceding discussion [22]. Understanding the characteristics of lime and portland cements as binders in mortars and stuccos is essential to accomplishing this objective.

TABLE 3—*Mortar mix selection* [21].

	Mortar group	Mortar mixes
↑	i or M	1:0:3
Decreasing Creep	ii or S	
Increasing Shrinkage	iii or N	1:2:9H 1:1:6 1:6+S
Increasing Strength	iv or O	1:2:9
↓	v or K	0:1:3H 1:3:12
		←equivalent strengths within each group→
		←increasing shrinkage
		←increasing creep

Historical Repairs: The Inappropriate Use of Portland Cement

In the early decades of the 20th century, portland cement was frequently used without sufficient understanding of its properties and their long-range consequences for building behavior. With time, the preservation community developed a better understanding of these issues. In 1966 with the passage of the National Historic Preservation Act, agencies (such as State Historic Preservation Offices or SHPOs) were created to help in this regard. By 1976, a standard, *The Secretary of the Interior's Standards for Rehabilitation*, appeared [23]. Due to inadequate dissemination of information, however, portland cement remained the product of choice for historical restoration.

Cotswold Cottage, Dearborn, Michigan

In 1929, Henry Ford purchased a Cotswold cottage in England. His intent was to have it shipped piece by piece to Dearborn, Michigan, and re-erected in Greenfield Village, an open-air museum consisting of a diverse array of residential, commercial, and industrial structures. Because of its then-current condition, he was advised to have it restored in-situ before dismantling. W. Cox Howman of Stow-on-the-Wold was hired to complete the work, and his invoices to Ford specify lime and sand for exterior mortarwork [24].

Twenty-six railroad cars brought the cottage, packed in cases and sacks, to Dearborn in April 1930. Reassembling began immediately using what Ford called "American methods" [25,26]. First, cement was added to the lime mortar with the intent of creating a tight bond with the stones. Then, this mortar was used in locations that had never seen mortar before. For example, the dry stone fence walls were rebuilt and laid with mortar; and the stone roof tiles, originally hanging off a batten/counterbatten system with wooden pegs, were "made safe with mortar." As the Village architect, E. Cutler, noted, "This job had lasted 400 years, and we wanted it to last another 400." [25, 27].

The methods used in 1930 were believed to be the best. Time has since shown that irreparable damage occurred: the rigidity of the portland cement mortar prohibited the building and the fence from absorbing seasonal movement, resulting in numerous broken stones and tiles and subsequent interior water damage [26].

Cannon's Point, St. Simons Island, Georgia

In the late 1700s and early 1800s, many structures along the southeastern coast of the United States were constructed of "tabby," an early form of poured masonry consisting of lime, sand, and oyster-shell, and erected in layer-like units. Between 1920 and 1960, with the best of intentions, residents on Georgia's islands sought to save these structures by repairing joints and replacing missing lime stucco with portland cement stucco [20, 28]. In virtually every case, these well-intentioned repairs did more harm than good, due to the performance

differences (as noted above) between the original tabby and its stucco—both made with lime, and the portland cement repairs. For example, Cannon's Point Plantation, constructed of tabby in the decades following 1794, was owned and operated by the Couper family on St. Simons Island and underwent such repointing and restuccoing—with disastrous results. In particular, the house chimney was repointed with a neat portland cement mortar (cement and water only) and stands today as a honeycombed testament to the problems that arise when incompatible materials are used. The bricks have been completely destroyed, eroding away due to the dense, neat cement mortar.

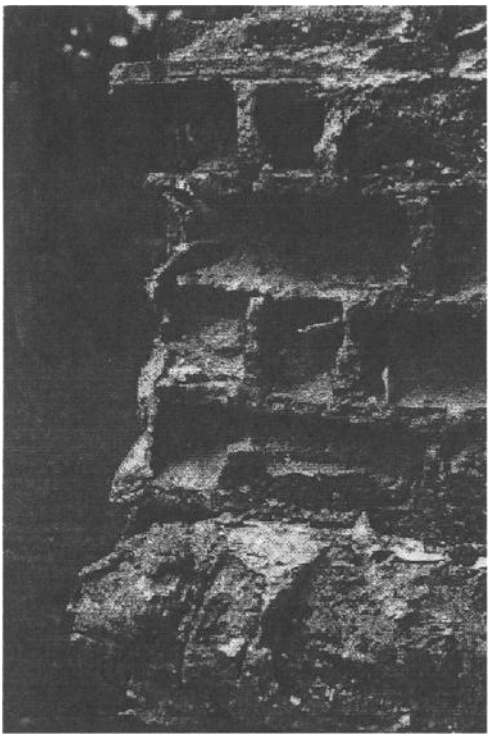

FIG. 1 – *The Effects of Incompatibility: Portland Cement Mortar with Handmade Tabby Bricks* [20].

Mexican Bricks, Keene, Texas

Understanding the effects of portland cement use in bedding mortar can be critical in diagnosing the possible causes of deterioration exhibited by historic masonry. This is particularly important in the American Southwest where a

significant number of historic structures are constructed of adobe or other relatively soft brick. Bedding mortar composed primarily of portland cement is too strong for this type of brick, and if used will eventually cause premature brick deterioration [11].

This issue surfaced in the 1960s and 1970s, as part of a debate regarding the general quality of handmade brick used in the erection of masonry structures, especially brick obtained from Mexico [29]. Some handmade brick from Mexico was alleged to be inferior. The evidence used to support this contention often incorporated photographs of historic structures displaying badly deteriorated walls characterized by significant loss of brick from spalling and a remnant honeycomb of bedding mortar [30]. It was implied that the condition of such structures was due to inferior brick.

Alternative hypotheses exist, however. This condition is reminiscent of that observed at Cannon's Point Plantation, where the problem was clearly related to the inappropriate use of portland cement in the repair of an historic tabby structure. This suggests that in some cases, the deterioration of the soft Mexican brick may have been accelerated by the inappropriate use of hard, impermeable, portland cement mortar.

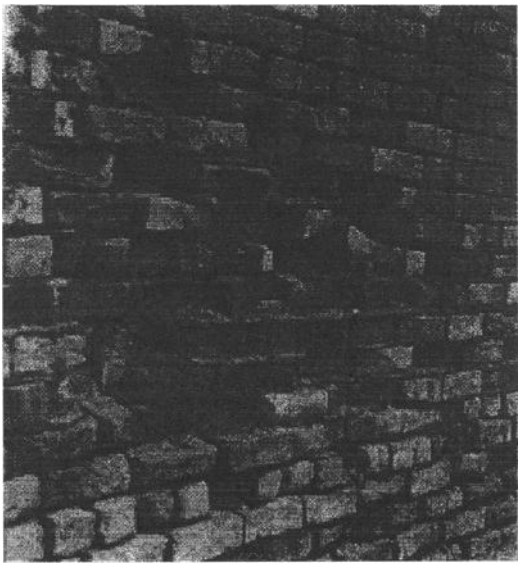

FIG. 2—*Deteriorated wall on building constructed of Mexican handmade brick.* [29]

The fundamental point to be made is that when historic masonry exhibits badly spalled walls and relatively intact mortar joints, as observed at Cannon's Point

and among some structures constructed with handmade brick, to assume that this is due to poor brick alone is to risk further problems. When confronted with historic masonry displaying these characteristics, it is imperative to evaluate the mortar as well as the brick. Merely replacing the brick with kind will not necessarily correct the condition of the wall over the long term. From a structural perspective, the brick may be perfectly adequate but if the mortar is too strong, or impervious to the transmission of water vapor, the brick will suffer [31]. The symptom is decayed brick. As in medicine, curing the symptom will not cure the problem. Where soft, or handmade, brick is used as a structural unit, as is often the case in historic structures, the use of lime mortars is highly desirable and, because of its strength and plastic qualities, should be the mortar of first choice.

The Tabby House, Cumberland Island, Georgia

In 1980, the National Park Service commissioned a condition report on The Tabby House, a tabby building (c.1804) on the south end of Cumberland Island, Georgia [32]. That report concluded that portland cement was not compatible with tabby and should not be considered an option in a restoration project. In spite of this warning, in the early 1990s a neat portland cement stucco (over a wire mesh) was applied to the structure. Within only a few years, the inappropriate nature of this restoration became evident. Buckling stucco, unsightly staining, and cracks on the exterior with mold, mildew, and peeling paint on the interior forced the Park Service to install a twenty-four-hour, seven-day fan merely to circulate air until the funds and the correct method of preservation could be found.

With the aid of a grant from Earthwatch and the collaboration of several National Parks, The Tabby House was fully restored in 1997. The cement stucco and mesh were removed and replaced with a stucco whose volume proportions were 1 part hydraulic lime, 1 part hydrated lime, and 4 parts sand. To date, the stucco has aged well.[3]

This example has an unfortunate postscript. As the restoration team for the Tabby House left Cumberland Island in 1997, after finishing their work, they drove through Brunswick, Georgia. One of the very first sites they saw was a commercial tabby structure enveloped in scaffolding. Workers were applying a wire mesh and portland cement stucco to the walls.

Review of these examples, especially the Tabby House on Cumberland Island, suggests several important points. As recently as the early 1990s, portland cement has been the material of choice in restoration projects involving pre-portland cement historic structures, even though recommendations from qualified professionals stipulate, unequivocally, that portland cement use would be inappropriate, even deleterious [32,33]. Again with particular reference to the Tabby House, it is clear that lime-based mortars and stuccos are quite durable and hold up very well with age.[3]

[3] Bjork, J., National Park Service, St. Marys, GA, personal communication with Lauren B. Sickels-Taves, Eastern Michigan University, Ypsilanti, MI, December 2001.

Recent Research and Developments

International Efforts

"Since the general introduction of portland cement for construction in Britain after 1945, considerable damage has occurred to the nation's stock of over 250,000 historic buildings. More recently it has become evident that cement can damage new builds too. The realization that policy of sustainable development during the 21st century and later is the only way for humanity to fulfil its expectations without destroying the environment has added new emphasis to the use of lime for construction" [34]. This statement reinforces and reflects the increased interest over the last few decades, in many countries, in the use of lime mortars and stuccos in the restoration of historic masonry structures. Based on an extensive literature search, and consulting with leading preservation professionals, it appears that of all the countries engaged in such restoration, Scotland has assumed a position of leadership in the global dissemination of such information to practitioners and the general public. The following section of this paper focuses primarily on information related to these trends in Scotland and the United States.

Scotland–

- Hydraulic lime has been manufactured, since before 1980, in Crouzilles, France, and has been shipped throughout Europe. Until the development of The Scottish Lime Centre Trust in the early 1990s, this French lime was promoted by the City of Edinburgh, Scotland [11].
- The Scottish Lime Centre Trust developed workshops in Charlestown, Fife, to supply lime, provide analytical services, and teach masonry techniques to restoration practitioners and the general public.
- The Scottish Lime Centre Trust produced a simple, easily understood guide on this subject: *Preparation and Use of Lime Mortars: An introduction to the principles of using lime mortars* in 1995 [35].

United States – The fact that the United States is not considered a leader in the dissemination of information and specification of lime mortars and stuccos can be attributed to several causes:

- The United States has considerable geographic extent, with a range of climatic conditions. This complicates the development of appropriate lime mortars and stuccos for use in the entire United States.
- In the United States, lime producers and users are not effectively organized at national or regional levels. Many companies offer lime products, but they are not commonly available at the retail level.
- Many companies offer mortar workshops, but only on a very local basis.
- The United States has no central clearinghouse for information on this subject, nor does it have ready access to references such as The Scottish Lime Centre publication noted above.

The relatively minor role of the United States in this area, behind Europe, is illustrated by a new study of lime mortars in the conservation of historic buildings [36]. Although this research was supported by the US-based Getty Conservation Institute, it is strikingly deficient in research contributions from the United States. This helps to substantiate the observation made earlier that the United States is not a leader in the dissemination about information in this area.

At an ASTM International Symposium held in 1996, Doebley and Spitzer noted the need for ASTM standards related to historic mortars [37]. In 2002 that need is still present. This is reflected in the recent resurrection of a task group on historic mortars, ASTM C12 taking on this role.

Symposia

In 1981, in Rome, the International Centre for the Study of the Preservation and the Restoration of Cultural Property (ICCROM) held a symposium on Mortars, Cements and Grouts used in the Conservation of Historic Buildings. This international symposium led the way in stressing the need to examine the use and abuse of mortars due to the vital role their properties play in the functioning of a structure [38].

It was another 12 years before similar international symposia were held. Both were sponsored by ASTM, and both contained pleas for the development of ASTM standards for historic mortars: *Standards for Preservation and Rehabilitation* in 1993 and *The Use of and Need for Preservation Standards in Architectural Conservation* in 1998 [7, 39].

Soon after, The International Union of Testing and Research Laboratories for Materials and Structures (RILEM) assembled preservationists in Paisley, Scotland, in 1999 to discuss historic mortars, their characteristics, and testing procedures by examining prevailing interdisciplinary activity. Belgium, Canada, China, Italy, Denmark, Great Britain, and the United States were just a few of the countries represented. The proceedings "revealed large gaps in factual knowledge...and a strong demand...for improved guidance for conservation practitioners" [40, 41].

Disseminating the Information: Lime Mortars and Stuccos

Even as late as the 1990s, information regarding the performance of lime mortars and stuccos was not generally available. *The Secretary of Interiors Standards for Rehabilitation* had been around 20 years, but it is a basic guide only, and not marketed to contractors [23]. To reach contractors, masons, and other practitioners, as well as the general public, multiple avenues for disseminating available information are required:

- ASTM material standards and codes addressing the use of lime mortars and stuccos;
- Explanatory guides directed at the general public;
- Regional, easily affordable workshops;

- Ready retail availability of lime products, perhaps through home improvement stores;
- Promotional or endorsed dissemination, focusing on the product not the name brand, through agencies such as SHPOs and local governments;
- Easily obtained assistance through agencies such as SHPOs and local government.

Standards in the United States: Lime Mortars and Stuccos

Although the United States has lagged behind some countries, notably Scotland, in the ability to readily obtain and use lime-based masonry products, it is **not** behind Europe in research and applications. Preservation professionals in this country have seen the need. In 1982, the National Endowment for the Arts funded a research project on mortars in preservation [11]. In 1998 and 1999, the National Center for Preservation Technology & Training (NCPTT) funded a project, "A Standard Method for the Analysis of Historic Cementitious Materials" [42]. The need for an ASTM standard on historic mortars was mentioned in the ASTM proceedings of both above-mentioned symposia [37,43]. The journal of the Association for Preservation Technology has, for years, published articles on mortars, thus disseminating information. One that has for years been popular for its practicality is "Tests for the Analysis of Mortar Samples" [19,44].

ASTM Subcommittee E06.24 on "Building Preservation and Rehabilitation Technology" was developed in the early 1980s to address, in part, the need for ASTM standards for historic mortars. While E06.24 has a task group charged with developing a standard on repointing historic buildings, its draft document has lingered in committee for years. ASTM C12 chose to supplement this task group one year ago by forming a similar task group to develop a standard on historic mortars.

At the risk of being redundant, it is still important to note that these professionals have either been stymied, or their work—in the form of specifications, standards, etc.—is not reaching those that are closely involved in the masonry work, the general public: the contractor, the mason, and the client. The problems here stem from dissemination of the results in an acceptable form to the general public. That need was stated in 1996 and is still present in 2002. To that can be added, in the authors' opinion, the need to approach the National Park Service's National Center for Preservation Technology and Training (NCPTT) to act as a clearinghouse. Through their web site, the general public could be linked to the various companies offering lime products, while we continue to find ways to get these products in local stores.

The questions, in the authors' opinion, remain: which organization/agency is going to step up to the plate in the United States and address these needs? Who has the authority to empower a team and their results for the betterment of our country and its historic buildings?

Current Applications

Many preservation professionals now examine and even analyze building materials as a part of restoration projects. In addition to restoring a structure, it is now important to understand what historic materials were used in that structure, and why. While this has proved largely beneficial to structures, the fact remains that preservation professionals are still being confronted with requests for codes—that may not exist, and with competition from lay people who gain their advice from non-preservation professionals or de facto preservationists such as employees at home improvement stores.

There are numerous, recent examples in which historic structures have been restored without using portland cement. As discussed below, among the key factors involved in the success of some of those projects is the use of lime rather than portland cement.

Funding and the SHPO: A Case Study

Old Baldy lighthouse is the oldest structure of its kind in North Carolina. Constructed in 1817, it is located on Bald Head Island, near the mouth of the Cape Fear River. It is an octagonal, stuccoed, brick building atop a stone foundation.

Each of the lighthouse's eight faces exhibits a mottled appearance, due largely to past repairs conducted without matching the original color and composition of the masonry. Those past repairs involved both lime-based and cement-based materials, with the latter being inappropriate in terms of color, strength, and texture. Due to their relative impermeability to water vapor, the use of cement-based materials has exacerbated moisture problems experienced by the lighthouse masonry. The resulting bloom and associated spalling has exposed the brick core in a number of locations [45].

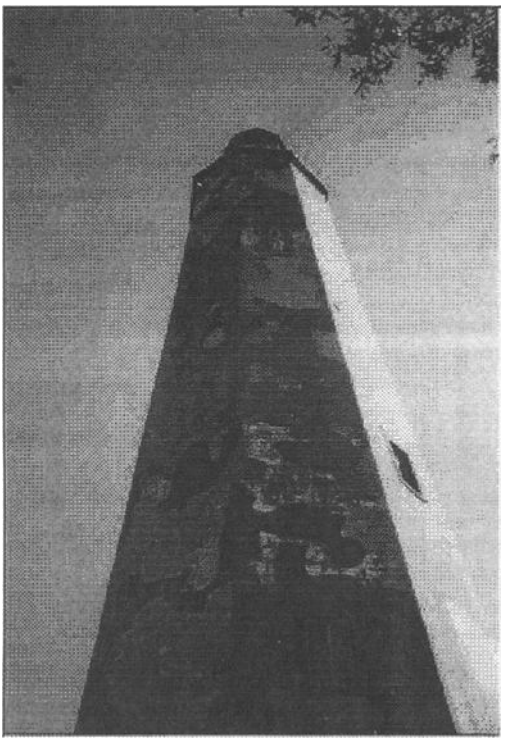

FIG. 3 — *Bloom and spalling as a result of portland cement repairs* [45].

Due to this spalling and an original diagnosis of "rising damp," a condition report was commissioned, funded in part by the National Trust for Historic Preservation, and directed by the North Carolina SHPO. The SHPO was on site during the fieldwork phase of the condition report and carefully asked questions. Investigators carefully documented the building's history, took samples of masonry materials, and analyzed them before proposing a restoration approach. They concluded that present problems are solely attributable to the use, over time, of portland cement [45]. Cement patches on the exterior and interior have created water-impermeable pockets, forcing the surrounding lime stucco areas to discharge unusually large amounts of water vapor.

According to the investigators, by regulating the sand used and returning to a lime binder, water and spalling problems will be avoided [45]. Proposed specifications require that the masonry materials used for restoration match the original materials in color, texture, composition, and size; they also require mortar and stucco proportions, by volume, of 1 part hydraulic lime, 1 part hydrated lime, and 4 parts sand.

By interacting on behalf of the owner, the National Trust and the SHPO increased the probability that this project would be successful. Analyses of the

mortars and stuccos confirmed the original materials and aided in specifying appropriate restoration materials. This project used at least two of the avenues noted in the preceeding section for gathering and disseminating information about lime mortars for restoration projects: a condition report and SHPO involvement. Lime will be used, but it will have to be ordered as it is not available locally.

The United States as a Leader

In the emerging "global community," the United States has assumed a leadership position in a variety of political, social, and economic arenas. There is a perception in some developing countries, especially those making the difficult transition from a command economy to a market economy, that this is true in historic preservation as well. The United States is perceived as a leader in historic preservation, and should be more active in making that perception a reality. In the discussion that follows, an example of this perception is provided and includes a review of the "leadership potential" that the preservation movement in the United States possesses, especially in promoting material compatibility.

Szarvasgede Manor, Hungary

In the small town of Szarvasgede, Hungary, a 16th-century manor house, the historic residence of the mayor, was sold in 1996 to a man with a mission. The new owner had grown up in a post-1950, Soviet-dominated Budapest, whose architecture could be compared with that of Paris, except that its buildings were not stone, but rather combinations of bricks and rubble, stuccoed with portland cement. After acquiring the Szarvasgede manor, the new owner wished to see it restored with the best materials and the best technology. He turned to the United States, and wanted this country to train Hungary in the cutting-edge preservation skills of documentation and material analyses.

With the help of a grant awarded under the auspices of Earthwatch, a team of United States citizens spent the summer of 1998 analyzing the building's archaeological history and construction materials. They identified lime as the original binder in the mortar and stucco [46]. The team saw the chance to avoid the use of portland cement as found in Budapest, and to teach the value of historic ingredients: how to determine what they are and how to incorporate them into a restoration project. One man understood the value of doing a restoration right the first time; and the United States team was able to make an important contribution: stressing the importance of using lime over cement in the restoration formulas. The United States participants had the opportunity to learn application skills from Old World craftsmen.

One of the most important points to be gleaned from this example is that a need for expertise in historic preservation was perceived, and the personnel responsible for obtaining that expertise turned to the United States. People in other countries evidently view preservationists in the United States as "leaders" in

the global preservation community. The challenge before us is to fulfill the promise of that international perception. To meet this challenge, specific steps should be taken.

Requests for Codes

The need for codes dealing with historic preservation projects was highlighted during a recent assessment of The Chimneys, a group of structures once belonging to Stafford Plantation on Cumberland Island, Georgia. The chimneys, constructed of tabby brick, are all that remain of a series of former slave cabins. Over time, due to structural instability and lack of maintenance, the chimneys have begun to lean inward into what once were the cabin interiors. The National Park Service requested a condition report, complete with specifications for repair [47]. During the site visit and discussions over expectations for the restoration mortar, it was asked if the specified restoration mortar would be to "code." The response, unfortunately, was: "there is no code governing this type of repair."

The condition report included analyses of mortar, stucco, and plaster; measured drawings; a chimney-by-chimney cost analysis; and proposed specifications for restoration. The proposed specification for restoration mortar called for volume proportions of 1:1:4 (hydraulic lime:hydrated lime:sand). Since the report was compiled by competent preservation professionals, it was not critical that a "code" exist for the client. However, the fact remains that a "code" was requested and was not available, either to preservation professionals or to the general public.

Conclusion and a Call for Action

In the United States, there is considerable indication that preservationists are ready to develop design provisions and material standards for historic mortars and stuccos. If such standards existed, contractors would be better informed whenever a historic project was undertaken without requiring the expertise of a professional preservationist; and clients and the historical masonry itself would not be compromised by lack of knowledge. Masons would have a standard by which to judge their work. The existence of such standards might also encourage the introduction of lime putties, hydraulic lime, and other lime products to the shelves of home improvement stores, further encouraging contractors to use them when appropriate.

This development can begin in two ways:

- With ASTM's new C12 task group working closely with E06.24;
- By establishing a central, probably governmental, clearinghouse for information. A collaboration with the NCPTT makes sense.

The next step might be determining how to get lime products out to local stores. In terms of critical structural properties, all masonry is not created equal.

Consequently, material compatibility is an extremely important issue. This is particularly true with regard to historic masonry, originally constructed and finished using lime-based products, and restored using portland cement mortars and stuccos. It is clear that in specific, and easily identifiable, historic preservation contexts, portland cement is not the automated product of choice in the 21st century. This position is substantiated by preceding discussions of the performance characteristics of portland cement-based products and their use in historic repairs. It is time to look back with forward thinking. An American specification at the turn of the 18th century called for a 1:2:9 mix, consisting of hydraulic lime, hydrated lime, and river sand by volume [48]. How did we move from that into the cure-all use of Portland cement? Let history **not** repeat itself; the challenge is upon us. "If not us, who? If not now, when?"

References

[1] McKee, H., *Introduction to Early American Masonry*, National Trust for Historic Preservation, Washington, D.C., 1973.

[2] London, M., *Masonry: How to Care for Old and Historic Brick and Stone,* National Trust for Historic Preservation, Washington, D.C., 1988, pp. 182–183.

[3] London, Mark, *Masonry: How to Care for Old and Historic Brick and Stone,* National Trust for Historic Preservation, Washington, D.C., 1988, p. 182.

[4] Pavia, S. and Bolton, J., *Stone, Brick & Mortar: Historical Use, Decay and Conservation of Building Materials in Ireland,* Wordwell Ltd., Wicklow, Ireland, 2000, pp. 251–252.

[5] Vitruvius, *The Ten Books of Architecture*, Translation by M.H. Morgan, Dover Publications, New York, 1960, pp. 45–49.

[6] Sickels-Taves, L., "Selecting mortar for historic preservation projects," *Masonry Construction*, Vol. 10, No. 10, 1997, pp. 533–534, 555, 557.

[7] Sickels-Taves, L., Ed., *The Use of and Need for Preservation Standards in Architectural Conservation, ASTM STP 1355*, ASTM International, West Conshohocken, PA, 1999.

[8] Doebley, C. and Spitzer, D., "Guidelines and Standards for Testing Historic Mortars," *Standards for Preservation and Rehabilitation, ASTM STP 1258*, S. J. Kelley, Ed., ASTM International, West Conshohocken, PA, 1996, pp. 285-293.

[9] Fontaine, L., Thomson, M. L., and Suter, G. T., "Practice and Research: The Need for Standards for Historic Mortars," *The Use of and Need for Preservation Standards in Architectural Conservation, ASTM STP 1355*, L.B. Sickels-Taves, Ed., ASTM International, West Conshohocken, PA, 1999, pp. 158–171.

[10] Pavia, S. and Bolton, J., *Stone, Brick & Mortar: Historical Use, Decay and Conservation of Building Materials in Ireland,* Wordwell Ltd., Wicklow, Ireland, 2000, p. 231.

[11] Sickels, L.-B., "Mortars in Old Buildings and in Masonry Conservation: A Historical and Practical Treatise," Ph.D. diss., University of Edinburgh, Scotland, 1987.
[12] London, M., *Masonry: How to Care for Old and Historic Brick and Stone,* National Trust for Historic Preservation, Washington, D.C., 1988, p. 117.
[13] Pavia, S. and Bolton, J., *Stone, Brick & Mortar: Historical Use, Decay and Conservation of Building Materials in Ireland,* Wordwell Ltd., Wicklow, Ireland, 2000, p. 246.
[14] London, M., *Masonry: How to Care for Old and Historic Brick and Stone,* National Trust for Historic Preservation, Washington, D.C., 1988, p. 116.
[15] Suter, G. T., Thomson, M. L., and Fontaine, L., "Mortar Study of Mechanical Properties for the Repointing of the Canadian Parliament Buildings," *Bulletin of the Association for Preservation Technology*, Vol. XXIX, No.2, 1998, p. 54.
[16] Sickels-Taves, L. B., "Creep, Shrinkage, and Mortars in Historic Preservation," *Journal of Testing and Evaluation, JTEVA,* Vol. 23, No. 6, Nov. 1995, p. 452.
[17] Pavia, S. and Bolton, J., *Stone, Brick & Mortar: Historical Use, Decay and Conservation of Building Materials in Ireland,* Wordwell Ltd., Wicklow, Ireland, 2000, p. 248.
[18] Sickels-Taves, L., "Selecting mortar for historic preservation projects," *Masonry Construction*, Vol. 10, No. 10, 1997, p. 534.
[19] Cliver, B., "Tests for the Analysis of Mortar Samples," *Bulletin of the Association for Preservation Technology*, Vol. VI, No.1, 1974, pp. 22–29.
[20] Sickels-Taves, L. and Sheehan, M., *The Lost Art of Tabby Redefined*, Architectural Conservation Press, Southfield, MI, 1999, p. 112.
[21] Sickels-Taves, L. B., "Creep, Shrinkage, and Mortars in Historic Preservation," *Journal of Testing and Evaluation, JTEVA,* Vol. 23, No. 6, Nov. 1995, pp. 447–452.
[22] Sickels-Taves, L., "Selecting mortar for historic preservation projects," *Masonry Construction*, Vol. 10, No. 10, 1997, p. 533.
[23] Morton, B. and Hume, G., *Secretary of the Interior's Standards for Rehabilitation*, National Park Service, Washington, D.C., 1976.
[24] File "Correspondence 1928–1929," Cotswold, E.I. #186, Archives, The Edison Institute, Dearborn, MI.
[25] File "Cutler, E. J. Interviews," Cotswold, E.I. #186, Archives, The Edison Institute, Dearborn, MI.
[26] Sickels-Taves, L., "Maintenance Booklet, Cotswold Cottage, Greenfield Village," Historic Structure Report, The Edison Institute, 1998.
[27] File "History," Cotswold, E.I. #186, Archives, The Edison Institute, Dearborn, MI.
[28] Sickels-Taves, L., "Understanding Historic Tabby Structures: Their History, Preservation, and Repair," *Bulletin of the Association for Preservation Technology*, Vol. XXVIII, No.2–3, 1997, pp. 22–29.

[29] Cook, S., *Mexican Brick Culture in the Building of Texas*, Texas A & M Press, College Station, 1998, pp. 249–250.
[30] Cook, S., *Mexican Brick Culture in the Building of Texas*, Texas A & M Press, College Station, 1998, p. 252.
[31] McKee, H. *Introduction to Early American Masonry*, National Trust for Historic Preservation, Washington, D.C., 1973, pp. 61, 72.
[32] Sickels, L.-B., "The Tabby House, Cumberland Island, Georgia: Paint and Mortar Study," Materials Report, National Park Service, 1980.
[33] Sickels-Taves, L. and Sheehan, M., "The Lost Art of Tabby Redefined: A Practical and Cultural Study," Earthwatch, Center for Field Research, Watertown, MA, 1997.
[34] "Hydraulic lime mortars for building – an introduction," URL: http://www.limesolve.demon.co.uk, Hydraulic Lias Limes Limited, Somerset, England, 5 November 2001.
[35] Gibbons, P., *Preparation and Use of Lime Mortars: An introduction to the principles of using lime mortars*, Historic Scotland, Edinburgh, 1995.
[36] Elert, Kerstin et al., "Lime Mortars for the Conservation of Historic Buildings," *Studies in Conservation*, Vol. 47, 2002, pp. 62–75.
[37] Doebley, C. and Spitzer, D., "Guidelines and Standards for Testing Historic Mortars," *Standards for Preservation and Rehabilitation, ASTM STP 1258*, S. J. Kelley, Ed., ASTM International, West Conshohocken, PA, 1996, p. 293.
[38] "Introduction," *Mortars, Cements and Grouts used in the Conservation of Historic Buildings*, ICCROM, Rome, 1982, p. 1.
[39] Kelley, S., Ed., *Standards for Preservation and Rehabilitation, ASTM STP 1258*, ASTM International, West Conshohocken, PA, 1996.
[40] "PRO 12: Historic Mortars: Characteristics and Tests," URL: http://www.rilem.org/rppro12.html, RILEM, Cachan Cedex, France, 5 November 2001.
[41] Bartos, P., Groot, C., and Hughes, J. J., Eds., *Historic Mortars: Characteristics and Tests*, PRO 12, RILEM Publications, France, 1999.
[42] Goins, Elizabeth, "A Standard Method for the Analysis of Historic Cementitious Materials," *NCPTT Notes*, No. 35, 2000, pp. 8–9.
[43] Fontaine, L., Thomson, M. L., and Suter, G., "Practice and Research: The Need for Standards for Historic Mortars," *The Use of and Need for Preservation Standards in Architectural Conservation, ASTM STP 1355*, L. B. Sickels-Taves, Ed., ASTM International, West Conshohocken, PA, 1999, p. 170.
[44] Sickels-Taves, L., and Hovey, L., "Lack of Material Preservation Standards Raises Global Concern," *APT Communique*, Vol. 26, No. 1, 1997, pp. 4–5.
[45] Sheehan, M. and Sickels-Taves, L., "Old Baldy Lighthouse: Report on Analysis and Specifications for Masonry Restoration," Condition Report, North Carolina State Historic Preservation Office, 2001.
[46] Sickels-Taves, L. and Sheehan, M., "A Medieval Farm Revisited: Architecture, Archaeology, and Historic Preservation in Eastern

Europe/Hungary," Earthwatch, Center for Field Research, Watertown, MA, 1998.

[47] Fischetti, D., Sickels-Taves, L., and Graton, A., "The Chimneys, Stafford Plantation: Findings and Preservation Report," Condition Report, The National Park Service, 2000.

[48] "Hybrid Mortars," *Lime Newsletter*, Vol. 2, No. 2, 2000, p. 8.

Anne B. Abell,[1] and John M. Nichols[2]

Investigation of the Rheology and Microstructure of Hydrated Lime and Sand for Mortars

REFERENCE: Abell, A. B., and Nichols, J. M., "**Investigation of the Rheology and Microstructure of Hydrated Lime and Sand for Mortars,**" *Masonry: Opportunities for the 21st Century, ASTM STP 1432*, D. Throop and R.E. Klinger, Eds., ASTM International, West Conshohocken, PA, 2003.

ABSTRACT: This paper presents the investigation and characterization of Type S hydrated lime in aged solutions with sand and with subsequent addition of Portland cement. The plastic mortar workability and flow as prescribed by ASTM Standards C207 and C270, the rheological properties, the microstructure of the lime-sand slurries, and the hardened microstructure and properties as prescribed by ASTM Standard C109/C 109Mhave been analyzed to identify the optimal relation of lime hydration product form to sand and the implications to selection of materials or manufacture of a hydrated lime type for constructability and performance.

KEYWORDS: lime, sand, workability, mortar, electron microscopy, morphology

Introduction

The importance of hydrated lime to the workability and water-tightness of mortars is well recognized. The water retention required of lime mortars is specified in ASTM Standard C207 and discussed in relationship to the selection of mortars in the Appendixes of ASTM Standard C270. The ability of a mortar to withstand repeated stresses without rupture of bond and heal autogenously is attributed to plastic flow, creep, and moduli of elasticity; all directly influenced by the presence of lime [1]. The process of carbonation, which can cause irreversible drying shrinkage and reduced corrosion resistance at surfaces, is beneficial by effectively closing off the access of moisture into hardened mortar by forming calcium carbonate crystals ($CaCO_3$ or $C\overline{C}$) that aid dimensional stability upon wetting and drying and is a chemical process directly involving lime hydration products of calcium hydroxide ($Ca(OH)_2$ or CH) [2]. The increase in strength with time after compaction of crushed aggregate materials treated with calcium hydroxide for base courses of Portland cement concrete pavements has been attributed to good interfacial bond from the carbonation products by scanning electron microscopy

[1] Assistant Professor, School of Architecture, University of Illinois, Temple Buell Hall, Champaign, IL 61820

[2] Senior Lecturer, School of Civil Engineering, Curtin School of Technology, Perth, Western Australia 6845

(SEM) studies [3]. The microscopy showed that there is good attachment of cement with carbonate (limestone) aggregates.

Typically, scanning electron microscopy is used to examine the hardened state of cement and mortar materials. These non-conducting materials must be dried and coated with a conductive material such as gold or carbon in order to be examined using the electron beam. The drying of hydrating materials can cause damage to the microstructure as water is removed from clay-like layers, and effectively freezes the form of hydration products, which may change with further hydration, and consumption of available water. Environmental scanning electron microscopy (ESEM), which is a relatively recent advance in the technology, allows observation of a wet specimen in a microenvironment at high magnifications without disturbing the development of the microstructure. Lange, Sujata, and Jennings [4] observed dissolution and precipitation processes in cement paste by examining wet pastes and by the addition of water to Portland cement within the specimen chamber of the microscope. They also examined the microstructure as the water was removed from the microenvironment and the resulting drying, cracking, and shrinkage of the microstructure.

The types of lime for masonry purposes are supplied as hydrated lime in dry form, with and without air entraining additives, or as a putty that is fully slaked and screened. The crystalline shape of the hydrated lime is variable, particularly with respect to aging, as shown by Rodiquez-Navarro, et al. [5]. Their study found from X-ray diffraction, nitrogen adsorption, and scanning electron microscopy that there was a size reduction and morphological or shape change between fresh and 14-month-old aged lime putties. The traditional use of aged or slaked lime to improve workability and water-tightness is based on experience, as evident by an ancient Roman law requiring lime to be slaked and stored under water three years before its use [6]. But the science underlying the material behavior is still not well understood, although the increase in surface area by the crystal size reduction has been suggested as a reason for the quality improvement [5] and rapid carbonation of lime mortars [7]. The benefit of adding the sand to a lime putty for a period prior to mixing with cement is also based on experience[3] [1][9]. Modern construction practices using the commercial forms of hydrated lime preclude the use of these aging techniques.

Nichols [10] completed a systematic investigation of pressed clay masonry shear walls subjected to dynamic loads. This research used a 1:1:6 mortar that had been used in repairs to the Catholic cathedrals after the 1989 Newcastle earthquake (M5.5). The masons had observed that this mortar provided improved workability when the lime component was delivered in the form of a putty. The laboratory work investigated a number of alternative methods for combining the lime, and, and cement. The masons observed improve workability with a sand-lime mix that had been allowed to stand overnight compared to dry lime mixes and lime putty mixes that had not.

If the enhancements attributed to the aging techniques can be characterized through understanding the microstructural relation of the lime to the sand in the wet state and the relationship of the lime-sand slurry to the cement hydration process, the lime could be

[3] Personal communications with masons.

supplied in a form tailored for the desired fresh and hardened masonry properties. This work studies the effects of aging lime putty and lime-sand slurries on the workability, microstructure and strength of Portland cement mortars using standard test methods and microscopy.

Experimental Procedure and Technique

The effect of aging lime-sand slurries on calcium hydroxide crystal size and shape, fresh mortar rheology and plastic flow, and compressive strength were of particular interest in this investigation. Lime-sand slurries and a lime putty were observed using an ESEM in the wet state and with removal of water. The addition of Portland cement to the sample surface was also observed in wet and dry states. Mortars made with Portland cement and the lime-sand-slurries were tested for rheological properties and flow, and formed into 2-in cube specimens for compressive strength testing. The mortars were also used in a brick prism for examination of the hardened microstructure.

Materials

Type S lime — special hydrated lime for masonry purposes — is the most commonly used form of hydrated lime in masonry mortars, particularly because it is able to develop high, earlier plasticity and higher water retentivity than normal hydrated lime (Type N). In addition Type S lime is allowed to have a maximum of 8% unhydrated oxides as by Standard Specification for Hydrated Lime for Masonry Purposes, ASTM C207, which does not limit the unhydrated oxide content for Type N lime. The hydrated lime used in this study was Type S hydrated lime (Standard Specification for Hydrated Lime for Masonry Purposes, ASTM C207). Type I Portland cement (Standard Specification for Portland Cement, ASTM C150) and masonry sand (Standard Specification for Aggregate for Masonry Mortar, ASTM C144) were used in the mortars.

A lime putty was formed by adding sufficient water to fully liquify the hydrated lime, and was aged for a minimum of one week before use in lime-sand slurries and mortars for this study. The putty had a specific gravity of 1.3. The proportions of the mortar components by weight were 1 part hydrated lime/lime putty to 1 part Portland cement to 6 parts masonry sand. The equivalent laboratory volume ratio is 2:1:4.5, which classifies as sand-rich Type O Cement-Lime mortar. Three mortars were constructed and designated Putty — made with the lime putty, 1 Hour — made when the lime-sand slurry was 1 hour old, and 4 Hour—made when the lime-sand slurry was 4 hours old. The lime, cement, and sand were mixed for 30 seconds when 1 part by volume of water was added and mixed for 30 seconds. Additional water was added to the lime-sand slurries until the point at which the sand grains could just easily flow past each other and mixed for 3 additional minutes. When the slurries mortars were mixed, the additional water was added until the coated sand particles formed a cohesive mass with the masonry paste and the sand grains could just easily flow past each other. The specific w/s ratios were not determined, as water was added for the desired workability.

A prism was constructed using bricks with IRA of 17.2 g/ 30 in^2 with a standard deviation of 0.34 g/30 in^2 and a bed with each mortar covering a third of the brick. The

prism was constructed to examine the resulting hardened microstructure upon water removal by brick absorption.

Rheology

Viscosity measurements were taken following Test Method A of Standard Tests Methods for Rheological Properties of Non-Newtonian Materials by Rotational (Brookfield type) Viscometer, ASTM D2196 for the Putty, 1 Hour and 4 Hour lime-sand slurries, and the lime putty. A Brookfield Viscometer Model LVF was used with a #4 spindle and rotational speed of 12 RPM having a scale factor of 500. The apparent viscosities after 8 minutes (for stabilization) are presented in Table 1. The viscosities can be referenced to those of water: 1 mPa·s, and glycerine: 1500 mPa·s. The 4 Hour lime-sand slurry has a distinctly lower viscosity than the 1 Hour and Putty mixes. Hydration of Portland cement produces an increase in viscosity, which suggests that the lime hydration products are not mechanically interlocking and resisting the flow. The putty without addition of sand shows the influence of sand particle suspension with minimal adhesion of lime hydration products on the surface of the particles (no aging time with addition of sand) by an increase of 8190 mPa·s. The increase in viscosity of the Putty mix with respect to the 1 Hour mix could be attributed to the presence of early age hydration products having large surface areas.

TABLE 1—*Viscosity of Lime-Sand Slurries and Lime Putty*

Slurry Type	Viscosity (mPa·s)
1 h	15500
4 h	11100
Putty	14300
Putty (no sand)	6110

Mortar Flow

Flow was determined for each mortar made from the lime-sand slurries in accordance with Standard Test Method for Compressive Strength of Hydraulic Cement Mortars, ASTM C109/C 109M by dropping the table 25 times. The resulting measurements are presented in Table 2. The flows are less than those anticipated for field mortars due to the criteria for the addition of water to the point where the sand grains would flow past each other. The 4 Hour mortar formed plastic cracks on top of the molded shape as it was dropped and also had surface bleed water.

Table 2 – *Flow of Mortars*

Slurry Type	Flow %
1 Hour	52
4 Hour	62
Putty	78

Compressive Strength

Compressive strength of 2-in. cube specimens was determined following Standard Test Method for Compressive Strength of Hydraulic Cement Mortars, ASTM C109. Two test specimens of each mortar mix were molded and moist cured for 7 days prior to testing. Results of the tests are reported in Table 3.

TABLE 3 —*Mortar Compressive Strengths*

Slurry Type	7 day Compressive Strength (psi)
1 h	620
4 h	808
Putty	774

Microstructural Characterization

Of particular interest to the workability of lime-sand slurry mortars is the influence of aging of the lime-sand slurry. As this material is composed of saturated lime water, lime hydration products and sand, optical microscopy can show little beyond the surface, while scanning electron microscopy requires the removal or freezing of the water. With the use of an environmental stage, the pressure can be elevated while still allowing sufficient pressure in the electron gun for the secondary-electrons to be detected[8]. A Philips XL30 ESEM-FEG scanning electron microscope was used with water vapor pressure and a cooling stage in this study. A 0.5 mm gaseous secondary electron detector (GSED) was used with a 20kV electron beam. With the stage chilled to 3° C and pressure of 6.4 torr, the sample experienced 100% relative humidity. As the pressure was reduced, the relative humidity dropped and water was removed from the chamber and specimen. The sample chamber with cooling stage (two water lines and serial cable), sample container, and GSED (above the sample) can be seen in Figure 1.

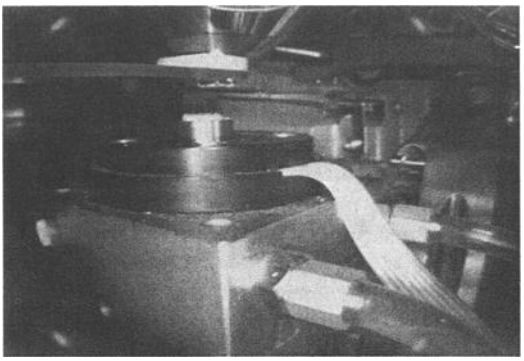

Figure 1 – *ESEM Sample Chamber*

The wet mode observation of all the lime-sand slurries and the lime putty revealed very little in the way of surface features. The surface tension of the lime solution

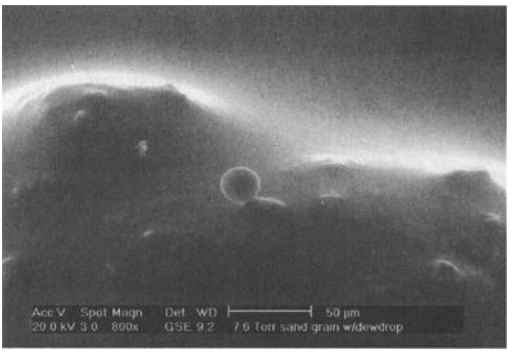

Figure 2 – *ESEM Wet Mode Feature: Water Droplet, Sand Grains, and Crystals*

remained fairly featureless with relief provided by sand grains and hydration products. Figure 2, from a preliminary investigation of a week old lime-sand slurry, shows the contrast between a water droplet that has formed with an increase in vapor pressure compared to the sea-like expanse with edges of elevated hydration crystals in relief (bright).

Lime Putty

The lime putty showed very similar features in wet mode, without the relief provided

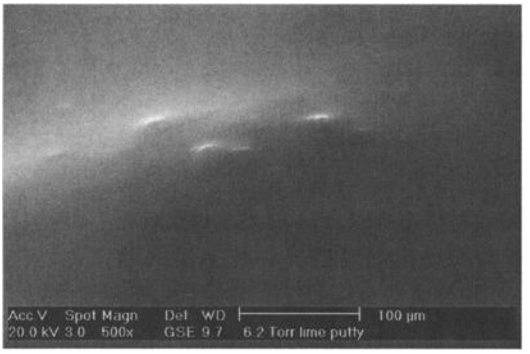

Figure 3 – *Lime Putty (wet mode)*

by presence of sand grains (Figure 3). Objects under the surface of the lime solution were difficult to distinguish because of the scattering of electrons, but faint cracks and hydration product close to the surface were visible. As the water vapor pressure was reduced, the sharpness of the features increased. Figure 4 shows the pressure reduction from 6.4 torr (100% RH) at 5.1 torr (a) to 4.8 torr (b).

Closer inspection of the smooth structure of the dried hydration products (Figure 5) shows that the individual crystals of calcium hydroxide are thin hexagonal plates varying in size from 0.1 µm to 1 µm.

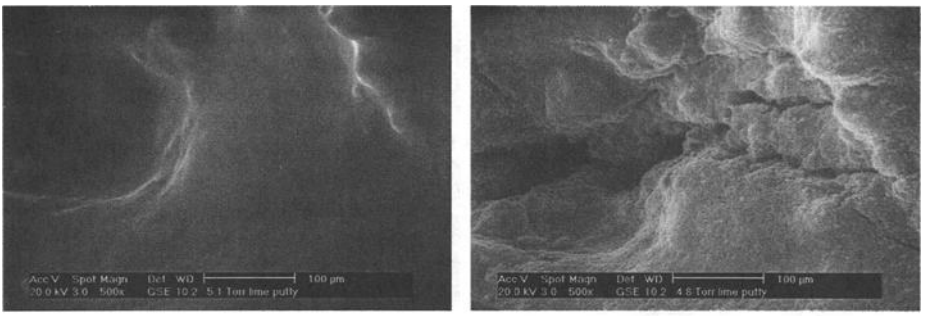

a) 5.1 torr b) 4.8 torr

Figure 4 – *Lime Putty Drying*

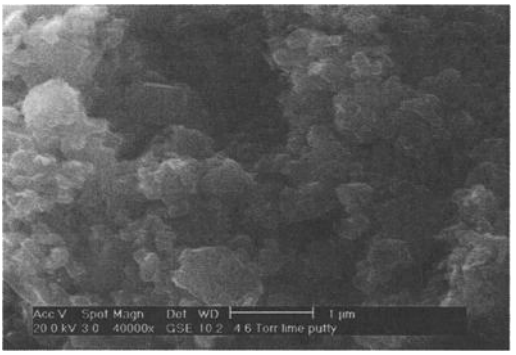

Figure 5 – *Calcium Hydroxide from Lime Putty*

1 Hour Lime-Sand Slurry

Relatively few surface features were found in wet mode for the 1 Hour lime-sand slurry, and were due again to elevation of sand grains and hydration products. Figure 6 shows the drying evolution at a sand grain. Figure 6b reveals the edge of a large hydration cluster to the right of the sain grain. This cluster and the smaller ones near it appear to be of generally hexagonal shape built up of layers. In general, the smooth coating of the sand grains appears very similar to the dried lime putty.

An interesting feature for the dried slurry appeared several times at the top surface of a sand grain of a dark flat crystal formation (Figure 7a). The darkness suggests that the formation is sufficiently thin to suppress secondary-electron effects. Higher magnification shows that the crystals are plate-like and thin, 1 µm or less, and intergrown. The very small hexagonal crystals are randomly forming the classic irregular "rosettes" of monosulfoaluminate in hydrated Portland cement. There also appears to be no adhesion of the bulk lime hydration product on the sand grains where these features are. The lime hydration product that is nearest to the bare area is less dense and level in appearance. These formations could be a result of the surface tension of the lime solution receding as water is removed by lowering the vapor pressure, stunting the crystal growth.

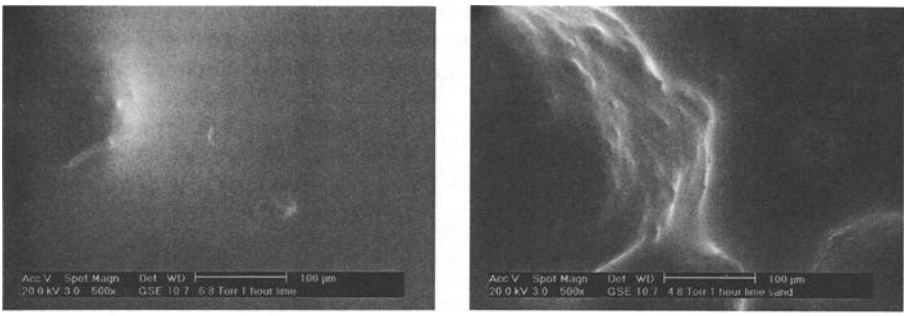

a) 6.8 torr b) 4.8 torr

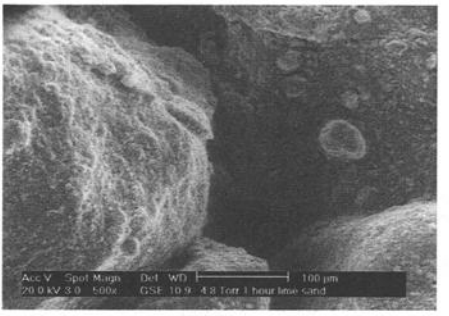

c) dried

Figure 6 – *1 Hour Lime-Sand Slurry Drying*

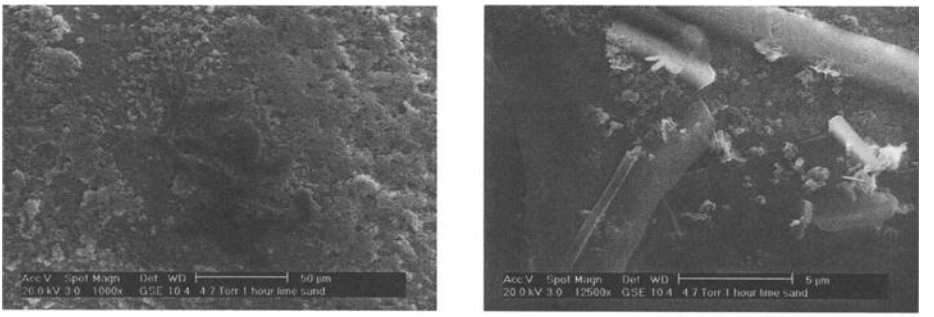

a) 1000x b) 12500x

Figure 7 – *Flat Crystal Formation in Dried 1 Hour*

4 Hour Lime-Sand Slurry

Somewhat more surface features were found in wet mode for the 4 Hour lime-sand slurry due to elevation of sand grains and hydration product. There was an increase in identifiable small hydration clusters on the sand grains and subsurface features. Figure

8a shows a lamellar feature on the scale of a sand grain not seen on the 1 Hour lime-sand slurry in wet mode. Higher magnifications (b & c) suggest that the submerged crystals are of similar form to the intergrown crystals seen in the dried 1 Hour lime-sand slurry (Figure 7b) but are of much greater thickness. Upon drying of the 4 Hour lime-sand slurry, the separations between the lamellæ in wet mode are actually the edges of overlapping sheets of hydration product (Figure 9), which appear bright because of the edge effect of the secondary-electrons. It is not clear if this feature was uniformly distributed within the 4 Hour lime-sand slurry, as the sample container was less than 1 cm in diameter, but it is possible that sliding of these sheets against each other contributes to the workability of this aged slurry and lower viscosity.

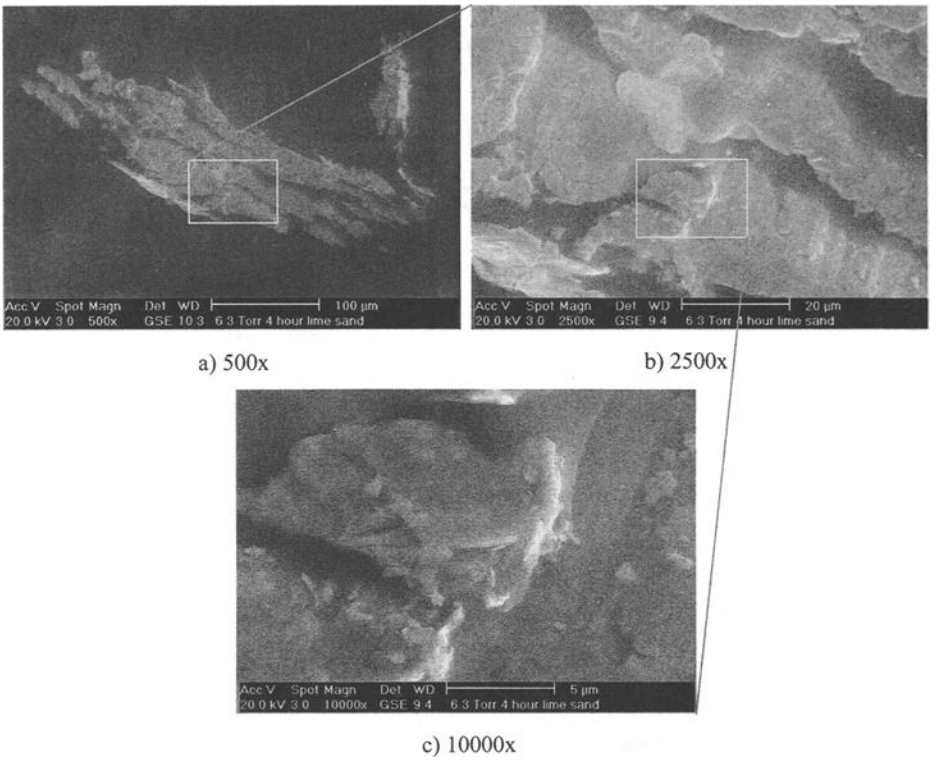

Figure 8 – *4 Hour Lime-Sand Slurry Lamellar Feature (wet mode)*

The dried bulk hydration product on the sand grains had similar topology to that of the 1 Hour lime-sand slurry, but was more porous, delicate, and stratified. Shrinkage cracks were not in evidence between grains, but there was a separation, almost plastic-like, of the porous sheets (Figure 10). The increase in surface area could easily contribute to water retentivity by capillary effects, to the bond by interlocking in the masonry unit surface, and to self healing by dissolution and precipitation upon wetting to fill cracks.

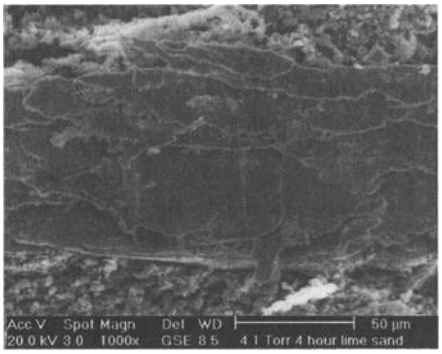

Figure 9 – *Dried 4 Hour Lime-Sand Slurry Lamellar*

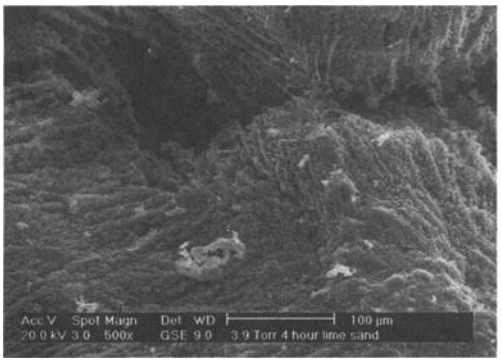

Figure 10 – *Dried 4 Hour Lime-Sand Slurry*

Addition of Portland Cement – Portland cement grains were added on the surface of a sample of 4 Hour lime-sand slurry. In wet mode, the grains are evident as their surfaces begin to dissolve in the saturated lime solution (Figure 11). As there is no evidence of hydration products with the Portland cement until the concentration of dissolved ions is large enough, the sample was only left in the microscope chamber for about 15 minutes

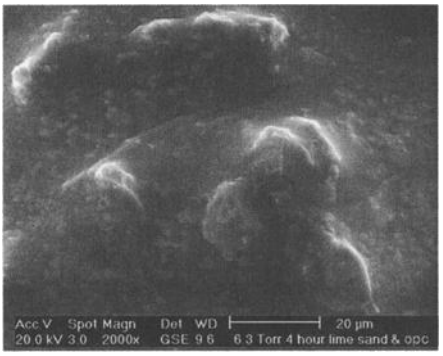

Figure 11 – *4 Hour Lime-Sand Slurry with Cement*

before the water vapor pressure was reduced. The dried structure of the lime hydration products is much like that of the 4 Hour lime-sand slurry, but with the addition of calcium silicate hydrate (C-S-H) needles and larger calcium hydroxide grains as identified in Figure 12.

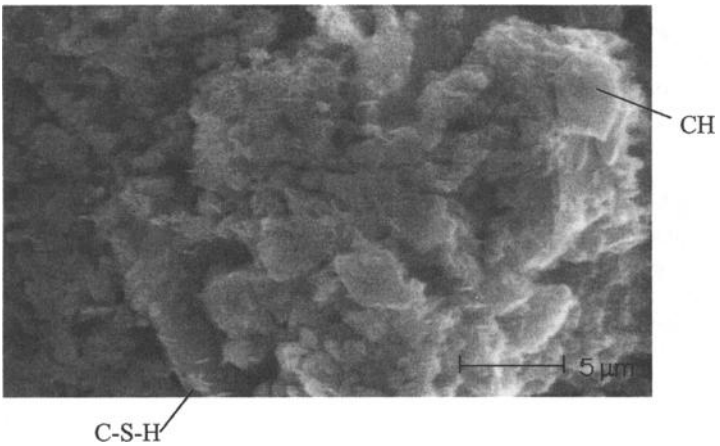

Figure 12 – *Dried 4 Hour Lime-Sand Slurry with*

Mortar Microstructure

The microstructure of the hardened mortar was examined using an optical microscope at a magnification of 30 times. The brick prism had been cut with a water-lubricated saw to expose the center of each mortar in the bed at 7 days. The cut surfaces showed a predominance of white calcium hydration product. The Putty mortar showed blocky crystal formation on the sand grain surfaces, gaps at the interfaces with grains, and pull-outs where grains had been. The 1 Hour mortar showed cracks around grains and single plate crystals in pull-outs and voids. There were more deep pull-outs and voids, and very little crystallization on the grains themselves. The 4 Hour mortar had crystal formations in the pull-outs, with little crystallization on the sand grains.

The observations suggest that the Putty and 1 Hour mortars experienced more shrinkage than the 4 Hour mortar. The crystal formation on the grains of the Putty could be an indication of interface adhesion contributing to a higher compressive strength.

Implications to Selection or Specification of Masonry Materials`

The differences in morphological characteristics of the 1 Hour and 4 Hour lime-sand slurry were most evident in the dried state observed with ESEM. Although wet mode observation of the 4 Hour lime-sand slurry showed a large thick flat crystal feature as opposed to the small thin flat crystal features on the surface of sand grains in the 1 Hour lime-sand slurry, the major difference was in the density and thickness of the bulk lime hydration product, and its form at grain to grain interfaces. The increase in surface features and the reduction of the size of these features in the 4 Hour lime-sand slurry

when Portland cement was introduced to the mortar could play a key role in the saturation of dissolved ions in solution to a concentration initiating precipitation of C-S-H, which is implicated in the strength of cement based materials due to its proportion in the cement hydration products and the high surface area interlocking. When sufficient thickness of hydration product has formed around a cement grain to prevent all of it from dissolving into solution indicating that sufficient water is available for continued hydration, higher strength is expected as well[2]. Increased amounts of calcium hydroxide crystals in the thicker coating may contribute to a decrease in strength if the crystals were oriented preferentially, like at aggregate interfaces in cement-based materials, but there is no distinct orientation in the 4 Hour lime-sand slurries. There does not appear to be a significant difference in the amount of large calcium hydroxide crystals oriented with their hexagonal surfaces parallel to sand grains in the 1 Hour and 4 Hour lime-sand slurries.

The investigation suggests that the amount of hydration product is more important to the workability and hardened properties of the mortar than the crystal morphology, which is different upon aging as well. Determining a catalyst for crystal shape and size may be of limited use. It would be of greater benefit to provide a sand that is lime-rich, or pre-treated like the crushed aggregate used in highway base courses in Florida[3] which have been exposed to moisture in the air and have hydration products formed on the aggregate before use in a mortar. This could be accomplished in much the same fashion by soaking the materials in lime slurry to a sufficient age, drying, packaging and marketing it as pre-limed masonry sand with "no need" to add additional lime. Material provided in this form may appeal to the time conscious contractor or mason. Future work on manufacturing techniques to reproduce lime-aged sands could provide further insight.

Summary

The effect of aging lime-sand slurries on calcium hydroxide crystal size and shape, fresh mortar rheology and plastic flow, compressive strength and hardened microstructure were investigated with respect to benefits as a result of physical attributes. Lime-sand slurries and a lime putty were observed using an ESEM in the wet state and with removal of water, and the addition of Portland cement to the surface of an aged lime-sand slurry was also observed in wet and dry states. Mortars made with Portland cement and the lime-sand slurries were tested for rheological properties and flow, and compressive strength, in addition to being used in a brick prism to observe the hardened microstructure in 'situ.

The results suggest that the increase in surface area of the lime hydration products resulting from small, lightly packed calcium hydroxide crystals in thick coatings on the aggregates is the primary influence on workability, water retentivity and bond. The aging process contributed more to the thickness and porosity of the coating than it did to changing the crystal formations. One way to incorporate this benefit into a manufacturable masonry material is suggested by pre-liming masonry sand.

Acknowledgments

Graymont Dolime (OH) Inc. and Chemical Lime Company generously supported this research. We thank Anne Werner for providing brick units and IRA characterization, and Scott Robinson of the Image Technology Group for his help with the ESEM at the Beckman Institute for Advanced Science and Technology.

References

[1] Staley, H. R., "A Petrographic Study of the Bond Between Bricks and Mortar," *Transactions of the British Ceramic Society*, Vol. 39, 1939-40, pp. 85–100.

[2] Mindess, S., and Young, J.F., *Concrete*, Englewood Cliffs: Prentice Hall, 1981, p. 498.

[3] Graves, R.E., Eades, J. L, and Smith, L. L., "Calcium Hydroxide Treatment of Construction Aggregates for Improved Cementation Properties," *Innovations and Uses for Lime, ASTMP STP 1135,* D.D. Walker, Jr., T.B. Hardy, D.C. Hoffman, and D.D. Stanley, Eds., ASTM International, West Conshohocken, PA, 1992, pp. 65–77.

[4] Lange, D. A., Sujata, K., and Jennings, H. M., "Observations of Wet Cement Using Electron Microscopy," *Ultramicroscopy*, Vol. 37, 1991, pp. 234–238.

[5] Rodriquez-Navarro, C., Hansen, H., and Ginell, W. S., "Calcium Hydroxide Crystal Evolution upon Aging of Lime Putty," *Journal of the American Ceramic Society,* Vol. 81, No. 11, 1998, pp. 3032–34.

[6] Ashurst, J., "Mortars for Stone Buildings," *Conservation of Buildings and Decorative Arts,* Vol. 2, J. Ashurst, and F.G. Dimes, Eds., London: Butterworths, 1990, pp. 78–96.

[7] Cazalla, O., Rodriquez-Navarro, C., Sebastian, E., Cultron, G., and del la Torre, M.J., "Aging of Lime Putty: Effects on Traditional Lime Mortar Carbonation," *Journal of the American Ceramic Society,* Vol. 83, No. 5, 2000, pp. 1070–76.

[8] Goldstein, J. I., Newbury, D. E., Echlin, P., Joy, D. C., Romig, A. D., Jr., Lyman, C. E., Fiori, C., and Lifshin, E., *Scanning Electron Microscopy and X-Ray Microanalysis,* 2nd ed., New York: Plenum Press, 1994, pp. 572–574.

[9] Baker, I.O., *Treatise on Masonry Construction, 10th ed.,* New York: Wiley, 1912, pg. 746.

[10] Nichols, J.M., *A Study of the Progressive Degradation of Masonry Shear Walls Subjected to Harmonic Loading*, Doctoral Thesis, University of Newcastle, Newcastle, NSW, 2000.

D. Herbert Nordmeyer[1]

High Pozzolan Mortars and Stuccos

REFERENCE: Nordmeyer, D. Herbert, **"High Pozzolan Mortars and Stuccos,"** *Masonry: Opportunities for the 21st Century, ASTM STP 1432*, D. Throop and R. E. Klingner, Eds., ASTM International, West Conshohocken, PA, 2003.

ABSTRACT: The Romans introduced and used pozzolanic mortars and cements. In recent years pozzolans are again being used, especially in concrete. With the modifications of ASTM C 270 to include C 595 and C 1157 cements, pozzolans are becoming more common in cement-lime mixes. Failures have been reported in fly ash modified mortars and stuccos, and specifications have been written that limit the amount of fly ash that can be added to a mortar. By combining expertise in masonry with expertise in pozzolans, we have worked with masons and plasterers to develop a line of high-pozzolan masonry cements, mortar cements, and plastic (stucco) cements. Mortars made from these cements exhibit excellent workability, water retention, resistance to the penetration of water, and bond strength. As a side benefit these mortars appear to be more acid resistant than cement/lime mortar or masonry cement mortar tested at our lab. This paper reviews the process of developing the cements and provides test data to demonstrate that they exceed current specifications.

KEYWORDS: fly ash, masonry cement, mortar, mortar cement, pozzolan, stucco cement

Introduction

The author's laboratory, operated by a materials supplier, is charged with oversight of a company-wide QA/QC program for manufactured products, including cements and stuccos. It is also charged with bringing emerging technologies to commercial reality. This paper deals with one example of that process, involving pozzolanic mortar. This material, invented by the Romans over two thousand years ago, has been improved substantially, and mortars and stuccos can be produced with high concentrations of pozzolans. Pozzolans improve the performance of those products, and are thus much more than inexpensive fillers. They also have been accepted with enthusiasm by masons. As a by-product of the research necessary to develop commercially successful pozzolans, it was found that selection of the proper pozzolan was extremely important. An addition rate of 20% pozzolan could be detrimental if the

[1] Product manager, ISG Resources, Inc., 5033 Callaghan Road, San Antonio, TX 78228

wrong pozzolan were used: conversely, with the right pozzolan, an addition rate of 40% could produce a very satisfactory product. While natural pozzolans such as volcanic ash work well, this paper emphasizes the use of fly ash, since it is the most commonly available pozzolan and also the most economical.

In this paper, it is assumed that the reader understands the terminology common to masonry cements and mortars. Because the reader may not be familiar with pozzolans and their reaction with lime, nor the differences between Class C and Class F fly ashes, background information on those subjects is reviewed below.

Pozzolanic Reactions

According to ASTM Standard Specification for Coal Fly Ash and Raw Natural Pozzolan for Use as a Mineral Admixture in Concrete (C 618), a pozzolan is "a siliceous or siliceous and aluminous material which in itself possesses little or no cementitious value but will, in finely divided form and in the presence of moisture, chemically react with calcium hydroxide at ordinary temperatures to form compounds possessing cementitious properties." Other definitions include that the silica or alumino-silicates are amorphous. Volcanic ash as well as many clays are natural pozzolans. Many clays that are non-pozzolanic can be made pozzolanic by calcining.

In simplified form portland cement is the milled product of a reaction between silica, alumina (i.e., clay), and calcium (i.e., limestone) at elevated temperatures. When portland cement reacts with water, hydrated calcium silicates, hydrated calcium aluminates, calcium hydroxide, and heat are produced. [1, 2]

A pozzolanic reaction is endothermic. It can be an amorphous clay and hydrated lime reacting at ordinary temperatures to produce hydrated calcium silicates and hydrated calcium aluminates that are similar to, or identical to, those produced by the hydration of portland cement. Compared with the speed of the portland cement hydration reaction, the pozzolanic reaction is slow. [1, 2]

Fly ashes are some of the most commonly used-pozzolans. They are formed, in part, by the clay contaminates in coal being heated to a high heat and cooled to form an amorphous glass.

In summation, the raw materials are similar. The resulting compounds are similar. The pathways are different.

Classes Of Pozzolans

ASTM C 618 identifies 3 classes of pozzolans: N, C, and F.

Class N pozzolans are natural pozzolans such as volcanic ash, diatomaceous earth, and rice hull ash. Normally these pozzolans have little or no calcium and by themselves have no cementitious properties. Some of them, such as meta-kaolin, have to be heated before their developing strong pozzolanic characteristics. The advantages of natural pozzolans are that they are more consistent than fly ashes, can be milled to the appropriate particle size, and many tend to be lighter in color than fly ashes. Most natural pozzolans are more expensive than fly ashes; as a result, they are not used as much as fly ashes.

Class C pozzolans are fly ashes that meet the Class C properties listed in C 618. The sum of the silica, alumina, and iron is between 50% and 70%. Calcium concentrations are not specified, but usually make up over 15% of the mass. These pozzolans when mixed with water exhibit cementing properties. In general terms, a portion of the material is pozzolanic, and a portion (that which is combined with calcium) is cementitious. The cementitious chemicals are not necessarily the preferred cement chemicals that are found in portland cement since the amount of calcium present is lower than is found in portland cement. Since Class C fly ash provides some cementing properties, the assumption is often made that Class C fly ash can replace more of the portland cement in mortar than can Class N or Class F. This assumption is not always true because time of set becomes difficult to control with high dosages of Class C ash and autoclave expansion may increase.

Class F pozzolans are fly ashes that meet the Class F properties listed in ASTM C 618. The sum of the silica, alumina, and iron is 70% or greater. The calcium concentrations are not specified, but are usually less than 15%. This class of pozzolans exhibits little or no cementing properties when mixed with water.

Both Class C and Class F pozzolans are by-products of coal combustion. Since the generating utility is more concerned with the production of electricity then the production of fly ash, the fly ash from a given plant will be variable. All formulation decisions need to be made based on that variability, not on averages.

ASTM C 618 specifies in the definition of fly ash that it results from the combustion of ground or powdered coal. There are combustion ashes that are produced by burning raw material other than coal. These ashes do not comply with the requirements of C 618.

Functions of Mortar

Mortar has many functions in a building. Some of these functions include holding brick apart, bonding brick together, and keeping moisture from penetrating the wall, as well as aesthetics. A mortar must not only satisfy the ASTM and Building Code requirements, but it must satisfy the needs of the mason on the job-site. What satisfies an engineer in a mortar and what satisfies a mason often seem mutually exclusive. The mason judges a mortar based on workability and production. Architects and engineers judge mortar based on performance, endurance, and its service during the life of the building. Additionally, we need to satisfy the builder and the owner of the building.

Only by understanding the needs of each can a superior product be developed. Rochelle C. Jaffe's article entitled "Understanding Mortar" in the February 2001 issue of *Masonry Construction* [3], provides an excellent explanation of these needs.

Conventional Technology

Mortars are a mix of cement (often masonry cement or portland-lime blends), sand, and water. When we use the term "masonry cement" or "mortar cement," we are referring to the dry powder. "Mortar mix" usually refers to a sanded dry powder.

Mortars and stuccos are made from similar materials. In fact, many plasterers use masonry cement, or masonry cement plus portland cement, as the cement in their stucco.

Most masonry cements that are produced at cement plants consist of a blend of portland cement clinker, limestone or other filler, and an air-entraining agent. [4] The components are usually milled together. The air-entraining agent is often chosen to act as a grinding aid. Type N masonry cements usually use about equal amounts of portland cement clinker and limestone. Type S and Type M masonry cements contain more portland cement clinker. When produced at blending plants, they often consist of the same components that have been milled or a blend of portland cement and hydrated lime. The cement/lime blends often follow the ASTM C 270 proportion mix ratio.

In recent years several products have come to market that can be added to portland cement to produce a mortar. These products are often called "mortar fat" and are often advertised as a replacement for hydrated lime. ASTM Task Group 12.09.02 on Alternate Mortar Materials is addressing the subject of mortar fats and their use. These products fall into two categories. The first is sodium-bentonite-clay-based [5, 6], and the second is a gum or resin. The bentonite-clay-based product may be pozzolanic. Both categories of "mortar fat" act as thickeners and plasticizers. While they perform many of the functions that hydrated lime does in a mix, they do not provide a calcium source for reaction with a pozzolan. Thus if they are used with a pozzolan, the pozzolan tends to take on the role of an inert filler. This is especially true if the bentonite clay product is used.

During the last 15 years mortar cements have come into the market. These are similar to masonry cements, except bond strength is measured and required. This usually requires an increase in portland cement over what a masonry cement of the same type would require.

Development of Technology

Pozzolanic mortars are not new. The Greeks learned to burn lime and hydrate it to make mortar. The Romans learned to combine burned lime with other products to make concrete and mortar. They used broken brick and tile that they had crushed, as well as sand and gravel, and mixed them with slaked lime and volcanic ash. An important and high-quality source of volcanic ash came from near Pozzoli, and thus was called pozzolan. The Iliad tells of making and curing pozzolanic floor tile, although that name was not used. The tile was placed on the roof to cure for two years before being used as floor tile. The Pantheon, probably the best-preserved building of the Roman Empire, was rebuilt in Rome in 200 AD using pozzolanic mortar and brick. There are many other buildings built by the Romans with pozzolanic mortar that are still around today. As centuries passed, the use of pozzolanic mortars faded from prominence in Europe, especially northern Europe. [2, 7, 8]

By the time what is now the United States was settled by Europeans, the predominant mortar was a mixture of lime putty and sand. With the development of the portland cement industry in the United States in the late 19th century, it became common to add portland cement to mortar to speed setting. This led to the traditional cement/lime

mortars. By the 1920s cement companies were developing masonry cement, a hydrated lime-free material that could be used to make mortar. [9]

In the late 1950s the author was employed by a company that developed and successfully marketed Type N pozzolanic masonry cement for several years. The formula was a blend of processed volcanic ash and hydrate lime, without any portland cement. The Fairway Motel in McAllen, TX, was built using this mortar. When it was torn down a few years ago we examined some of the mortar. It remained in excellent shape. The bond was sufficient to interfere with salvaging the brick.

Modern Application of Pozzolanic Mortar and Stucco Technology

Pozzolans can be introduced to mortars in several ways.

Cement-Lime Mortars

Pozzolans can be used in mortars under ASTM Specification for Mortar for Unit Masonry (C 270). This specification provides for cement-lime mortars to be made with several different cements, including ASTM C 595 Type 1P cement. This is a blended hydraulic cement that contains between 15% and 40% pozzolan and meets certain physical standards. We have been on a number of jobs where C 270 Type N and Type S cement-lime mortars were made with Type 1P cement. We are not familiar with any mortar or stucco jobs using Type 1P cement where a failure occurred due to a Class N or Class F pozzolan in the cement.

In recent years there have been discussions about allowing mortar fat to be used instead of hydrated lime to produce cement-lime mortars. This author is aware of failures that occurred when mortar fats were added to Type 1P cements, and failures that occurred when the pozzolan was added at the job site. Neither of these actions falls under ASTM C 270. One of the worst failures was on a stucco job in San Antonio, TX. A mortar fat was added to Type 1P cement. The job was painted with elastomeric paint (to cover the cracks) two days after the stucco was applied. Job-site samples revealed 160 psi (1.1 MPa) after seven days. The contractor maintained that he had mixed cement-lime stucco according to the instructions on the bottle.

Cements that are produced under ASTM Standard Performance Specification for Hydraulic Cement (C 1157) can also be used as the cement for cement-lime mortars. ASTM C 1157 does not limit the use of pozzolans but does provide that the generic names of the raw materials be listed in descending order.

Masonry Cement and Mortar Cement

Pozzolans can be incorporated into mortar by including the pozzolan in cement produced under ASTM Standard Specification for Masonry Cement (C 91), or with ASTM Standard Specification for Mortar Cement (C 1329). These standards do not in themselves limit the amount of pozzolan that can be used in their production.

Cement-Lime Stuccos

ASTM Standard Specification for Application of Portland Cement-Based Plaster (C 926) provides the same function for mixing stucco as C 270 provides for mixing mortar. Like ASTM C 270, ASTM C 926 allows the use of Type 1P blended hydraulic cement (as well as several other types) that falls under ASTM C 595.

Stucco Cement

Pozzolans can be incorporated into mortar by including the pozzolan in cement produced under ASTM Standard Specification for Plastic (Stucco) Cement (C 1328). This standard does not in itself limit the amount of pozzolan that can be used in the production of stucco cement.

Cheap Filler

The above methods are the legitimate ways in which pozzolans can be introduced into mortars and stuccos. Contractors regularly inquire about job site additions of pozzolans. We are aware of no standard or code that allows this. From the shortcuts that we have seen taken with job-site mixing, we would be averse to allowing such mixing.

In recent years, many groups have attempted to use fly ash in mortar and stucco. Most have approached the subject from a "cheap filler" point of view, and have obtained less than satisfactory results. We suspect, but have no proof, that a majority of these groups have not taken the time to understand what pozzolans can and cannot do. In reviewing mortar specifications across the country, we regularly note a caveat against the use of fly ash. Some ASTM meeting participants have suggested banning the use of fly ash in mortar. Fly ash can degrade mortars and stuccos if used in an inappropriate manner as evidenced by the text of a letter from Mr. William Hime.[2]

> "Recently, investigation of several large projects involving low-strength mortar or stucco have revealed that the proprietary cementitious component contained fly ash. Petrographic studies indicated that, due to minimal curing (as is common with masonry or stucco), the fly ash not only hadn't reacted pozzolanically, but also had delayed (effectively, prevented) proper hydration of the cement."
>
> "These investigations indicated that fly ash should not be employed in such a system, or if employed should be accompanied by a warning that extended wet curing should be used. If a proprietary system can be designed to be effective under such poor-cure conditions, it should be so stated."

When pozzolans are used as cheap fillers, the author agrees with Mr. Hime.

---

[2] Letter from William Hime with Wiss, Janney, Elstner Associates, Inc. to Herb Nordmeyer with ISG Resources, Inc., October 3, 2001.

To use pozzolans effectively and prevent curing problems, several steps must be taken that are commonly omitted.

Balanced Formulas —While a stoichiometrically-balanced formula is usually not possible if one wants to meet workability and other requirements, one should stay as close to a stoichiometrically-balanced formula as possible. As a result, most components of the mix become cementitious rather than some of them functioning as fillers. If high levels of fly ash are used, then a source of calcium ions must be present. The most common source of calcium ions is hydrated lime. If present in a stoichiometrical concentration the water retention will be high enough to prevent the premature dehydration of the mortar.

Careful Selection—The raw materials need to be carefully selected to assure that they are compatible. Use of ashes that have a continuing water demand should be avoided.

Meet Standards—The pozzolanic cement, be it a blended hydraulic cement, a masonry cement, a mortar cement, or a stucco cement, must be tested and meet all of the requirements of the standard, not just the strength requirements.

Advantages of Pozzolanic Mortars

The advantages of pozzolans in concrete are well known and are listed in many references. [10]

Following are a few of the many advantages of including pozzolans in mortars and stuccos:

Workability

Workability is one of the qualities that cannot be accurately measured in the lab with scientific instruments. Water retention measures some aspects of workability, but we do not have a test that can address the trowelability of a mortar. Many pozzolanic particles are relatively round. This is especially true of fly ash particles. As a result, they act like "ball bearings" in the mortar or stucco mix, and good workability can be obtained with a lower concentration of entrained air.

Table 1 lists the results of tests that were performed on a commercially available Type N pozzolanic mortar cement (PMC-N) and a commercially-available Type N cement-lime mortar cement (CLMC-N) by the University of Texas at Arlington.[3] Water retention results are virtually identical.

[3] Final Report, Masonry Mortar Investigation, from John H. Matthys with Construction Research Center, University of Texas at Arlington, to D. Herbert Nordmeyer, with Best Masonry & Tool Supply, San Antonio, TX, May 1997.

TABLE 1 —*Pozzolanic and Cement-Lime Mortar Cements*

Parameter	Pozzolanic Mortar Cement Type N psi (MPa)	Portland-Lime Mortar Cement Type N psi (MPa)
7-day Compressive Strength (C 1329)	823 (5.7)	1 758 (12.1)
Number	6	6
Standard deviation	13.7	88.6
28-day Compressive Strength (C 1329)	1 269 (8.8)	1 934 (13.3)
Number	6	6
V %	50.6	96.4
28-day Compressive Strength (C270)	1 005 (6.9)	1 818 (12.5)
Number	3	3
V %	45.8	05.4
Water Retention (C 270)	94.5%	93.5%
Entrained Air (C270)	4.9%	5.8%
Flexural Bond Strength, 28-day, 15 joints	78.1 (0.54)	78.0 (0.54)

Growth In Strength

It is well documented throughout the literature that pozzolanic cements continue to gain strength for an extended period of time. [11] Table 2 demonstrates that Type IP cement continues to gain strength long after Type I cement has essentially stopped gaining strength.

A rule of thumb is that the 7-day strength of a conventional mortar is 75% of the 28-day strength. Pozzolanic mortars that are made with Class N or Class F pozzolans do not gain strength as fast. The author reviewed quality control test results from two plants that produce Type N and Type S pozzolanic masonry cements. The results for the two plants are pooled. Based on 99 Type N samples, the 7-day strength was 57.7% (5.5% standard deviation) of the 28-day strength. Based on 184 Type S samples, the 7-day strength was 62.7% (4.7% standard deviation) of the 28-day strength.

TABLE 2—*Compressive Strength Gain Hydraulic Cements Type 1 and 1P.*

Type (as listed on bag)		1	1P
% Pozzolan		0%	35%
No. of samples is listed in brackets [ ]			
3-day Compressive Strength		3 750 (25.9) [10]	2 520 (17.4) [10]
7-day Compressive Strength		4 340 (29.9) [10]	3 450 (23.8) [10]
28-day Compressive Strength		5 620 (38.8) [10]	5 080 (35.0)[10]
90-day Compressive Strength		6 000 (41.4) [4]	6 840 (47.2) [5]
365-day Compressive Strength		6 020 (41.5) [2]	8 000 (55.2) [3]
		Percentage Strength Gain	
3 to 7 days	%	16.0%	37.0%
7 to 28 days	%	29.0%	47.0%
28 to 90 days	%	7.0%	35.0%
90 to 365 days	%	0.3%	17.0%

Table 3 presents the results of tests of several masonry cements. Pozzolanic masonry cements gain strength at a slower rate than conventional masonry cements, but they continue to gain strength.

ASTM C 1329 data in Table 1 demonstrates that the 7-day strength of the pozzolanic mortar cement was 65% of the 28-day strength. With the portland-lime mortar cement, the 7-day strength was 91% of the 28-day strength.

With well-designed pozzolanic mortars, we have found the 90-day strength was often 140–150% of the 28-day strength.

With the continued strength gain, care must be taken so that the ultimate strength is not excessive. The tendency of some specifiers to require a higher strength mortar than needed should be avoided. If a brick wall cracks, the mortar should be weak enough so the crack is in the mortar, not in the brick.

Water Resistance

By incorporating a particle size that complements the cement particle size, and by including a compound that will react in a cementitious manner with the lime that is

TABLE 3 — *Compressive Strength Gain Masonry Cements ASTM C 91.*

Sample Number	1	3	4	5
Type (as listed on bag)	N	S	N/S	S
% Pozzolan	63%	46%	0%	0%
	psi (MPa)	psi (MPa)	psi (MPa)	psi (MPa)
Each sample point is the average of three cubes.				
7-day Comp. Str.	800 (5.5)	1 710 (11.8)	2 940 (20.3)	2 200 (15.2)
28-day Comp. Str.	1 650 (11.4)	2 320 (16.0)	3 270 (22.6)	2 760 (19.0)
90-day Comp. Str.	2 360 (16.3)	3 490 (24.1)	3 530 (24.3)	3 030 (20.9)
365-day Comp. Str.	3 220 (22.2)	4 910 (33.9)		
	Percentage Strength Gain			
7 to 28 days	106%	36%	11%	25%
28 to 90 days	43%	50%	8%	10%
90 to 365 days	36%	40%		

liberated, the mortar made with pozzolanic technology is more resistant to the movement of water than conventional mortar. Table 4 illustrates the results of ASTM E 514 testing with high-pozzolan masonry cement mortar Type N (PMC-N), high pozzolan mortar cement mortar (PMorC-N), and a popular conventional Type N masonry cement (CMC-N) in Texas. Trinity Blend clay brick by ACME Brick Company were used for the tests. The test was run as a demonstration during a seminar. ASTM Standard Test Method for Water Penetration and Leakage Through Masonry (E 514) served as a guide but was not followed precisely. Modifications included (1) one rather than three panels for each type of cement, (2) rather than curing the walls for a minimum of 14 days, the walls were cured for 12 days, (3) rather than run the test for 4 hours, the test was run for 9 hours. A commercial bricklayer built the walls. His preferred masonry cement was the conventional masonry cement that was tested. He stated that he had never to his knowledge used a pozzolanic masonry cement or mortar cement before.

Autogenous Healing

Autogenous healing is well known in portland cement-lime mortars. [12] Since strength-gaining chemical reactions continue to occur with pozzolanic cements for an extended period of time, if a fracture occurs in the mortar, autogenous healing can occur. We cannot comment on the effectiveness of such healing in the field but the following indicates that it occurs under laboratory conditions.

TABLE 4 — *Water Penetration Tests.*

Parameter	Pozzolanic Masonry Cement Type N	Pozzolanic Mortar Cement Type N	Conventional Masonry Cement Type N
% Pozzolan	60%	50%	0
One panel per type of cement			
Units			
Test Area ft^2 (m^2)	12	12	12
Time of test (hours)	9	9	9
Time to first collection of water (minutes)	180	240	15
Water collected Gallons (liters)	0.12 (0.45)	0.07 (0.26)	19 (71.9)
Flow rate ml/hr per ft^2	4.2	2.4	665.7
Flow rate ml/hr per m^2	0.39	0.22	61.8

Several years ago we set a few high-pozzolanic masonry cement cubes aside that we had tested for compressive strength at 28 days, but had not smashed them to the point that they broke into pieces. After a period of time, we retested the cubes and observed that the strength had increased. We then expanded the test and over a year collected over 500 data points with different formulas, different times of initial test, and different times to final test.

Table 5 lists six high-pozzolan Type N masonry cement cubes that were tested at 28 days and then 70 days later. Samples were cured under C 270 conditions for 28 days. After the original test and until the retest occurred, the cubes were stored on a lab bench at room temperature and humidity. Each cube was made with the same formula and contained 65% pozzolan. Samples have been placed in descending order of the 28-day compressive strength. The retest compressive strength was close to the strength that we would have anticipated if the cubes had not been tested at twenty-eight days. Although not listed in Table 5, tests run with conventional masonry cement consistently showed a lower compressive strength on the retest.

Flexural Strength

By adding internal bracing between hydrated cement particles, the flexural strength increases. If a wall moves, there is less likelihood of the wall cracking. We ran tests in the mid-1990s using shop-fabricated equipment that did not meet ASTM standards. Since the tests were non-standard, the data is not reported here. Well-designed pozzolanic mortars showed higher flexural strength than cement-lime mortars.

Poorly-designed pozzolanic mortars showed worse flexural strength than masonry cements.

TABLE 5 – *Autogenous Healing of High-Pozzolan Mortars.*

Sample Number	Compressive Strength at 28 Days psi (MPa)	Compressive Strength at 98 Days psi (MPa)	Strength Gain (%)
1	950 (6.6)	1 530 (10.6)	161%
2	930 (6.4)	1 510 (10.40	162%
3	860 (5.9)	1 260 (8.7)	147%
4	850 (5.9)	1 180 (8.4)	139%
5	830 (5.7)	1 280 (8.8)	154%
6	790 (5.5)	1 310 (9.0)	166%
Std. Dev.	60.8	142.4	10.3%

Flexural Bond Strength

Flexural bond strength tests were run according to C 1329-96. That standard specifies that a Type N mortar cement must exceed 0.5 MPa (70 psi) flexural bond strength and a Type S mortar cement must exceed 0.7 MPa (100 psi). Our testing demonstrated that commercially available Type N pozzolanic mortar cement with more than 50% pozzolan comfortably passed. This testing was repeated by a third-party testing facility, and equal results were attained. We do not know of a commercially-available Type S pozzolanic mortar cement. A laboratory-formulated Type S mortar cement with over 40% pozzolan comfortably passed the 100-psi limit.

Reduced Efflorescence

Most masonry and stucco will effloresce under certain conditions. Virtually all experts agree that efflorescence is caused by a number of factors. After that, there is not a great deal of agreement among the experts. [13]

The need for flexural bond strength is usually associated with seismic areas or high-wind areas. We have found that good flexural bond strength and good workability, when combined with good workmanship, result in fewer hairline cracks at the mortar-brick interface. This results in less penetration of water into the wall. Less water penetrating the wall results in reduced efflorescence.

Permanent efflorescence (alkaline earth efflorescence) is usually caused by calcium hydroxide being carried to the surface and reacting with carbon dioxide from the atmosphere to form calcium carbonate. By reacting with the lime that is liberated when

the portland cement particles hydrate, pozzolans reduce the extent of calcium carbonate efflorescence.

Alkali efflorescence is usually caused by water carrying sodium and potassium salts in the building materials to the surface. To the extent that a pozzolanic mortar reduces the water entering a wall, it reduces the alkali efflorescence. The pozzolan does not tie up the sodium or potassium salts.

Acid Resistance

Over the last several years we have worked on a project that concerned acid resistance of concrete. One of our lab technicians placed pozzolanic mortar and conventional mortar samples in a 1.0-pH sulfuric acid bath to see what would happen. He found that the acid attacked the conventional mortar at a much higher rate than the pozzolanic mortar. Since then we have tested with other acids. We found that a well-balanced, well-cured pozzolanic masonry formula is much more acid resistant than conventional masonry-cement mortar or portland-lime mortar. Is this the answer to acid rain attacks on mortar? We don't know, but it would be worth studying.

Reduced Global Warming and Landfill Space

Separate and apart from producing a better mortar, with concerns about global warming, cement manufacturers in the US will sooner or later have to reduce their carbon dioxide emissions. Pozzolanic mortar technology will help. Besides reducing carbon dioxide emissions, use of pozzolanic mortars reduces the load on industrial landfills.

Section 6002 of the Resource Conservation and Recovery Act requires that, when federal funds are used, procurement agencies use products of the highest percentage of recovered materials as practical. [14]

What We Look For in An Ash

Just about any pozzolan can be used as cheap filler in a mortar or stucco. To produce a quality mortar or stucco, we found that the pozzolan must be carefully selected. ASTM Standard Test Method for Sampling & Testing Fly Ash or Natural Pozzolans for Use as a Mineral Admixture in Portland-Cement Concrete (C 311) includes a test for the strength activity index with portland cement. We have found that running this test using a 35% cement replacement gives a better indication as to the performance of the ash as a mortar than the conventional 20% replacement.

Mortar color cannot vary; therefore, we must have consistent ash color. We have found that color variations due to carbon in the ash are temporary variations. Even if we know they will take care of themselves in a year or so, the customer must not be asked to wait a year or so to obtain a consistent color.

We look for a low and consistent foam index. Because this test did not exist, we had to create it. Mortars need entrained air. If carbon or scoria is present in sufficient quantities to impact the air-entraining admixtures, then the cost of entraining air will increase. If the foam index is variable, then the mortar air content will be variable. Even

if the mortar air content is within specifications, a variable air content reduces the mason's productivity.

We look for a very low free-calcium-oxide content. Free calcium oxide leads to low water retention and premature stiffening of the mortar. Additionally, it may lead to the burning of the hands of the masons.

We look for consistent quality. An ash source must be characterized for consistency, and then the formulas are developed for the worst conditions. With greater variability of the ash, less ash can be used and more problems will develop.

Putting It Together

We have found that the laboratory personnel must be able to lay brick and to stucco so they understand the craft. If they cannot, they do not have a feel for mortar and stucco on a trowel. The ability of the lab personnel to lay brick and to stucco allows the lab personnel to be able to talk to the tradesmen who test the products. It allows the two groups to speak the same language.

Tradesmen must be a part of the development team. They must be able to describe a mortar or a stucco in terms such as "I love it." If they cannot, then a viable product does not exist.

Conclusions

With the revival of discussions of global warming and the Kyoto Protocol, we will see greater use of fly ash in mortars and stuccos.

Pozzolans, including fly ash, can be used to develop masonry cement, mortar cement, stucco cement, and blended-hydraulic cement that makes excellent mortar and stucco. Failure to understand how pozzolans work, as with failure to understand how any component works, can lead to failures.

References

[1] Richard Helmuth, *Fly Ash in Cement and Concrete,* 203 pp., Portland Cement Association, 1987.

[2] F. M. Lea, *The Chemistry of Cement and Concrete*, Chemical Publishing Company, Inc., 3rd edition, 1971, pp. 1-10.

[3] Rochelle C. Jaffe, "Understanding Mortar," *Masonry Construction*, Vol. 14, No. 2, (February 2001), pp. 20–26.

[4] F. M. Lea, *The Chemistry of Cement and Concrete*, Chemical Publishing Company, Inc., 3rd edition, 1971, pp. 531–532.

[5] Margaret Thompson, "Can Lime be Replaced? Saying It Replaces Lime Doesn't Make it Lime," *Masonry Construction*, Vol. 13, No. 3, (March 2000), pp. 29–32.

[6] Charles D. Meadowcroft, "Can Lime be Replaced? Lime Alternates Are Not And Do Not Want To Be Lime!" *Masonry Construction*, Vol. 13, No. 3, (March 2000), pp. 29–33.

[7] David Moore, *The Roman Pantheon, The Triumph of Concrete,* University of Guam Station, 1995, pp. 91–92.

[8] David Moore, *The Roman Pantheon, The Triumph of Concrete,* University of Guam Station, 1995, pp. 14–47.

[9] John P. Speweik, *The History of Masonry Mortar in America 1720-1995.* GemLime Group, L. P., (undated).

[10] Craig J. Cain, "Mineral Admixtures," *Significance of Tests and Properties of Concrete and Concrete-Making Materials*, Paul Klieger and Joseph F. Lamond, editors, ASTM STP 169C, ASTM International, West Conshohocken, PA, 1994, pp. 500–508.

[11] F. M. Lea, *The Chemistry of Cement and Concrete*, Chemical Publishing Company, Inc., 3rd edition, 1971, pp. 435–439.

[12] Robert S. Boynton and Kenneth A. Gutschick, *Durability of Mortar and Masonry*, *Masonry Mortar Technical Notes # 1*, 6 pp., National Lime Association, 1964.

[13] Robert S. Boynton and Kenneth A. Gutschick, *Efflorescence of Masonry*, *Masonry Mortar Technical Notes # 4*, 8 pp., National Lime Association, 1966.

[14] Richard Helmuth, *Fly Ash in Cement and Concrete,* 203 pp., Portland Cement Association, 1987, pp. 5–6.

Scott Berman,[1] Debera F. Drage,[2] and Michael J. Tate[3]

The Effect of Acid Rain on Magnesium Hydroxide Contained in Cement-Lime Mortar

Reference: Berman, S., Drage, D. F., and Tate, M. J., "**The Effect of Acid Rain on Magnesium Hydroxide Contained in Cement-Lime Mortar,**" *Masonry: Opportunities for the 21st Century, ASTM STP 1432,* D. Throop and R.E. Klingner, Eds., ASTM International, West Conshohocken, PA, 2003.

Abstract: The effect of acid rain on mortar durability is not well understood. In particular, little work has been done on the reaction of magnesium hydroxide in dolomitic Type S hydrated lime with sulfuric acid compounds. In this study, this reaction is investigated using two different exposure situations, each involving distilled water and sulfuric acid (4.5 pH) as leachants. In the first situation, the leachability of the Type S hydrated lime is examined through packed-bed column testing. In the second situation, hardened mortar samples were placed in both distilled water and sulfuric acid (4.5 pH) solution for one week. Inductively Coupled Plasma-Atomic Emission Spectroscopy (ICP) was used to determine the magnesium content of the raw materials, hardened mortars and leachate. Magnesium levels of the leachate samples were consistently low and did not appear to be affected significantly by the presence of sulfuric acid.

Keywords: magnesium hydroxide, sulfuric acid, durability, mortar, Type S hydrated lime, efflorescence, solubility, dolomitic, acid rain, masonry

Introduction

Hardened mortar is exposed to a wide range of environmental conditions that influence its durability. Important qualities of mortar include the ability to withstand freeze-thaw cycles, to undergo autogenous healing, to resist water penetration and minimize efflorescence. This paper focuses on the effect that acid rain (specifically sulfuric acid) may have on the magnesium hydroxide component of dolomitic hydrated lime.

[1] Quality Assurance Manager, Graymont Inc., 670 E. 3900 South #200, Salt Lake City, UT 84107.
[2] Senior Laboratory Technician, Graymont Inc., 670 E. 3900 South #200, Salt Lake City, UT 84107.
[3] Building Lime Sales Manager, Graymont Dolime (OH) Inc., 21880 West State Route 163, Genoa, OH 43430-0158.

Dolomitic Type S hydrated lime is commonly used in cement-lime mortar applications throughout the United States and Canada, and has demonstrated durability under a broad range of environmental conditions. Dolomitic hydrated lime is manufactured by burning dolomitic limestone containing 35 to 46 % magnesium carbonate to produce quicklime. Water is then added to quicklime at high pressure to produce Type S hydrated lime [1], whose chemistry is defined in the Standard Specification for Hydrated Lime for Masonry Purposes (ASTM C 207). As shown in Table 1, Type S hydrated lime must consist primarily of calcium and magnesium hydroxides.

Table 1 - *ASTM C 207 requirements.*

Parameter	Type S Hydrated Lime
Calcium & Magnesium Oxides (nonvolatile basis), min., %	95
Carbon Dioxide (as-received basis), max., %	
• If sample is taken at place of manufacture.	5
• If sample is taken at any other place	7
Unhydrated Oxides (as-received basis), max., %.	8

As seen in Table 2 [2] the solubility of magnesium hydroxide in water is extremely low. Both calcium and magnesium carbonate, the main components of dolomitic limestone, are more soluble than magnesium hydroxide [3]. Magnesium hydroxide, however, can react with sulfuric acid to produce magnesium sulfate compounds that are much more soluble in water (Table 2). Since sulfuric acid is a potential component of acid rain, this creates concern that mortars containing magnesium hydroxide could effloresce and have poor durability.

Table 2 – *Magnesium compound solubility.*

Chemical Compound	Cold (0 C) (g/100 cc)	Hot (100 C) (g/100 cc)
Magnesium Carbonate	0.0106	
Magnesium Hydroxide	0.0009[18]	0.0040
Magnesium Oxide	0.00062	0.0086[30]
Magnesium Sulfate	26.000	73.80000
Magnesium Sulfate Heptahydrate	71.000[20]	91.000[40]
Magnesium Sulfate Monohydrate		68.400

Though the efflorescence of soluble salts in mortars has been examined extensively, there has been little examination of the effect of sulfuric acid on magnesium hydroxide contained in mortars. This study examines the interaction of these two materials using leachate tests on dolomitic Type S hydrated lime in packed-column testing, and also leachate testing of hardened Type S and N mortars soaked in a water bath.

Materials

Portland Cement

The cement used met the requirements of the Standard Specification for Portland Cement Type I (ASTM C 150) and was locally obtained in bag form.

Mason's Lime

The dolomitic hydrated lime used met the requirements of ASTM C 207 Type S and was obtained from the manufacturer.

Sand

A standard sand consisting of equal parts by weight of standard graded Ottawa sand and standard 20-30 Ottawa sand was used in conformance to the requirements of the Standard Test Methods for Physical Testing of Quicklime, Hydrated Lime, and Limestone standard (ASTM C 110 13.2.4).

Deionized Water

High-purity (Class 1) deionized water was used throughout this work. This water was produced with a high capacity, multi-bed, ion exchange system (Water Specialties, Inc., Sandy, UT). The system includes multi-step ultra filtration down to 0.1μm with ultraviolet sterilization.

Acidic Water

High-purity deionized water and ultrapure sulfuric acid were used to make the solutions used in the leaching columns. Sulfuric acid was added to produce a solution with a pH of 4.5, typical of acid rain in much of the United States [4].

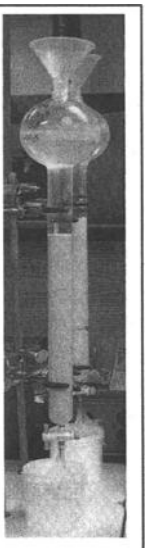

Figure 1 - *Leach Column Apparatus*

Experimental Procedures

Column Tests

The leaching columns used in this work were Kontes chromaflex columns (# SZ 252), 28 mm in diameter and 400 mm long, with a 500 mL reservoir and an overall length of 625 mm (Figure 1). Three leaching columns were used for each leachant. A piece of glass wool was stuffed into the bottom end (end with stopcock) of each column to keep material from flowing out of the column. Samples of the Type S hydrated lime (130 grams) were placed in each leaching column, and were tightly packed into the columns using a vibrating table. This was done to help eliminate air pockets from forming in the materials as the leaching liquid permeated through the column. Collection containers were placed below each column to collect the leachate, and were covered with parafilm to help stop evaporation of the collected leachate. The stopcocks of the leaching columns were placed through the parafilm

so that the collected leachate would drip directly into the covered containers. These materials were leached for 5 days using approximately 225 mL of either deionized water or acidic water (deionized water adjusted to a pH of 4.5 with sulfuric acid). The resulting leachate was then analyzed for magnesium by Inductively Coupled Plasma-Atomic Emission Spectroscopy (ICP).

Puck Tests

Two different mortar mix designs (Type N and Type S) were used to make the pucks. In both cases, the mortar was mixed to the proportion specification of the Standard Specification for Mortar for Unit Masonry (ASTM C 270). The mortar pucks were prepared in accordance with procedures in ASTM C 110–00 Section 10, with the proportions shown in Table 3. Water was added to the blended mortar to achieve a flow of 110 + 5%, using the methods of the Standard Test Method for Flow of Hydraulic

Table 3 – *Puck test mix designs.*

ID Code	Mortar Type	Portland Cement	Type S Hydrated Lime	Standard Sand	Water
A	Type N	94 g	40 g	480 g	100 mL
B	Type S	94 g	20 g	360 g	72 mL

Cement Mortar (ASTM C 1437–99). Once material of the correct consistency or flow was obtained, the mortar was placed into ring molds approximately 100 mm in diameter. The ring molds were filled to a height of 9.5 mm (3/8 in.), the thickness of a typical mortar joint. The pucks were allowed to partially set up before removing the rings, because otherwise the pucks would not have maintained their shape. The pucks were allowed to cure at room temperature for a few days prior to analysis. Each puck was oven dried at 110° C for 24 hours. The pucks were cooled in a desiccator and then weighed. These weights were recorded so that they could be compared to the final weight of the pucks after leaching. The pucks were then placed into a 600 mL beaker to which 0.5 L of leaching solution was added. A piece of parafilm was placed over the top of each beaker to limit evaporation of the leaching solutions. After 5 days the pucks were removed from the solutions and dried for 24 hours at 110° C. The weights were compared to the initial weights. The leaching solutions were then analyzed by Inductively Coupled Plasma-Atomic Emission Spectroscopy (ICP) for magnesium.

Dried pucks composed of each type of mortar before and after leaching were crushed in a jaw crusher to minus 6.4 mm (1/4 in.). This material was then finely ground using a disk pulverizer. The resulting material was 100% minus 250μm (60 mesh). These samples, along with representative splits of the materials used to produce the pucks, were then digested with lithium tetraborate in accordance with the Standard Test Method for Major and Trace Elements in Limestone and Lime by ICP and Atomic Absorption (AA) (ASTM C 1301–95).

To analyze the pucks the ICP was calibrated with the following Certified Reference Materials (CRM): DH 3506 (MgO 0.43%), DH 0902 (MgO 20.52%), NIST 88b (MgO 21.03%), IRSID 701-1 (MgO 0.6%) and IPT 44 (MgO 2.93%). Figures 2 and 3 show the

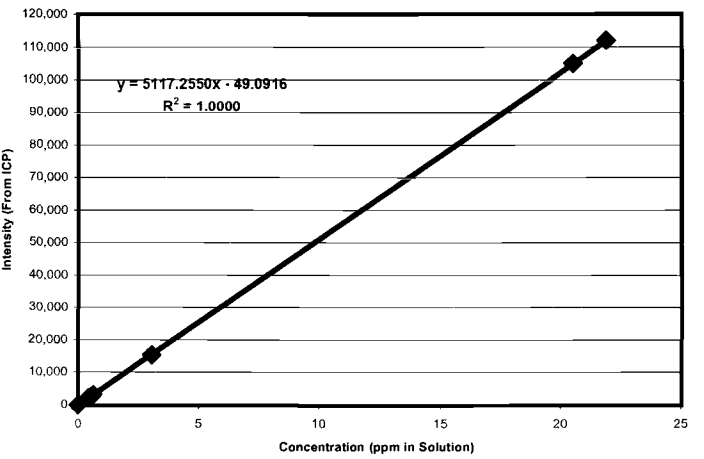

Figure 2 - *Magnesium (Mg 279 079 nm) - calibration curve, intensity vs.* Certified Reference Standards - Used to Calibrate ICP for Solid Materials

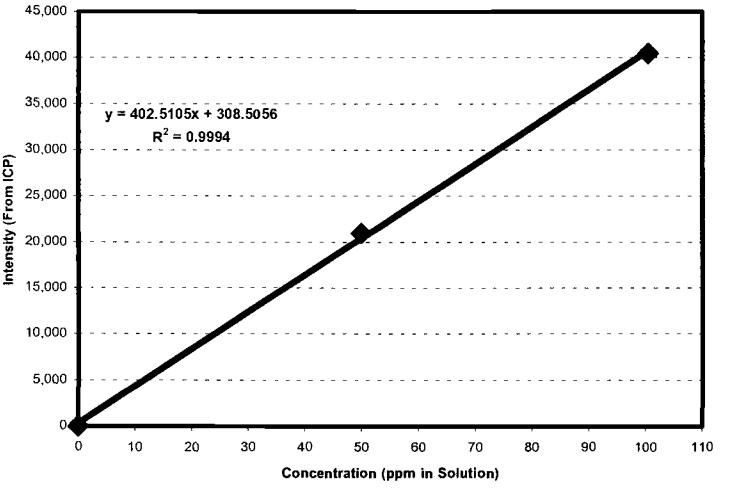

Figure 3 - *Magnesium (Mg 279.079 nm) - Calibration Curve, Intensity vs. Concentration* Liquid Standards - Used to Calibrate ICP For Leachate Solutions

calibration curves for the solid materials and leachate respectively. These CRMs cover a broad range of magnesium concentrations. The linearity and large operating range of an ICP make it possible to analyze samples with concentrations from fewer than one part per million (ppm) to more than one part per hundred (six orders of magnitude).

Analytical Procedure

The instrument used to perform the elemental analysis was a Perkin Elmer Optima 3000 ICP. Instrument operating parameters are listed in Table 4. The sample introduction system consists of a cyclonic spray chamber and a Meinhard Type A nebulizer. The instrument was optimized for magnesium (Mg – elemental analite) and cobalt (Co – internal standard). Cobalt is used as an internal standard to compensate for minor changes in barometric pressure, temperature, pH of analite solutions and/or surface tension differences of analite solutions.

Table 4 - *Instrument operating parameters.*

Instrument	Perkin Elmer Optima 3000
Plasma	All Argon
Forward Power	1150 W
Reflected Power	<5 W
Coolant Gas Flow	15.0 L/min
Auxiliary Gas Flow	0.5 L/min
Nebuliser Gas Flow	0.85 L/min
Peristalic Pump	Perkin Elmer
Uptake Route	About 0.7 mL/min
Nebuliser	Concentric Type A
Spray Chamber	Cyclonic
Scanned Region	167-782 nm
Internal Standard	Co 10 ppm

Reagent-grade cobalt chloride was used to prepare the internal standard solution of cobalt. This material was put into solution with high-purity deionized water to yield a final concentration of 4000 ppm (mg mL^{-1}). This solution was then added to each of the sample solutions, as well as the calibration standards (solutions) to yield a final concentration of 10 ppm cobalt in solution.

The magnesium calibration solutions were made from a single-element 10000 ppm ICP standard supplied by Inorganic Ventures (Lakewood, NJ). This solution was diluted with the appropriate amount of high-purity deionized water to produce a series of calibration solutions ranging from 0 ppm to 100 ppm.

The solid samples were fluxed with high-purity lithium tetraborate, and the resulting fusing beads were dissolved (put into solution) using ultra-pure hydrochloric (36%) and nitric (70%) acids.

Results

Column Tests

Table 5 - *Leachate Column Test Results.*

Leachant	Sample MgO Content (ppm)			Average MgO (ppm)
	1	2	3	
Deionized Water	0.03	0.07	0.04	0.05
Acidic Water	0.03	0.02	0.01	0.02

The magnesium oxide content of leachate created by exposing a packed bed of Type S hydrated lime to deionized water and a simulated acid rain solution is given in Table 5.

This table shows that the magnesium oxide (MgO) content of the leachate created with the acidic water was slightly lower than the values obtained with deionized water. This indicates that the dolomitic Type S hydrated lime was essentially unaffected by a sulfuric acid solution with a pH of 4.5. In all cases, the levels of magnesium oxide found in the leachate were extremely low.

Puck Tests

Table 6 - *Mortar puck magnesium concentrations.*

Puck Type	Sample MgO (%)			Average Sample MgO (%)
	1	2	3	
Type N Mortar				
- Unsoaked	1.64	1.69	1.51	1.61
- Deionized Water	1.92	1.89	1.90	1.90
- Acidic Water	1.47	1.36	1.57	1.47
Type S Mortar				
- Unsoaked	1.56	1.29	1.27	1.37
- Deionized Water	1.64	1.30	1.49	1.48
- Acidic Water	1.25	1.57	1.23	1.35

The magnesium content of Type N and S mortar pucks before and after soaking is given in Table 6. Tables 7a and 7b display the change in weight of Type N and S mortar pucks after soaking in both deionized and acidic water.

Magnesium oxide concentrations of the raw materials were

Silica sand	0.01%
Portland Cement	3.00%
Type S Hydrate	30.49%

Table 7a - *Type N mortar puck weight.*

Puck Type	Sample Weight (g)			Average Sample Weight
	1	2	3	
Deionized Water				
- Weight Before	78.24	89.60	87.17	85.00
- Weight After	78.84	90.34	87.59	85.59
- Difference	-0.60	-0.74	-0.42	-0.59
Acidic Water				
- Weight Before	87.61	84.06	85.36	85.67
- Weight After	88.25	84.69	85.73	86.22
- Difference	-0.64	-0.63	-0.37	-0.55

Magnesium oxide levels measured for the pucks were, in general, slightly lower than their theoretical concentration in the Type N and Type S mortar patties of 2.45% and 1.88% respectively. Type N mortar patties show more magnesium than Type S patties because the former have higher levels of dolomitic Type S hydrated lime.

Weights of the mortar pucks increased

slightly under exposure to deionized water, and also to acidic water. In the case of the Type S mortar, exposure to acidic water resulted in a slightly larger gain. For the deionized water samples, the gain in weight was attributed to further hydration of the cement in the mortar mix. For the acidic water samples, the gain could be attributed to both cement hydration and to the formation of sulfate compounds. In both the Type N and Type S mortar samples there did not appear to be any significant degradation of the mortar due to exposure to sulfuric acid.

Table 7b - *Type S mortar puck weight.*

Puck Type	Sample Weight (g) 1	2	3	Average Sample Weight
Deionized Water				
- Weight Before	93.47	87.51	108.64	85.00
- Weight After	94.51	88.42	109.88	85.59
- Difference	-1.04	-0.91	-1.23	-0.59
Acidic Water				
- Weight Before	93.47	87.51	108.64	96.54
- Weight After	94.51	88.42	109.88	97.60
- Difference	-1.04	-0.91	-1.23	-1.06

Despite the increase in sample weight, the percentage of magnesium in the mortar increased slightly when the mortar was soaked in deionized water. The reason for this increase is unclear. The differences, however, were small.

Magnesium oxide concentration of the leachate created by soaking the mortar pucks is shown in Table 8a and 8b. Results for Type S mortar indicate slightly higher magnesium oxide concentrations when the pucks were soaked in the sulfuric acid solution. The difference, however, was small. Despite containing more lime, the Type N mortar samples showed no significant leaching of magnesium oxide. Use of acidic water had no apparent effect. In all cases, the amount of magnesium oxide in the leachate was extremely low.

Table 8a - *Puck leachate magnesium concentration Type S mortar.*

Leaching Medium	Puck Leachate MgO (ppm) A1	A2	A3	Avg. MgO (ppm)
Deionized Water	0.00	0.01	0.02	0.01
Acidic Water	0.04	0.01	0.00	0.03

Table 8b - *Puck leachate magnesium concentration Type N mortar.*

Leaching Medium	Puck Leachate MgO (ppm) B1	B2	B3	Avg. MgO (ppm)
Deionized Water	0.00	0.00	0.01	0.00
Acidic Water	0.00	0.00	0.00	0.00

Discussion

This study indicates that exposure to acidic water (pH of 4.5) does not cause a significant release of magnesium compounds from Type S hydrated lime or from Type S and N hardened cement-lime mortar.

These results are not surprising, because they are consistent with efflorescence research and field experience that indicates that magnesium compounds are not primary contributors to the efflorescence of mortar. A study of the source of efflorescence in Southern California indicated that the main sources of efflorescence are alkalis of sodium

sulfate (Na_2SO_4) and potassium sulfate (K_2SO_4) [5]. Ritchie also determined in laboratory experiments that Na_2SO_4 and K_2SO_4 were the main components of efflorescence seen in piers made with cement-lime mortar [6]. Lime, and particularly dolomitic lime, typically has extremely low levels of sodium and potassium sulfates [7].

Magnesium hydroxide has been shown to react with sulfuric acid in water-treatment applications. In those applications, dolomitic hydrates are added as dilute slurry. The packed-bed and hardened-mortar tests conducted in this study are different from those applications, in two key ways. First, calcium-based alkalis have been shown to be more reactive than magnesium-based alkalis in dolomitic hydrated lime. Hardened mortar has a larger concentration of calcium-based alkalis than does a dilute slurry. Second, the pH of the solution is important. Water-neutralization processes can treat process water with a pH of 3 or less. This test used a weakly acid solution simulating acid rain. The higher pH of this solution likely resulted in lower reactivity with the alkalis contained in the lime. Given the presence of calcium-based alkali and a weak acid, a potential explanation for the low levels of magnesium seen in the leachate samples is the poor reactivity and solubility of magnesium hydroxide.

The processing of hydrated lime begins with the disassociation of carbon dioxide from calcium and magnesium carbonates at high temperatures. Magnesium carbonate disassociates at a much lower temperature (402-480°C) than calcium carbonate (898°C) [8]. The result from this disassociation is a combination of calcium and magnesium oxides (quicklime). In processing dolomitic limestone, high kiln temperatures are necessary to disassociate completely the calcium carbonate portion of the stone. This results in the magnesium portion becoming "hard burnt," which lowers its reactivity.

The exothermic reactivity of dolomitic quicklime with water is well defined. Reported heats of hydration and reaction for calcium hydroxide ($Ca(OH)_2$) and magnesium hydroxide ($Mg(OH)_2$) are 15300 cal/g mole and 8000 to 10000 cal/g mole respectively [8]. Slaking-rate tests indicate that dolomitic quicklime samples typically reach a lower maximum temperature at a slower rate than quicklime samples containing over 95% calcium oxide (CaO). Calcium oxide hydrates readily at atmospheric pressure. Magnesium oxide, in contrast, requires high pressure or long periods of soaking in water to hydrate completely.

Both calcium hydroxide and magnesium hydroxide have low solubility in water. Calcium hydroxide, however, is much more soluble (0.077 to 0.185 g/100 cc) than magnesium hydroxide (0.0009 to 0.004 g/100 cc) [2]. The greater solubility of calcium hydroxide enhances its ability to react with the acid hydrogen ion (H^+) to form a water molecule and a calcium salt such as calcium sulfate ($CaSO_4$).

Boynton indicates that lime's effectiveness as an alkali depends on the rate at which it goes into solution or becomes available, and on its solubility [10]. In weakly acidic solutions, this becomes more critical. The rate of solution of dolomitic hydrate tends to decrease as the pH of the acid increases due to the magnesium oxide component [10]. The solubility of the resulting salts is also important. Calcium sulfate has poor solubility (0.16-0.30 g/100cc) [2]. Insoluble salts can form on the outside of hydrate particles, further limiting the reactivity of the hydrated lime.

Preferential reactivity of calcium hydroxide over magnesium hydroxide is seen in other applications as well. Perhaps the most directly applicable comparison comes from research on flue-gas desulfurization. Sorbent (dry) injection studies show that dolomitic hydrated lime can perform well in these applications due to its high specific surface. In this reaction, sulfur dioxide reacts preferentially with the calcium hydroxide contained in dolomitic hydrated lime[11].

Conclusions

1. Magnesium compounds in mortar have low solubility when exposed to both deionized water and a simulated acid rain solution with a pH of 4.5.
2. The reaction of sulfuric acid (pH of 4.5) with Type S hydrated lime does not significantly increase the solubility of magnesium compounds in the lime.
3. The reaction of sulfuric acid (pH of 4.5) with Type S and Type N cement-lime mortars does not significantly increase the solubility of magnesium compounds in the mortar.

References

[1] What is Lime?, URL: http://graymont-oh.com/whtslime/whtslime.html, Graymont Dolime (OH) Inc., Genoa, OH, November 1, 2001.
[2] Weast, R.C., *CRC Handbook of Chemistry and Physics*, CRC PRESS, Inc., Boca Raton, FL, 1979, pp. B-51-B-144.
[3] Boynton, R.S., *Chemistry and Technology of Lime and Limestone*, Second Edition, John Wiley & Sons, Inc., 1980, p. 207.
[4] Acid Rain, URL:www.epa.gov/airmarkets/acidrain/, U.S. Environmental Protection Agency (EPA), Washington, DC, June 26, 2001.
[5] Bolme, B.W. and L.P. Berriman, "Investigation of the Source of Efflorescence of Brick Masonry," Stanford Research Institute, Clay Products Promotional Fund, 1960.
[6] Ritchie, T., "Efflorescence Produced on Ceramic Wicks by Masonry Mortars," The Journal of the American Ceramic Society, Vol. 38, No. 10, October, 1955.
[7] Boynton, R.S. and Gutschick, K.A., "Efflorescence of Masonry," Masonry Mortar Technical Notes #4, National Lime Association, 1966
[8] Boynton, R.S., *Chemistry and Technology of Lime and Limestone*, Second Edition, John Wiley & Sons, Inc., 1980, pp. 160-161.
[9] *International Critical Tables*, National Academy of Sciences – National Research Council, Volume V, McGraw-Hill, 1929, pp. 195-196.
[10] Boynton, R.S., *Chemistry and Technology of Lime and Limestone*, Second Edition, John Wiley & Sons, Inc., 1980, pp. 213-216.
[11] Dahlin, R.S., Beittel, R., and Gooch, J.P., *Pilot-Scale Evaluation of LIMB Technology*, United States Environmental Protection Agency Project Summary, EPA/600/S7-87/019, September 1987.

Richard J. Godbey[1] and Margaret L. Thomson[2]

Emley Plasticity Testing: First Steps to a Precision and Bias Statement

REFERENCE: Godbey, R. J. and Thompson, M. L., **"Emley Plasticity Testing: First Steps to a Precision and Bias Statement,"** *Masonry: Opportunities for the 21st Century, ASTM STP 1432*, D. Throop and R. E. Klingner, Eds., ASTM International, West Conshohocken, PA, 2002.

Abstract: Plasticity is an important physical property of masonry mortar and stucco (plaster). Quality workmanship and economic use of materials by masons and plasterers requires highly plastic mortar and stucco. Hydrated lime enhances the plasticity of masonry mortar and stucco by providing excellent water retention and workability.

In 1919, after nearly 10 years of work, chemist Warren Emley developed a method to quantify plasticity. In essence, plasticity testing as developed by Emley quantifies the quality of lime in terms of water retention and workability. Nearly 100 years later, the measurement of plasticity continues to be definitive in ASTM Specification for Finishing Hydrated Lime (C206) and ASTM Specification for Hydrated Lime for Masonry Purposes (C207) utilizing procedures and apparatus outlined in ASTM Test Methods for Physical Testing of Quicklime, Hydrated Lime, and Limestone (C110). This paper reviews the history of the plasticity test method, laboratory methods, instrument nuances, and the need to establish ASTM precision and bias statements for the test method.

Keywords: Plasticity of Hydrated Lime, Emley Plasticity, Masonry Mortar, Plaster, Stucco, Finishing Hydrated Lime, Precision and Bias.

[1] B.Sc., Project Manager, National Building Construction, Chemical Lime Company, 8000 W. Lake Mead Dr., Henderson, NV 89015.

[2] Ph.D., Technical Manager, National Building Construction, Chemical Lime Company8000 W. Lake Mead Dr., Henderson, NV 89015.

Background and Introduction:

Nearly a century ago, Warren E. Emley, a chemist with the National Bureau of Standards, published a technical paper titled *Measurement of Plasticity of Mortars and Plasters* [1]. Emley introduces his paper by stating, "If one plaster is more plastic than another, it means that the plasterer can cover more square yards in a given time...which, of course, will reduce the cost...Furthermore, the more plastic material entails less physical and mental fatigue on the part of the plasterer, and he is thereby led unwittingly to produce a better quality of work...For these reasons, the measurement of plasticity is not a question of academic interest only, but is of real practical importance to everyone who uses or pays for any mortar or plaster." Mortars and plasters with good plasticity can help control the costs of construction projects through ease of use and subsequently, improved quality.

Trades workers use terms such as "buttery", "workable" and "fat" to describe mortars and plasters with inherently good plasticity. Conversely, terms such as "sticky", "rubbery" and "harsh" are used to describe mortars and plasters with less than ideal plasticity. Emley showed that masonry mortar and plaster made from cement, lime and sand is more plastic than mortar and plaster made from cement and sand alone. Without the addition of lime, the masonry mix design is too harsh and too quick drying. Lime improves the plastic property of a mix design by increasing water retention and workability.

In the beginning, Emley worked to define the property of mortar and plaster plasticity so that comparisons of plasticity could be determined. By focusing on the particular use of mortar and plaster, he derived a definition set forth in two parts: 1) "That material is the more plastic which has the greater ability to retain its water against the suction of the surface to which it is applied", and 2) "That material is the more plastic which requires the less work to spread it." His definition clearly had the trades in mind because he restated his definition to mean: "A plastic material is one which works freely and easily under the trowel and has marked ability to hold its water." With these simple concepts in mind, Emley began the search for a quantitative measure of plasticity.

Starting in 1909, Emley would explore six different plasticity principles: 1) Colloidal content, 2) Viscosity, 3) Compressive strength, 4) Range of plasticity, 5) Rate of drying, and 6) the Carson blotter test. Studying and testing these principles required the design and construction of 20 different instruments. Finally, after 10 years of work, a method and test instrument was developed to adequately test plasticity. Emley's plasticimeter measures plasticity of mortar and plaster by mimicking the work required of a mason or plasterer against the suction of a building surface (e.g. brick, concrete block, or stucco scratch and brown coats). The instrument is equally successful in measuring the inherent plasticity of lime putty and Emley did extensive work with the instrument to characterize and classify lime putty made from hydrated lime.

The Emley Plasticimeter used today in the characterization of lime is the direct descendent of Emley's 1919 instrument (Figure 1). The modern version of Emley's plasticimeter is used to specify lime plasticity as required in ASTM Specification for Finishing Hydrated Lime (C206) and ASTM Specification for Hydrated Lime for

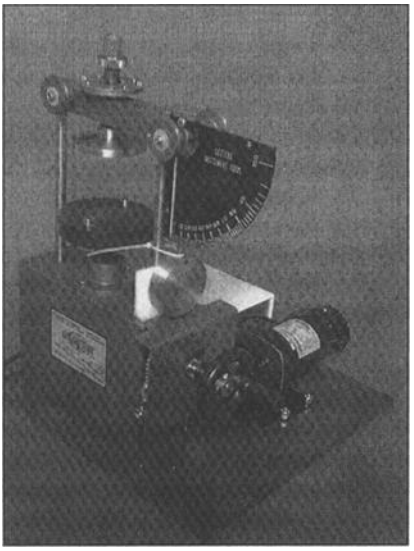

Figure 1: The Modern Emley Plasticimeter[3].

Masonry Purposes (C207). Mandatory plasticity instrument constants, consistency of lime putty made from hydrated lime, base plate specifications and plasticity determination are outlined in ASTM Test Methods for Physical Testing of Quicklime, Hydrated Lime and Limestone (C110).

In introductory terms, the modern test using the Emley Plasticimeter measures over time the degree of stiffening of lime putty made from hydrated lime mixed with water to a standard consistency (viscosity). The test instrument measures increasing force as the stiffening putty is slowly rotated and upwardly squeezed against a disk attached through pulleys to a weighted needle-like arm superimposed over a calibrated scale. At the end of the test, the degree of stiffening is assigned a unitless plasticity figure as determined by a calculation specified in C110. This calculation has two terms that relate directly back to Emley's two-part definition of plasticity: water retention and workability. Water retention is related to the total elapsed time of the test. Workability is related to the force recorded by the scale reading. C-206 and C207 require lime putty mixed from designated hydrated lime to have a minimum plasticity figure of 200. C206 and C207 do not place an upper limit on the plasticity of lime putty mixed from designated hydrated lime.

In summary, we think masons and plasterers will agree with Emley; the advantage of water retention and workability (plasticity) in mortars and stuccos is that the worker can lay more brick or cover more wall area in a given time with less physical and mental effort. Mortar and stucco products that are easier to use result in higher quality workmanship.

[3] Photo courtesy of Geotest Instruments Corp., Evanston, IL. Geotest is currently the only known manufacturer of Emley Plasticimeters.

Hydrated Lime Plasticity Specifications:

Two types of hydrated lime are designated in C206: 1) Type N—Normal hydrated lime for finishing purposes and 2) Type S—Special Hydrated lime for finishing purposes. Both these hydrates are suitable for use in scratch, brown, and finish coats of plaster, for stucco, for mortar, and as an addition to portland-cement concrete. Both hydrates must meet minimum plasticity requirements. C206 lime putty made from Type N hydrated lime must be soaked in water prior to plasticity testing for a period of 16 to 24 hours. C206 Type S hydrated lime putty made from hydrate is not soaked prior to plasticity testing and plasticity testing must begin within 30 minutes after mixing the dry hydrate with water. It should be noted that a hydrated lime designated as C206 can be used in all applications of masonry mortar requiring a C207 hydrated lime except where the properties of an air-entrainment hydrated lime are desired or required. Masonry mortar that would benefit from air-entrained hydrated lime must meet the Type SA or NA designation found in C207. Air-entraining lime should not be used as a finishing lime.

Four types of hydrated lime are designated in C207: 1) Type N-Normal Hydrated lime for masonry purposes, 2) Type NA-Normal air-entraining lime for masonry purposes, 3) Type S-Special hydrated lime for masonry purposes and 4) Type SA-Special air-entraining lime for masonry purposes. C207 Types S and N are suitable for use in mortar, in scratch and brown (but not finish) coats of cement plaster, for stucco, and for addition to portland-cement concrete. C207 Types SA and NA are air-entrained products suitable for use as above where air-entrainment properties are desired. C207 Type S and SA hydrated lime is differentiated from C207 Type N and NA hydrated lime by the ability to develop high and early plasticity and higher water retention. C207 Type N hydrate does not have a specification for plasticity, but C207 Type S and SA must earn the distinction of being special by meeting minimum plasticity requirements. Because Type S and SA lime must develop immediate plasticity upon mixing with water, C207 lime putty made from Type S and SA hydrated lime is not soaked in water prior to testing. Plasticity testing of Type S and SA hydrated lime must commence within 30 minutes after mixing the dry hydrate with water.

Instrument Constants:

Emley developed a sophisticated tool to measure and quantify the plasticity of lime used in modern and historic masonry construction projects. The three biggest differences between Emley's original plasticimeter and the instrument used today is the omission of a upward force measuring mechanism, a change in the speed of rotation and the shape of the scale disk in contact with the lime putty material. Emley's original instrument measured the force exerted on the top disk in a vertical direction. He found this motion and force "not interesting" and the modern version used for lime putty mixed from hydrated lime does not have this feature. Also, Emley's original version had a vertical shaft rotation at the rate of one revolution in 6 minutes 30 seconds. The modern version used to classify lime putty rotates at a slightly longer interval of 6 minutes 40 seconds. For studying the plasticity of mortar and plaster, Emley utilized a conical disk at the top

of the instrument. The modern machine used to study lime putty made from hydrated lime utilizes a flat disk.

Modern day constants of the machine are specified in C110 (Table 1). The constants include required specifications outlining absorption of base plates, dimension of base plates, dimension of the disk, vertical shaft speed and torque on the disk when the scale reading is 100.

Table 1 – *Emley Plasticimeter Instrument Constants*

Absorption of Porcelain Base Plate	Minimum of 40 g in 24 hours
Rate of Base Plate Absorption	See Table 2 Below
Dimensions of Base Plate	25 mm thick by 100 mm Diameter
Dimension of Disk	0.8 mm thick by 76 mm Diameter
Speed of Vertical Shaft	1 Revolution in 6 min. 30 s.
Torque on Disk when Scale = 100	1.41 N•m

Base plates are required to meet the rate of absorption standards set forth in C110 7.2.3.2 (Table 2).

Table 2 –*Rate of Base Plate Absorption*

Time, min.	Water Absorbed, mL
1	8 to 14
2	5 to 7.5
3	4 to 6.5
4	4 to 6
5	3.5 to 5.5

Base Plates:

Base plate absorption characteristics are critical to the plasticity figure determination for the specification of hydrated lime used in finishing and masonry construction projects. These base plates function as an absorbent surface to remove water from the lime putty being tested. As water is withdrawn from the lime putty it will begin to stiffen. This degree or rate of stiffening is less rapid with putty of high plasticity and more rapid with putty of low plasticity.

The Emley Plasticimeter requires the use of carefully made absorptive base plates 25 mm thick and 100 mm in diameter made of porcelain or hydrous calcium sulfate (gypsum plaster; $CaSO_4 \cdot 2H_2O$). Porcelain base plates may be reused after plasticity testing if carefully cleaned following protocols of ASTM C110 7.2.2. Plaster base plates used in Emley's original work were reused after drying in an oven at 70 °C. Presently, C110 does not clearly state that plaster base plates are to be used only one time following plasticity testing, but the authors interpretation of the standard leads us to believe that plaster base plates are to be disposed of after a single use. Regardless of which type of plate is used, base plates require two independent water absorption measurements: 1) The

total amount of water absorbed in a 24 hour period (40 g minimum, no maximum) and 2) the rate of water absorption in 5 minutes when tested over a diameter of 70mm.

Testing base plates for total absorption is a simple matter requiring only that the plates be immersed in water at room temperature for a period of 24 hours. C110 specifies that a plate shall not absorb less than 40 g of water. Prior to testing, C110 specifies that porcelain base plates be dried overnight at temperatures between 100 °C and 110 °C. Plaster plates will crack if dried at these elevated temperatures. C110 specifies drying plaster plates overnight over calcium chloride at room temperature. Typical results for plaster plates dried overnight at room temperature in a desiccator charged with calcium chloride show that the base plates tested readily meet the minimum requirement of 40g water absorbed (Table 3).

Table 3 – *Typical Plaster Base Plate Total Absorption*

Plate #	Weight After Soaking (g)	Weight Before Soaking (g)	Grams H2O Absorbed (g)
1	292.9	229.0	63.9
2	294.1	229.1	65.0
3	275.5	214.8	60.7
4	276.3	215.0	61.3
5	289.0	226.3	62.7
6	298.8	231.7	67.1
7	278.4	213.2	65.2
8	293.4	228.6	64.8
9	293.8	230.1	63.7
10	274.0	214.0	60.0
Average	286.6	223.2	63.4
Std. Dev.	9.5	7.8	2.2

The maximum amount of water absorbed after 24 hours is not specified in C110. Most of the plaster plates that the authors have tested over a period of months show a typical total absorption in the range of 55 to 75 mL. Of course, plates that absorb too much or too little water after an immersion period of 24 hours will either be too porous or too dense to meet the rate of absorption requirements of C110. In intralaboratory work, the dry weight of typical plates can be used as a non-destructive test to determine the density of the plates prior to testing. Plates of similar density will have similar absorption characteristics. The authors have found that case lots of plates with widely varying dry weights (standard deviation in excess of 10) should be rejected.

C110 does not specify the apparatus required for the measurement of base plate rate of water absorption. However, Note 4 of ASTM C110-00a does describe a water absorption measuring apparatus that may be used. This non-mandatory apparatus consists of a buret sealed onto an inverted glass funnel with an inside basal diameter of 70 mm. The buret allows the measurement of water being absorbed by the base plate and the inverted funnel provides the required 70 mm testing surface. The note states that the funnel may be

attached to the base plate by melted paraffin, however, the note cautions that the "paraffin should not be too hot" and "a little experience will indicate when it is of the proper consistency." Typical results from the author's testing with this apparatus show that the method has merit (Table 3). However, it is the author's opinion that Note 4 is too vague to be of use for establishing standardized rate of absorption apparatus. The apparatus description should be fully developed within C110.

Table 3: ***Typical Results of Emley Base Plate Rate of Absorption Testing Using Buret and Modified 70mm Flask (25 plates per case lot; 5 tested).***

Time (min.)	ASTM Minimum Value Water Absorbed (mL)	ASTM Maximum Value Water Absorbed (mL)	Test 1 Results Water Absorbed Per Minute (mL)	Test 2 Results Water Absorbed Per Minute (mL)	Test 3 Results Water Absorbed Per Minute (mL)	Test 4 Results Water Absorbed Per Minute (mL)	Test 5 Results Water Absorbed Per Minute (mL)	Average Water Absorbed Per Minute (mL)	Standard Deviation Water Absorbed Per Minute (+/- mL)
1	8.0	14.0	10.5	11.6	12.0	11.0	11.4	11.3	0.6
2	5.0	7.5	5.0	4.6	5.0	5.4	4.8	5.0	0 3
3	4.0	6.5	4.4	4.4	4.2	4.4	4.2	4.3	0.1
4	4.0	6.0	4.0	3.8	4.2	4.2	3.8	4.0	0.2
5	3.5	5.5	3.6	3.6	3.6	4.0	3.8	3.7	0.2
Total Water Absorbed (mL)	24.5	39.5	27.5	28.0	29.0	29.0	28.0		

Apparatus developed true to the intent and spirit of C110 Note 4 (gravity head pressure, use of a modified buret, style of modified funnel, etc.) can be problematic. First, the glass funnel requires specialized skills for modification and the small neck formed by removal of the funnel stem tends to trap air at the funnel-buret connection. Second, with wax, an effective seal is not apparent by observation and the seal is easily broken when handling the apparatus prior to testing. As an alternative to a modified glass funnel attached with melted wax, the authors were successful using an apparatus consisting of a glass buret sealed onto a modified Nalgene Erlenmeyer flask by the use of a common rubber stopper with the funnel adhered to the top surface of the base plate by two-part epoxy. The advantage to using epoxy adhesive is that no stress or strain is induced into the plaster base plate matrix by apparatus requiring clamping or other external forces to maintain a watertight seal. The disadvantage to using epoxy adhesive is that the test is destructive to the base plate's top surface during funnel removal and the base plate must be disposed after testing (Figure 2).

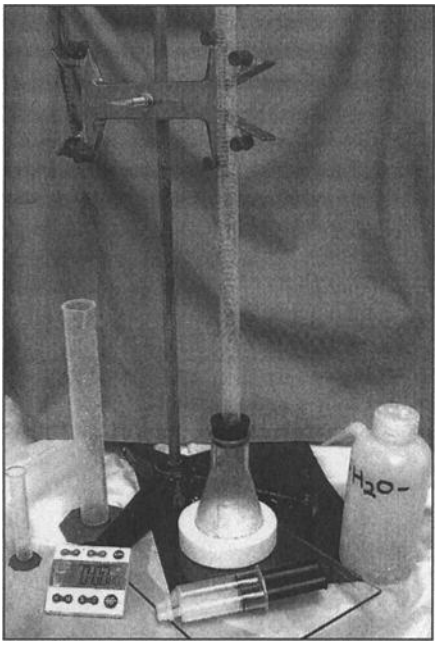

Figure 2. ***The Author's Base Plate Rate of Absorption Apparatus.***

One inherent weakness in the author's base plate testing method is experimental error introduced in the first minute of observation. At the start of the test, the operator manually fills the buret while starting a timer. Varying fluid head pressure and buret filling time are at least two sources of experimental error introduced during the first minute. The fact that the water column in the buret is constantly falling while the apparatus is being filled is problematic. The author's method requires back calculation of the water absorbed in the first minute. This requires careful use of the apparatus and careful measurement of all fluids used before, during and after the test. Even with careful use of the equipment, early research shows that typical base plate rate of absorption testing using a buret and modified flask may be in error by as much as plus or minus 10 to 12 %.

At least one laboratory known to the authors has developed base plate test methodology allowing the reuse of plaster base plates following water absorption testing (June 2001 ASTM Conference[4]). This lab uses a clamping device with a gasket to effect a watertight seal. An additional difference in this lab's approach is that fluid head pressure is applied to the inverted surface of a base plate against the force of gravity. Absorption character tested in this manner relies on the pressure differential across the

[4] ASTM June Committee Week, Committee C07 on Lime, June 24-29, 2001, Norfolk, VA.

testing diameter and capillary suction of water into the plate matrix. This novel approach to a watertight seal does have merit; the ability to reuse the plate after absorption testing is cost and labor efficient. A preliminary joint study with this laboratory has shown that testing of the same plates using the two different methodologies shows general results within the minimum and maximum absorption tolerances within C110 (Table 4). Additional work needs to be done on an intra and interlaboratory basis to establish specifications for base plate rate of water absorption apparatus.

Table 4 – *Results of Interlaboratory Base Plate Rate of Absorption Testing*

Sample ID Number	Lab ID	Absorbed Water at 1 minute (mL)	Absorbed Water at 2 minutes (mL)	Absorbed Water at 3 minutes (mL)	Absorbed Water at 4 minutes (mL)	Absorbed Water at 5 minutes (mL)	Total Water Absorbed (mL)
1A	Lab #1	9.0	4.8	4.2	3.8	3.8	25.6
	Lab #2	11.5	6.5	5.2	4.3	3.8	31.3
2A	Lab #1	13.0	5.6	4.8	4.4	4.2	32.0
	Lab #2	10.5	7.0	6.0	5.0	4.5	33.0
3A	Lab #1	7.4	5.0	4.2	4.0	3.4	24.0
	Lab #2	10.1	6.0	5.0	4.2	3.8	29.1
4A	Lab #1	11.0	4.8	4.6	3.8	3.8	28.0
	Lab #2	9.3	6.1	5.0	4.2	3.7	28.3
5A	Lab #1	11.2	5.8	5.0	4.6	4.4	31.0
	Lab #2	10.6	6.9	5.7	4.8	4.2	32.2

Lime Putty Consistency:

At the time of testing, the base plate is loaded with a lime putty of standard consistency molded with a conical ring 40mm in height with an inside diameter of 70 mm at the base and 60 mm at the top. Standard consistency is determined by following mixing protocol and measurement with a modified Vicat apparatus as outlined in C110 6.3.2 and C110.6.3.3. C110 states that the significance of standard consistency is that "it is necessary to have a uniform or standard consistency (viscosity), since the property measurement is affected by the consistency level."

Emley studied the effect of consistency on plasticity and noted that consistency has "little influence on plasticity." He states: "If a lime paste is not plastic, no amount of water which may be added to it can render it so. The converse of this is also true; a plastic lime remains plastic, regardless of the quantity of water which may be added to it. Of course, these statements are true only when the material is really plastic—when it does not approach too closely to either the solid or liquid conditions. Any plasterer will verify these statements, and they can be corroborated with a trowel at any time." However, Emley does concede that consistency does have some effect and a standard is needed to make reasonable comparisons of different hydrates. He says: "In cases where greater accuracy is desired, as when comparing similar hydrates, the consistency must be considered and accurately measured."

The work that Emley did to classify plasticity is validated because he made all his experiments with lime putty of standard consistency as determined by a modified slump

test. While he found that consistency is not the most important characteristic of plasticity, the work is only validated when a standard consistency is used. C110 does not offer precision and bias of the consistency determination test method. Work needs to be done to derive an interlaboratory data set for precision and bias related to putty consistency. This work will need to be done as a subset of interlaboratory plasticity tests on known hydrates. Ruggedness testing within each individual lab will determine if the current standard for lime putty consistency is tight enough.

Plasticity Determination:

Emley spent 10 years in the pursuit of a method to measure plasticity. At the end of this journey he stated: "...it is not difficult to build a machine and say that it will measure plasticity. The difficulty lies in offering convincing and acceptable proof that the machine will fulfill the claims made for it." Today, Emley's work has resulted in an instrument that is used to designate hydrated lime used in masonry construction.

After hydrated lime has been made into lime putty by mixing with water and molded to shape on an absorptive base plate, the instrument measures the degree of stiffening of the lime putty as water is withdrawn. This degree of stiffening is recorded by the machine operator from scale readings taken at 1-minute intervals until the test ends. The test is considered over when one of three conditions exists: 1) the scale reading reaches 100, 2) any reading is less than the one before and 3) the scale reading remains constant for three consecutive readings and the specimen has visibly ruptured or broken loose from the base plate. These two factors, elapsed time to end of test and scale reading, are used in calculating the unitless plasticity figure (Equation 1).

Plasticity Formula: $$P := \sqrt{F^2 + (10 \cdot T)^2} \quad (1)$$

where

P = plasticity figure
F = scale reading at the end of the test, and
T = time in minutes from the time when the first portion of lime putty was put into the ring mold centered on the absorptive base plate.

It takes a fair amount of operator experience to follow and interpret all the nuances associated with the plasticity test method. Putty consistency, base plate total and rate of absorption, and end of test determinations require good laboratory practice. Mechanical devices wear out over time and it is important to have plasticimeters recalibrated periodically so that the determinations remain reliable. An internal study done with two different machines shows the importance of maintaining plasticity equipment. The first machine was calibrated to meet all the machine constants required by C110. The second machine had been taken out of service because the mechanical drive mechanism was worn and the instrument rotation was slow. A slower rotation prolongs the length of the test resulting in a (significantly) higher plasticity figure (Figure3).

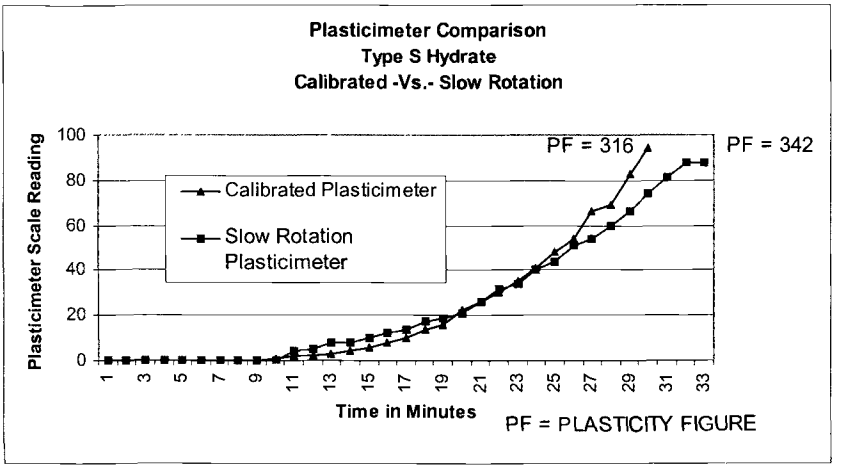

Figure 3. ***Plasticimeter Comparison: Calibrated Instrument Versus Non-Calibrated.***

Conclusion:

Because of the importance of plasticity in designating C206 and C207 hydrated lime, it is important to establish precision and bias statements for lime putty consistency, total and rate of base plate absorption and plasticity determinations. Rate of water absorption apparatus with more clearly defined user friendly operational procedures should be specified within C110. Emley's tool to measure plasticity is valuable to manufacturers of hydrated lime, construction specifiers, building department and code officials, and perhaps most importantly, the end users such as masons and plasterers. Precision and bias statements developed through round robins with labs that measure plasticity and meeting the rigorous standards of ASTM will support the statistical validity of the plasticity test method.

In summary, the cooperative work to be done to establish precision and bias data for submission to ASTM for balloting includes:

- Lime putty consistency of putty mixed from hydrated lime.
- Continued development of clearly defined procedures, apparatus, materials and measurement of base plate rate of absorption.
- Development and specification of calibration requirements for plasticimeters.

References:

[1] Emley, W.E., "Measurement of Plasticity of Mortars and Plasters." Technologic Papers of the Bureau of Standards. No. 169. Department of Commerce. Government Printing Office. Washington, DC, June 1920.

John J. Hughes[1], David S. Swift[2], Peter M.J. Bartos[1] and Philip F.G. Banfill[2]

A traditional vertical batch lime kiln: thermal profile and quicklime characteristics.

REFERENCE: Hughes, J. J., Swift, D. A., Bartos, P. J. M., and Banfill, P. F. G., "**A Traditional Vertical Batch Lime Kiln: Thermal Profile and Quickline Characteristics,**" *Masonry: Opportunities for the 21st Century, ASTM STP 1432*, D. Throop and R. E. Klingner, Eds., ASTM International, West Conshohocken, PA, 2002.

Full scale calcination of high calcium limestone using traditional methods was performed in the batch process Experimental Lime Kiln (ELK). The ELK is equipped to monitor temperature, air flow and gas compositions and also has significant insulation to ensure minimum lateral energy loss during burning. Internal kiln wall temperatures of up to 550°C, and kiln core temperatures of 850°C, within the range of calcium carbonate disassociation have been achieved for several hours with predictable temperature/time gradients. A mixed feed solid fuel : stone ratio of 1:9 was employed resulting in limestone conversion to quicklime of 75% ± 9. The heat balance efficiency is approximately 45%. However, this may not be a useful indicator of overall efficiency of binder production, especially in a open-top batch process traditional kiln. The hydration behaviour of the low-temperature traditional quicklime is more varied than high-temperature commercially produced quicklime, made from the same stone. The low temperature material hydrates more slowly, reaches a lower temperature and maintains a peak temperature plateau for longer than the high-temperature quicklime. The traditional quicklime also produces as much as 50% non-hydrated residue during the tests. This suggests an origin for "lime inclusion" texture in historic mortars. Mortars produced using traditional hot mixing processes are petrographically similar to historic mortars. The recognition of distinctive quicklime microstructures may also provide a diagnostic tool for quality control in small-scale traditional lime production.

Keywords: masonry conservation, lime:sand mortar, lime kiln, calcination, quicklime, heat of hydration

Introduction

Masonry binders in historic buildings are dominated by lime based materials. These often exhibit unparalleled durability, and compatibility with masonry units. Past decades have seen a considerable increase in the awareness of the benefits in using appropriate

materials, those that are truly compatible with the existing fabric, for the conservation and repair of historic masonry buildings. The use of inappropriate hydraulic mortars, where none were used originally, has caused damage to historic fabric such as increased stone decay and the early loss and failure of mortars.

Many research projects have focussed on the specification of appropriate replacement mortars for use in historic masonry repair. Effort was initially directed toward the identification of the composition of mortars, especially the ratio of binder to aggregate, and the hydraulic or non-hydraulic composition of the binder itself using wet chemical techniques [e.g.1-3]. Increasingly more information is sought on the detailed composition and texture of historic binders [4].

Detailed information is vital for the correct formulation and use of repair and restoration mortars. Previous analysis by the authors on historic mortars from Scotland, have revealed features relating to the raw materials used, the burning process and the hydration and use of mortars [5,6]. Comparisons with current commercially available limes also reveal differences compared with their Scottish, historic counterparts [7]. This has raised the question of whether our current limes, produced using modern high efficiency processes and often not for construction purposes, are truly compatible with the historic masonry.

To this end, the Experimental Lime Kiln (ELK), located at Charlestown in West Fife, Scotland, was constructed to conduct fundamental research into the production of masonry binders using traditional methods. The purpose of the project was to respond to the need for better lime-based masonry binders for use in building conservation.

Methods

This pilot project looked at the production of masonry binders using traditional limestone burning methods using the Experimental Lime Kiln (ELK). The ELK is a batch mode single shaft vertical lime kiln with a maximum capacity of approximately 24 tonnes of combined fuel and stone (see Fig's 1 & 2). Full computerised instrumentation is incorporated into the ELK, allowing the continuous monitoring of temperature, inlet air velocity and pressure, exhaust gas CO_2, CO, O and temperature and pressure. Nine K-type thermocouples are mounted recessed by 1.5cm, but exposed, within the refractory brick lining of the kiln shaft, at 1m intervals over the 5m internal height of the kiln shaft. Another thermocouple is available for insertion along a further three inspection conduits, permitting measurement within the kiln charge during burning. Unfortunately the gas compositions were not measured in any of the burns discussed in this paper.

Identical materials and firing conditions were used over three successive firings. The project comprised the following sections:

- Use of the Experimental Lime Kiln to calcine limestone on a large scale.
- The recording of the process and determination of approximate first values for efficiency.
- Determination of the heat of hydration characteristics of the materials produced and their comparison with commercially available materials.
- Manufacturing of mortars and their petrographic characterisation.

- Characterisation of the microstructure of the raw binder.

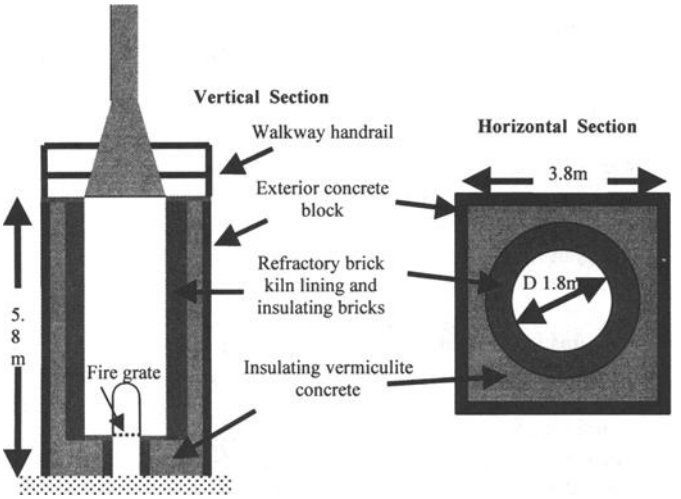

Figure 1. Cross sectional views of the Experimental Lime Kiln

Figure 2 The Experimental Lime Kiln at Charlestown, Fife, Scotland

SiO_2	0.11
TiO_2	0.00
$Al2O_3$	0.05
$Fe2O_3$	0.13
MnO	0.03
MgO	0.41
CaO	55.44
Na_2O	0.09
K_2O	0.01
P_2O_5	0.01
LOI	43.49
TOTAL	**99.77**

Table 1 - Shap limestone average chemical analysis (XRF).

Raw materials

The limestone used is burnt commercially for the production of quicklime at Shap in Cumbria, England. This has allowed the direct comparison of the commercial, high-temperature product, made using modern techniques, and the low-temperature material produced using traditionally based methods in the ELK, both made from the same

limestone. Table 1 shows the chemical composition of the limestone as sampled from the kiln fill. It is a high calcium limestone that returns a theoretical maximum available lime content of 98.9 %. After the firings the degree of calcination of the stone was determined by measuring and comparing the weight of a sample of quicklime with that of a similar volume of uncalcined stone.

The fuel used was a mixture of 1 part high volatility Pet-coke and 1 part low volatility anthracite added at a concentration of 1 part fuel to 9 parts stone, by weight, mixed in the kiln. The stone particle size was 100-150mm and the fuel smaller at 25mm. The fuel type was chosen for a clean burn with a low ash content , not for its traditional use. For the third firing the total fill amounted to 17160kg of combined fuel and stone, of which 1560kg was fuel, making an actual fuel:stone ratio of 0.9:9.1.

Temperature distributions in the Experimental Lime Kiln

Figure 3 shows the locations of thermocouples in the ELK, and Figure 4 depicts the temperature distributions during the third burning. Initially temperatures do not rise for 2.5 hours. At this point the draught was assisted by a fan attached to the air intake below the grate. This increase in air velocity encouraged the first rise in temperature. The temperature, as recorded by the recessed thermocouples, reaches a maximum of just below 550°C after approximately 24 hours, and peaks at different times at different sections of the kiln. The temperature, as measured along the thermocouple conduits A, B, C and D, recorded a maximum in excess of 700°C. The exhaust gas temperature reaches a maximum of 500°C during the apparently most intense burning period between approximately 17 and 22 hours burning time. The periods of sustained temperature maxima at or above approximately 90% of maximum temperature range from 2-5 hours.

Figure 5 shows the temperature distribution within the upper right portion of the ELK during the third firing at 15 hours burning duration, as recorded by moving a thermocouple along the A, B, C, D thermocouple conduits. This is at a time where the maximum temperature measured at the kiln wall is 500°C. The temperature distribution in the kiln wall also shows a smooth relationship to the kiln core temperature, with a fairly steep temperature gradient from the burning zone to the outer wall. This qualitatively indicates the efficiency of the insulation, with outer wall temperatures continuing at ambient environmental levels even when the kiln core is at calcination temperatures. The kiln was cool before the burning was started, so the temperature development seen here represents that from ambient environmental conditions (approx. 15°C). Thermocouple T9 was not used as it sits above the stone in the kiln and would not record useful temperature information. Thermocouple T3 was also not utilised during burning due to its proximity to the additional thermocouple conduit D, which was used to record temperature profile through the kiln wall.

Looking more carefully at the spatial temperature-time distributions as indicated in Figure 4, it is possible to determine the dynamic evolution of the burn. Temperature increases progressed up the back and front initially, parallel with the fire grate running from back to front across the kiln. This is associated with the increased draft in these locations, where air flow is less restricted. Maximum temperature was reached at the

lower left section of the kiln, perhaps indicating an inhomogeneity in fuel distribution at this point. As burning progressed up through the kiln temperature maxima decrease to approximately 450°C. Burning is neither static nor uniform throughout the kiln, and indicates the differing calcination conditions that occur in the kiln-fill.

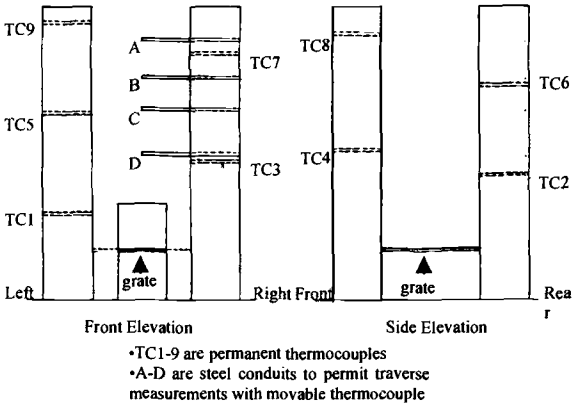

Figure 3 Schematic diagram of ELK showing locations of thermocouples

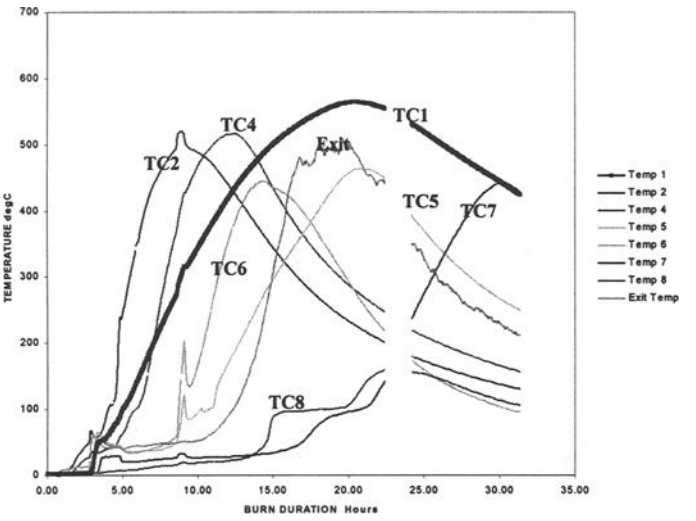

Figure 4. Temperature distributions with time for ELK burn 3. See Fig 2 for locations of thermocouples.

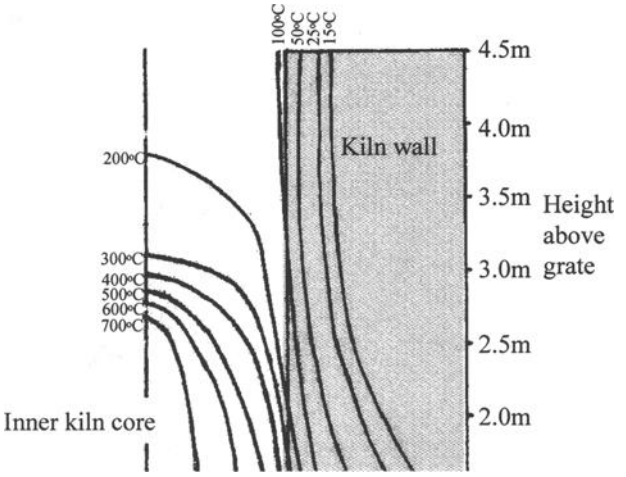

Figure 5 Temperature profile in the ELK during Burn 3 at 15 hours. Measured using movable thermocouple in conduits A,B,C & D (see Fig.3).

Degree of Calcination and first estimation of efficiency

Lump quicklime from the ELK was weighed several times to gain an average weight plus deviation value for a fixed volume of material. This was then compared with a similar number of weighings of the same volume of uncalcined stone. Using an average loss on ignition value for the stone of 43.49% to represent 100% calcination (see table 1) this leads to a degree of calcination of approximately 75 ± 9 %. However, this must be viewed with caution as it is very approximate and will benefit in future from determination of actual bulk density of the quicklime.

The efficiency of a lime burning process is given by Boynton [8] as:

$$\% \text{ Thermal Efficiency} = \frac{\text{Theoretical Heat Requirement X \% available oxide content}}{\text{Total heat requirement}}$$

This was developed for practical use by Hill and Mason [9] further as:

$$\% \text{ Thermal Efficiency} = \frac{\text{Theoretical Heat Requirement x \% available oxide content}}{\text{calorific value of fuel x mass fuel kg/t of quicklime produced}}$$

To calculate this as a first approximation we used the chemical composition (Table1) of the stone to calculate the theoretical heat requirement to be 3151Mj/kg, the theoretical available lime content as 98% or 0.98 (derived from the chemical analysis), the calorific content of the fuel as 33.9Mj/kg (from generic values in Boynton 1980 [8] and Oates

[10]), and the weight of fuel per tonne of quicklime produced as 150kg/t (assuming the weight of quicklime corresponds to the median calcination figure of 75%). So:

$$\% \text{ Thermal Efficiency} = \frac{3151 \times 0.98}{33.9 \times 150} = 0.607 \text{ or } 60.7\%$$

It must be borne in mind that this is an approximate figure and the relationship between the weight of quicklime produced and the weight of fuel needed per tonne is not satisfactory at this time. The equation assumes total calcination and no appreciable limestone core. We understand that we have approximately 25% core in our quicklime or 75% of the total weight of quicklime is available for reaction. If we multiply the available lime content by this figure we get an efficiency of 45.8%, probably nearer the real figure. Further work and improved data gathering is required to increase the certainty of efficiency calculations.

The gas discharge temperature of the kiln is 550oC. This means that a great deal of heat is being removed from the kiln without contributing to calcination. It is very high compared to modern kiln discharge temperatures of nearer 100°C. This is certainly provides some support for the assertion that the ELK has high lateral insulation, but does bring into question the overall efficiency in comparison to modern techniques. However, the ELK is an open-topped traditional kiln, so these estimates of its efficiency may indicate that it is an efficient kiln of this type. However insufficient data is available at this time.

Heat of Hydration of traditionally produced quicklime

After calcination in the ELK, quicklime was sampled regularly from the kiln during unloading and stored in air-tight plastic containers until testing took place. Quicklime from the ELK-Burns and commercially available material were then subjected to a heat of hydration test. The method adopted combined apparatus constructed to EN 459-2 "Building Lime: Part 2. Test methods", with samples prepared to ASTM C110 "Standard Test Methods for Physical Testing of Quicklime, Hydrated Lime and Limestone". After crushing, ELK lump lime was screened through a 3.35mm aperture sieve.

The commercially produced quicklime is produced in a Maertz Parallel Flow Regenerative Kiln at between 1200-1300°C. This high-temperature quicklime is supplied granulated, with a particle size between 6 and 1 mm. It was also screened through 3.35mm, before testing. However, the ELK-produced quicklime had an apparent grain size distribution very different from the commercially produced material. Hydration tests were also performed on grain size separates from the ELK quicklime to establish the influence of grain size on the results.

During the tests temperatures were noted at various intervals up to 1 hour. After each test the contents of the Dewar flask were passed through a 150μm sieve and the residue dried at 105°C and weighed to obtain the "slaking residue". Commercially produced Shap quicklime was compared with quicklime produced in the ELK from the second and third

firings. They were tested at the same time, the ELK burn 2 material being some 2 months older than that from ELK burn 3.

Comparison of ELK Burn-2 & 3 quicklime & commercially produced quicklime.

Figures 6 & 7 display data from tests performed on different quicklime sub-samples taken from the products of the second and third firing of the ELK with Shap limestone. The results from Burn 2 (Fig. 6) show a variation in reactivity between different samples from the same firing. After a rapid increase over the first 30 seconds, times to 50°C range from 14 to 26 minutes, with maximum temperatures reached around 55-62°C. Each sub-sample used for testing was crushed separately from lump quicklime, and was not taken from a previously homogenised sample. Unhydrated and unburnt residues were not determined for these tests of the Burn 2 material.

Figure 7 displays results for a crushed bulk, homogenised, sample from the 3rd ELK burn. This material had a time to 50°C of approximately 9 minutes, for both samples, and a maximum temperature of 63°C. This sample had a slaking test residue of 34.7% that contained unburnt fragments of limestone and numerous small quicklime particles that had failed to reduce or hydrate during the test.

Figure 8 shows the results from the testing of 3 sub-samples of the commercially produced high-temperature Shap quicklime. It has a time to 50°C of approximately 3-4 minutes and maximum temperature of 73°C. The slaking residue retained on the 150μm sieve after one test, was 13.3% by weight of the total quicklime added to the test.

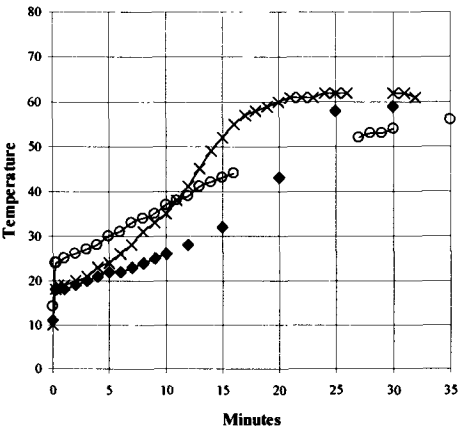

Figure 6 Heat of hydration of 3 samples of ELK Burn 2 , high calcium Shap quicklime.

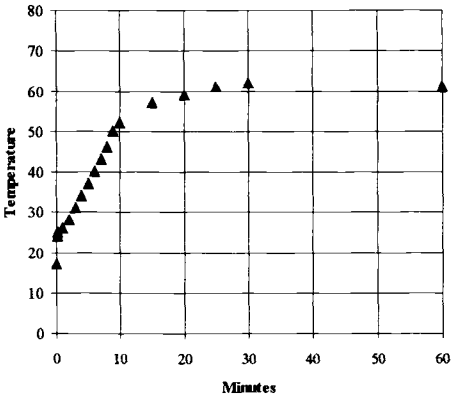

Figure 7. Heat of hydration of a bulk quicklime sample from ELK Burn No. 3

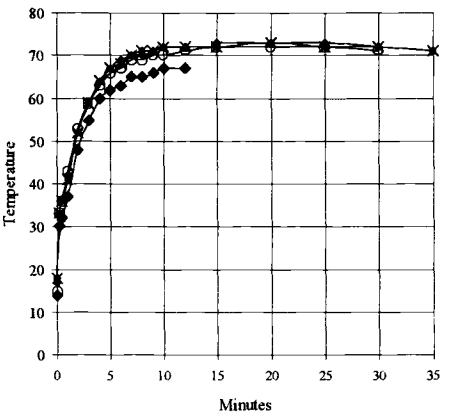

Figure 8. Heat of hydration results for 3 samples of commercially produced high calcium Shap quicklime

Grain size effects: ELK-Burnt Shap Quicklime.

The material tested from the ELK firings was crushed in a jaw crusher to reduce it from the 15-20cm lump lime size in order to pass the 3.35mm sieve. This generated a grain size distribution in the sample that appeared to contrast strongly with the commercially prepared material. In order to asses the likely contributions of grain size to the results obtained, the bulk sample was sieved through 3.35, 2 and 1mm aperture size sieves. Each grain size fraction was then tested separately.

The grain size/weight distribution of the crushed quicklime from Burn 2 is given in Fig.9. The results of the hydration tests for quicklime from ELK-Burn 2 and 3 are presented in Fig.10. It is clear that it is very hard to separate the curves for the different grain sizes, so it apparently has no significant effect on the results of the bulk samples. The slaking residues for the grain size fractions from ELK-Burn 2 and 3 were also examined and are presented in Figure 11 and 12. For Burn 2 quicklime a larger proportion of the coarser quicklime grains disintegrate in the test compared with the finer material. A similar temperature increase generated by the finer grained quicklime is achieved by the reaction of a smaller amount of material. This is interpreted as being achieved by an increase in surface area in the finer material, though it is not clear why more of this material does not break down through reaction during the test. The slaking residue for Burn 3 is less than that for Burn 2, though still significant at up to 33% of the total weight of quicklime tested. The same pattern is seen of the finer grain size quicklime producing a larger slaking residue.

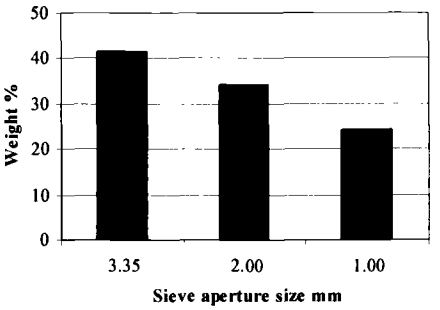

Figure 9. Grain Size Distribution of crushed quicklime from ELK burn 2

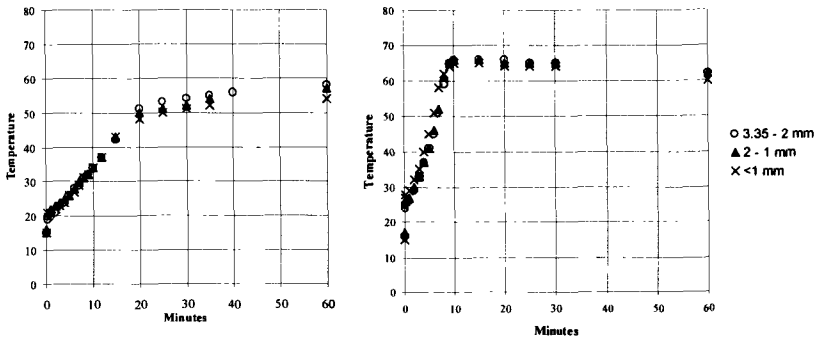

Figure 10. Heat of hydration of grain size separates of crushed ELK burn 2 (left) and ELK-Burn 3 (right) quicklime.

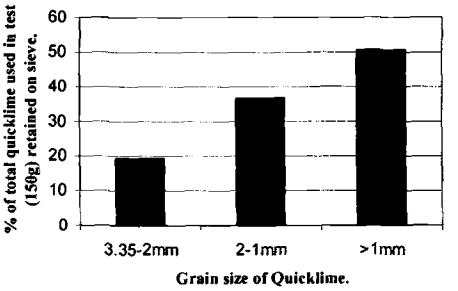

Figure 11. ELK produced quicklime Burn 2: % Residue retained on 150um sieve after 1 hour heat of hydration testing

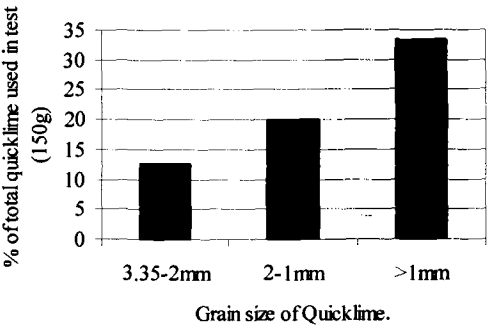

Figure 12. ELK produced quicklime Burn 3: % Residue retained on 150um sieve after 1 hour heat of hydration testing

Quicklime microstructures.

A Hitachi S4100 Cold Field Emission Scanning Electron Microscope was used to qualitatively compare the microstructures of the commercially produced quicklime, calcined at 1200-1300°C in a modern kiln, with the microstructures of the quicklime produced in the ELK at lower temperatures of around 700-900°C.

Figures 13 and 14 show examples of coalesced structures in the commercially produced high-temperature material. Figures 15 and 16 show typical microstructures of the low-temperature quicklime from the ELK. The textures in the low-temperature quicklime are very varied, however, but no examples of microstructure comparable to that seen in the high-temperature material were discovered. The low-temperature quicklime exhibits larger apparent surface area whereas the high-temperature material has a lower apparent surface area, but a larger volume of apparent porosity. This may account for the increased hydration reactivity of the high-temperature quicklime, as suggested by

Boynton [9]. The form and size of the crystallites of CaO in the respective quicklime samples is related to temperature of calcination and to residence time [11]. This is an established relationship, through which it may be possible to calibrate microstructure in quicklime produced from a particular limestone to conditions within the kiln.

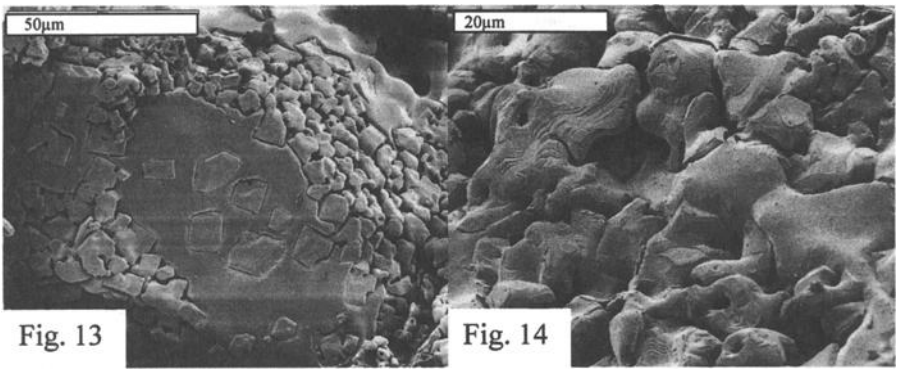

Figure 13 (left) and 14(Right). Commercially produced quicklime from Shap limestone, showing coalesced textures, Temp. approx. 1200-1300°C

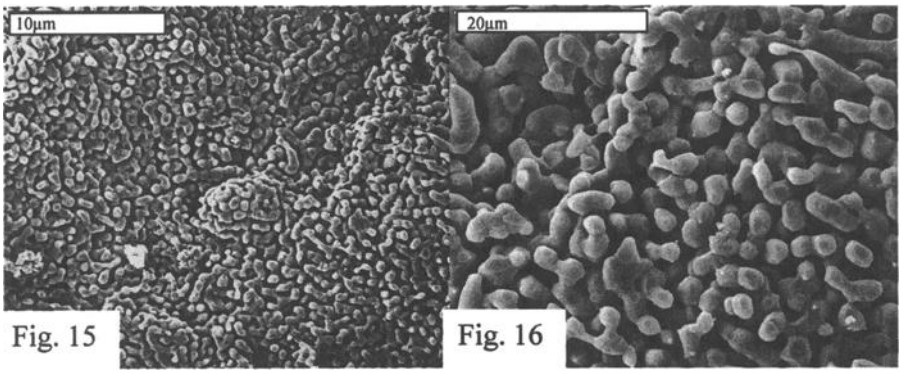

Figure 15 (Left) and Fig.16 (right) Quicklime produced from Shap limestone in the ELK, showing dimensions of CaO crystallites and porosity.

Mortar production and petrographic analysis

Mortar was produced from the low-temperature ELK quicklime, and made into 40 x 40 x 160mm prisms and 50mm cubes. The "hot" hand-mixing method was used, where quicklime, sand and water are added directly together, no putty being made and matured in advance. Specimens were de-moulded after 4 days and cured at 20°C and 60%± 10 % humidity. Thin sections of mortar were made after 5 months and examined using a conventional petrographic polarising microscope.

Hot mixing of lime based mortars produces a distinctive texture, of a mortar with numerous lime inclusions or "lime lumps"; white, spherical particles of possibly unmixed binder. They are commonly seen in historic mortars. They do not contain aggregate, and an origin in over or under-burnt lime has been suggested [7]. The mortars mixed for this project exhibited such a texture, and many specimens suffered from late hydration of particles leading to expansion and disruption. Figures 17 and 18 show a five month old lime mortars produced with the hot mixing method exhibiting distinctive early age shrinkage cracking, but also a lime inclusion texture- distinct to indistinct areas of lime that contain no aggregate.

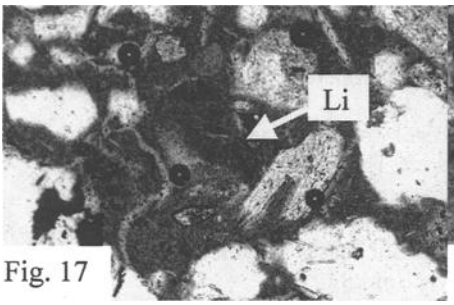

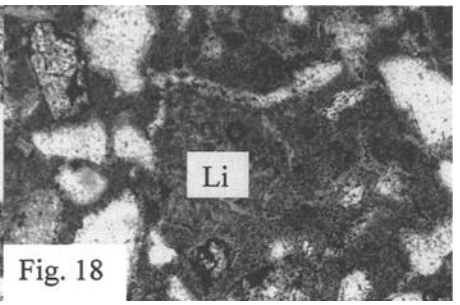

Figure 17 and 18. Photomicrographs of 5 month old hot mixed lime mortar mixed using quicklime produced in the ELK. Showing distinctive young mortar shrinkage cracks and also lime inclusion texture (Li). Field of view 1mm.

Discussion & Conclusions

The high-temperature commercial quicklime, produced from the Shap limestone, is more reactive than the low-temperature ELK produced quicklime. This applies to the rate of initial temperature increase and for the maximum temperature reached. Quicklime from the low-temperature ELK burns show a shallow temperature increase and lower peak temperature, but a longer period of sustained temperature. The results from different samples ELK quicklime indicate that variability in reactivity may be characteristic.

The slaking residue from the heat of hydration tests was found to be quicklime that had not slaked or broken down, and pieces of limestone core. The large slaking residue from the low-temperature ELK quicklime contrasts with the smaller residue from the high-temperature commercial quicklime. This indicates the more complex hydration behaviour of the traditionally produced material, and also a likely source of lime inclusions in the material. It is increasingly clear that lime inclusions are a major component of historic mortars and may act as a "buffer" of carbonate material within an ageing mortar, allowing redistribution and "self healing". Lime lumps can be generated from commercial lump lime as well, so it is possible their occurrence is controlled more by particle size and mixing method. The characteristic slaking behaviour of the low-

temperature ELK quicklime may be due to the large quantity (up to 50%) of non-slakable residue. This may inhibit temperature rise by acting as a heat sink during the tests.

There is also a contrast in the observed microstructure of the high-temperature commercial and low-temperature traditional quicklimes. More coalesced structures are formed in the high-temperature commercial quicklime, that are not encountered in the low-temperature ELK material. It may be possible to use the microstructural characteristics of quicklime for quality control and temperature/residence time calibration. This is important when looking at a traditional process, which produces varied material, as direct temperature monitoring within a batch kiln is limited to specific points around the periphery and within the kiln core. In order to probe the temperature distributions and residence time characteristics within such a kiln, some character of the material produced may need to be studied. It may be possible to build up a dynamic picture of the kiln's behaviour to better understand the properties of the materials produced.

The kiln is well insulated to minimise lateral heat loss, and the temperature evolution is predictable and controllable, by manipulating draft. Thermal efficiency of is approximately 45%, though the reliability of the data used and the assumptions made in arriving at this value need to be better constrained. However, this is a traditional type open-topped batch kiln, where a considerable amount of heat is lost out of the top of the kiln. An efficiency of 45% may be good for this type of kiln.

Several other issues still remain to be resolved:

- The exact correspondence of microstructures to temperature and residence time is still unclear, and how it may be able to help us understand the dynamics of a small scale kiln.
- The physical and chemical properties of the quicklimes produced need to be investigated in more detail, including surface area and porosity to relate clearly to temperatures and residence times in the kiln.
- The fresh and hardened properties of mortars produced from the quicklime are still to be quantified and compared to historic examples. Properties to be investigated include putty properties, mortar workability, strength, permeability, porosity and durability (e.g. freeze thaw).

Traditional methods of binder production (and this is ***binder*** production ***not*** lime production) result in a material that is different from commercial production, even using the same stone. This is not surprising or new, but the properties of the materials are not researched to date. It is possible that the performance of these materials may be good, even though they do not meet current standards for lime production, the added variability being beneficial for performance in some, as yet, unconstrained way. The results of hydration and the experience of making mortars indicate that it is possible to produce materials with an appearance closer to historic ones.

References

[1] Jedrzejewska, H., "Old mortars in Poland: a new method of investigation", *Studies in Conservation*, **5**, No. 4, 1960, pp.132-138.

[2]Cliver 1974 Cliver, E. B. "Tests for the Analysis of Mortar Samples", *Bulletin of the Association for Preservation Technology*, **6**, No.1, 1974, pp.68-73.

[3] Stewart, J. & Moore, J., "Chemical Techniques of Historic Mortar Analysis", in *"Mortars, Cements and Grouts used in the Conservation of Historic Buildings"*, Nov 3-Nov 6, ICCROM, Rome, 1981, pp.297-310.

[4] Callebaut et al. (2000) Callebaut K., Viaene W., Van Balen K. and Ottenburgs R., "Petrographical, mineralogical and chemical characterisation of lime mortars in the Saint Michael's church (Leuven, Belgium)" in *"Historic Mortars: Characteristics and Tests"*, Bartos P.J.M, Groot C.J.W.P & Hughes J.J. (eds.), RILEM, PRO12, 2000, pp.115-126.

[5] Hughes J.J., Cuthbert, S.J. & Bartos M.J., "Alteration Textures in Historic Scottish Lime-Mortars and the implications for practical mortar analysis", in *Proceedings of the 7th Euroseminar on Microscopy Applied to Building Materials*, Delft June 29-July 2 1999, Pietersen H.S., Larbi J.A. and Janssen H.A. (eds.), 1999, pp.417-426.

[6] Hughes J.J., Cuthbert S.J. "The petrography and microstructure of medieval lime mortars from the west of Scotland: Implications for formulation of repair and replacement mortars.", *Materials and Structures*, Vol. 33, 2000, pp594-600.

[7] Leslie A.B and Hughes J.J., "Complex structure and mineralogy of historic Scottish mortars – implications for replacement mixes and repair strategies", *Proceedings of the 8th Euroseminar on Microscopy Applied to Building Materials*, Athens, September 4-7th 2001, pp. 443-450.

[8] Boynton R.S., "Chemistry and Technology of Lime and Limestone", Wiley – Interscience publication, John Wiley and Sons, 1980

[9] Hill N. and Mason K., "Calculating the energy efficiency of a lime burning process," *World Cement*, March, 1997

10] Oates, J.A.H., "Lime and Limestone, Chemistry and Technology, Production and Uses", Wiley-VCH, 1998.

Margaret L. Thomson[1]

Pozzolan-Lime Mortar: Limitations of ASTM C593.

Reference: Thomson, M. L., "**Pozzolan-Lime Mortar: Limitations of ASTM C593.**" *Masonry: Opportunities for the 21st Century, ASTM STP 1432*, D. Throop and R.E. Klingner, Eds., ASTM International, West Conshohocken, PA, 2003.

Abstract: Alone, neither a pozzolan nor hydrated lime is capable of setting under water. They are not hydraulic. When combined and mixed with water, however, the resulting reaction products are hydraulic. There is a renewed interest in pozzolan-lime binders, in particular for historic masonry. ASTM C593 provides a limited resource in defining suitable pozzolans to be used with lime for masonry mortars and exterior plasters. One of its limitations is that the specified pozzolan-lime weight ratio is not representative of a traditional volumetric ratio of one volume part binder to three volume parts sand. In addition, the standard requires accelerated curing, which is unrealistic for pozzolan-lime mortar.

Preliminary results indicate that using specific ratios of pozzolan to lime and a vapor curing regime, as required by ASTM C593, does not necessarily promote the optimum pozzolanic reaction as tested by compressive strength. Results from ASTM C593 therefore do not represent the expected field behavior of pozzolan-lime mortars. The requirements of that standard should be modified with respect to pozzolan-lime ratios and curing conditions.

Keywords: pozzolan, lime, mortar, hydraulic lime

Introduction

There is a renewed interest in the use of pozzolan-lime binders, especially for the repair and restoration of historic masonry mortars [1,2,3]. The standard most applicable to the production of pozzolan-lime mortar and the assessment of pozzolan and lime reaction is Specification for Fly Ash and Other Pozzolans for use with Lime (C593). That standard requires that mortar materials be batched by weight, and does not account

[1] Ph.D. Technical Manager, National Building Construction, Chemical Lime Company, 8000 W. Lake Mead Drive, BMI Complex, Henderson, Nevada, 89015, margaret.thomson@chemicallime.com

for variations in material bulk density. This is problematic because masonry mortar is traditionally mixed by volume.

C593 also specifies that the mortar be cured for 7 days in an elevated-temperature vapor cabinet, and for the remaining 21 days in a 100% RH cabinet. Accelerated curing conditions are common in the testing of concrete (Method of Making, Accelerated Curing, and Testing of Concrete Compressive Test Specimens, C684) [4], but the same approach should not be applied reflexively to pozzolan-lime mortar, where the nature of the pozzolan can vary.

The objective of this paper is to examine the flow and compressive strength of several types of pozzolan-lime mortars, and to examine the relationship between those properties and the procedures required by C593. Portions of C593 that appear to be inconsistent or unrealistic are identified, and suggestions are made for improving them.

Material Selection

In this study Type C flyash, volcanic ash, and calcined clay were chosen to represent a range of pozzolan types. Type C fly ash is derived from coal-burning power plants and is composed of amorphous alumina-silicate glass, free lime (CaO), and iron phases. Naturally occurring, consolidated volcanic ash is composed primarily of amorphous alumina-silicate glass. Calcium present in the consolidated ash does not occur as free lime, but is tied up in other phases, most commonly feldspar. Naturally occurring clay is calcined to alter its original alumina-silicate sheet structure to create an essentially amorphous or weakly crystalline habit. All the materials were obtained from commercial vendors and are used commercially as pozzolans.

Table 1 is a summary of chemical analysis of the three pozzolans investigated. Interestingly, the CaO, SiO_2 and Al_2O_3 values of the fly ash and the volcanic ash show similar values and ratios. The calcined clay is essentially silica and alumina only.

Table 1 – *Chemical analysis of pozzolans used in this study.* [1]

	Type C Flyash	Volcanic Ash	Calcined Clay	Type S Hydrated Lime
CaO	10.49	8.08	0.02	43.00
MgO	2.50	1.90	0.03	28.37
SiO_2	60.67	60.18	52.92	0.16
Al_2O_3	16.77	18.98	44.64	0.11
Fe_2O_3	5.47	4.48	00.44	0.26
Na_2O	1.91	1.96	0.08	0.00
K_2O	1.11	1.12	0.08	0.00
LOI	1.06	4.34	1.89	27.87
Total	99.98	101.40	100.10	99.77

[1]Analysis completed on Leeman Labs, Inc., Model PS1000 UV, Induced Coupled Plasma (ICP)

Chemstar Type S hydrated lime meeting the requirements of C207 (Specification for Hydrated Lime for Masonry Mortar) was chosen because it meets the chemical requirement of providing a hydroxide for the pozzolanic reaction, and also contributes to the plastic and hardened properties of a masonry mortar. Graded standard sand was used, conforming to the requirements of C778 (Specification for Standard Sand).

Test Procedure

One mortar group was proportioned by weight using C593, but using a larger batch size to provide more material. The second mortar group was proportioned by volume. A traditional mix of 2:1:9 by volume of pozzolan, lime and sand, respectively, was chosen for comparison. Volume values were converted to weights using bulk density values. Mixing procedures followed C593, Section 9. Mix parameters are presented in Table 2.

The vapor cabinet was set up as required by ASTM C593. The mortar molds were placed in the vapor cabinet. After the required time there, the cubes were demolded and moved into a 100% RH cabinet.

The second curing regime was set up in a site-built humidity cabinet consisting of a wooden frame covered with low-perm 6 mil plastic construction film. The humidity was maintained at 50% ± 3% RH using pails of water open to the air, and the temperature was held at 22° ± 3°C. The humidity values were determined and recorded daily until stable, then weekly using a Vaisala HM141 Humidity and Temperature Instrument. The mortar cubes were demolded after 96 hours in the 50% RH room and placed for the duration of the prescribed curing period on a counter top of untreated marine grade plywood.

Compressive strength testing was conducted on a calibrated Tinius Olsen, 200 N/m^2, Super L Universal Testing Machine. Testing was conducted at 14 days, 28 days and 49 days to estimate long-term strength gain.

Results of Testing

Table 2 summarizes the mix designs and flows of the mortars studied here. The ratios of water to binder for the two mix designs show a wide variation, reflecting the specific surface of each pozzolan. The flyash required the least water to achieve the same flow, and the calcined clay required the most. In the C593 mixes, the ratio of pozzolan to lime by weight had a constant value of 2;for the 2:1:9 mixes, in contrast the flyash shows a high weight ratio of 5.5, and the calcined clay shows a ratio of 1.9. This variation is consistent with the variations in bulk density between those materials. The weight ratios of binder to sand of the C593 mixes remained at a constant value of 0.37. The 2:1:9 volume mixes were consistently lower in binder (richer in sand), with weight ratios of 0.30 for the flyash, 0.20 for the volcanic ash and 0.13 for the calcined clay mortar.

Table 2 – *Mix design and flow.*

	Pozzolan (g)	Lime (g)	Sand (g)	H_2O (g)	Flow (%) 10 drops	H_2O/ Binder	Binder/ Sand	Pozz/ lime
ASTM C593								
Type C Flyash (50% RH)	540.0	270.0	2220.0	575.0	66	0.63	0.37	2
Volcanic Ash (50% RH)	540.0	270.0	2220.0	630.0	67	0.78	0.37	2
Calcined Clay (50% RH)	540.0	270.0	2220.0	1000.0	73	1.23	0.37	2
Type C Flyash (Vapor)	540.0	270.0	2220.0	575.0		0.63	0.37	2
Volcanic Ash (Vapor)	540.0	270.0	2220.0	630.0		0.78	0.37	2
Calcined Clay (Vapor)	540.0	270.0	2220.0	1000.0		1.23	0.37	2
Volume 2:1:9								
Type C Flyash (50% RH)	566.2	102.1	2220.5	480.0	69	0.72	0.30	5.5
Volcanic Ash (50% RH)	343.6	102.1	2220.4	425.0	73	0.95	0.20	3.4
Calcined Clay (50% RH)	197.4	102.1	2220.5	500.0	75	1.67	0.13	1.9
Type C Flyash (Vapor)	566.2	102.1	2220.5	480.0		0.72	0.30	5.5
Volcanic Ash (Vapor)	343.6	102.1	2220.4	425.0		0.95	0.20	3.4
Calcined Clay (Vapor)	197.4	102.1	2220.5	500.0		1.67	0.13	1.9

Table 3 and Figure 1 summarize the compressive strengths for each mortar. Compressive strengths show a wide variation among pozzolan types. The calcined clay-lime mortars proportioned to meet C593 have the highest compressive strength of the pozzolan-lime mortar types, regardless of the curing regime (7.52 N/m^2, 9.85 N/m^2). The second and third strongest, respectively, are the volcanic ash-lime C593 design, vapor cured (6.16 N/m^2), and the Type C flyash 2:1:9 proportion, cured at 50% RH (5.78 N/m^2).

Differences in strengths among the calcined clay mortars appear to be more related to the binder to sand proportions than to the curing regime. The C593 calcined clay-lime mortars have an equivalent volume ratio of 2 parts calcined clay to 1 part lime to 4.5 parts sand. This is considerably more binder-rich than a more traditional mortar of 1 part binder to 3 parts sand. Curing has a secondary influence, with the vapor curing showing slightly higher strength gains than the 50% RH cabinet samples.

The difference in strength among the Type C flyash-lime mortars shows no clear relationship to curing regime, binder-sand ratio or pozzolan-lime ratio. The vapor-cured C593 mix has a higher tested compressive strength than the 2:1:9 equivalent, but the 2:1:9 50% RH cured mixes have a higher tested compressive strength than the C593 equivalent. The lower pozzolan-lime ratio of the C593 mix appears to require the accelerated curing of the vapor cabinet to promote reaction. Moreover, the higher pozzolan-lime ratio of the 2:1:9 mixes appears to be more appropriate ratio to promote reaction under 50% RH curing. The C593 mortar in 50% RH showed no strength gain from the 28-day test time to the 49-day test time.

The difference in strength among the volcanic ash-lime mortars appears to be related to curing regime. The vapor-cured mortars have the highest compressive strength, with the C593 mix design being the higher of the two. The 2:1:9 mix mortars cured under 50% RH showed no significant strength gain from 14 to 49 days. This suggests that over time there was no significant pozzolanic reaction resulting in the development of cementitous minerals.

Table 3 – *Compressive strengths.*

	14 day (N/m^2)	St. Dev. (n=3)	28 day (N/m^2)	St. Dev. (n=3)	49 day (N/m^2)	St. Dev. (n=3)
ASTM C593						
Type C Flyash (50% RH)	1.20	0.05	1.23	0.03	1.01	0.06
Volcanic Ash (50% RH)	1.81	0.12	2.19	0.24	2.18	0.20
Calcined Clay (50% RH)	7.03	0.14	7.63	0.37	7.52	0.48
Type C Flyash (Vapor)	2.94	0.15	3.91	0.08	4.51	0.06
Volcanic Ash (Vapor)	6.03	0.14	5.64	0.12	6.16	0.62
Calcined Clay (Vapor)	6.08	0.55	6.95	0.46	9.85	0.24
Volume Proportion: 2:1:9						
Type C Flyash (50% RH)	4.25	0.03	5.40	0.39	5.78	0.44
Volcanic Ash (50% RH)	0.92	0.06	0.88	0.01	0.87	0.19
Calcined Clay (50% RH)	3.06	0.30	3.14	0.06	3.12	0.06
Type C Flyash (Vapor)	2.55	0.04	2.94	0.05	2.85	0.12
Volcanic Ash (Vapor)	4.31	0.14	3.33	0.07	2.95	0.18
Calcined Clay (Vapor)	4.25	0.28	4.70	0.11	4.53	0.02

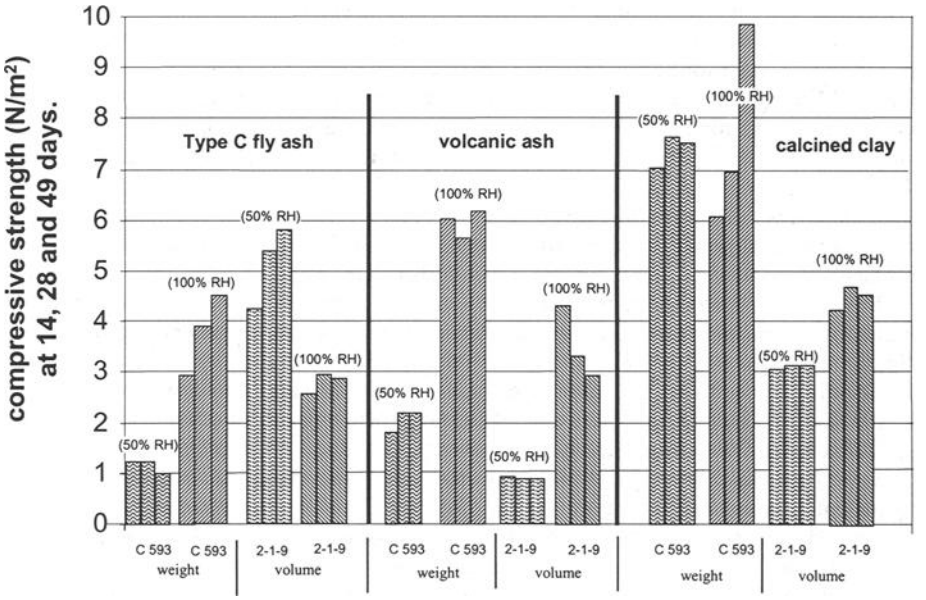

Figure 1 – *Compressive strength data.*

Discussion

This work is intended to provide a basis for discussion in Subcommittee C07.07 leading to possible modification of C593 to develop testing procedures specific to pozzolan-lime mortars. Limitations of the current standard are its requirement for proportioning by weight, and it prescribed curing conditions. In this section, each is briefly discussed.

The requirements of C593 for proportioning by weight ignore the traditional mortar proportions of 1 part binder to 3 parts sand by volume. Calculation of the volume proportions of the C593 mortars prepared for this study show that none of those mortars meets these traditional proportions, and are all binder-rich compared to commonly used mortars. The flyash mortar has a volumetric binder:sand ratio of 1.61; the volcanic ash is 1.55; and the calcined clay is 1.01. Volumetric binder:sand ratios should range from 1:2¼ to 1:3, as for C270 (Specification for Mortar for Unit Masonry).

The accelerated curing methods required by C593 are not appropriate for determining the suitability of a pozzolan-lime mortar for masonry. Accelerated methods are common in concrete testing, because the cement has its own heat of hydration, and the accelerated curing is meant to conserve this heat for reaction, rather than add to it. Without significant free lime, however, pozzolan-lime mortars do not have heat of hydration; the vapor heat method of C593 provides heat that is not normally present. This added heat enhances the reactions for the calcined clay-lime and volcanic ash-lime mortars, resulting in anomalously high compressive strengths. Because of this, C593 cannot be considered an accurate predictor of the long-term compressive strength of pozzolan-lime mortars.

Using compressive strength as a measure of the extent of pozzolanic reaction, it is clear from Table 3 and Figure 1 that using prescribed weight ratios of pozzolan to lime and a vapor curing regime does not necessarily promote an optimum pozzolanic reaction. If the intent of C593 is to provide a test methodology to evaluate the potential of a pozzolan-lime reaction, limiting the pozzolan-to-lime ratio to a single weight value defeats its purpose. The test methodology needs to allow for different pozzolan-to-lime weight ratios, in order to accommodate variations in bulk density and to allow for consistent volumetric ratios of binder to sand.

This study does not provide enough information to identify the appropriate relative humidity for curing. Curing at 100% RH does give an indication of the pozzolanic reaction, but it does not address the role of carbonation in strength gain. Further investigation of curing regime is required to evaluate this.

Pozzolan-lime mortars can provide compressive strengths of 5 N/m^2, more than adequate for most masonry applications. Compressive strength, however, is not the only requirement of a mortar. Further investigation of the properties of pozzolan-lime mortars is needed to establish the range of performance properties suitable for masonry mortars. An appropriately modified C593 will be a valuable tool in such investigations.

Acknowledgments

I am grateful to Chemical Lime Company for their continued support. Mr. Rich Godbey provided his usual quality of workmanship in setting up the testing apparatus and his perspicacity in discussing the finer points of mortars. Drs. Paddy Grattan-Bellew and Rolf Feldman, retired from the National Research Council of Canada, Institute for Research in Construction, first interested me in pozzolans. The editors are thanked for their comments, which greatly improved the manuscript.

References

[1] Borona, G. and Binda, L., "Study of the Pozzolanicity of some Bricks and Clays," *Proceedings of the 10th International Brick and Block Masonry Conference*, Vol. 3, Calgary, 1994, pp. 1189–1197.

[2] Martirena Hernández, J.F., Middendorf, B., Gehrke, M. and Budelmann, "Use of Wastes of the Sugar Industry as Pozzolana in Lime-Pozzolana Binders: Study of the Reaction, *Cement and Concrete Research*, Vol. 28, No. 11, 1998, pp.1525–1536,

[3] Shi, C., "Studies of Several Factors Affecting Hydration and Properties of Lime-Pozzolan Cements, *Journal of Materials in Civil Engineering*, 2001, pp. 441–445.

[4] Mehta, P. K., "Concrete, Structure, Properties and Materials", Prentice-Hall, Inc, 1986, pp. 450.

Units

Ian R. Chin[1]

Spalling of Brick

Reference: Chin, I. R., **"Spalling of Brick,"** *Masonry: Opportunities for the 21st Century, ASTM STP 1432*, D. Throop and R. E. Klingner, Eds., ASTM International, West Conshohocken, PA, 2003.

Abstract: Brick is normally selected for use in exterior walls and paving by owners and designers because of its durability, appearance, and low maintenance. However, occasional spalling of the exposed surface of brick in service has occurred that has created concerns on the durability of brick and on the accuracy of the preconstruction indicators of brick durability established by the masonry industry. Investigations of spalled brick performed by the author have revealed that this spalling is primarily caused by water that gained access into the brick. Compressive forces in the wall can also cause spalling of brick. The water absorption preconstruction indicators of brick durability specified by C216 for Grade SW brick were found to be reliable for standard size brick in properly designed and constructed walls exposed to normal weather conditions. However, they may not be reliable for uncored special size brick that are larger than standard size brick, and for brick exposed to weather conditions that are more severe than the C67 freezing and thawing test conditions. Brick that are longer than 8 in. (203 mm) were found to be less durable due to under firing than brick in the same run that are 8 in. (203 mm) or less and that were properly fired. This paper presents information on the causes of spalling of brick as determined from the investigations and on recommendations to minimize spalling of brick on buildings and paving.

Keywords: coatings, compressive forces, corrosion, cryptoflorescence, durability, glazed brick, spalling of brick, water absorption

Introduction

In the United States of America, the durability of brick has been established by its successful long-term performance in structures that are more than 200 years old in a variety of climatic conditions. This demonstrated successful durability of brick is one of the primary reasons why brick is selected by owners and designers for use in buildings. However, occasional spalling of brick has occurred on several buildings and other

[1] Vice President, Principal, and Unit Manager, Wiss, Janney, Elstner Associates, Inc., 120 North LaSalle, Suite 2000, Chicago, IL 60602.

structures. This spalling has occurred on non-glazed brick as well as on glazed brick and on brick that were properly manufactured as well as on brick that were not properly manufactured.

Manufacture of Brick

Brick are made with finely ground clays and shales thoroughly mixed with water to obtain proper plasticity and with materials such as manganese for color changes. The plastic material is then shaped into brick shapes by extrusion, machine molding, or hand moulding. The unfired shaped brick are then dried to limit their moisture content and fired in a kiln at temperatures that vary up to 2,000 degrees F (1,100 degrees C). The color range of brick is determined by the type of clay materials used and by the firing temperature used by the manufacturer. Coatings can also be applied to brick to change its appearance. After firing, brick are allowed to cool. They are then sorted and placed into cubes of about 500 brick for transportation and distribution.

Glazed Brick

Glazed brick are brick that have a bonded ceramic finish on the exposed surface. Single fired glazed brick are manufactured with the glaze applied to the unfired brick and the brick and glaze fired together in a single firing. Double fired glazed brick are manufactured with the glaze applied to a fired brick unit which is fired a second time to fuse the glaze to the brick.

ASTM Specifications

ASTM specification for Facing Brick (Solid Masonry Units Made from Clay or Shale) (C216), specifies the requirements for non-glazed facing brick; ASTM Specification for Glazed Brick (Single Fired, Solid Brick Units) (C1405), specifies requirements for single fired glazed brick; ASTM Specifications for Ceramic Glazed Structural Clay Facing Tile, Facing Brick, and Solid Masonry Units (C126) specifies requirements for double fired glazed brick when the firing temperature of the glaze is greater than 1500 degrees F (815 degrees C); and ASTM specification for pedestrian and light traffic brick (C902) specifies requirements for pedestrian and light traffic paving brick.

Durability of Brick

The measure of the durability of a particular brick for use in a building may be initially estimated by evaluation of its performance in similar existing buildings located in a climatic condition that is similar to the new building. Such information is usually available from the brick manufacturer or distributor. However, because the properties of a particular brick that has performed successfully on existing buildings could be different from the brick manufactured for the new building, laboratory testing of brick for new buildings should be performed to obtain a measure of its durability.

Currently, C216 uses one of the following sets of physical properties of brick determined from laboratory testing performed in accordance with ASTM Methods for

Sampling and Testing of Brick and Structural Clay tile (C67), to indicate the durability of brick at the time of purchase:

1. Compressive strength, water absorption by 5-h boiling, and saturation coefficient (ratio of absorption of 24-h submersion in cold water to that after 5-h submersion in boiling water),
2. Compressive strength, water absorption by 5-h boiling, and "cold water absorption of any single unit of a random sample of five brick does not exceed 8%", or
3. Compressive strength, and a sample of five brick "passes the freezing and thawing test as described in the Rating Section of the Freezing and Thawing Test Procedures of Test Methods C67." One cycle of the C67 freezing and thawing test calls for brick that are soaked/thawed in water at 75 degrees F (24 degrees C) for four hours to be exposed to a temperature of 16 degrees F (-9 degrees C) for 20 hours. Fifty (50) cycles of this test is required, after which, the brick should not break, crack or lose more than 0.5% of its original weight.

Spalling of Brick

For this paper, spalling is defined as fracturing and delamination of the exposed exterior face of brick to a depth of approximately ¼ in. (6 mm). Spalling of brick is primarily caused by the action of water that gains access into brick. Spalling of brick can also caused by applied compressive forces that exceed the ultimate compressive strength of the brick.

Spalling of Brick Due to Action of Water

It is recognized within the masonry industry that properly designed and constructed masonry walls are not impermeable to water penetration, and that when water passes through brick masonry walls it penetrates through minute separations between the brick units and mortar joints in the wall [1]. Of course, the poorer the design and/or construction of the masonry wall, the greater the amount of water that is able to penetrate the wall. Water can also enter brick masonry walls around copings, sills, roof flashing, and through deficiencies in sealant joints, and by condensation. The water that penetrates into brick masonry walls normally leaves the wall via capillary action and evaporation from the exterior face of the wall and through weep holes at flashings in cavity walls. In some cases, the water that penetrates brick masonry walls can cause spalling of brick as discussed below:

Spalling of Brick Due to Freezing of Water Absorbed by Brick

One hundred laboratory freeze/thaw cycles of saturated brick has resulted in reduction of compressive and flexural strength of brick and in an increase in the extent of water absorption of brick [2]. Since the C67 freezing and thawing test calls for only 50 freeze/thaw cycles, brick that meet the durability requirements of C216 and that are exposed to moisture conditions and to accompanying freezing and thawing cycles that are

more severe that the C67 freezing and thawing test conditions may, therefore, spall under these severe exposure conditions.

The vast majority of conditions under which brick are used in exterior walls on buildings do not normally expose the brick to repeated freezing and thawing cycles while the brick are saturated with water in a manner that is similar to the C67 freezing and thawing test conditions. Consequently, except for a few conditions, spalling of brick due to freezing and thawing of water absorbed by the brick does not often occur.

Conditions which have resulted in spalling of saturated brick due to freezing and thawing include the following:

Improperly manufactured brick --Spalling of improperly manufactured brick was observed in the exterior walls on a building in Wisconsin, USA. The walls are a 1 ft, 0 in. (305 mm) thick, multiple wythe masonry wall system consisting of an exterior wythe of brick work and an interior wythe of 8 in. (203 mm) thick concrete block. The exterior wythe of brick work was tied to the concrete block with a header course of brickwork at every seventh course. The brick between the header course are nominally 4 in. x 2-1/4 in. x 8 in. (102 mm x 57 mm x 203 mm) standard size units laid in a running bond. The brick in the header course are uncored dubrick which are special sized brick that are two brick wide and are nominally 8 in. x 2-1/4 in. x 8 in. (203 mm x 57 mm x 203 mm) [3]. The use of dubrick in lieu of standard size brick in the header course maintained the running bond pattern of the brick work in the wall and concealed the existence of the header course. The color of the standard size stretcher brick is brown and the color of the special size dubrick is orange and brown.

Spalling of approximately 20% of the dubrick occurred on the building, as shown in Figure 1. Spalling of the brown stretcher brick did not occur.

The dubrick in the header course span across the collar joint in the wall. This configuration made the dubrick more exposed to water that penetrated the wall than the standard size stretcher brick that did not span across the collar joint.

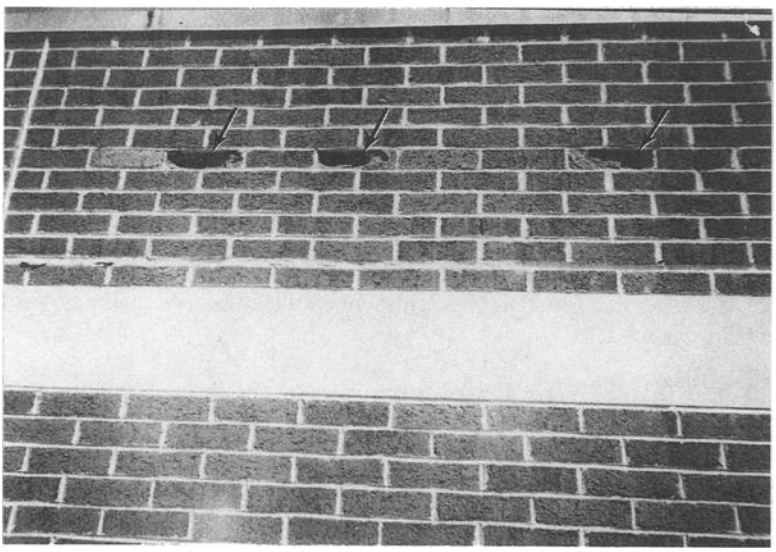

Figure 1--*View of spalled dubrick due to cyclic freezing of saturated brick*

The vast majority of the spalled dubrick on the building occurred within the first 15 years of the life of the building. Subsequently, the rate of the spalling reduced significantly to about one to five spalled brick units per year. Spalling occurred in both orange and brown dubrick with more spalling occurring in the orange dubrick than in the brown dubrick.

Petrographic examination of samples of spalled dubrick revealed that the brick contain cracks and laminations that are indicative of cyclic freezing of saturated brick, and that the brick were poorly constituted and under fired, as demonstrated by severe laminations and variation in internal color of the brick.

Eleven spalled dubrick and five non-spalled dubrick were removed from the building and were tested in accordance with C67 to determine the 24 hour cold water absorption and the 5 hour boiling water absorption properties of the brick at the time of the test. Although these properties will most likely not be equal to the properties of the brick at the time of purchase, they are used in this paper to obtain a measure of the accuracy of the water absorption preconstruction indicators of brick durability specified by C216 for brick at the time of purchase. The results of the tests are presented in Table 1. The test revealed the following:

Table 1--*Water absorption testing of spalled and non-spalled header brick dubrick*

Dubrick	Orientation	Spalled	Absorption, %		Saturation Coefficient	Grade SW
			24h cold water	5h Boiling Water		
1	N	No	6.09	9.28	0.66	Yes
2	N	Yes	8.97	11.29	0.75	Yes
3	N	Yes	11.46	14.19	0.81	No
4	W	Yes	17.46	19.26	0.92	No
5	W	Yes	8.46	11.19	0.76	Yes
6	S	Yes	8.43	11.40	0.74	Yes
7	S	Yes	16.51	18.43	0.90	No
8	S	Yes	18.67	19.84	0.94	No
9	E	Yes	8.72	12.18	0.72	Yes
10	E	No	9.56	12.47	0.77	Yes
11	E	Yes	12.84	15.50	0.84	No
12	S	Yes	6.16	9.19	0.67	Yes
13	S	Yes	7.97	10.32	0.77	Yes
14	W	No	5.85	8.86	0.66	Yes
15	E	No	5.53	9.24	0.60	Yes
16	E	No	10.16	12.98	0.78	Yes
Average			10.46	13.12	0.78	Yes

1. All of the five non-spalled dubrick tested met the saturation coefficient requirement of Grade SW brick.
2. All of the five dubrick tested that do not meet the saturation coefficient requirement of Grade SW brick are spalled.
3. Six of the eleven spalled dubrick tested met the saturation coefficient of Grade SW brick.

As mentioned above, spalling of the brown, standard size stretcher brick did not occur. Water absorption testing of 18 stretcher brick removed from the building revealed that all of the brick tested met the saturation coefficient requirement of grade SW brick and that they have the following average properties:

- 24h cold water absorption: 2.92%,
- 5h boiling water absorption: 5.56%, and
- Saturation coefficient: 0.53.

These tests indicate that the water absorption preconstruction indicators of brick durability for C216, Grade SW brick are reliable for standard size brick units but may not be reliable for uncored special size brick, such as dubrick, that are larger than standard size brick.

Measurement of 55 randomly selected brick (13 spalled dubrick, 33 non-spalled dubrick , and nine stretchers) was made. The results of the measurement are as shown in Table 2.

Table 2—*Results of measurement of randomly selected brick*

Length, in.	**Dubrick**		**Stretcher Brick**
	Spalled	**Non-spalled**	
7-3/4		2	
7-7/8		4	7
8	1	19	2
8-1/8	3	5	
8-14	6	3	
8-3/8	3		
	13	33	9

1. The length of 12 of the 13 (92%) spalled dubrick measured was greater than 8 in. (203 mm) and varies from 8-1/8 in. to 8-3/4 in. (206 mm to 222 mm).
2. The length of 25 of the 33 (75%) non-spalled dubrick measured was 8 in. (203 mm) or less.
3. The length of all of the nine brown stretcher brick measured was 8 in. (203 mm) or less. As previously stated, spalling of the brown stretcher brick did not occur.
4. Twelve of the 20 (60%) dubrick measured that were greater than 8 in. (203 mm) long were spalled.

As previously stated, the petrographic examination revealed that spalled dubrick were under fired. These measurements, therefore, indicate that the dubrick on this building, that are slightly longer than 8 in. (203 mm) were under fired and are less durable due to being under fired than dubrick that are 8 in. (203 mm) or less.

The investigation determined that spalling of 20% of the dubrick on this building occurred because, as determined by the petrographic analysis, the spalled dubrick were poorly constituted, were under fired, and did not meet the saturation coefficient

requirement required for grade SW brick at the time of purchase; that the vast majority of the remaining non-spalled dubrick are most likely of better quality and are not expected to spall; and that non-spalled dubrick that are greater than 8 in. (203 mm) long may potentially spall in the future.

To minimize spalling of brick in walls due to cyclic freezing, this investigation indicates that the specific brick to be used, especially uncored special size brick that are larger than standard size brick, should be tested prior to placement in the wall to verify that they meet the durability requirements of C216 for SW brick. In addition, the wall should be designed and constructed to minimize the amount of water that is able to penetrate the wall, and to collect and rapidly drain out of the wall water that penetrated the wall. ASTM Guide for Reduction of Efflorescence Potential in New Masonry Walls (C1400), provides guidance on how to achieve this design and construction intent.

Spalling of paving brick -When paving brick are placed in paving systems that do not have adequate vertical and horizontal drainage characteristics, the brick will become saturated from ponded water and if the saturated brick are exposed to repeated freezing and thawing over a period of time, the brick may spall, as shown in Figure 2. This exposed condition is more severe than the C67 freezing and thawing test conditions.

This type of brick spalling can be minimized by sloping the top of the paving at least ¼ in. per foot (20 mm per m), place sand in the joints between brick units, and provide a well compacted sub base with good vertical drainage characteristics [4].

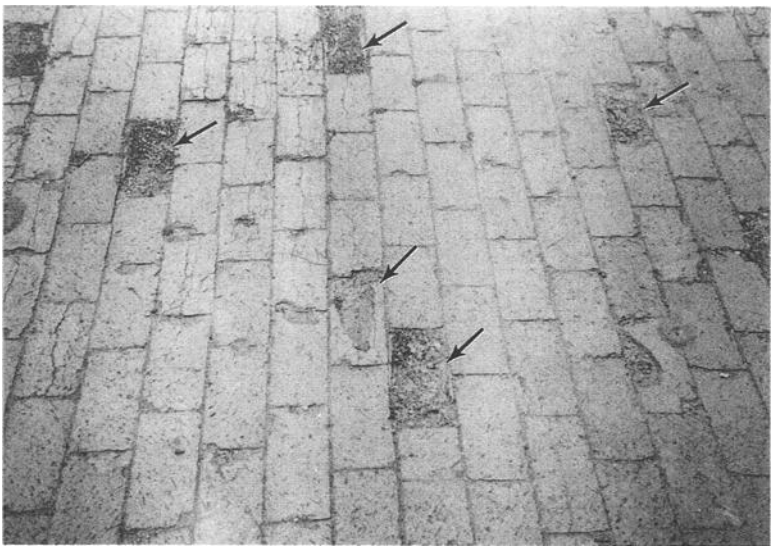

Figure 2--*View of spalled paving brick due to cyclic freezing of saturated brick*

Spalling of Glazed Brick Due to Freezing of Water and to Cryptoflorescence Behind the Glaze

Currently, C1405 uses one of the following sets of physical properties of brick determined from laboratory testing performed in accordance with C67 to indicate durability of single field glazed brick for exterior use at the time of purchase.

1. Compressive strength, 24h cold water absorption, and saturation coefficient,
2. Compressive strength, and 24h "cold water absorption of any single unit shall not exceed 6%", or
3. Compressive strength, and a sample of five brick "passes the freezing and thawing test described in the rating section of the freezing and thawing test procedures of test method C67".

C1405 also requires the glaze on single fired glaze brick not to "craze, spall, or crack when subjected to one cycle of autoclaving".

Currently, for double fired glazed brick, where the firing temperature of the glaze is greater than 1500 degrees F (815 degrees C), C126 specifies a required compressive strength and for the glaze on the brick not to "craze, spall or crack when subjected to one cycle of autoclaving in the crazing test". C126 does not specify water absorption, saturation coefficient or freezing and thawing test requirements to predict the durability of double fired glazed brick as does C216 for non-glazed face brick and C1405 for single fired glazed brick. C126 requires that "where ceramic glazed units are required for exterior use, the manufacturer shall be consulted for material suitable for this purpose." In this case, the manufacturer will most likely rely on historical performance of their brick in exterior exposures as a prediction of glazed brick durability in exterior walls for a particular building.

Similar to non-glazed brick walls, glazed brick walls are not impermeable to water penetration. However, unlike non-glazed brick, the water that penetrates a glazed brick wall cannot evaporate through the impervious glaze on the face of the brick and may become trapped behind the glaze [5]. Freezing of this water can result in internal forces due to confined expansion of the frozen water that are large enough to spall the glaze on the brick, as shown in Figure 3.

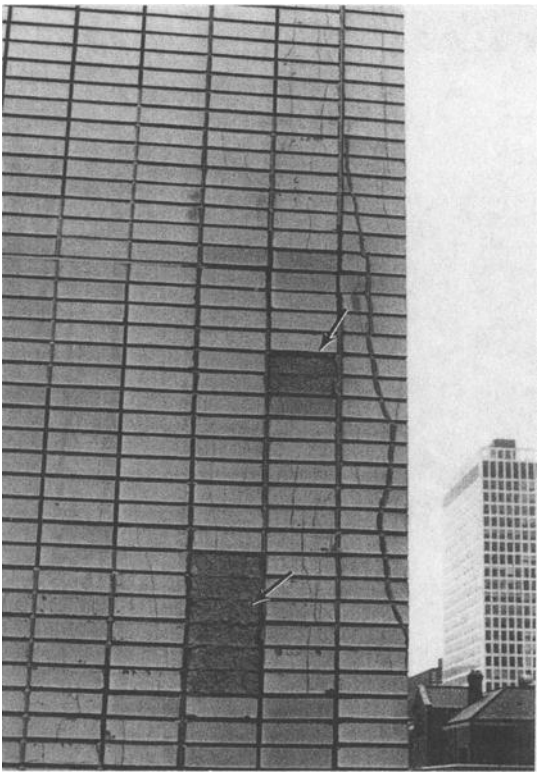

Figure 3--*View of spalled glazed brick due to freezing of moisture trapped by the glaze*

If the materials in a glazed brick wall contain water-soluble compounds, the water that penetrates the wall will dissolve these compounds and bring them towards the exterior surface of the brick. The water and the water-soluble compounds will be prevented from passing through the exterior face of the brick by the glaze. Forces resulting from the build-up of the deposit of the water soluble compounds behind the glaze (cryptoflorescence) can cause the glaze to spall, as shown in Figure 4.

To minimize the occurrence of spalling of glazed brick on buildings, specify and test project specific glazed brick for conformance with app0licable ASTM standards. In addition, the amount of water that is able to penetrate the glaze brick wall, and the potential for the development of efflorescence in the wall should be minimized. C1400 provides information, that if implemented, will reduce water penetration and efflorescence potential in new masonry walls. In addition, the wall should be designed as a vented cavity wall with a proper flashing and weep hole system. The total area of the vents in the wall is recommended by some engineers to be 1/3500 of the area of the wall. The vents should be located adjacent to the top of the wall uniformly along the length of the wall. These vents should be used in conjunction with non-wick type weep holes at the bottom of the wall to form the venting system for the wall.

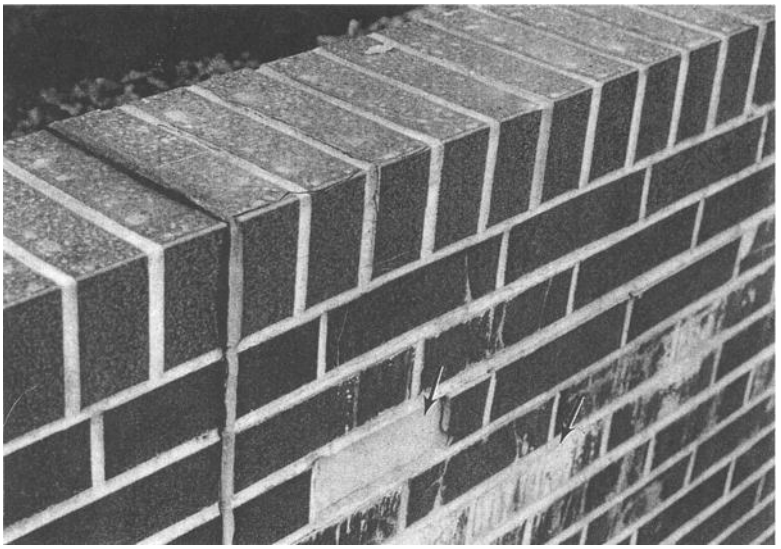

Figure 4--*View of spalled glazed brick due to cryptoflorescence*

Spalling of Brick Due to Freezing of Water and to Cryptoflorescence Behind Coating on Brick

Coatings are sometimes placed on the exterior surfaces of leaky brick masonry walls in an attempt to reduce the amount of water that is able to enter the wall. When the applied coatings prevent water that had entered the wall from evaporating, spalling of the brick can occur from freezing of the water, as shown in Figure 5. Spalling of the brick can also occur due to forces from the build-up of water-soluble compounds in the wall trapped by the coating (cryptoflorescence), as shown in Figure 6. Similar spalling of brick can also occur on walls that were decoratively painted or were covered with stucco, as shown in Figures 7 and 8, respectively.

To prevent these types of spalling of brick from occurring, the use of coatings, paint, and stucco on brick masonry should be avoided.

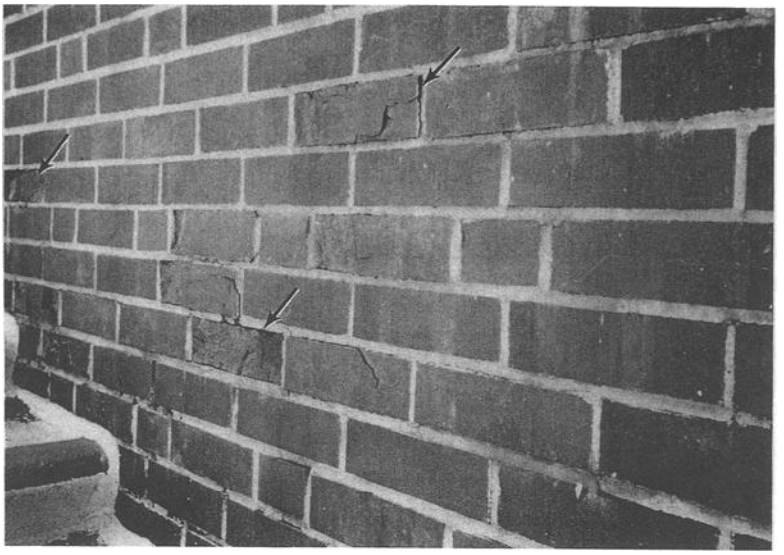

Figure 5--*View of spalled brick due to cyclic freezing of moisture trapped by coating on brick*

Figure 6--*View of spalled brick due to cryptoflorescence behind coating on brick*

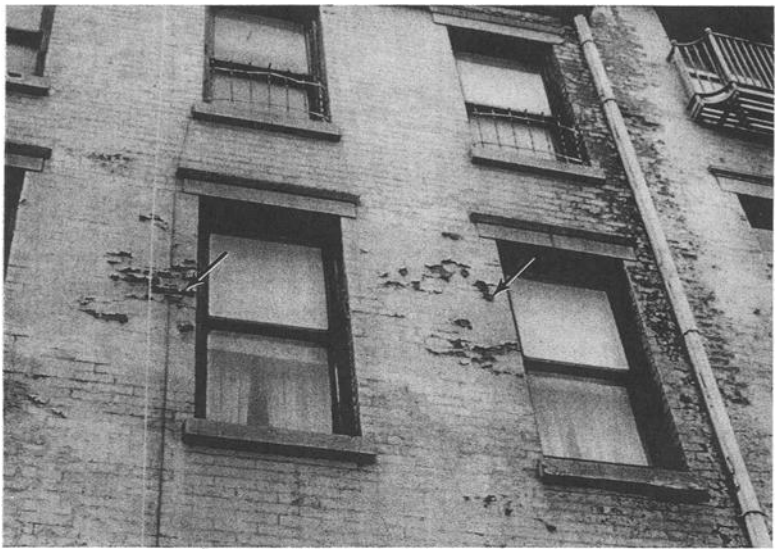

Figure 7--*View of spalled brick due to cyclic freezing of moisture trapped by paint on brick*

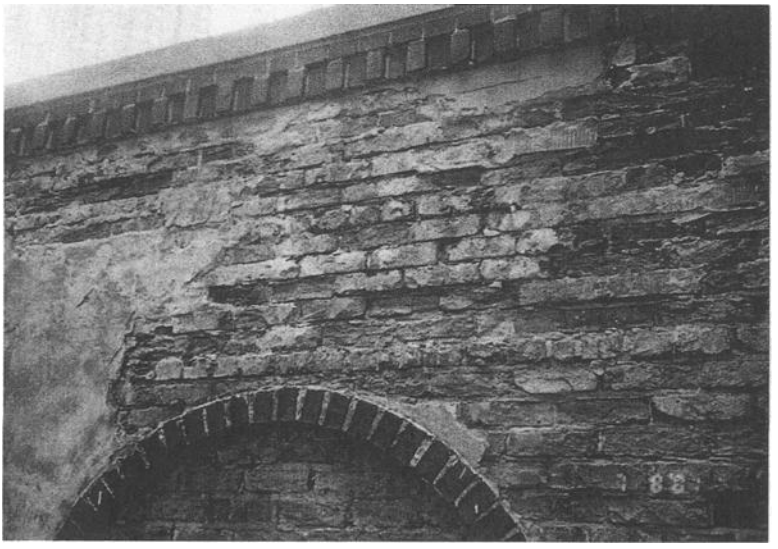

Figure 8 - *View of spalled brick due to cyclic freezing of moisture and to cyptoflorescence behind stucco coating on brickwork*

Spalling of Brick Due to Compressive Forces in Wall

Brick veneer in the exterior walls on tall buildings is often supported on horizontal shelf angles with a horizontal expansion joint between the bottom of the shelf angle and the brick veneer below to reduce the compressive stresses in the veneer. The shelf angles are attached to the structural frame of the building.

At the shelf angles, differential vertical movements occur as a result of upward vertical expansion of the brickwork due to temperature increases and moisture absorption of the brick, and as a result of downward movement of the shelf angle due to shortening of the structure, deflection of the spandrel beam which supports the shelf angle, and to deflection of the shelf angle.

When these differential vertical movements are not accommodated, the brick work and the shelf angle come in contact with each other. When this condition occurs, significant compressive stresses can develop in the brickwork at the shelf angles, which can cause the brick to spall, as shown in Figure 9. To keep this type of spalling from occurring, a horizontal expansion joint should be placed between the bottom of the shelf angle and the top of the brick wall to accommodate the differential vertical movements.

Figure 9--*View of spalled brick due to compressive forces at shelf angle*

When brick masonry walls are constructed between exposed reinforced concrete columns in long buildings, as shown in Figure 10, spalling of brick in the wall can occur due to differential horizontal movements from horizontal expansion of the brickwork and horizontal shrinkage of the concrete frame, as shown in Figure 11. To avoid this type of spalling, vertical expansion joints should be placed between the brickwork and the exposed reinforced concrete columns.

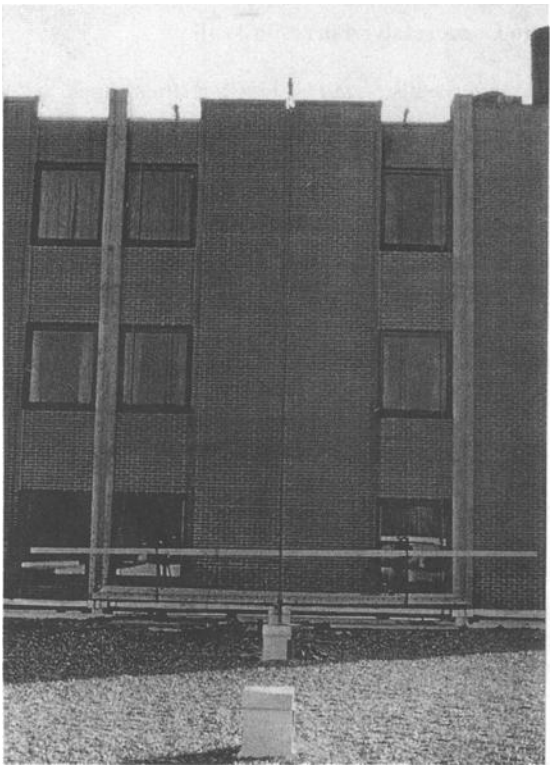

Figure 10--*View of brick wall constructed between concrete columns on a long building*

Figure 11--*View of spalled brick due to horizontal compressive stresses in wall*

Conclusions

Occasional spalling of brick has occurred in exterior walls on buildings and in paving. The cause(s) of the spalling included the following:

1. Freezing of water in poorly constituted and under fired brick,
2. Freezing of water in paving brick exposed to weather conditions that are more severe than the C67 freezing and thawing test conditions,
3. Freezing of water in glazed brick,
4. Cryptoflorescence behind the glaze on glazed brick and behind coatings, paints, and stucco applied on brick,
5. Compressive forces due to differential vertical and horizontal movements in the wall.

The water absorption preconstruction indicators of brick durability for C216 Grade SW brick were found to be reliable for the standard sized brick units evaluated. However, they may not be reliable for uncored special size brick that are larger than standard size

brick such as dubrick which are 8 in. x 2-1/4 in. x 8 in. (203 mm x 57 mm x 203 mm) in size.

Brick that were not properly fired (underfired) were found to be slightly longer than the ones that were properly fired, therefore, brick from the same run that are longer than the other brick may not be as durable.

Recommendations

Perform the following to reduce spalling of brick:

1. Perform preconstruction testing on brick specifically manufactured for the project especially on uncored special size brick that are larger than standard size brick.
2. Use brick that meet the durability requirements of the ASTM standard.
3. Design and construct walls to minimize water penetration and efflorescence potential in the walls in accordance with C1400.
4. Use vented cavity walls for exterior walls with glazed brick.
5. Avoid the use of paint, coatings, and stucco on exterior brick masonry walls.
6. Design and construct brick paving with a proper drainage system.

References

[1] "Water Resistance of Brick Masonry, Design and Detailing, Part 1 of III," Technical Notes 7 revised, Brick Institute of America, Reston, VA, February 1985, pp. 1.

[2] Palmer, L.A. and Hall, J.V. "Some Results of Freezing-and-Thawing Tests Made with Clay Face Brick," Proceedings of the American Society for Testing and Materials, Volume 30, Part II, Philadelphia, PA, 1930.

[3] Plummer, Harry C. and Reardon, Leslie J., Principles of Brick Engineering, Structural Clay Products, Washington, DC., 1943, pp. 20.

[4] Chin, I. R. and Monk, C.B., "Design of Pavements to Resist Weathering," Proceedings of the Second North American Masonry Conference, Donald W. Vannoy and James Colville, Eds, The Masonry Society, 1982, Section 35.

[5] "Ceramic Glazed Brick Facing for Exterior Walls," Technical Notes 13, Brick Institute of America, Reston, VA, March 1982, pp.1.

DISCUSSION

T. Young [1] *(written discussion)*— Is there a minimum vapor transmission rate for a coating to avoid spalling?

I. Chin (author's closure)— The minimum range of water vapor permeance for a coating on brick to allow the transmission of moisture from the interior of the wall through it and avoid spalling of brick due to freezing of entrapped water is 5 to 10 perms. However, regardless of their water vapor permeance, coatings will not allow the transmission of efflorescence compounds in the wall through them. This trapped efflorescence will result in spalling of the brick from the pressure caused by the build up of efflorescence behind the coating (cryptoflorescence).

[1] Lynwood, WA 98036

Christopher L. Galitz[1]

Variability In Brick Unit Test Results

Reference: Galitz, C. L., "**Variability in Brick Unit Test Results,**" *Masonry: Opportunities for the 21st Century, ASTM STP 1432*, D. Throop and R.E. Klingner, Eds., ASTM International, West Conshohocken, PA, 2003.

Abstract: For centuries, brick masonry has been used as a structural and non-structural material, with requirements for strength and other properties often specific to a particular project. To determine these properties, various ASTM and other test methods have been standardized and incorporated into building codes and project documents. The results of standardized testing are typically used as verification that a particular brick meets the property requirements of a particular project. Unfortunately, there is a high degree of variability in some test results. This is due to a combination of variations in actual material properties and variations in the way a particular test method is performed from laboratory to laboratory and operator to operator.

This paper reports statistical analyses of previously published and unpublished test results for compressive strength, IRA, absorption, and other properties of various brick tested at a number of laboratories in the United States. Variability in the results is quantified and statistical significance of the variations presented. Recommendations for modifications to standardized tests, including the number of specimens tested as a sample is also presented. Topics including precision, bias, and sampling methods are discussed as they relate to the testing methods and results presented.

Keywords: brick units, strength testing, statistical variation, absorption testing, precision and bias, sampling methods, sample sizes

Introduction

In the manufacture of brick units, or nearly any other product, there is inherently a variation from unit to unit that can have a significant effect on the performance of that product. In the case of brick, the performance of the product is judged based on results of various types of tests performed in accordance with the ASTM Standard Test Methods for Sampling and Testing Brick and Structural Clay Tile (C 67). Further, in the performance of these tests, even with identical units, there is variation from person to person or laboratory to laboratory in precisely how the test is performed, which adds a further variation in the test results.

In an ideal case, every brick unit manufactured would be tested in accordance with

[1]Senior Project Director, LZA Technology, 641 Avenue of the Americas, New York, New York 10011.

ASTM standards to define exactly the properties of that particular run of units. However, this is a practical impossibility. Therefore, it is necessary to find the compromise between the practicality of being able to ship out as many units as possible and testing a sufficient number of units to have an accurate estimate of the properties of the entire population of units being shipped. The variability from test result to test result must be considered in deciding how accurate the estimate of the properties needs to be and thus how many of the units need to be tested to produce that estimate.

The intent of this paper is to characterize the sources of the variability of test results and present data that quantifies the amount of variability that should be expected. With this information, the paper will go on to present a statistical analysis of the data with pertinent conclusions and recommendations based on that analysis. It is not the intent of the paper to produce results that apply to every brick unit size or type. However, the methods presented can be applied by specifiers, manufacturers, or investigators to apply to specific brick products not included within the scope of this paper.

Sources of Variability

The process of brick manufacture and testing involves three distinct phases that may affect the ultimate results. The first phase is the manufacture of the units themselves. In this step, the selection of raw materials, the type and relative wear of the equipment, and the handling procedures each introduce potential variability in actual material properties. The second phase is in the selection of units to be tested. In a run of brick, it is evident from visual inspection that at least the aesthetic characteristics vary depending on location on kiln car and many other factors. These same factors can introduce variation in the physical properties of the units themselves. Therefore, depending on which units are chosen to represent the run of brick, test results can vary. The third phase is the testing of the units. Each laboratory typically has its own setup of equipment, its own training procedures, and its own interpretation of the language of the testing standard. All of these taken together can lend significant variability to the reported test results.

Brick Testing Methods

Typically, brick units to be used in façade applications are to meet the durability requirements of ASTM Standard Specification for Facing Brick (Solid Masonry Units Made from Clay or Shale) (C 216), and other requirements for appearance as specified in project documents. These requirements necessitate determination of size, weight, cold water absorption (24-hr abs.), boiling water absorption (5-hr abs.), saturation coefficient, and compressive strength (strength). In addition, tests that are sometimes, but not typically, performed for face brick include initial rate of absorption (IRA) and modulus of rupture (MOR). All these tests are defined within ASTM C 67. Each test method has a requirement for the number of brick units (specimens) to be tested with results averaged to give the data for the sample. Table 1 lists the sample sizes for each of the listed test methods as well as the typical requirements used.

Table 1 – *Typical requirements for brick testing and results*[1]

Test	Specimens	Units	Average	Min[2]	Max[2]
Length	10	in.	7-5/8	7-3/8	7-7/8
Width	10	in.	3-5/8	3-1/2	3-3/4
Height	10	in.	2-1/4	2-5/32	2-11/32
Gross Area	10	sq. in.	27.64	25.81	29.53
24 hr abs.	5	% dry wt.	--	--	8.0[3]
5 hr abs.	5	% dry wt.	17.0	--	20.0
Sat. coeff.	5	ratio	0.78	--	0.80
Strength	5	psi	3000	2500	--
IRA[4]	5	g/30 sq. in./min.[5]	N/A	5[6]	30[6]
MOR[4]	5	psi	N/A	N/A	N/A

[1] All requirements are based on standard modular (4 in. by 8 in. nominal size) brick, Grade SW, Type FBS, as defined in ASTM C 216.

[2] For each specimen within sample

[3] Requirement to meet Absorption Alternate (all specimens)

[4] Tests not required to meet ASTM C 216 standards.

[5] Hereafter referred to as g/min.

[6] Typical range for the majority of brick

Testing Results

During 1996 to 2000, a total of four series of round robin tests of brick units were conducted nationally, coordinated by the Cement and Concrete Reference Laboratory (CCRL) of Gaithersburg, Maryland [1]. In each series, two sets of brick units were shipped to the participating laboratories that then tested the brick and reported the results. Of the eight sets, seven were standard modular and one was a 4 in. x 12 in. nominal brick. The results were then combined and analyzed using the methods of the ASTM Standard Practice for Conducting an Interlaboratory Study to Determine the Precision of a Test Method (E 691). The analysis reduced each of the eight data sets to an average (mean), standard deviation, and coefficient of variation (CoV). The CoV is defined as the standard deviation divided by the mean and gives a non-dimensional measure of the spread of the data for each data set. The CoVs are comparable over the full range of the eight sets to give overall values of all the brick represented by the samples. Table 2 lists the average values and standard deviations for each of the eight samples and the weighted average CoVs for each test method. The number of labs listed is the total for all eight sets, after outlying data values were removed from consideration.

Table 2 – *Results of CCRL's interlaboratory studies*

Test	# Labs		1	2	3	4	5	6	7	8	CoV
Length	154	Mean	7.63	11.77	7.63	7.98	7.53	7.65	7.65	7.64	0.5%
		S.D.	0.03	0.03	0.02	0.04	0.04	0.10	0.03	0.04	
Width	154	Mean	3.56	3.66	3.57	3.70	3.46	3.52	3.59	3.61	0.8%
		S.D.	0.02	0.02	0.02	0.03	0.02	0.07	0.01	0.03	
Height	153	Mean	2.26	2.28	2.27	2.22	2.24	2.25	2.23	2.27	1.0%
		S.D.	0.02	0.02	0.02	0.02	0.04	0.05	0.02	0.02	
Area	147	Mean	27.19	43.18	27.25	29.51	26.02	27.04	27.43	27.55	1.1%
		S.D.	0.23	0.38	0.16	0.37	0.26	0.84	0.19	0.28	
Weight	148	Mean	1536.1	2922.8	1536.5	2014.2	1475.2	1727.7	1655.5	1930.3	0.7%
		S.D.	4.3	9.1	4.8	23.8	20.0	23.7	7.4	11.1	
24 hr	151	Mean	9.0	3.7	9.6	4.0	8.4	9.4	6.0	3.0	10.6%
		S.D.	1.1	0.7	0.2	0.6	0.5	1.1	0.5	0.3	
5 hr	152	Mean	10.6	4.7	10.6	6.3	9.9	13.1	7.5	3.9	10.6%
		S.D.	1.1	0.7	0.6	0.8	0.7	1.8	0.7	0.4	
S.C.	138	Mean	0.88	0.80	0.89	0.61	0.85	0.70	0.76	0.74	4.6%
		S.D.	0.03	0.03	0.04	0.04	0.05	0.06	0.03	0.02	
Strength	153	Mean	7418	10721	7196	12467	10236	3489	13174	14591	29.2%
		S.D.	2084	3763	2228	4060	3709	1426	2064	2120	
IRA	116	Mean	45.1	8.9	28.6	15.0	21.4	65.7	10.0	4.6	44.4%
		S.D.	33.2	6.5	9.4	4.8	8.1	27.3	2.0	1.7	
MOR	114	Mean	1382.7	1762.5	1072.6	1494.2	1115.3	706.5	1169.2	1306.9	45.1%
		S.D.	781.1	1012.3	481.3	551.0	387.4	268.2	566.8	600.2	

Precision and Bias of Results

The results presented in Table 2 are in some cases significantly variable. Specifically, one of the most commonly run tests, that for determining compressive strength, has a coefficient of variation of 29.2%. Using ASTM E 691 to determine an appropriate precision and bias statement for the compressive strength test method, the CoV is multiplied by twice the square root of two to give a between laboratories precision value of 82.6% reproducibility. This effectively means that if two laboratories perform compressive strength testing of samples of the same run of brick units, the average strength values reported by the two labs can differ by as much as 82.6% and still be within the range predicted by the test method. The bias associated with compressive strength testing is none, as the test method defines the property.

It was recognized by Robinson et. al that variability in test results was present and in some cases, was undesirable [2]. They designed a research study to limit specifically the variability in the results by hand-picking brick from kiln cars in specific and

consistent locations and conducting some of the ASTM C 67 test methods on those brick within the same laboratory. The number of specimens for each method was increased to better characterize the variability. Based on the sources of the variability explained above, the second and third phases were effectively removed, leaving only the variability within the manufacturing process. The results from the interlaboratory study summarized in Table 2, the resulting precision values described above, and the variations based on the research of Robinson, et. al are included in Table 3.

Table 3 – *Interlaboratory precision values and results from Robinson, et. al*

Test	CCRL data		Robinson, et. al data	
	CoV	Precision	# specimens	CoV
Length	0.5%	1.4%		
Width	0.8%	2.2%		
Height	1.0%	2.9%		
Gross Area	1.1%	3.1%		
Weight	0.7%	2.0%		
24 hr abs.	10.6%	30.0%	180	4.1%
5 hr abs.	10.6%	30.0%	180	3.0%
Sat. coeff.	4.6%	12.9%	180	1.4%
Strength	29.2%	82.6%	55	27.0%
IRA	44.4%	125.6%	336	11.0%
MOR	45.1%	127.5%	60	28.6%

From Table 3, it can be seen that the variability in results from the interlaboratory study typically stems partially from material variation and partially from sample selection and testing. Further, the relative proportions of the components of the variability differ from test to test. The most commonly used, compressive strength, has a variability in results based nearly completely on variation in the product itself, as displayed in the Robinson, et. al paper. Consideration of the data also shows that the seemingly high degree of variation in results of the interlaboratory study is reasonable and the accuracy of the test methods can be further studied.

Accuracy and Sample Sizes

ASTM Standard Practice for Calculating Sample Size to Estimate, With a Specified Tolerable Error, the Average Characteristic for a Lot or Process (E 122) presents methods for determining the number of samples (or specimens) required to give an estimate for an average value of a normal population, within a specified range, with a specified level of confidence. For example, the method can be used to determine how many brick units would need to be tested to determine the average compressive strength of all brick units of that run within 10%, with a confidence of 90%. Conversely, the

method can be used to determine the confidence that the current ASTM C 67 test methods estimate the average properties of the population within a given percentage.

The steps involved in determining a sample size sufficient to predict accurately the mean of a population are first to determine the required level of confidence, second assign the appropriate value of f given for that level of confidence, third determine an acceptable error, e, and finally compute the number of specimens, n, using Equation 1.

$$n = \left(\frac{f \cdot CoV}{e} \right)^2 \tag{1}$$

By specifying n and the level of confidence, the error in Equation 1 becomes

$$e = \sqrt{\frac{(f \cdot CoV)^2}{n}} \tag{2}$$

Using Equation 2 and the number of specimens of each of the test methods considered above, values for e can be computed. In this instance, the accuracy with which we would be 90% confident our brick test would predict the true mean of the population of brick units being sampled and tested. These values for e are presented in Table 4. Note that for a 90% level of confidence, f is 1.64.

Table 4 – *Accuracy of ASTM C 67 test results*

Test	n	CoV	e	Example value and e	
Length	10	0.5%	0.3%	7-5/8 in.	0.023 in.
Width	10	0.8%	0.4%	3-5/8 in.	0.015 in.
Height	10	1.0%	0.5%	2-1/4 in.	0.011 in.
Gross Area	10	1.1%	0.8%	27.64 sq. in.	0.22 sq. in.
Weight	5	0.7%	0.5%	1600 g	8 g
24 hr abs.	5	10.6%	7.8%	8.0%	0.62%
5 hr abs.	5	10.6%	7.8%	17.0%	1.33%
Sat. coeff.	5	4.6%	3.4%	0.78	0.027
Strength	5	29.2%	21.4%	3000 psi	642 psi
IRA	5	44.4%	32.6%	20 g/min.	6.52 g/min.
MOR	5	45.1%	33.1%	1200 psi	397 psi

Inspection of the accuracy values in Table 4 reveals that for the example values given, the error in the testing results predicted at a 90% level of confidence in some cases far exceeds the ranges specified and/or commonly used, as listed in Table 1. This variability in results may or may not be acceptable, depending on project requirements and project-specific test results.

Increasing Accuracy of Results

The accuracy, or relative inaccuracy, of testing results is linked to the manufacture of the units, selection of the specimens that constitute the sample to be tested, and the way in which the units are tested. To produce more consistent, and therefore more accurate, results implies limiting the variability in each of these stages. However, it would be a practical impossibility to produce identical units, select ideal specimens, and make every testing laboratory in the world identical in equipment and training. Therefore, the accuracy of the results can only be practically increased by increasing the number of specimens tested, thereby increasing the percentage of the population represented by the sample.

It is common practice to hold the acceptable error associated with a predicted average value at 10%. In the case of some brick testing methods, this value may be too restrictive and in the case of others, too loose. For some project requirements, most notably in loadbearing brick masonry applications, increasing accuracy may only be required where the actual results are close to the minimum or maximum acceptable values. For example, a brick that tests to a compressive strength of 8000 psi with a predicted error of 1000 psi may be perfectly acceptable for a project that requires only a 5000 psi strength. Therefore, results of the standard tests should be carefully compared to project requirements before increasing the number of specimens to be tested.

Conclusions

Fired clay brick masonry units are highly variable in physical properties. Further, laboratories conducting the test methods contained in ASTM C 67 introduce additional variability in reported results. This variability is expected due to variations in materials, manufacturing conditions, sample selection and testing conditions.

Examination of test results for eight sets of brick specimens tested by approximately 150 laboratories reveals a predictable variability for the results of most ASTM C 67 test methods. This variability has an associated error value that for the majority of the methods is well within the industry standard acceptable error of 10%. However, in the cases of compressive strength, initial rate of absorption, and modulus of rupture, the predicted error of the results significantly exceeds the acceptable error value.

Due to practicalities in the manufacturing and testing processes, it is most appropriate to decrease the variability in test results by increasing the number of specimens to be tested. However, in many applications, the variability of the results using the standard number of specimens may be perfectly acceptable and the increase in the number of tested specimens would not be necessary.

References

[1] Proficiency Sample Program, The Cement and Concrete Reference Laboratory, Gaithersburg, Maryland, 1996-2000.

[2] Robinson, G.C., Borchelt, J.G., and D. A. Brosnan, "Attempts to Obtain a Standard Research Brick from Commercial Production", *Proceedings of the Seventh North American Masonry Conference*, The Masonry Society, Boulder, CO, June 1996, pp. 759-772.

Eric J. Seaverson,[1] Denis A. Brosnan,[2] James C. Frederic, Jr.,[2] and John P. Sanders[2]

Predicting the Freeze-Thaw Durability of Bricks Based on Residual Expansion

Reference: Seaverson, E. J., Brosnan, D.A., Frederic, Jr., J.C., and Sanders, J.P., "**Predicting the Freeze-Thaw Durability of Bricks Based on Residual Expansion,**" *Masonry: Opportunities for the 21st Century, ASTM STP 1432,* D. Throop and R. E. Klingner, Eds., ASTM International, West Conshohocken, PA, 2003.

Abstract: The response of saturated brick masonry units to internal freezing water was studied in an attempt to improve the accuracy of freeze-thaw durability predictions currently described in ASTM C 67. Cryogenic dilatometry was employed to study the change in length, or response, of water-saturated brick during freeze-thaw cycles. In all cases, a permanent, or residual, expansion was observed.

Residual expansion varied from approximately 0.01% to 0.08% for different commercially available brick for a single freeze-thaw cycle. No strong correlation was found between residual expansion and physical properties cited in current ASTM specifications.

Research on lab-fired extruded brick showed that the amount of residual expansion is related to the "maturity," or amount of "heat work" expended, in firing of the brick. Comparison of lab- and plant-fired brick with similar water adsorption values yielded considerable differences in residual expansion, reflecting a lack of correlation between physical properties and durability.

Residual expansion may be a quantitative index reflecting the freeze-thaw durability of brick, and may result in a more definitive and faster test procedure than that described in ASTM C 67.

Keywords: freeze-thaw durability, residual expansion, brick

Introduction

Since the 1920s, the physical properties of brick have been extensively studied in order to ascertain physical property requirements that constitute a durable brick. [*1*] One

[1] Staff Engineer, Simpson Gumpertz & Heger Inc., 297 Broadway, Arlington, MA 02474
[2] Professor and Director, Associate Director, and Research Associate, respectively, The National Brick Research Center, Clemson University, 100 Clemson Research Boulevard, Clemson, SC 29634

durability issue that is still being studied is the relationship between physical properties and freeze-thaw durability. ASTM C 216 specifies physical property requirements that classify facing bricks as "Severe Weather Grade" (SW) or "Moderate Weather Grade" (MW). These classifications are, in effect, predictions of freeze-thaw durability of the brick. Using the ASTM standards, the majority of modern SW brick do not exhibit freeze-thaw failures in service. Unfortunately, in some instances, facing brick that qualify as SW in the ASTM requirements have exhibited freeze-thaw failures, and some brick that do not meet the physical property requirements are known to be durable in service.

From years of research on the freeze-thaw durability of brick, the general physical properties that attribute to freeze-thaw durability are known. Unfortunately, there are complex interactions between physical properties in brick, and accurate prediction of field durability based on physical properties beyond about 80% accuracy has not been achieved in North America.

As a means for prediction, performance-based freeze-thaw testing has become a preferred approach by many researchers. [2–4] Typically, these tests may not fully simulate the stresses imposed in an actual freezing and thawing event. According to Franke and Bentrup, existing European performance-based tests failed to properly predict frost resistance in one of every five cases. [5] In addition, some researchers believe that durability is related to the pore structure and particularly to the smallest pore fraction, leading some researchers to rely solely on pore-structure-related durability indices. [6–7]

Water expands approximately 9% by volume during the phase change from liquid to solid (ice). Freezing water that expands within the pore phase of a brick induces internal expansive stresses and the brick exhibits an increase in volume. The increase in volume of the brick material is typically within the elastic response region, but some inelastic response takes place. With each freezing and thawing cycle, the inelastic response can result in fracture of a relatively small number of vitreous bonds on a microscopic scale in a "fatigue-like" process, leading to permanent expansion, or it can, over time, result in the initiation and propagation of a relatively major crack leading to freeze-thaw failure. [8]

The objective of this study was to quantify the expansion phenomena on freezing of saturated brick to understand the mechanism of freeze-thaw failures, and determine how the response to freezing is affected by the degree of firing.

Procedure

In the first phase of this study, seven different commercially available brick were obtained from six North American manufacturers in the fired state. The brick were chosen based on raw material constitution and forming processes as are typical of North American manufacturing conditions (Table 1). Each brick was tested in accordance with the American Society of Testing and Materials (ASTM) Method C 67. Mercury intrusion porosimetry was employed to determine the pore structure of each brick.

Table 1 – *Commercial Bricks Employed In Cryogenic Dilatometry Studies*

Brick	Forming Process	Composition
A	Extruded (three cores)	Clay with about 10% sawdust (by volume)
B	Extruded (ten cores)	Kaolin/Shale (50% shale)
C	Extruded (three cores)	Clay
D	Extruded (solid)	Shale
E	Molded	Clay
F	Dry Pressed	Shale
G	Dry Pressed	Fireclay

For the second phase of this study, one additional brick, primarily composed of shale, was obtained from a manufacturer in both the dried and fired state. The brick obtained in the dried state were lab-fired with simulated production cycles to yield several adsorption levels. The freeze-thaw behavior of the lab-fired brick were compared to plant-fired brick of the same composition. The goal of this investigation was to determine if the residual expansion measurements were capable of distinguishing between samples of the same type of brick with different physical properties.

To monitor differential linear expansion during freeze-thaw cycles, a Netzsch 402C dilatometer was used. The dilatometer with the cryogenic "furnace" is capable of measuring at temperatures between 932 °F (500 °C) and -256 °F (-160 °C) with a linear sensitivity of 4.9×10^{-8} (1.25 nm). The typical freeze-thaw cycle consisted of cooling from 68 °F (20 °C) to 5 °F (-15 °C) at 0.9 °F (0.5 °C) per minute, holding at 5 °F (-15 °C) for two minutes, and heating from 5 °F (-15 °C) to 68 °F (20 °C) at a rate of 0.9 °F (0.5 °C) per minute. Cooling of the specimen chamber was carried out with nitrogen gas (originating from liquid nitrogen) without contact between the specimen and cooling gas. During testing, the specimen chamber was purged with helium at a rate of 0.002 cubic feet (50 ml) per minute to remove moisture in the specimen chamber and prevent condensation and freezing of water vapor on moving parts in the instrument.

For the evaluation of fired brick, whole brick of each type were randomly selected from the brick provided by each manufacturer. Test specimens were cut from the internal section of each brick. Test specimens were approximately 0.25 in. (6.4 mm) square by 1 in. (25.4 mm) long. Testing was primarily conducted at full saturation (i.e. 5 hour boiling-water absorption) and at orientations parallel and perpendicular to the depth of the brick (nominal 2.5 in. or 63.5 mm dimension). Although higher than a typical in-service brick may experience, fully saturated specimens were tested to "magnify" differences between samples. A limited number of specimens were tested at a saturation level of 24-hour cold-water absorption. A few dry specimens were tested to demonstrate that all expansion phenomena originated from the consequences of freezing of absorbed water.

For lab-fired brick, simulated production firing cycles were first performed on fully dried brick to achieve the desired physical properties. After the lab firing, these bricks were prepared for measurement in the same manner that has been described for the plant-fired brick. All lab firings were conducted in a natural-gas-fired furnace.

Preparation of the specimens for testing at a level of full saturation was accomplished using vacuum submersion (approximately 14.5 psi or 1 bar). Because the

specimens lost a small amount of moisture during a single freeze-thaw cycle in the dilatometer, specimens were re-saturated in the vacuum after each freeze-thaw cycle.

Results and Discussion

Physical Properties of Commercial Brick

Physical properties for each brick type are listed in (Tables 2 and 3). The properties listed in (Table 2) are those cited in ASTM C 216, or other properties that previous investigators have related to durability. All samples included in this study passed the ASTM C 67 freezing and thawing test (50 consecutive cycles).

For the mercury porosimetry data, the percent of pores with diameters less than 3.94×10^{-4} in. (10 μm) and 3.94×10^{-5} (1 μm) are indicated in (Table 3). The majority of water that enters a brick is drawn by capillary action. Because capillary action ceases to occur in pores with diameters greater than 3.94×10^{-4} in. (10 μm), the amount of pores less than that are considered. Many investigators have investigated the pore sizes that contribute to freeze-thaw failure. Findings of such studies suggest that the water in pores with diameters less than 3.94×10^{-5} (1 μm) is responsible for freeze-thaw failures. [*5*]

Table 2 – *Average Physical Properties of Brick Specimens (ASTM C 67)*

Brick	Forming Method	Compressive Strength psi (MPa)		MOR psi (MPa)		CWA (%)	BWA (%)	C/B Ratio	IRA g/30 in^2 (/193 cm^2)
A	Extruded	7,893	(54.4)	994	(6.9)	10.32	16.23	0.64	35 (225)
B	Extruded	8,211	(56.6)	1,673	(11.5)	10.69	11.85	0.90	40 (256)
C	Extruded	12,853	(88.6)	1,528	(10.5)	4.02	5.43	0.74	11 (71)
D	Extruded	16,731	(115.4)	1,810	(12.5)	4.48	7.16	0.63	10 (65)
E	Molded	12,034	(83.0)	1,271	(8.8)	5.84	8.67	0.67	12 (78)
F	Pressed	10,665	(73.6)	1,683	(11.6)	6.64	8.6	0.77	58 (372)
G	Pressed	12,135	(83.7)	8,03	(5.5)	4.69	6.24	0.75	34 (217)

By initial inspection, all plant-fired samples are classified as SW (severe weather) by physical property requirements in ASTM C 216, except Sample B, which has a C/B ratio of 0.90 (The ASTM requirement is less than 0.78). Upon further inspection, because Sample B passed the freezing and thawing test (50 consecutive cycles), ASTM C 216 classifies Sample B as SW by the "freezing and thawing alternate."

Table 3 – *Mercury Porosimetry Results for Brick Samples*

Brick	Porosity (%)	Median Pore Diameter 10^{-3} in. (μm)	Pores < 3.94×10^{-4} (10 μm) (%)	Pores < 3.94×10^{-5} (1 μm) (%)
A	27.26	0.09 (2.37)	78.3	22.8
B	24.55	0.02 (0.45)	94.0	83.8
C	14.49	0.06 (1.44)	91.7	32.3
D	17.77	0.81 (2.07)	90.3	22.1
E	21.90	0.06 (1.49)	92.2	25.9
F	14.03	0.21 (5.43)	78.8	11.7
G	12.36	0.16 (3.97)	69.1	26.6

Dilatometer Testing

All dilatometer test results were corrected for the thermal characteristics of the apparatus using the manufacturer's standard software. Typical behavior of the saturated specimens during freeze-thaw cycles is illustrated in (Figures 1 and 2). (Figure 1) is a time-based plot, with a solid line indicating differential expansion and a dashed line indicating specimen temperature. (Figure 2) is a temperature-based plot of the same data. The solid line in Figure 2 indicates differential expansion during the cooling portion of the freeze-thaw cycle, and the dashed line indicates differential expansion during the heating portion of the cycle.

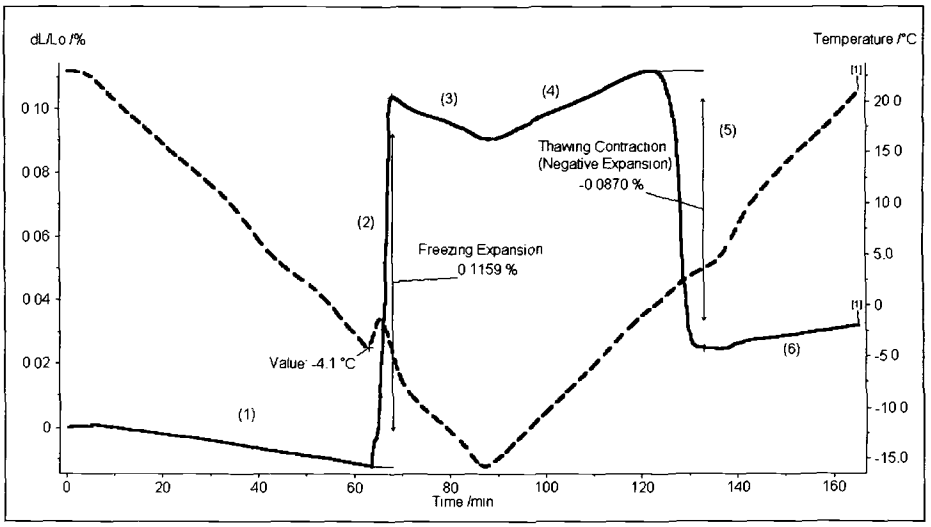

Figure 1 – *Typical Behavior of Fully Saturated Specimens (Time-based plot)*

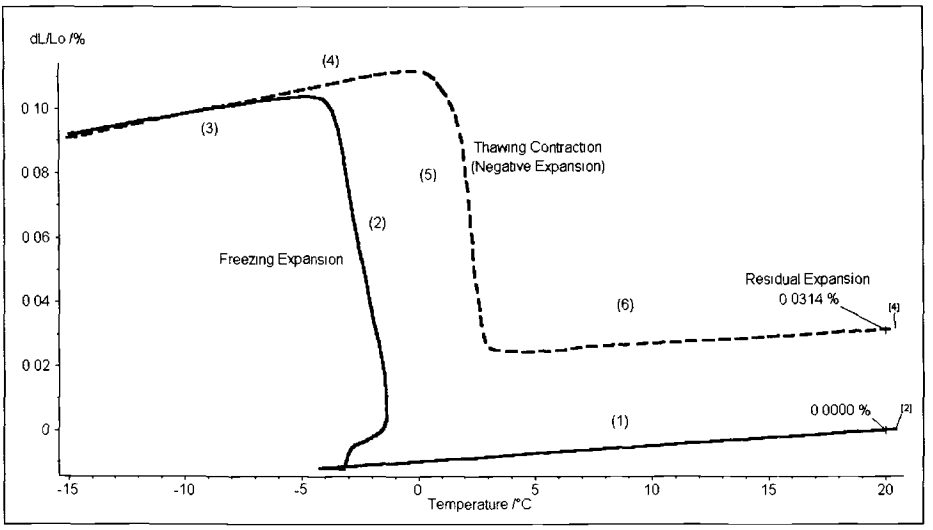

Figure 2 – *Typical Behavior of Fully Saturated Specimens (Temperature-based plot)*

Testing starts by cooling the specimen below room temperature. As the specimen begins cooling, it slowly decreases in length, indicated by (1) on the plots. For the specimen shown in (Figures 1 and 2), at approximately 25 °F (-4.1 °C), the water within the pores of the specimen freezes, causing a large expansion, indicated by (2). The water appears to freeze within the brick at a temperature somewhat below 32 °F (0 °C) due to heat-transfer effects, pressure in the pores, and the presence of soluble salts within the brick.

The increase in length caused by the phase change of water is termed "freezing expansion." As cooling of the brick continues, the specimen length slowly decreases, as indicated by (3). After reaching the desired minimum temperature of 5 °F (-15 °C), the specimen is heated back to room temperature. As heating begins, the specimen slowly increases in length, as indicated by (4). At approximately 32 °F (0 °C), the phase change of the ice occurs (returning back to liquid), releasing the pressure in the pores and causing the specimen to decrease in length, as indicated by (5). The decrease in length may be called "thawing contraction" (indicated by negative expansion). As heating continues to room temperature, the specimen slowly increases in length, as indicated by (6).

Differential expansion between cooling and heating cycles can be seen above 32 °F (0 °C) in (Figure 2). This differential expansion is called "residual expansion" and, for all specimens, residual expansion was measured at 68 °F (20 °C) as a convenient point of reference. To ensure that unsaturated brick specimens did not exhibit permanent expansion during a freeze-thaw cycle, dry specimens were tested in the dilatometer. As expected, the dry brick exhibited only reversible expansion on exposure to the temperatures of these tests.

(Figures 3 and 4) illustrate the residual expansion for the seven plant-fired samples, for the specimens cut parallel (PA) and perpendicular (PE) to the brick depth, respectively. Values shown on both graphs are the average cumulative residual expansion

over five freeze-thaw cycles. As seen in both figures, residual expansion for all samples increased with each additional freeze-thaw cycle. Additionally, the residual expansion for Samples E (molded brick) and A (extruded brick) are predominantly greater than all other samples in the PA and PE orientation, respectively.

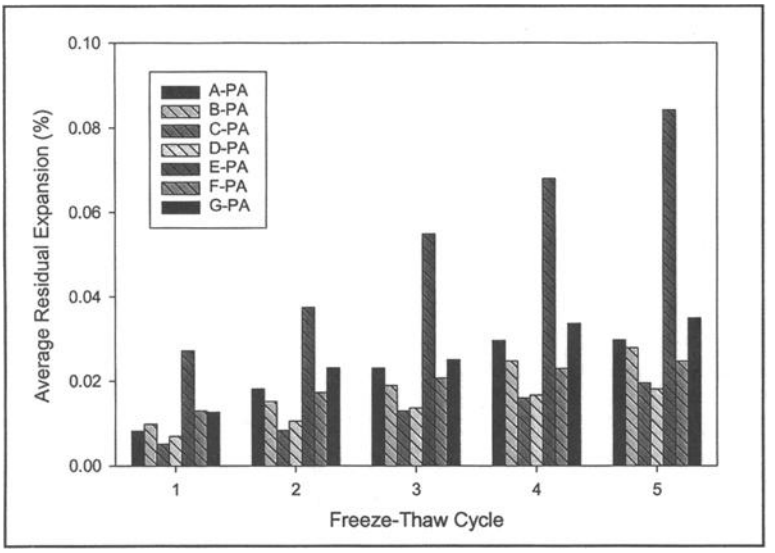

Figure 3 – *Residual Expansion for Parallel Specimen Orientation (to brick depth) at Full Saturation*

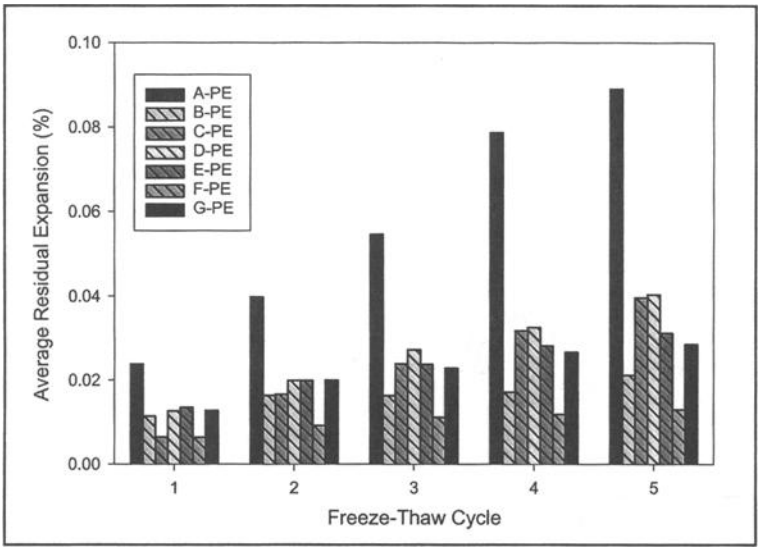

Figure 4 – *Residual Expansion for Perpendicular Specimen Orientation (to brick depth) at Full Saturation*

A comparison of average residual expansion for Sample A in both orientations (parallel (PA) and perpendicular (PE) to sample depth) is given in (Figure 5). Linear regression lines were fitted to each data set to identify the general trend of the data. For three of the four extruded brick types (Samples A, C, and D), residual expansion was greater in the PE orientation than the PA orientation. Sample B data illustrated similar residual expansion in both orientations for the first two freeze-thaw cycles, and then the residual expansion in the PA orientation slightly outweighed the expansion in the PE orientation.

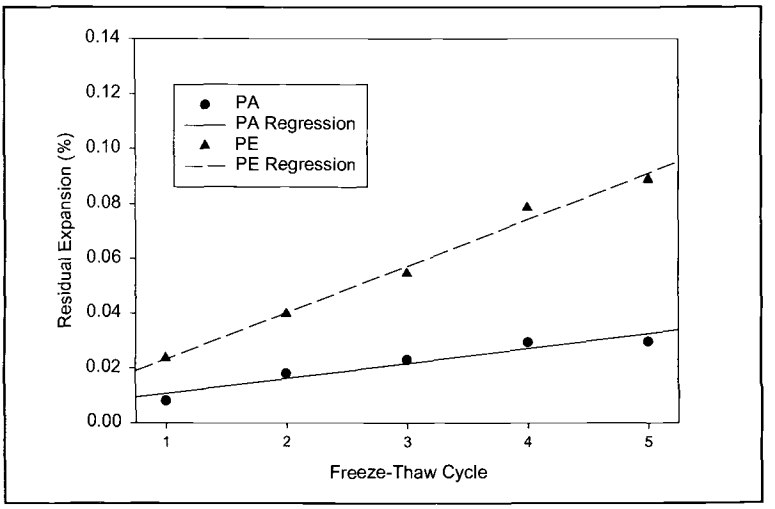

Figure 5 – *Residual Expansion Plot For Specimen A*

A comparison between the freezing expansion and its corresponding residual expansion was conducted for each individual freeze-thaw cycle (i.e., non-cumulative). (Figure 6) illustrates a typical plot of this type. The data for each sample generally illustrate that residual expansion for each individual freeze-thaw cycle decreased with each additional cycle, and that the freezing expansion was relatively larger than the residual expansion.

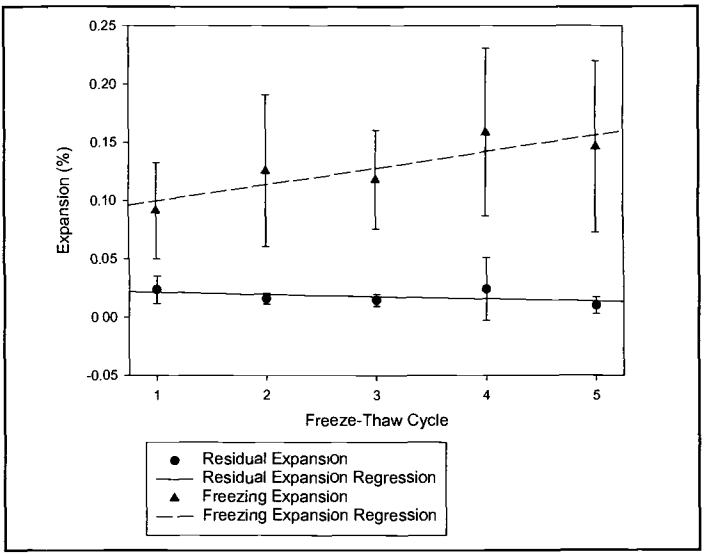

Figure 6 – *Comparison Between Residual and Freezing Expansion*

Statistical analysis comparing residual and freezing expansion for each cycle was completed. Data indicated that residual expansion is not correlated to freezing expansion; the highest correlation coefficient determined was 56%. Additionally, for many of the samples, freezing expansion increased as residual expansion decreased.

To examine the effect of saturation on the amount of residual expansion, Sample C specimens were tested at 24-hour cold-water absorption (CWA). Similar to the samples that were fully saturated, Sample C at CWA experienced greater residual expansion for samples cut perpendicular to sample depth than parallel. As expected, values of residual and freezing expansion for the vacuum-saturated specimens were of a larger magnitude than specimens at CWA. Although at a lesser magnitude, additional findings were similar to that noted for Sample C at full saturation.

Statistical Analysis

Linear and multi-variant correlation analysis was completed comparing residual and freezing expansion values to physical properties. Generally, the following results were determined by the analysis:

- There is no correlation between residual or freezing expansion and single physical properties specified by ASTM C 67.
- There is no correlation between residual or freezing expansion and pore characteristics determined by mercury porosimetry.
- Considering physical properties simultaneously (ASTM C 67 and/or porosimetry) does not enhance the correlation to residual or freezing expansion.

Freezing Expansion Characteristics of Lab Fired Brick

In the second phase of this study, several lab firings were performed on an all-shale, extruded brick to achieve a range of physical properties. Up to twenty-five residual expansion measurements were made on multiple samples from each firing. In addition to the residual expansion measurements on fully saturated samples, water adsorption properties, mercury intrusion porosimetry, and the performance-based freeze-thaw procedures were conducted (C 67 Freezing and Thawing Test (interrupted method) and the procedure described by Vickers). [*4*] For the sake of comparison, plant-fired brick of the same composition were also included in this study. Lastly, the durability index described by Maage was calculated from the mercury intrusion porosimetry data for each group of samples. [*7*]

The physical property measurements are summarized in (Table 4). The plant-fired sample had similar water adsorption properties to the lab-fired A sample, with some notable differences in the pore size distribution. A comparison of the pore size distributions as measured by mercury intrusion porosimetry is contained in (Figure 7).

Table 4 – *Summary of Physical Property Measurements*

Sample	Cold-Water Absorption (%)	Boiled-Water Absorption (%)	C/B Ratio	Cumulative Residual Expansion (%)	Pores < 3.94 x 10^{-4} (10 μm) (%)	Pores < 3.94 x 10^{-5} (1 μm) (%)	Maage Durability Index
Plant-Fired	6.58	8.56	0.77	0.16 (20 Cycles)	96.6	16.7	59
Lab-Fired A	7.09	9.33	0.76	0.11 (25 Cycles)	96.0	24.5	48
Lab-Fired B	11.53	13.48	0.85	0.16 (20 Cycles)	97.0	51.7	37
Lab-Fired C	16.11	17.08	0.94	0.58 (25 Cycles)	96.1	90.1	30

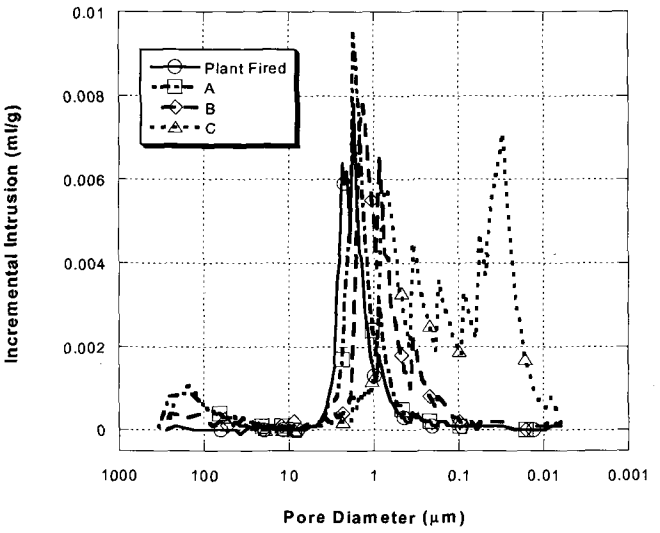

Figure 7 – *Comparison of Pore Size Distributions*

Lab-fired Samples B and C were both intentionally "under fired" to determine the residual expansion behavior due to increased porosity and less favorable pore size distributions. For the plant-fired sample, the Maage durability index indicated that this brick would fall into the category of questionable durability, while all of the lab-fired samples would fall into the "not durable" category. [7]

The cumulative residual expansion behavior is displayed in (Figure 8), while the residual expansion behavior per cycle is displayed in (Figure 9). Similarly, a summary of

the cumulative residual expansion measurements is given in (Table 4). In the cryogenic dilatometric measurements of residual expansion, lab-fired B samples and the plant-fired samples both failed around 20 cycles, with failure preceded by a sharp increase in expansion, as seen in (Figure 9). These samples failed with a crack running through the body perpendicular to the direction of measurement in the dilatometer. A summary of the failures observed in this procedure is summarized in (Table 5).

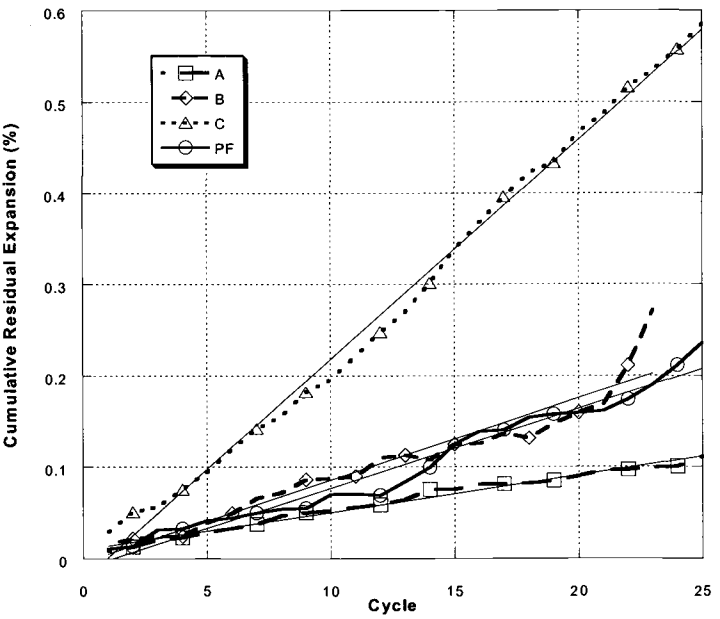

Figure 8 – *Comparison of Cumulative Residual Expansion*

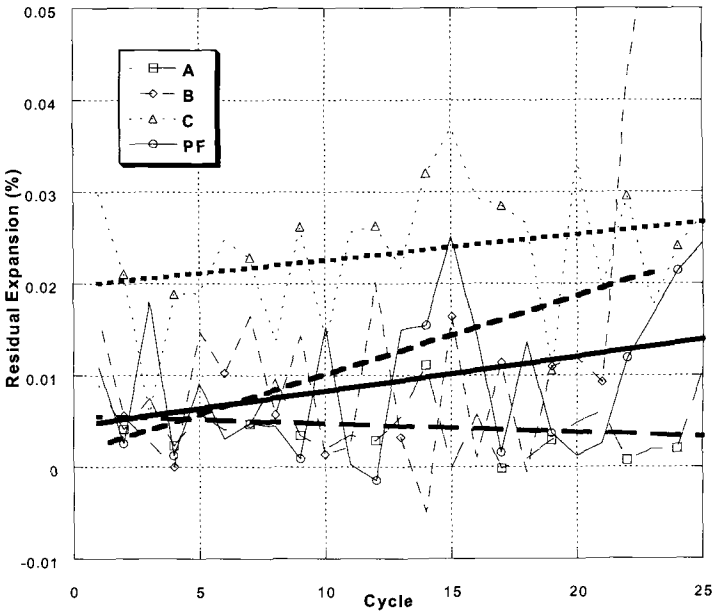

Figure 9 – *Comparison of Residual Expansion per Cycle*

Table 5 – *Results of Freeze Thaw Evaluations*

	Cryogenic Dilatometry	ASTM C 67 Procedure	Vickers Procedure [*4*]
Cycles	25	50	50
Number of Samples	3	5	5
Plant-Fired	Failure @ 21 Cycles (2 of 3 samples)	No Failures	No Failures
Lab-Fired A	No Failures	No Failures	No Failures
Lab-Fired B	Failure @ 21 Cycles (2 of 3 samples)	No Failures	No Failures
Lab-Fired C	Partial Failure (spalling of samples)	Failed at 5 Cycles (all samples)	Failed at 5 Cycles (all samples)
Failures	3	1	1

While the lab-fired C samples had a very large residual expansion, they did not fail catastrophically in the residual expansion test. By contrast, these samples tended to "shell" material off of the surface (or fragment), which had the effect of rounding the

edges of the samples. As Sample C was the most "underfired" of the lab-fired brick, a different failure mode was suggested for very high absorption or "soft" brick.

Despite the similar physical properties of lab-fired Sample A and the plant-fired sample, these samples had significant differences in the cumulative residual expansion measurements (Figure 8). This difference can also be seen in the residual expansion measurements (Figure 9) where lab-fired Sample A showed a decline in the magnitude of residual expansion with repeated cycling, while the opposite was true for the plant-fired sample. As would be expected, lab-fired Sample C, which had the highest water adsorption and the finest pore size distribution, had the highest cumulative residual expansion and the largest magnitude of residual expansion.

For the lab-fired samples, the magnitude of cumulative residual expansion and residual expansion followed a trend of higher water adsorption, yielding higher residual expansions. The fact that the residual expansion trend for the plant-fired sample does not follow the trend of the lab-fired samples suggests that durability is a complicated relationship between a number of physical properties and microstructural development, which may include the degree of vitrification (thermal history), porosity, pore size distribution, pore morphology, and mechanical properties. [*5*]

The results of the performance-based, freeze-thaw durability evaluation procedures are summarized in (Table 5). In these procedures, only the lab-fired C samples, which had the highest water adsorption values, displayed failures. These limited results suggest a major difference in sensitivity between the cryogenic dilatometry test and the test designed for larger specimens. In comparing tests, it is suggested that the cryogenic dilatometry test measures the "intrinsic response" of a brick to freezing and thawing, whereas brick using larger test specimens reveal effects due to other factors, such as freezing rates and geometric effects.

Conclusions

Residual expansion is the measure of the amount of permanent damage incurred by a brick from internally freezing water during freeze-thaw cycles. Residual expansion of the fully saturated, plant-fired brick specimens varied between 0.01% and 0.08% for all commercial brick tested after five freeze-thaw cycles. Residual expansion can be attributed to the effect of breaking vitreous bonds on a microscopic scale within the brick. Repeated freeze-thaw cycles resulted in a fatigue-like behavior. However, cumulative residual expansion continues to increase, suggesting that microscopic damage can progress to a point that a major flaw develops, resulting in a freeze-thaw failure in some brick.

It was determined from this testing that the amount of residual expansion incurred with a single freeze-thaw cycle does not correlate with the total amount of freezing expansion during testing. Statistical analysis comparing freezing expansion for all samples, and also the extruded samples only, showed relatively positive correlations with absorption values. As one would expect, the general trend indicated increasing freezing expansion with increasing absorption values.

Generally, the current ASTM freeze-thaw prediction method is based on the theory that freeze-thaw failures can be attributed and estimated by the absorption

characteristics of the fired product. On the contrary, the research indicates that the amount of water a brick absorbs is not related to the amount of residual expansion (the theorized cause of freeze-thaw failure) that will occur. Instead, the results show that the amount of water absorbed is not of great importance for prediction, but rather how the brick responds to a given amount of absorbed water.

Dilatometer testing demonstrated that residual expansion can be used to describe the response of saturated brick during freeze-thaw cycles. Residual expansion allows a quantitative property measurement that is not biased by production method, raw materials, and fired physical properties.

Statistical analysis using linear and multi-variant models revealed no correlation between residual expansion and physical properties of brick. If residual expansion is a significant measure of the cause of freeze-thaw failures, then freeze-thaw prediction using physical properties or performance-based freeze-thaw test procedures cannot be considered more than an estimate of performance.

Dilatometer test results also demonstrated that there are differences in the freezing response as a function of orientation. The effect of orientation was especially noted in the extruded brick specimens, but was also observed for the molded and dry, pressed brick. Such results suggest that cumulative freeze-thaw damage results in shear stresses near the face of the brick in the wall. The results of tensile and shear stresses, primarily resulting from expansion phenomena, appear to be the cause of most freeze-thaw failures.

Comparison of lab-fired samples of an extruded brick body showed that the residual expansion measurements discriminate between samples with different physical properties. A general trend of increasing residual expansion with increasing water adsorption was observed for lab-fired samples of the same, shale-based, raw material. Interestingly, residual expansion measurements reveal a difference between samples of the same composition with apparently similar physical properties that were fired under different conditions. As such, no correlation was found between the residual expansion measurements and physical properties, characteristics of the pore size distribution, or the results of performance-based freeze-thaw procedures.

Given the wealth of literature documenting conflicting results between existing durability evaluation techniques based on physical properties or performance-based tests, it is clear that a new method of predicting potential durability is needed. Residual expansion measurements offer the potential for such a procedure. Residual expansion measurements have the advantages of offering a direct and quantifiable measurement of the actual damage incurred in freeze-thaw events.

References

[1] McBurney, J. W. and Lovewell, C. E., "Strength, Water Absorption and Weather Resistance of Building Bricks Produced in the United States," *Proceeding of ASTM,* Vol. 33 [Part II], 1933, pp. 636–650.

[2] Butterworth, B. and Baldwin, L. W., "Laboratory Tests and the Durability of Bricks, V. The Indirect Appraisal of Durability (Continued)," *Transactions of the British Ceramic Society,* Vol. 63, No. 11, 1964, pp. 647–661.

[3] Kaskel, B.S., "Uni-Directional Freezing and Thawing Durability Tests for Brick Masonry Panels," *Masonry: Esthetics, Engineering, and Economy,* ASTM STP 1246, 1996, pp. 149–159.

[4] Vickers, M.A., "Comparison of Laboratory Freeze-Thaw Procedures," *Masonry: Design and Construction, Problems and Repair,* ASTM STP 1180, 1993, pp. 240–249.

[5] Franke, L. and Bentrup, H., "Evaluation of the frost resistance of bricks in regard to long service life," *Ziegelindustrie International,* Vol. 46, No 7-8, 1993, pp. 483–492.

[6] Friese, P, "Predictions of the frost resistance of bricks," *Ziegelindustrie International,* Vol. 48, No. 12, 1995, pp. 952–963.

[7] Maage, M., "Frost resistance and pore size distribution of bricks," *Ziegelindustrie International,* Vol. 43, No. 9, 1990, pp. 472–481.

[8] Brosnan, D.A. and Frederic, J.C., "Fatigue Properties of Traditional Ceramic Products," *British Ceramic Proceedings,* Vol. 2, No. 60, 1999, pp. 361–362.

Robert D. Thomas[1] and Vilas Mujumdar[2]

Determining Concrete Masonry Unit Compressive Strength Using Coupon Testing

Reference: Thomas, R. D., and Mujumdar, V., "**Determining Concrete Masonry Unit Compressive Strength Using Coupon Testing,**" *Masonry: Opportunities in the 21st Century, ASTM STP 1432*, D. B. Throop and R. E. Klingner, Eds., ASTM International, West Conshohocken, PA, 2003.

Abstract: In 1990, provisions were added to ASTM Methods for Sampling and Testing Concrete Masonry Units (C 140) to permit the evaluation of the compressive strength of concrete masonry units that were of an unusual size or shape, by cutting a rectangular coupon from the face shell. These provisions were added to permit evaluation of units whose shapes or size do not lend themselves to testing full-size and to accommodate limitations of testing equipment. The testing on which these provisions were based have not previously been published in a peer-reviewed journal or proceedings. This paper presents the results of two sets of testing programs that provided the basis for the development of coupon testing provisions. Since the provisions have been approved for use in ASTM C 140, two additional testing programs have been performed to evaluate those provisions. This paper evaluates the coupon testing provisions of ASTM C 140 with respect to the available data.

Keywords: CMU, compressive strength, concrete masonry, concrete masonry unit, coupon, height to thickness ratio, length to thickness ratio, testing

Introduction

Concrete masonry units are frequently used in structural, load-bearing applications. Designers must have confidence in understanding the ability of concrete masonry units to resist compressive stresses to predict structural performance of masonry assemblies. Historically, testing procedures for concrete masonry units have been performed on full-size units. These units are capped to uniformly distribute compressive stresses across the bearing surfaces normal to the vertical direction of loading. However, most concrete masonry units are placed in construction such that only the face shells of the units are mortared. Thus, concrete masonry unit testing procedures do not necessarily replicate

[1] Vice President of Engineering, National Concrete Masonry Association, 13750 Sunrise Valley Drive, Herndon, VA 20171

[2] Executive Director, California Concrete Masonry Association of California and Nevada, 6060 Sunrise Vista Drive, Citrus Heights, CA 95610

compressive load distribution throughout the unit that might be experienced in service. However, the standard procedures have worked effectively as a quality assurance method and to provide designers an indication of the capacity of the concrete masonry unit to resist compressive loads.

As production capabilities improved, unit shapes evolved to better accommodate reinforcing and metal connectors. Some of these unit shapes, such as bond beam units and open-ended units that were designed to accommodate grout, do not lend themselves to testing the entire unit because of geometry. Also, specified compressive strengths of units have increased due to structural demands. The required platen thickness in testing standards has increased for reliable compression testing. These demands have made many existing compression machines inadequate for testing an entire concrete masonry unit. Therefore, Committee C 15 of the American Society of Testing and Materials considered it necessary to provide alternative methods for evaluating unit compressive strength. One of these alternatives, coupon testing, is the subject of this paper.

The 1990 edition of ASTM C 140, Sampling and Testing Concrete Masonry Units, included new provisions for modifying full-size units when necessary to produce a specimen for testing in compression. Permissible modifications included:

- Removing unsupported projections
- Reducing the height of specimens with reduced webs
- Reducing unit size to achieve a specimen that is fully-enclosed in a four-sided cell or cells, and
- Saw-cutting a coupon of a height to thickness ratio (H:T) of 2:1 and a length to thickness ratio (L:T) of 4:1 from the face shell of each unit.

This paper presents and reviews previously unpublished research conducted by the following:

- 1986 — Concrete Masonry Association of California and Nevada (CMACN), at Riverside Cement Technical Service Laboratory
- 1987 — Concrete Masonry Association of California and Nevada (CMACN), for Graystone Concrete Block Company, at Kaiser Cement Technical Service Laboratory
- 1994 — National Concrete Masonry Association (NCMA)
- 1995 — Concrete Masonry Association of California and Nevada (CMACN), at three different laboratories

Review of ASTM Testing Requirements

The 2001 edition of ASTM C 140 includes three basic options (Fig. 1) for obtaining test specimens from concrete masonry units for the purpose of compression testing. These provisions are largely unchanged from those included in the standard in 1990 when coupon provisions were added.

Option 1, Full-Size Specimens

If there are unsupported projections whose length is greater than their thickness, those are to be removed by saw-cutting. If the units contain reduced webs, the face shell

projecting above the full-bearing surface is removed provided the resulting specimen height is not reduced by more than one-third of the original unit height.

Option 2, Reduced Specimens

Reduce the size of the unit to produce a compression specimen that has no face shell projections or irregular webs and has a fully enclosed cell or cells with a 100% bearing surface.

Option 3, Coupons

Saw-cut a coupon from the face shell of each unit such that the height of the coupon is twice its thickness and the length is four times its thickness. The thickness of the coupon shall be as large as possible and not less than 1.25 in. (32 mm).

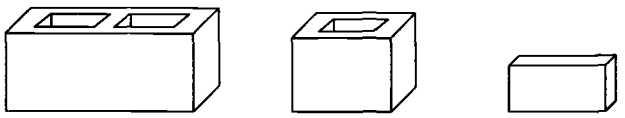

Fig. 1 —*Typical Concrete Masonry Compression Test Specimens*

The three options were added to ASTM C 140 to provide for provisions in testing a range of unit sizes and shapes and to accommodate testing machine limitations for size and capacity. The four sets of reported data are evaluated considering these three options.

1986 CMACN Test Data

The tests conducted by the Concrete Masonry Association of California and Nevada (CMACN) at Kaiser Cement Technical Service Laboratory were performed on a single production set of 8 × 8 × 16 in. (203 × 203 × 406 mm) (nominal, width × length × height) hollow concrete masonry units. Five concrete masonry units were tested full-size. Five additional units were reduced to approximately half-length with a complete center web and tested. Twelve different coupon sizes were saw-cut from full-size units. For each size, one coupon was cut from the lower half and one from the upper half of three units. The results of the testing are summarized in Table 1.

At the time of the testing, the following basic conclusions were drawn:

- Half-length units tested higher than full-size units (approximately 3%).
- Most coupon strengths tested higher than full-size units (ranging from approximately 90–125% of full-size units, depending on coupon size).
- In general, strengths decreased as coupon H:T or L:T increased.

- Coupons taken from the bottom of the unit tested lower than those from the top of the unit (8% higher on average).

TABLE 1 —*Summary of Compressive Strengths of Specimens from 1986 CMACN Data* [1, 2, 3], *psi (MPa).*

Coupon Height, in., (mm)	Coupon Length, in. (mm) 3.75 in. (95 mm) L:T = 3	5 in. (127 mm) L:T = 4	6.25 in. (159 mm) L:T = 5	7.5 in. (191 mm) L:T = 6	Full Size Unit	Half Length Unit
2.5 in. (64 mm), H:T = 2	3490 psi (24.1 MPa)	2870 (19.8)	2820 (19.4)	2940 (20.3)	2790 (19.2)	2890 (19.9)
3.75 in. (95 mm) H:T =3	2930 (20.2)	2920 (20.1)	2750 (19.0)	2690 (18.5)		
5 in. (127 mm), H:T = 4	2990 (20.6)	2990 (20.6)	2720 (18.8)	2570 (17.2)		

[1]The thickness of all coupons was 1.25 in. (32 mm).
[2]Each strength value in the table represents an average of six coupon specimens, three saw-cut from the upper half of a concrete masonry unit and three from the lower half.
[3]The raw data for this data set is not available. Therefore, standard deviation and coefficients of variation cannot be reported.

1987 CMACN Test Data

The tests conducted by the Concrete Masonry Association of California and Nevada (CMACN) at Riverside Cement Technical Service Laboratory were also performed on a single production set of 8 × 8 × 16 in. (203 × 203 × 406 mm) (nominal, width × length × height) hollow concrete masonry units. Five concrete masonry units were tested full-size. Five additional units were reduced to approximately half-length with a complete center web and tested. Ten different coupon sizes were saw-cut from full-size units. For those coupons having a height of 2.5 inches (64 mm) or less, three coupons could be obtained from a single unit. Therefore, for this coupon size, one coupon was taken from each of the bottom, middle, and top of each of three units. For other coupon sizes, one coupon was cut from the lower half of a unit and one from the upper half of each of four units. The results of the testing are summarized in Tables 2 and 3.

The following observed trends in the data are consistent with that seen in the 1986 CMACN data:

- Compressive strengths decreased with increasing H:T ratio.

However, the following observed trends from this data are not consistent with the 1986 CMACN data:

- Compressive strengths increased with increasing L:T ratio.
- Half-length units tested lower than full-size units (approximately 3%).
- Most coupons strengths tested lower than full-size units (ranging from approximately 70–127% of full-size units, depending on coupon size).

- Coupons taken from the bottom of the unit tested higher than those from the top of the unit (4% higher on average).

TABLE 2 — *Summary of Compressive Strengths of Specimens from 1987 CMACN Data, psi (MPa).*

Coupon Height, in. (mm)	Coupon Length, in. (mm) 2.5 in. (64 mm) L:T = 2	5 in. (127 mm) L:T = 4	7.5 in. (190 mm) L:T = 6	Full Size Unit	Half Length Unit
1.25 in. (32 mm), H:T = 1	4760 psi 32.8 (MPa)	...	...	3740 (25.8)	3610 (24.9)
2.5 in. (64 mm), H:T = 2	3320 (22.9)	3470 (23.9)	3900 (26.9)		
3.75 in. (95 mm), H:T = 3	2620 (18.1)	3700 (25.5)	3410 (23.5)		
5 in. (127 mm), H:T = 4	2610 (18.0)	3170 (21.9)	3450 (23.8)		

[1]The thickness of all coupons was 1.25 in. (32 mm).

[2]Each coupon value for coupons having a height of 2.5 inches (64 mm) or less represents an average of nine specimens, three saw-cut from the upper portion of a concrete masonry unit, three from the middle portion, and three from the lower portion. Each coupon value for other coupon heights represents an average of 8 specimens, four saw-cut from the upper half of a concrete masonry unit and four from the lower half.

TABLE 3 — *Comparison of Strengths and Variations from Specimens from 1987 CMACN Data.*

Specimen Size (L:H:T)	Compressive Strength, psi (MPa) Average	% of Full Unit Strength	Average Coefficient of Variation, %
Full Size	3740 (25.8)	100	5.4
Half-Length	3610 (24.9)	97	3.5
2:1:1 Coupon	4760 (32.8)	127	7.7
2:2:1 Coupon	3320 (22.9)	89	5.5
2:3:1 Coupon	2620 (18.1)	70	11.4
2:4:1 Coupon	2610 (18.0)	70	7.8
4:2:1 Coupon	3470 (23.9)	93	7.0
4:3:1 Coupon	3700 (25.5)	99	5.0
4:4:1 Coupon	3170 (21.9)	85	9.4
6:2:1 Coupon	3860 (26.6)	103	7.8
6:3:1 Coupon	3410 (23.5)	91	12.6
6:4:1 Coupon	3450 (23.8)	92	9.4

The following observed trends could not be compared to that of the 1986 CMACN data:

- Coupons taken from the middle of the unit tested lower than those from the bottom of the unit (8% lower on average).

- The coefficient of variation of coupon test results was typically significantly higher than that of tests on full-size and half-length specimens.

1994 NCMA Data

The National Concrete Masonry Association (NCMA) tests only considered the coupon proportions (L:H:T = 4:2:1) that were added to ASTM C 140 in 1990. However, unlike the earlier testing efforts discussed here, the NCMA data considers two different production sets from each of two different unit sizes. The tests also include a larger number of specimens, 30, per variable. Coupons were taken from the bottom, middle and top of 30 hollow concrete masonry units having nominal dimensions of 8 × 8 × 16 inches (203 × 203 × 406 mm) (width × length × height). Coupons were taken from the bottom and top of 30 concrete masonry units having nominal dimensions of 12 × 8 × 16 inches (305 × 203 × 406 mm).

Those coupons taken from 8 in. (203 mm) CMU measured 1.25 × 2.5 × 5 in. (32 × 64 × 127 mm)(W × H × L), while those taken from 12 in. (305 mm) CMU measured 1.5 × 3 × 6 in. (38 × 76 × 152 mm). The results of the testing are summarized in Tables 4 and 5.

The following trends were observed in the 1994 NCMA data:

- Coupons taken from the bottom of units typically tested higher than those taken from other locations (on average, 9% higher than those from the top and 21% higher than those from the middle as shown in Figs. 2 and 3).
- Coupons taken from the bottom of units demonstrated lower coefficients of variation in compressive strength tests than those taken from other locations (Table 5).
- Half-length units typically tested higher than full-size units (on average, 4 % higher) but there was greater variability in the results (Figures 2 and 3).
- Coupon strengths typically tested higher than full-size units (on average, 12% higher) but there was greater variability in the results (Figures 2 and 3).

TABLE 4 — *Summary of Compressive Strength and Coefficient of Variations from NCMA 1994 Data, psi (MPa).*

Specimen Set[1,2]	Property	Specimen Configuration		
		Full Size	Half-Length	All Coupons
8NW	Average Strength, psi (MPa)	2770 (19.1)	3020 (20.8)	3370 (23.2)
	% of Full Unit Strength	100	109	122
	Coefficient of Variation, %	6.9	9.2	9.3
8MW	Average Strength, psi (MPa)	3450 (23.8)	3570 (24.6)	3440 (23.7)
	% of Full Unit Strength	100	103	100
	Coefficient of Variation, %	12.8	12.6	16.1
12NW	Average Strength, psi (MPa)	2890 (19.9)	2870 (19.8)	3470 (23.9)
	% of Full Unit Strength	100	99	120
	Coefficient of Variation, %	5.4	5.5	11.1
12MW	Average Strength, psi (MPa)	2730 (18.8)	2880 (19.9)	2920 (20.1)
	% of Full Unit Strength	100	105	107
	Coefficient of Variation, %	4.8	9.9	12.5
All Sets Combined	Average Strength, psi (MPa)	2960 (20.4)	3090 (21.3)	3300 (22.8)
	% of Full Unit Strength	100	104	112
	Coefficient of Variation, %	7.5	9.3	12.2

[1] 8 = Coupons from 8 in. (203 mm) CMU, 12 = Coupons from 12 in. CMU
[2] NW = Coupons from normal weight CMU, MW = Coupons from medium weight CMU

TABLE 5 — *Effects of Coupon Location on Strength and Variation from NCMA 1994 Data.*

Specimen Set [1,2]	Compressive Strength, psi (MPa)			Coefficient of Variation, %		
	Top	Middle	Bottom	Top	Middle	Bottom
8NW	3660 (25.2)	2940 (17.2)	3520 (24.3)	11.5	8.1	8.2
8MW	3160 (21.8)	3050 (21.0)	4120 (28.4)	20.6	15.3	12.4
12NW	3420 (23.6)	...	3530 (24.3)	13.1	...	9.0
12MW	2690 (18.5)	...	3140 (21.7)	14.6	...	11.7
All Sets Combined	3233 (22.3)	2999 (20.7)	3575 (24.6)	14.6	11.7	10.3

[1] 8 = Coupons from 8 in. (203 mm) CMU, 12 = Coupons from 12 in. CMU
[2] NW = Coupons from normal weight CMU, MW = Coupons from medium weight CMU

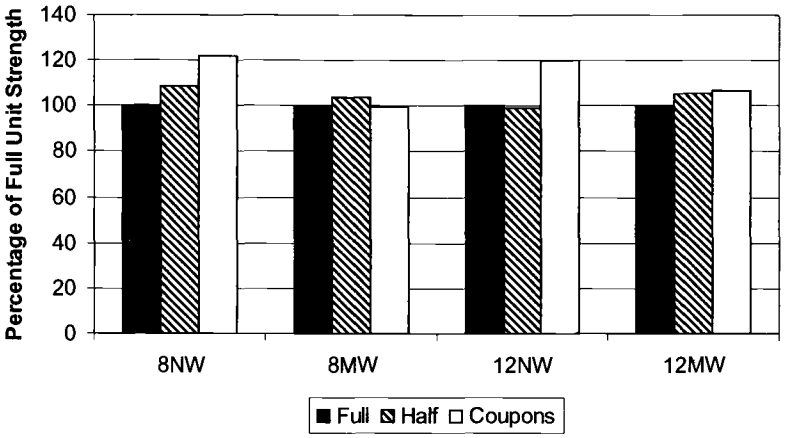

FIG. 2 – *Influence of Specimen Configuration on Compressive Strength, from Each Set in NCMA 1994 Data.*

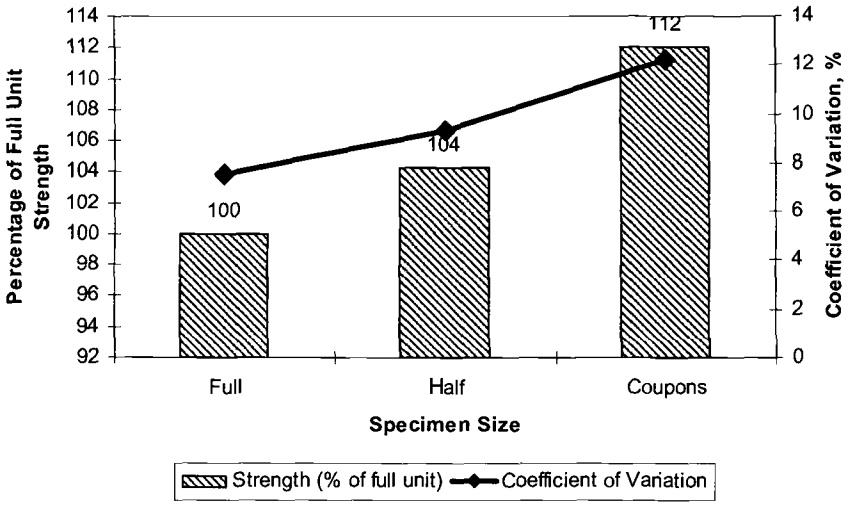

FIG. 3 — *Influence of Specimen Configuration on Compressive Strength and Coefficient of Variation, Combined Values from NCMA 1994 Data.*

1995 CMACN Test Data

Research performed in 1995 by the Concrete Masonry Association of California and Nevada in 1995 also only considered the coupon proportions (L:H:T = 4:2:1) that were added to ASTM C 140 in 1990. In this testing program, the research included two sets of units: 1) lightweight standard concrete masonry units, and 2) medium split-face concrete masonry units with a single open web (A-shaped unit). Both sets of units had nominal dimensions of 8 × 8 × 16 in. (203 × 203 × 406 mm) (width × height × length).

To obtain the half-length specimens from the split face units, the projecting face shells were removed to result in a rather symmetrical, four-sided, single-cell, hollow specimen (similar to other half-length specimens referred to in this paper). The full-size, split-face units were capped and tested as manufactured, without removing or altering the face shell projections.

Coupons were only taken from the mid-height area of the unit. For the split face units, coupons were taken from both face shells (split and non-split). The thickness of the coupon was not equal to the thickness of the face shell containing the split surface. The face shell thickness on the split-face side of the unit was large enough that the coupon could have smooth sides and thus uniform cross-section. This configuration required five saw cuts: top, bottom, both ends and one side.

All specimens from each type of unit were taken from a single production set. Full-size and half-length specimens were tested in addition to coupons. Five specimens were tested from each unit configuration. In addition, an identical set of specimens was distributed to three different testing laboratories. The results of the testing are summarized in Tables 6, 7, and 8.

TABLE 6 — *Summary of Compressive Strength and Coefficient of Variations from CMACN 1995 Data for Lightweight Concrete Masonry Units.*

Lab Number	Property	Specimen Configuration		
		Full Size	Half-Length	All Coupons
1	Average Strength, psi (MPa)	2230 (15.4)	2187 (15.1)	2212 (15.3)
	% of Full Unit Strength	100	98	99
	Coefficient of Variation, %	1.7	4.0	5.8
2	Average Strength, psi (MPa)	2126 (14.7)	2238 (15.4)	2360 (16.3)
	% of Full Unit Strength	100	105	111
	Coefficient of Variation, %	3.6	3.9	5.8
3	Average Strength, psi (MPa)	2194 (15.1)	2172 (15.0)	2374 (16.4)
	% of Full Unit Strength	100	99	108
	Coefficient of Variation, %	4.6	5.1	8.4
All Sets Combined	Average Strength, psi (MPa)	2183 (15.1)	2199 (15.2)	2315 (16.0)
	% of Full Unit Strength	100	101	106
	Coefficient of Variation, %	3.8	4.3	7.1

TABLE 7 — *Summary of Compressive Strength and Coefficient of Variations from CMACN 1995 Data for Medium Weight, Split-Face Concrete Masonry Units.*

Lab Number	Property	Specimen Configuration		
		Full Size	Half-Length	All Coupons
1	Average Strength, psi (MPa)	3263 (25.0)	3638 (25.1)	3807 (26.2)
	% of Full Unit Strength	100	111	117
	Coefficient of Variation, %	4.5	4.3	7.1
2	Average Strength, psi (MPa)	3534 (24.3)	3776 (26.0)	4132 (28.5)
	% of Full Unit Strength	100	107	117
	Coefficient of Variation, %	1.7	2.7	6.5
3[1, 2]	Average Strength, psi (MPa)	3544 (24.4)	3312 (22.8)	3861 (26.6)
	% of Full Unit Strength	100	93	109
	Coefficient of Variation, %	1.7	3.5	7.1
All Sets Combined	Average Strength, psi (MPa)	3440 (23.7)	3576 (24.7)	3933 (27.1)
	% of Full Unit Strength	100	104	114
	Coefficient of Variation, %	4.8	6.5	7.4

[1] Lab 3 reported an apparent "tension-type" failure in one of the projecting face shells of three different full-size units. The compression tests of these three units were not omitted from data reported above since there appeared to be no notable influence on strength.

[2] Lab 3 reported an apparent "tension-type" failure in both of the projecting face shells of one full-size unit. The compression test of this unit was omitted from data reported above since a notable influence on strength was observed. Therefore, the data for full units for Lab 3 above represents only four test specimens.

TABLE 8 — *Influence of Coupon Location from 1995 CMACN Test Data.*

Lab No.		Face shell from Which Coupon was Taken	
		Smooth Face	Split Face
1	Average Strength, psi (MPa)	3819 (26.3)	3795 (26.2)
	Coefficient of Variation, %	7.7	7.0
2	Average Strength, psi (MPa)	4360 (30.0)	3904 (26.9)
	Coefficient of Variation, %	2.7	2.2
3	Average Strength, psi (MPa)	3897 (26.9)	3824 (26.4)
	Coefficient of Variation, %	7.8	6.5
All Labs Combined	Average Strength, psi (MPa)	4025 (27.8)	3841 (26.5)
	Coefficient of Variation, %	8.5	5.3

The conclusions drawn from the 1995 CMACN test data include the following:

- There was outstanding correlation between laboratories for tests on the lightweight concrete masonry units and good correlation between laboratories for tests on the medium weight, split-face, single open-end concrete masonry units.
- Coupons tested higher than full-size units (6% higher for lightweight units and 14% higher for normal weight units) and had greater coefficients of variation (Fig. 4).
- Half-length units tested slightly higher than full-size units (1% higher for lightweight units and 4% higher for normal weight units) and had slightly higher coefficients of variation (Fig. 4).
- Those coupons taken from the smooth face averaged 5% higher than those taken from the split-face side and had a slightly higher coefficient of variation (Table 8).
- The influence of specimen configuration was greater in the higher strength medium weight units (Fig. 4).

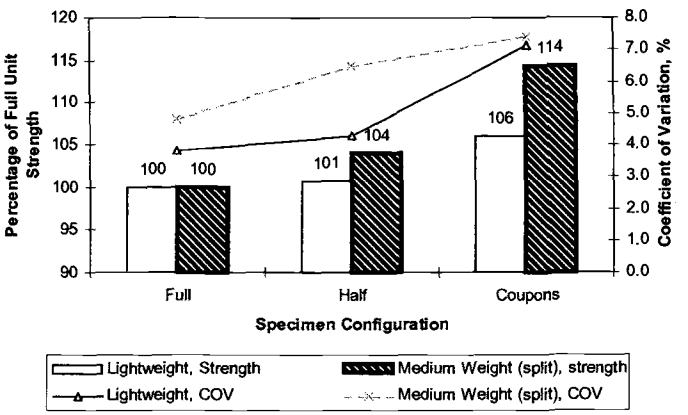

FIG. 4 — *Effect of Specimen Configuration on Compressive Strength, From 1995 CMACN Data.*

Discussion

When considering the data available from the three research programs conducted by CMACN and the one research program conducted by NCMA, there are a number of inconsistencies in the results that complicate evaluation of the data. However, the following basic conclusions appear to be reasonable:

- Half-length concrete masonry specimens test higher in compression than full size units, but results are more variable.
- Coupon specimens test higher than both half-length and full size specimens, but results are more variable.
- Coupon sample location influences compressive strength results. (The influence of sample location may depend on production methods.)
- Coupon proportions influence compressive strength results. (Strengths decrease with increasing height to thickness ratios (H:T). Also, in general, strengths decrease with increasing length to thickness ratios (L:T), although not as much as for H:T.)

Based on the two sets of CMACN data that was conducted before adding coupon testing provisions into ASTM C 140, it is not obvious why a coupon ratio of 4:2:1 (L:H:T) was selected. It appears that some subjectivity was applied in addition to evaluation of results. The 4:2:1 specimens did not provide the most comparable results to full-size specimens in the 1986 or 1987 test data. In 1986, the best correlation was provided by the 5:3:1 coupons and by the 4:3:1 coupons in 1987. Although we do not have the benefit of seeing the variation in the results of the 1986 data, the 4:3:1 coupons also had less variability than the 4:2:1 coupons. The height to thickness ratio of 2:1 may have been chosen to be consistent with other established test methods (such as those for concrete and mortar cylinders) for evaluating the compressive strength of concrete materials.

If the decision was first made to use a 2:1 height to thickness ratio, the test data prior to 1990 supports the selection of a 4:1 length to thickness ratio. The L:T of 4:1 was slightly more representative of full unit strengths than the L:T of 2:1 in the 1987 data with less variation. The L:T of 3:1 from the 1986 data may have been eliminated from consideration because it yielded 25% higher strengths than the full-size units.

With only the 1986 and 1987 data to use as the basis for developing coupon provisions, it is unfortunate that the 1987 data is not consistent with the other data sets now available in terms of relationship between coupon and full-size specimen strengths. Nearly all of the coupon proportions tested in the 1987 series produced coupons lower in strength than full-size units. Thus, at the time coupons were added to the standard, it was likely considered that coupons produced an approximate, if not conservative prediction of full unit strengths.

The two data sets conducted after 1990 were intended to evaluate the 4:2:1 coupon provisions. Given the discussion above, should these provisions remain in their current state? To facilitate discussion, the following set of assumptions are made to simplify issues:

1. Compressive strength data of full-size units, half-length units, and coupons produce a normal distribution of results (although data sets did not consistently produce normal distributions).
2. Compressive strengths of coupons are 10% higher than full units and half-length specimens are 5% higher than full units (Table 9).
3. Coefficients of variation for full units are 5%, for half-length 7.5%, and for coupons 10% (Table 9).

The assumptions are not based specifically on any one data set or calculated from a combination of data sets, but are rounded approximate numbers selected for discussion purposes.

TABLE 9 — *Assumed RelationshipBetween Different Specimen Configurations.*

	Full Size Units	Half-Length Specimens	Coupons
Compressive strength (% of full size unit strength)	100	105	110
Coefficient of Variation, %	5	7.5	10

ASTM Specification for Loadbearing Concrete Masonry Units (C 90) includes a required average compressive strength of 1900 psi (13.1 MPa) based on a set of three specimens and a minimum compressive strength of 1700 psi (11.7 MPa) of any specimen in the set. Assuming 5% coefficient of variation for full-size unit tests, the 200 psi (1.4 MPa) difference between 1900 and 1700 psi represents 2.1 standard deviations. For a set of 30 full-size specimens whose average is 1900 psi with 5% coefficient of variation, this represents a 98 % confidence level that any single full-size unit test will exceed 1700 psi. (For only three specimens there is 93 % confidence level.) Similar confidence level information for half-length and coupon specimens based on the assumed relationships from Table 9 is shown in Table 10. This information is shown graphically in Fig. 5.

Coupons and half-length specimens provide similar lower bond confidence values despite having higher average strengths.

TABLE 10 —*Influence of Specimen Configuration on Confidence Level that a Single Specimen will Exceed Minimum Required Value.*

	Full Size Units	Half-Length Specimens	Coupons
Average Compressive Strength, psi (MPa)	1900 (13.1)	1995 (13.8)	2090 (14.4)
Coefficient of Variation, %	5	7.5	10
Standard Deviation, psi (MPa)	95 (0.7)	150 (1.0)	209 (1.4)
Number of Standard Deviations between Average and 1700 psi (11.7 MPa)	2.11	1.97	1.87
Confidence Level (based on 30 specimens)	98%	97%	96%
Confidence Level (based on 3 specimens)	93%	92%	91%

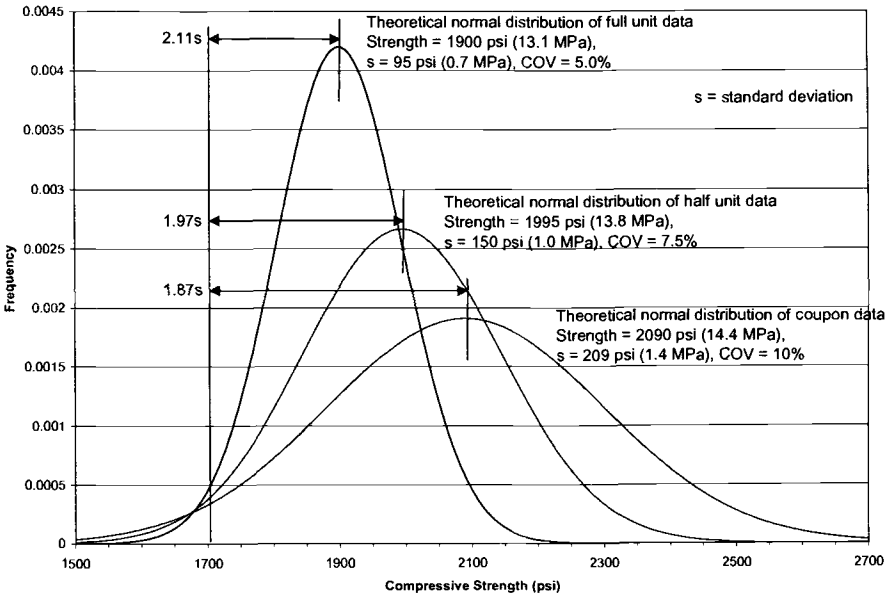

FIG. 5 – *Theoretical Normal Distributions of Test Results for Different Specimen Configurations.*

Conclusions

- Full-size unit testing should be encouraged since it results in the most consistent and reliable test results. However, options for testing other specimens saw-cut from full-size units should be maintained for practicality reasons (need for testing special unit shapes and limitations of testing machines).
- When full-size units cannot be tested, half-length concrete masonry units should be the next preferred method. Coupons should be the least preferred option, but the coupon method should be maintained.
- Coupon proportions for L:H:T should remain at 4:2:1 unless additional research shows that other specimen sizes would produce more consistent or reliable results. The 4:2:1 ratio results in a specimen that can be reasonably handled and tested in the laboratory. Maintaining these provisions permits easier comparisons of future investigations to past work and history.
- Because one of the data sets (1986 CMACN data) was not consistent with the other data sets regarding relative strengths of coupons to full-size units, additional research should be conducted before revisions are made to ASTM C 140 test provisions. This research should consider various block shapes, sizes, and mix designs to make sure relationships hold consistent for these variables.
- The procedures for testing reduced length specimens and coupons produce higher coefficients of variation in compressive strength tests, approximately 7.5% and 10% respectively, compared to approximately 5% for full size units.
- Due to increased variation in compression test results of reduced size specimens, there is not a significant difference in the confidence level provided by any of the three methods permitted by C 140 for exceeding a lower bound value.
- Given the increased variation for testing reduced size specimens, consideration should be given to increasing the number of specimens required for testing when these specimens are used.
- Difficulties in the reliability in capping and testing small specimens are believed to contribute to the higher variability in strength results observed in coupons. Consideration should be given to researching the effectiveness of an unbonded capping system or other methods of capping and testing coupons that could reduce variability.

References

[1] Isaak, M., "Report on a Compression Testing Program of Concrete Masonry Units (CMU's) Comparing Full Size Units, Half Size Units, and Coupons," Concrete Masonry Association of California and Nevada, Citrus Heights, CA, 1995.

[2] "Draft Report: Evaluation of Coupon Compressive Strength Provisions of ASTM C 140," Project No. 93-174, National Concrete Masonry Association, Herndon, VA, 1994.

[3] "Compression Coupon Test Program," Concrete Masonry Association of California and Nevada, Citrus Heights, CA, 1987.

[4] "Compression Coupon Tests for Greystone Block by Kaiser Cement Technical Service Lab," Concrete Masonry Association of California and Nevada, Citrus Heights, CA, 1986.

Assemblies

Edward A. Gerns and Lisa M. Chan[1]

The Evolution and Development of Lateral Anchorage Systems in Masonry Cladding Systems

Reference: Gerns, E. A. and Chan, L. M., "**The Evolution and Development of Lateral Anchorage Systems in Masonry Cladding Systems,**" *Masonry: Opportunities for the 21st Century, ASTM STP 1432*, D. Throop and R. E. Klingner, Eds., ASTM International, West Conshohocken, PA, 2003.

Abstract: Early skeletal frame buildings utilized numerous exterior cladding materials. Brick, terra cotta, and stone were all used, with economics frequently dictating both the location and quantity of materials. Early methods of anchoring these masonry cladding materials were varied and frequently experimental. With increased understanding of the behavior of cladding systems relative to both environmental forces as well as interaction with the structural systems, lateral anchorage systems evolved and achieved better performance. This paper will review the historical development of lateral anchorage systems over the past 125 years. A review of products, materials, code requirements and representative details will be presented. The intent of the paper will be to present a comparative timeline of lateral anchorage development to assist in understanding the concurrent evolution of masonry facade cladding systems.

Keywords: metal, lateral anchors, masonry

Introduction

Masonry has been used as a building material for thousands of years. Prior to the 1870s, solid masonry walls functioned as both the building's structural system and the enclosure for the interior spaces. One of the most dramatic changes in building construction was the result of the industrial revolution of the late nineteenth century. Advances in the understanding of the chemistry of iron as well as the ability to alter its metalographic properties led to the introduction of steel as a building material. With the ability to economically manufacture steel shapes, the skeleton frame building system soon developed. The rapid evolution of lateral anchorage over the last 125 years is the direct result of the introduction of steel into the construction of buildings.

[1]Consultant and Senior Architect/Engineer, respectively, Wiss, Janney, Elstner Associates, Inc., 120 North LaSalle, Suite 2000, Chicago, IL 60602.

Iron has been used in building construction for more than 3000 years. Though sparingly used, iron rods, chains, cramps and straps have played a critical part in the construction and stability of many major buildings throughout history. The corrosion of iron has long been known as a potential problem, and corrosion inhibiting systems have included boiling the iron in tallow, covering it with pitch or varnish, or coating it in molten tin, otherwise known as galvanizing [1].

The development of lateral anchorage systems in facades in general, and in masonry construction specifically, resulted from the interaction of numerous factors including cladding materials, structural systems, environmental forces, and experimentation. These factors similarly influenced other interrelated aspects of facade design and construction, and they should be considered in a discussion of lateral anchorage.

The incorporation of lateral anchorage in facade systems would not have been an issue in building construction had wall systems remained monolithic. During the building boom following the Industrial Revolution, economics and architectural trends necessitated the development of methods to achieve the desired finished wall surface while minimizing the quantity of the more expensive materials that would be hidden within the wall system. Initially the facing and backup materials were constructed as a solid wall, but eventually the decorative facing was physically separated from the backup wall.

When the exterior facing material was separated from the backup wall, the lateral anchors had to span the intervening cavity. To resist the lateral loads caused by wind or earthquakes, stiffer anchors were needed to transfer both inward and outward lateral loads from the cladding, across the cavity, and into the backup wall system.

The facing material can be attached to the backup material in several ways, including direct adhesion, keying, and the use of discrete anchors. One method of adhesion is bonding the face material to the backup by completely filling the intervening collar joint with mortar. Keying utilizes masonry units that extend into the backup at specific intervals to engage the mass of the backup wall. A more developed system of keying consists of discrete metal anchors that are embedded into the backup material at a specific horizontal and vertical spacing. Both keyed and discretely anchored systems rely on either friction between the anchor and the wall materials or interlocking of the various components to tie the system together.

A brief review of the evolution of architectural aesthetic trends, cladding materials, and construction practices between 1870 and 2000 provides valuable insight into the evolution of lateral anchorage systems specifically, as well as the curtainwall system in general.

1870–1920: The Age of Experimentation and the Development of the Curtainwall

The period from 1870–1900 was an experimental period in the development of cladding systems. No significant precedent had been established for the construction of tall buildings prior to this time. The ever-increasing height of buildings during this period quickly revealed the shortcomings of the bearing wall system. By the 1890s bearing walls had reached their practical limit with the construction of the 16-story Monadnock building in Chicago with 6-feet-thick (1.8 m) exterior walls at the ground floor [2].

Building Code Requirements

A review of building code requirements during this period reflects the trepidation regarding the "thinning" of the exterior wall envelope. Building codes in most of the major cities in the United States in the late nineteenth century defined the required minimum wall thickness based on the height of the building. In Chicago and New York, the prescribed thickness of the wall varied over the height of the building, with thinner walls permitted at the upper stories [3]. Though empirical in nature, these requirements reflected a general understanding that the forces acting on exterior load bearing walls were cumulative, with each portion of wall required to carry the load of all of the portions above.

Building codes of the late nineteenth century addressed the entire building enclosure as a single entity relative to lateral loads. Beginning around 1890, building codes in New York and Chicago specifically addressed wind load requirements for the main structural system of the building and not the cladding. The prescribed wind loads generally varied between 20 (958 Pa) and 30 pounds per square foot (1437 Pa) of wall area [2]. These wind loads were resolved by wind bracing within the building's structural system, but because the magnitude of these loads was insignificant in comparison to the weight of the relatively massive masonry wall systems, they were generally disregarded as design criteria for the exterior cladding.

Whereas the weight and stiffness of the wall system helps to resist wind loads, seismic loads are a function of the mass or weight of an individual component or system undergoing seismic acceleration in a given direction. Not surprisingly, significant dates in the evolution of the seismic code corresponded to major seismic events, beginning in 1906 [4]. Similar to the code's consideration for wind loads, for the most part, the seismic code requirements addressed the behavior of the entire structure rather than individual components. The behavior of the individual components was to become critical with the development of the framed structural system and the curtainwall.

Framed Structural Systems

Cast and wrought iron structural components had been used prior to 1800, but the limitations of these materials restricted the development of iron-framed structural systems. Although originally extolled as inexpensive and resistant to both fire and rust, cast iron was a brittle material that lacked tensile strength. Therefore, early buildings with framed structural systems utilized cast iron compression components coupled with wrought iron beams, which were much stronger in tension and flexure. Several failures within this period illustrated the tendency of cast iron elements to fail due to small imperfections [1]. Additionally, cast iron was soon revealed to be susceptible to both fire and corrosion. In the pursuit of enhanced capacity and performance, the use of cast iron in structural applications was quickly superseded by wrought iron and, as it became available, steel. The material properties of steel were more consistent than those of iron, with good compression strength, tensile strength, and ductility. Because of this consistency and superior performance, steel was used for both column and beam members in later framed buildings.

Following the development of mass-produced rolled steel sections in the 1850s, two building framing systems evolved that ultimately led to modern skyscrapers. The cage building system utilized steel spandrel beams to support both the floor loads and the exterior wall. In a skeleton system, the support of the exterior cladding system was separated from the support of the primary building loads. Both the cage and skeleton systems allowed the exterior wall to function as an enclosure rather than as part of the primary structural system. Therefore, the facade could be treated as a skin that wrapped the skeletal frame. This skin or curtainwall was still required to provide weather protection and transfer wind loads to the structural frame but was no longer required to support the interior floor loads [5].

Curtainwall Systems

Since the curtainwall was not part of the structural system of the building, the need to vary the thickness of the exterior wall was eliminated. Supported at each floor level, the exterior wall needed only to be thick enough to support itself, resist wind loads, and provide necessary weather and fire protection. The backup wall material was typically independent of the facing material, and its primary function was to enclose the steel frame to provide fire protection [6]. In many instances, the lateral anchorage for the facing material was attached to or embedded in the backup wall.

Although the properties of steel were significantly improved over those of iron in terms of tensile strength and ductility, two characteristics of steel members remained problematic—susceptibility to fire and corrosion. Throughout the development of steel-framed high-rise buildings, increasing importance was focused on the issue of fire protection. Testing revealed that a thin layer of masonry or plaster could protect steel members during a fire. This discovery led to embedding the structural frame system within the masonry backup wall, thus providing necessary fire protection as well as minimizing the intrusion of the frame into useable floor space. It was also believed that encasing the steel would protect it from corrosion [6]. Some early curtainwall systems were detailed to allow for an air cavity around the perimeter members. The isolation of the steel from the surrounding masonry was thought to reduce the likelihood of corrosion while maintaining a fireproof member. This system was quickly found to be ineffective, and the complete encasement of the perimeter members followed.

Corrosion became an increasingly significant problem with the introduction of carbon steel lateral anchorage components within wall systems. Metals had been used in walls prior to this period. However, the pieces were small relative to the mass of the wall and were located well within the thickness of the wall, thus protecting them from exposure to corrosive elements. With the thinning of the curtainwall system, the steel members supporting the cladding and the various steel elements providing lateral anchorage were nearer to the surface of the wall. Thus, as the wall began to age and the deterioration of the joints within the cladding allowed increasing amounts of moisture to enter the wall system, the corrosion of the embedded steel was inevitable.

Cladding Materials

Following this period of experimentation with the construction practices and design related to skeleton frame construction, the steel and concrete-framed structural systems were adopted for many major new high-rise buildings after 1900. Early skeletal frame buildings utilized numerous exterior cladding materials. Brick, terra cotta, and stone were all used, with economics frequently dictating both the location and quantity of materials. Early methods of anchoring these masonry cladding materials were varied and frequently experimental. With increased understanding of the behavior of cladding systems relative to interaction with both environmental forces as well as structural systems, lateral anchorage systems evolved further to achieve better performance.

Brick Masonry

Clay brick has been used as a construction material for thousands of years. Early examples of primitive brick were hand pressed and sun dried. Mechanization in the 1850s led to firing of the brick in kilns to achieve a harder, more durable material. In a continued attempt to minimize the potential for fire, brick became a very popular building material in the 1880s. Advances in the production capacity of kilns in brick plants resulted in brick becoming an economical building material [1].

Brick was commonly incorporated into the facades of buildings to provide a uniform appearance and to accentuate decorative elements of the facade. Typically, a more uniform, harder, and more durable face brick was used for the exterior wythe of the wall while softer, less expensive brick was used for the backup wythes. Early brick walls were typically monolithic. Brick headers were used to tie adjacent wythes together. The popularity of the uniform appearance of the running bond pattern led to alternate methods of creating a monolithic wall. Codes in cities such as New York and Chicago required bonding every sixth course into the backup. One alternative to exposed header courses was the use of a blind header system, also known as a diagonal or herring-bone bond, in which the inside corners of the face bricks were cut to accommodate bonding bricks laid diagonally within the wall (Fig.1). Another method involved cutting the face brick lengthwise and setting a header course behind the cut bricks to key the system together. These systems were cumbersome to construct and were rarely used due to increased labor and associated costs. Though not recommended, the bond of the mortar within the collar joint was occasionally relied upon to adhere the face brick to the backup brick. A more reliable system that was more economical than the blind header systems was the incorporation of steel or galvanized iron straps or wire ties (Fig. 1). These ties were installed in the bed joints every sixth course.

Even at the turn of the century, the potential problems of corroding steel were recognized as a shortcoming of the incorporation of metal ties. It was believed, however that by the time the wire had corroded away, the mortar would have cured to the point to "keep the face brick in place" [7]. Another "modern" method published around 1900 was the use of perforated steel ties typically about 1/8-inch thick (3 mm) with "about half of the metal punched out" [7]. Literature of the time recommended that heavier ties be dipped in hot asphalt or galvanized.

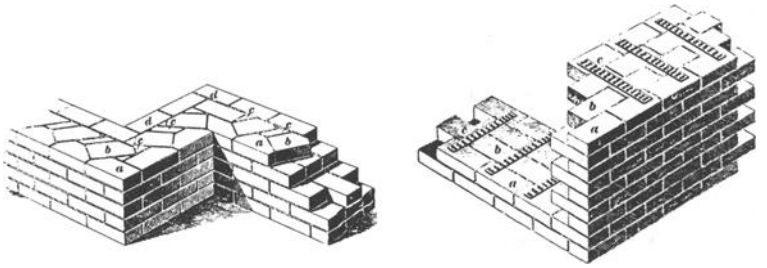

Figure 1 - *Blind header bonding of brick masonry wall and early metal tie system [7].*

The introduction of cavity walls around 1900 necessitated the development of metal anchorage systems that could resist wind loads. These early hollow wall systems were usually limited to small buildings and residential construction. The cavity was introduced to reduce thermal bridging and moisture migration that was sometimes a problem with solid walls. As in solid walls, the exterior face brick was tied to the backup wythes by various configurations of headers, blind headers, or metal ties. The desire to minimize water migration across the cavity led to various anchor geometries that attempted to reduce both mortar bridging and water migration across the anchor (Fig. 2). Wire ties and light gage straps were recommended to be installed 24 inches (0.6 m) on center in every fourth course. Stronger ties were to be installed every eighth course [7].

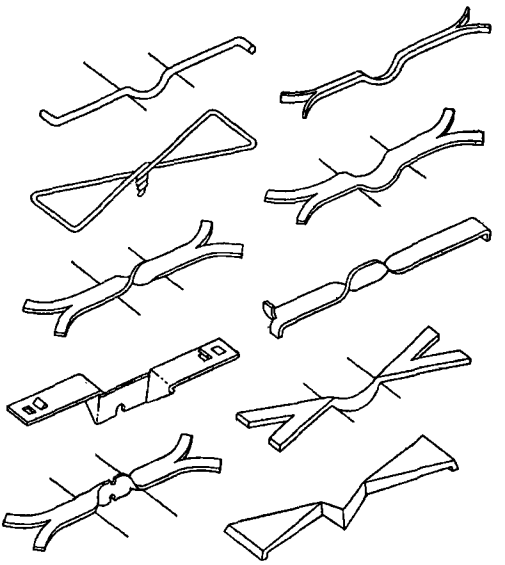

Figure 2 – *Cavity wall metal anchorage systems* [7].

Continued attempts to reduce the cost of the backup material in residential and small commercial buildings resulted in composite veneered wall systems consisting of a brick

facing with a wood-frame backup. The exterior wythe of brick was tied to the wood sheathing on the exterior face of the wood studs with wire ties or bent straps. Tie spacing was recommended at every other brick in every fifth course of brickwork.

Terra Cotta

Terra cotta, much like brick, has been used for thousands of years in construction. Prior to the eighteenth century it was primarily used for roofing, flooring, and sculpture. Traditionally, terra cotta was made by hand pressing a mixture of clay with pulverized terra cotta or brick into molds. Stiffener webs were added to pieces to help maintain their shape. Terra cotta pieces were generally no larger than 24 inches (0.6 m) in any direction to minimize distortion. After the pieces were formed and stiffened, they were dried, fired, and cooled, a process that could take up to two weeks. A vitrified glaze was often applied to the piece before firing a second time, or the original slip glaze was also utilized as the finished surface. Although mass production of terra cotta began in the 1860s, use of the material was not widespread until the 1890s. During the nineteenth century, terra cotta was regarded as "artificial stone," an economical alternative to carved stone. Because repetitive ornamental pieces could be cast from one mold, terra cotta offered economy and decorative flexibility.

Limitations of the material, specifically the tendency of the larger pieces to warp, dictated the size of the units and influenced the methods of support and lateral anchorage [1]. Horizontal framing members such as shelf angles supported the weight of the terra cotta cladding at each floor level, with terra cotta units bearing directly on the support member and subsequent pieces stacked on the pieces below. These terra cotta units were filled with a combination of mortar and brick and were built concurrently with the backup wall in an attempt to bond and key the facing material to the backup wall. In addition, while the wall was being constructed, various types of bent bars were installed to anchor the terra cotta to the backup and provide stability to the system until the mortar had cured. Pieces were generally referred to as *balanced* pieces if they were within the plane of the wall, such as ashlar coursing. Pieces that projected from the plane of the wall, such as cornices or other decorative features, were considered *unbalanced* and required stabilization during construction. Smaller pieces usually incorporated only a single anchor embedded into the top surface, while two anchors were customary for larger pieces. Typical specifications of the time suggested anchor spacing criteria for ashlar coursing of 24 inches (0.6 m) horizontally. Since most pieces were rarely taller than 24 inches (0.6 m), anchors were usually not installed in the bottom of pieces [8].

In some cases individual units or entire courses of terra cotta were hung from horizontal supporting members. These pieces were generally not filled with mortar in order to minimize their weight. Hung pieces, such as window lintels, were supported by horizontal bars inserted into holes in the side webs and hung on hooked bars. The hanger hooks, known as J-bolts, were suspended from shelf angles, hooked over the top flange of an embedded structural member, or hooked through a hole in the web of a member. The hooks and bars were typically 5/8-inch-diameter (15 mm) steel elements protected from corrosion by either galvanizing or a tar coating. Complex terra cotta assemblages such as cornices often combined balanced, unbalanced, and hung pieces requiring an extensive

steel framework to provide gravity and lateral support and overturning resistance for the terra cotta (Figures 3 and 4).

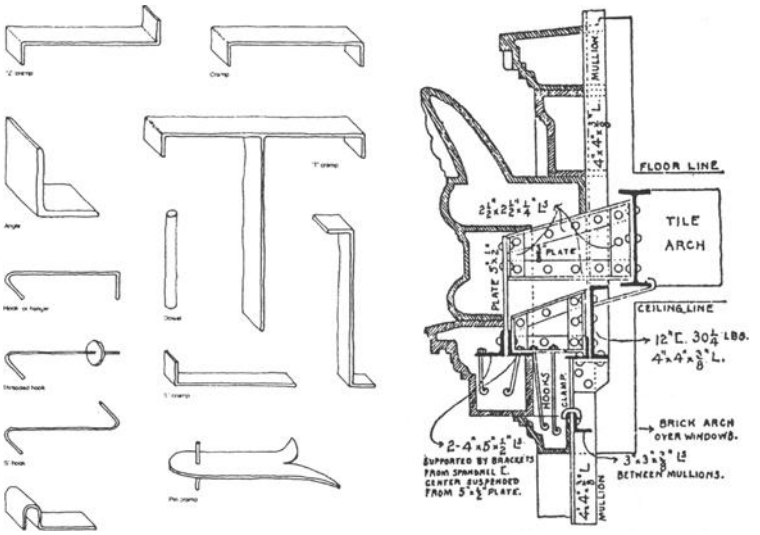

Figure 3 – *Representative terra cotta anchors and support detail [2].*

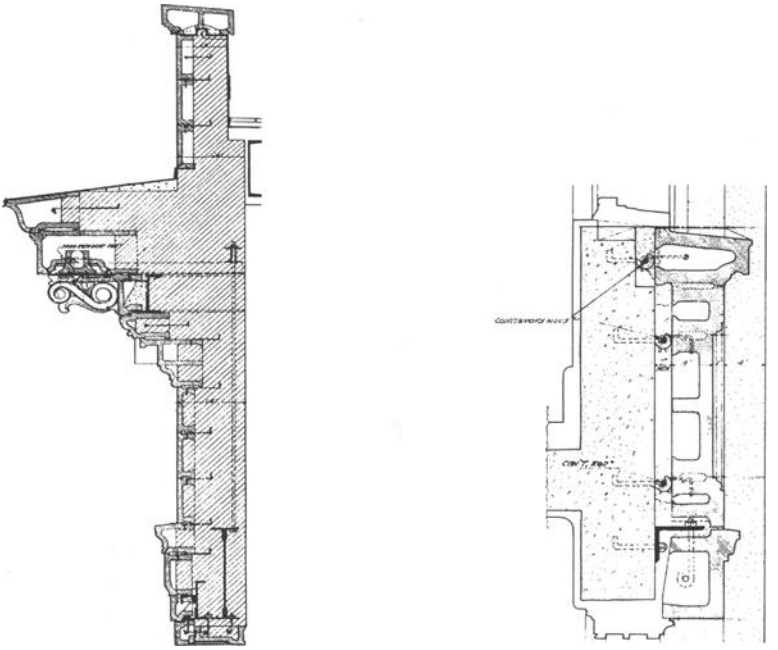

Figure 4 – *Terra cotta cornice and spandrel details from National Terra Cotta Society, Standard Construction 1927 edition.*

Stone

Stone remains one of the only natural materials used in construction. Stone is characterized according to its geologic characteristics as sedimentary, igneous, or metamorphic. Examples of these types of stone are limestone, granite, and marble, respectively. Historically, stone was removed from quarries and then hand cut with saws to create blocks or slabs of the desired size and shape. The size of the individual pieces was limited by the machines and conveying systems of the time. The characteristics of the stone tended to dictate how it was used in buildings.

The individual stone blocks were assembled to create walls of either a single wythe or multiple wythes of stone. Historically, stone walls were constructed similarly to brick walls, although the individual stone pieces were larger than bricks. Multi-wythe walls were often tied together with stones of alternating thickness to key the system together, similar to a brick header system. A typical keyed system employed individual stones that were the full width of the wall. One such through-bond stone was installed for each 10 square feet (0.93 m^2) of wall area. Iron cramps were also sometimes used to tie individual stone blocks together within a wythe or to tie adjacent wythes [7].

The thickness of stone used during the early part of the twentieth century typically varied between 4 and 8 inches (10 and 20 cm), although very expensive stone may have been cut as thin as 2 inches (5 cm). The stone was applied as facing to a brick or clay tile backup wall. Lateral anchorage for stone during this time period was very similar to that of ashlar terra cotta utilizing a combination of keying and bent bars and rods to tie the facing material to the backup masonry. Individual stones of greater thickness keyed the stone facing into the backup wall. Additionally, Z- or C-shaped steel or iron cramp anchors were installed to anchor the stone to the backup when the piece was taller than 18 inches (0.46 m). One end of the cramp anchors was embedded into the backup, and the other end was inserted into a hole or slot in the top or side of the stone panel. If a stone was longer than 30 inches (0.76 m), two cramp anchors were required. The limestone industry recommended a minimum of one anchor per limestone piece and a maximum spacing of 24 inches (0.6 m) between anchors. Further, anchors were recommended in both the top and bottom of pieces that were taller than 30 inches (0.76 m)[9].

1920–1940: The Age of Transition

In the 1920s building heights began to increase dramatically, and the need for lateral anchor systems to accommodate vertical movement was recognized. Over time, structural framing tends to creep and deflect under loading, and fired masonry materials tend to expand as they absorb moisture. In tall buildings, the accumulation of this shortening of the structural frame accompanied by both moisture and thermal expansion of the masonry led to the accumulation of significant compressive stresses within the facade. As the cladding systems aged and water infiltration increased, these stresses were further exacerbated by the accumulation of corrosive scale on the shelf angles used to support the exterior cladding material. Recognition of the combined effects of frame shrinkage, material expansion, and other building movements resulted in conceptual changes in the design of lateral anchorage and cladding systems. The stone industry

began to incorporate special horizontal joints to accommodate these movements. Initially two systems evolved: lead relieving joints at the mid-height of each floor and early forms of soft joints, such as felt and mastic joints, below shelf angle supports.

During the 1920s the increasing popularity of the more streamlined Art Deco style led to a significant reduction in the use of ornamental terra cotta. Limestone and the economical alternative cast stone became desirable cladding materials since they could be used as larger panels, which were becoming popular. As the previously compact individual cladding units became thinner and larger, the need for lateral anchorage to resist wind loads was recognized. The larger, thinner panels were subjected to significantly greater bending stresses than the more compact pieces, and the size of the piece resulted in significantly greater forces exerted on each anchor. Thus, the lateral anchors gained increasing structural significance as a component of the cladding system. Literature of the time indicates that lateral anchors were available in a variety of materials, including galvanized steel, copper, brass, zinc, monel and even aluminum [10]. A less expensive anchor material was steel painted with linseed oil.

Though previously used in brick construction, air cavities began to be included in stone-clad wall systems in the 1930s as a way to accommodate variability in the thickness of stone panels. In a solid wall system, the cladding material resists inward lateral loading through direct contact with the backup wall; however, with the introduction of a cavity, lateral anchorage must be provided to resist both inward and outward lateral loads on the cladding material.

Limestone panels, typically 4 inches (10 cm) thick, were the most common stone cladding material used during this time. Though panels of larger sizes were used, limestone panels were usually less than 12 square feet (1.1 m^2) in area. Various types of strap and rod anchors continued to be embedded into the top or sides of limestone facing panels, providing resistance to both inward and outward lateral loads. To accommodate the need for vertical movement within the wall system, multi-piece lateral anchorage systems incorporating a continuous vertical component attached to the backup wall or cast into the concrete columns, spandrel beams, or fireproofing became popular. The most common of these was the *dovetail* anchor system that consisted of a continuous vertical track and individual strap anchors with trapezoidal tails that fit into the tapered track. Another was called the *tie-to* anchor system consisting of a continuous vertical bar with equally spaced loops that were embedded into the concrete or masonry backup. Individual looped rod anchors engaged the vertical bar and were set into the horizontal joints between cladding panels. The *anchor clip and loop* system consisted of a U-shaped rod that was embedded into the backup with the closed portion extending out from the backup material (Fig. 5). Then a U-shaped strap was hooked over the exposed portion of the rod, and the other end of the strap was inserted into the top surface of the stone facing panels [10].

Other types of stone, including granite and marble, were cut into panels as thin as 1½ inches (3.8 cm) or more commonly 2 inches (5 cm), but these materials were used much less frequently than limestone for exterior cladding. Literature during this period recommended laterally anchoring granite and marble panels with ¼-inch-diameter (6 mm) galvanized or coated steel rods set into the horizontal joints between panels to a depth of ¾ to 1¼ inches (1.8 cm to 3 cm), depending on the thickness of the stone. Mortar spots or plaster of Paris spots within the cavity resisted inward loads. By the late

1930s, installing two ¼-inch-diameter (6 mm) copper or aluminum rods into the sides of the panels was recommended [*11*].

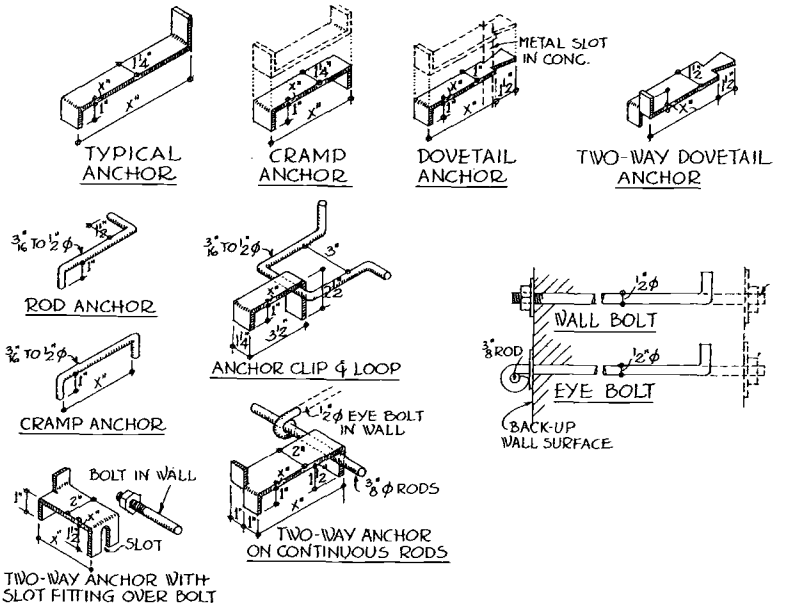

Figure 5 – *Representative lateral anchorage systems for limestone [9].*

Lateral anchorage for brickwork during this period remained largely unchanged. Header bonded walls were still used; however, galvanized corrugated strap ties were much more common. These types of ties were intended to restrain outward movement of the brick facing, but they were ineffective in resisting inward loading. Most of the brickwork facades of this period maintained a fairly narrow collar joint that was usually partially or completely filled with mortar to resist inward loading.

1940–1970: Modernism

After World War II the building boom, economics, and the rise of the Modern movement again changed the building industry with the introduction of the glass and metal curtainwall system. Continuing the evolution of facades hung from a supporting structure, the exterior skin of buildings during this period was constructed from very thin panels of glass, metal, stone, and precast concrete supported by extruded aluminum framing that spanned between floors.

During this period the cavity wall system evolved rapidly. Significant damage resulting from water infiltration and subsequent corrosion of the steel anchorage necessitated a shift in the general approach of the design and construction of wall systems. The recommended width of cavities continued to increase, and the

understanding of the need to create a clear separation between the exterior and interior backup wall for water control and thermal isolation was further recognized.

By the 1950s the anchor spacing rule-of-thumb for individual stone panels was one lateral anchor per 3 square feet (0.28 m^2) of panel area [*12*]. Increasing the size of the panels led to longer or even continuous members set into the edges of panel to provide lateral anchorage. During this period, small panels were also incorporated into panelized systems with much more substantial anchorage systems.

Precast concrete was developed in the 1950s and became popular as an economical alternative to stone cladding. Precast cladding systems offered advantages over conventional cladding systems during both fabrication and installation. Colored aggregate, tile, stone, and brick were frequently used in panels to create a variety of architectural motifs. For smaller inlaid materials such as tile and brick, lateral anchorage was achieved through the bond of the concrete to the inlaid facing materials. Larger pieces of stone or tile were anchored to the concrete with stainless steel wires inserted into holes in the back of the facing material and cast into the concrete. The size of precast panels was restricted between 1940 and 1960 by the limitations of the equipment available for handling large pieces. Many of the early precast cladding systems were set similarly to the cast stone, stone, and terra cotta systems of the time. The true economy of the precast panel system was not realized until very large panels were fabricated off-site and then installed onto the structural frame with cranes or other equipment.

The use of clay tile and concrete block as backup materials led to the development of ladder and truss type wall reinforcement during this period. In lieu of brick backup, the larger units of these materials became popular because they were less expensive, lighter and had lower installation costs. The modular sizing of the concrete block backup units and modern face brick was conducive to the introduction of new lateral anchorage techniques. The ladder and truss type systems were developed to permit the backup and face wythes to work together while also allowing for differential movements between the wythes of masonry. Generally the joint reinforcement consisted of parallel thin galvanized wires connected by intermediate wires either perpendicular to or diagonal to the parallel wires. Various configurations of reinforcement have been introduced, depending on the composition of the wall and the necessary structural performance of the system.

In stone cladding systems, the use of horizontal lead relieving joints continued until the 1960s in walls that employed a keyed course of stone to partially support the stones between shelf angle locations. As sealant technology evolved to provide greater compressibility of sealant materials, "soft" joints began to be incorporated below shelf angle supports at every other floor. Later systems employed soft joints at each floor with intermediate cladding units stacked between shelf angle locations. As larger panels were used, this system eventually developed into the independent support of individual components or panels. Because individual pieces were supported rather than entire stories of material, the anchorage systems began to provide both gravity support and lateral support. The reduced load meant that individual stone support anchors could be extruded out of aluminum. Furthermore, the anchors were often discontinuous and modified so that a portion of the horizontal leg was bent upward to provide lateral support to the stone above and a portion was bent down to engage the stone below the anchor. This anchor is commonly called a *split-tail* anchor. Smaller steel angles were

sometimes used with bars or plates welded to the end of the horizontal leg to engage both the stones above and below the anchor (Figure 6).

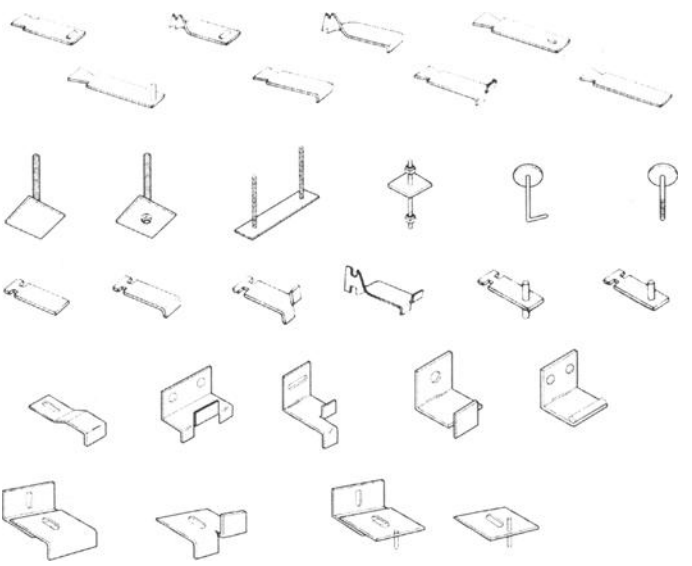

Figure 6 – *Lateral anchorage components. Drawing from Dur-o-Wal product literature.*

1970–2000: Post Modernism

In the later 1970s the rise of the postmodern aesthetic led to the incorporation of traditional facade geometries within a thin stone system. The new systems had to be flexible enough to accommodate multiple anchorage points while still remaining economical. These included more sophisticated precast concrete panels and shop-fabricated trusses with various materials bolted to the frame. Many of these systems required that the lateral anchorage of the stone be positioned on the back face rather than within the edges of the pieces, which had been the conventional method. Though anchorage systems for soffits had employed the use of friction or wedge type anchors in the back face of the stone, the new thinner stone panels could not accommodate these types of anchors. As a result various types of non-friction-type shallow inset anchors were developed within the stone industry. Different types of routing machines were developed that could create flared slots in the back of the stone. The concept of the geometry of these proprietary anchors was similar to toggle bolts. By this period, the stone industry was recommending the use of stainless steel or other non-corrosive metals for all anchorage components in direct contact with the stone. Design of lateral anchorage during this period began to focus on accommodating wind loads. The prescribed design wind loads were based on the probability of a maximum wind gust during a 50-year cycle and were typically between 20 and 50 pounds per square foot (958

Pa and 2395 Pa). The wind design requirements of coastal and mountain areas were significantly higher.

Increasingly stringent seismic code provisions led to the need for very light cladding systems in seismically active areas. These requirements and the continued attempt to reduce building costs resulted in the introduction of new experimental cladding systems. In an attempt at further economy, facing materials such as stone, ceramics, and even brick were cut as thin as ¼ inch (6 mm) and applied to a backing material to create a composite panel. The primary body or core of the panel was composed of honeycomb aluminum, insulation, lightweight concrete, or various wood products. The facing material was adhered to the core with various adhesive materials or modified grouts or mortars. These panels were then used and installed in much the same manner as their stone and precast predecessors (Figure 7).

2000 and Beyond

Modern cladding systems are a complex assemblage of various materials. The infinite variables that affect the performance of a building in general and cladding systems in particular make it almost impossible to anticipate all of the design parameters that should be considered. Lateral anchorage, though seemingly a simple concept, has evolved much like every other aspect of building construction. Undoubtedly more experimental systems will be introduced as building claddings evolve.

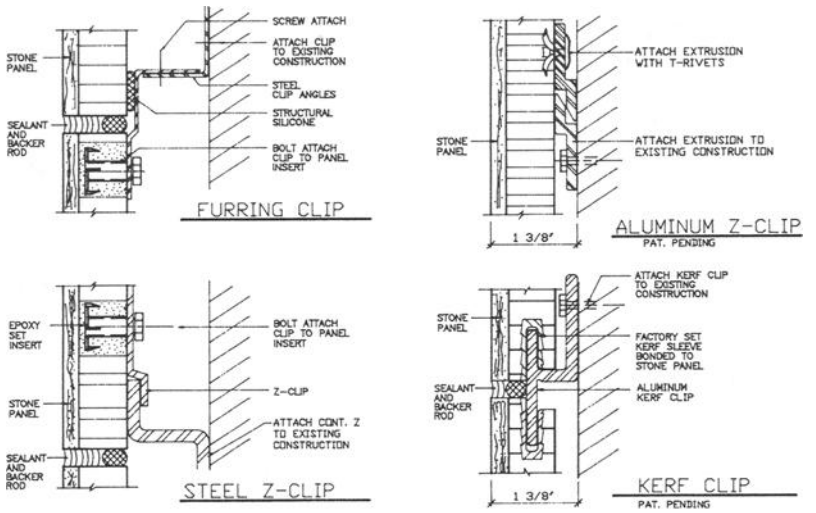

Figure 7 – *Representative lateral anchorage of composite panels from product literature for Ultra-Lite Stone by Stone Panel, Inc.*

References

[1] Elliot, Cecil, *Technics and Architecture; The Development of Materials and Systems for Buildings*, The MIT Press, Cambridge, MA, 1993, pp. 23–73.

[2] Freitag, Joseph, *Architectural Engineering, High Building Construction*, John Wiley and Sons, New York, NY, 1895, pp. 89–110.

[3] Birkmire, William, *The Planning and Construction of High Office-Buildings*, John Wiley and Sons, New York, NY, 1905, pp. 98–118.

[4] Holmes, W., "The History of U. S. Seismic Code Development," *Past, Present and Future Issues in Earthquake Engineering, Proceedings of the 50th Annual Meeting of the Earthquake Engineering Research Institute*, San Francisco, CA, 4–7 February, 1998.

[5] Yeomans, David, *Construction Since 1900: Material*, B. T. Batsford Ltd, London, England, 1997, pp. 33-40.

[6] Freitag, J. K., *The Fireproofing of Steel Buildings*, John Wiley and Sons, New York, NY, 1899.

[7] Lavicka, William, *The Art of Architecture, Engineering and Construction in 1899*, Chicago Review Press, Chicago, IL, 1980.

[8] Birkmire, William, *Skeleton Construction in Buildings*, John Wiley and Sons, New York, NY, 1894.

[9] *A Portfolio of Detail Plates and General Information*, Indiana Limestone Institute, Bedford, IN, 1949.

[10] Ramsey, C. G. and Sleeper, H. R., *Traditional Details for Building Restoration, Renovation, and Rehabilitation, from the 1932-1951 Editions of Architectural Graphic Standards*, ed. J. Belle, J. R. Hoke, and S. A. Kliment, Eds., John Wiley and Sons, New York, NY, 1990, p. 63.

[11] Sleeper, H. R., *Architectural Specification*, John Wiley and Sons, New York, NY, 1940 pp. 78-140.

[12] Mulligan, John, *Handbook of Brick Masonry Construction*, McGraw Hill Book Company, New York, NY, 1942.

Jason J. Thompson,[1] Craig T. Walloch,[2] and Robert D. Thomas[3]

Predicting Grouted Concrete Masonry Prism Strength

Reference: Thompson, J. J., Walloch, C. T., and Thomas, R. D., "**Predicted Strength Gain of Grouted Concrete Masonry Prisms,**" *Masonry: Opportunities in the 21st Century, ASTM STP 1432*, D. B. Throop and R. E. Klingner, Eds., ASTM International, PA, 2002.

Abstract: The structural performance of masonry is in part influenced by the relative and absolute compressive strength of the units, mortar, and grout. However, during the period immediately following masonry construction, the compressive strength of a given assemblage is often uncertain, as these materials have had insufficient time to fully cure. Further, with a near infinite number of combinations of unit, mortar, and grout strengths, designers have historically had little guidance related to available individual component properties when selecting a specified compressive strength of masonry for design purposes.

In response to these needs, this paper analyzes a database of prism compression tests, which incorporate varying material properties into their construction. Based on the results of the prism tests, a prediction model is proposed that provides a correlation to the unit strength, mortar type, grout strength, and prism configuration to the measured prism compressive strength at varying ages of curing.

The prediction model is based on 14 sets of prisms that were constructed and tested to measure the influence of age on the strength of grouted masonry prisms. The prisms were all constructed using the same materials and construction methods and were tested at ages of 0, 1, 2, 3, 4, 5, 6, 7, 14, 21, 28, 35, 42, and 56 days following grouting. Additional 28-day strengths of grouted prisms from other research programs were used to validate the model and to further correlate the influence of mortar type, unit strength, grout strength, and prism configuration on the measured versus predicted prism strength.

Keywords: aspect ratio, CMU, compressive strength, concrete masonry, concrete masonry unit, grout, masonry, mortar, predicted strength, prism, testing variables, unit, water content.

[1] Structural Engineer, National Concrete Masonry Association, 13750 Sunrise Valley Drive, Herndon, VA 20171.

[2] Technical Services Manager – Masonry Products, W. R. Grace & Co. – Conn., 62 Whittemore Avenue, Cambridge, MA 02410.

[3] Vice President of Engineering, National Concrete Masonry Association, 13750 Sunrise Valley Drive, Herndon, VA 20171.

Introduction

Frequently, situations arise whereby the strength of a grouted masonry assemblage requires evaluation prior to reaching 28 days of curing. Other times, the strength of a grouted assemblage needs to be estimated based solely upon the physical properties of the individual components used in construction. The lack of documented information pertaining to these two issues continues to result in construction delays and over-specifying necessary material properties. As such, contractors and designers alike are obliged to rely upon personal experience and estimates of 28-day strengths based on interim tests. Lacking such experience, a risk of increasing the overall cost of construction can be introduced by over-specifying, under-estimating, or misinterpreting material strengths.

To address this need, a research project was undertaken that consisted of testing 14 sets of grouted concrete masonry prisms after 0, 1, 2, 3, 4, 5, 6, 7, 14, 21, 28, 35, 42, and 56 days of curing. Based on the rate of strength gain established with these results, a prediction model is proposed that allows users to estimate the compressive strength of a prism based solely on curing time.

A next step in the analysis was to develop a generic form of the prediction equation to allow its use with various material properties, thereby establishing a correlation to the influence of mortar type, unit strength, grout strength, and prism configuration on the measured versus predicted prism strength. Finally, results of additional research programs were introduced to verify the prediction capability of the proposed prism strength model.

Material Properties

Concrete Masonry Units

The prisms of this research investigation were constructed with conventional hollow concrete masonry units with specified dimensions of 7 5/8 × 7 5/8 × 15 5/8 inches (194 × 194 × 397 mm). All of the units were manufactured at the same time and were of identical configuration with two square cores and square corners on both ends.

The units were tested full-size in accordance with ASTM Test Methods for Sampling and Testing Concrete Masonry Units and Related Units (C 140), the results of which are summarized in Table 1. At the time of prism construction, the units had cured for more than 28 days. Although drying shrinkage was not evaluated, all other properties of the concrete masonry units complied with the applicable requirements of ASTM Specification for Loadbearing Concrete Masonry Units (C 90).

To facilitate construction and evaluation, the prisms of this research project were constructed of half-length units (consisting of a single enclosed cell with full webs on each end). As such, the pertinent properties of these reduced size units were also determined for analysis purposes. The average cross-sectional properties determined for the half-size units included a net cross-sectional area of 34.9 in^2 (22500 mm^2), a gross cross-sectional area of 63.1 in^2 (40700 mm^2), and a percent solid of 55.2%.

TABLE 1 — *Average Tested Properties of Concrete Masonry Units.*

Unit Property	Full-Size Units
Net Area Compressive Strength	3630 lb/in^2 (25.0 MPa)
Oven-Dry Density	131.7 lb/ft^3 (2110 kg/m^3)
Absorption	8.0 lb/ft^3 (128 kg/m^3)
Average Dimensions	
•Width	7.62 in. (194 mm)
•Height	7.60 in. (193 mm)
•Length	15.54 in. (395 mm)
•Minimum Face Shell Thickness	1.29 in. (33 mm)
•Minimum Web Thickness	1.20 in. (30 mm)
Percent Solid	52.3 %

Mortar

Mortar Proportioning and Mixing — Type S portland cement/lime mortar was used to construct each of the prism specimens. The mortar constituents were mixed by volume in accordance with ASTM Specification for Mortar for Unit Masonry (C 270) to the following proportions: 1 part portland cement conforming to ASTM Specification for Portland Cement (C 150), one-half part Type S hydrated lime conforming to ASTM Specification for Hydrated Lime for Masonry Purposes (C 207), and 4½ parts masonry sand conforming to ASTM Specification for Aggregates for Masonry Mortar (C 144).

Potable water was added to the mortar during the mixing at the discretion of the mason to produce a workable consistency. All mortar was mechanically mixed for approximately 10 minutes. Any mortar unused 1½ hours after initial mixing was discarded. Retempering of the mortar was permitted once, but stiff mortar or mortar that had hardened due to hydration was not used.

Mortar Testing — Mortar was sampled during specimen construction for the purpose of documenting mortar properties in accordance with ASTM Test Method for Preconstruction and Construction Evaluation of Mortars for Plain and Reinforced Unit Masonry (C 780). The compressive strength of the mortar was determined using 2-inch (50.8 mm) cubes cured for a period of 28 days. The documented mortar strength was 3200 lb/in^2 (22.0 MPa). The observed consistency cone penetration of the plastic mortar was 53 mm (2.1 inches).

Grout

A local ready-mix concrete/grout supplier furnished the grout used in this research. The slump was measured in accordance with ASTM Test Method for Slump of Hydraulic Cement Concrete (C 143). Water was added to the grout on-site to produce a slump of 10-½ inches (267 mm) before placement.

Compliance with ASTM Specification for Grout for Masonry (C 476) was documented using the property specification of that standard. The tested 28-day grout strength, determined in accordance with ASTM Test Method for Sampling and Testing Grout (C 1019), was measured at 2300 lb/in^2 (15.9 MPa).

Masonry Prism Construction

Two journeyman masons with more than 30 years combined experience in masonry construction fabricated the test specimens using good construction techniques in accordance with the national masonry specification ACI 530.1/ASCE 6/TMS 602 [1] and ASTM Test Method for Compressive Strength of Masonry Prisms (C 1314).

Each prism consisted of two half-length units (saw-cut from full size units) laid in a stack bond configuration on a full mortar bed. The resulting outside dimensions of the prisms were approximately 7 5/8 inches (194 mm) wide by 15 5/8 inches (397 mm) high by 7 5/8 inches (194 mm) long. Approximately one week after construction, the concrete masonry prisms were filled with grout in one lift and consolidated and reconsolidated using mechanical vibration. Subsequent to the initial loss of water from the grout due to absorption by the units, a small amount of grout was added to the top of the specimens as necessary to bring the grout level with the top surface of the prisms.

Immediately following grouting, the prisms were sealed within plastic bags to minimize water loss due to evaporation. Approximately 48 hours prior to testing, the prisms were removed from the plastic bags and allowed to equalize with the temperature and moisture conditions of the laboratory environment. The only deviation to this procedure pertained to the prism tests conducted during the first few days after grouting. These prisms did not have an equal amount of time to equalize with the environment and therefore may have had higher moisture contents than those prisms tested at later ages. Nonetheless, the higher prism moisture content, and its impact on the measured compressive strength, is considered to be an inherent property of early-age prism tests. Therefore, no attempt was made to correct for the relatively high moisture content of the early-age prisms except as described in the following analysis.

In total, 14 sets of prisms were constructed and tested in accordance with ASTM C 1314, with each set consisting of five individual specimens for a total of 70 prisms. Each set of prisms corresponded to each day of testing at 0, 1, 2, 3, 4, 5, 6, 7, 14, 21, 28, 35, 42, and 56 days following grouting.

Test Results and Observations

Table 2 provides a summary of the results of the testing program, which includes the day the prisms were tested relative to the day they were grouted along with the compressive strength corrected in accordance with C 1314 for each of the five specimens in each set.

The Day 0 prisms were tested without grout to represent the characteristics of the prisms immediately after plastic grout is placed. However, a freshly grouted prism would have imparted moisture into the concrete masonry units. Since relatively high moisture content reduces the tested compressive strength of concrete masonry units and prisms [2], the actual tested values for Day 0 prisms were reduced by 10% to reflect an estimated prism strength with plastic grout. The value of 10% assumes that the tested Day 0 prism had a moisture content of approximately 40%, whereas a corresponding set of grouted prisms would have had a moisture content of approximately 70%. No other results include this correction. In addition, the recorded net area strength from the Day 0 hollow

prisms was converted into a gross area strength to permit comparison with other grouted prisms (where the net cross-sectional area is equal to the gross cross-sectional area).

TABLE 2 — *Prism Test Results.*

Day	Individual Prism Strengths, lb/in^2 (MPa)	Average, lb/in^2 (MPa)	Standard Deviation, lb/in^2 (MPa)	Coefficient of Variation %
0	1440 (9.9), 1400 (9.7), 1460 (10.1), 1350 (9.3), 1440 (9.9)	1420 (9.8)	48.6 (0.3)	3.4
1	1690 (11.6), 1620 (11.1), 1730 (11.8), 1700 (11.6), 1730 (11.8)	1690 (11.6)	43.2 (0.3)	2.6
2	1890 (12.9), 1870 (12.8), 1750 (11.9), 1960 (13.4), 1910 (13.0)	1880 (12.8)	76.9 (0.5)	4.1
3	1910 (13.0), 1970 (13.5), 1960 (13.4), 1990 (13.6), 1850 (12.6)	1940 (13.2)	57.0 (0.4)	2.9
4	1990(13.6), 1960 (13.4), 2000 (13.6), 1990 (13.6), 1820 (12.4)	1950 (13.3)	75.6 (0.5)	3.9
5	2170 (14.8), 2120 (14.5), 2100 (14.4), 2060 (14.1), 2090 (14.3)	2110 (14.4)	39.5 (0.3)	1.9
6	2100 (14.3), 2090 (14.2) 2240 (15.3), 2010 (13.7), 2060 (14.0)	2100 (14.3)	86.6 (0.6)	4.1
7	2110 (14.4), 2150 (14.6), 2220 (15.1), 2250 (15.4), 2220 (15.2)	2190 (14.9)	58.3 (0.4)	2.7
14	2510 (17.2), 2640 (18.0), 2390 (16.3), 2380 (16.3), 2560 (17.5)	2500 (17.0)	111.2 (0.8)	4.4
21	2760 (18.8), 2740 (18.7), 2690 (18.4), 2670 (18.3), 2640 (18.0)	2700 (18.4)	48.2 (0.3)	1.8
28	2800 (19.1), 2690 (18.3), 2760 (18.8), 2660 (18.1), 2680 (18.3)	2720 (18.5)	59.3 (0.4)	2.2
35	2900 (19.8), 2840 (19.4), 2990 (20.4), 2940 (20.1), 2970 (20.3)	2930 (20.0)	62.5 (0.4)	2.1
42	2770 (18.9), 2610 (17.8), 2640 (18.0), 2850 (19.5), 2730 (18.6)	2720 (18.6)	96.6 (0.7)	3.6
56	3090 (21.1), 3040 (20.8), 2930 (20.0), 2970 (20.3), 3020 (20.6)	3010 (20.6)	63.3 (0.4)	2.1

Analysis of Results

Influence of Curing Time on Prism Strength

As a means of predicting the results reported in Table 2, Eq. 1 was derived as a best fit to the documented prism compressive strengths. The relationship of the measured prism strength gain to the predicted prism strength gain is illustrated in Figure 1. The r^2 for Eq. 1 is to equal 0.98, showing good correlation between the predicted and measure values.

$$P_{ST} = 393 \ln(D + 1) + 1400 \quad (1)$$

The metric equivalent of Eq. 1 is:

$$P_{ST} = 2.71 \ln(D + 1) + 9.7$$

where

P_{ST} = predicted prism compressive strength, lb/in^2 (MPa).
D = number of days of curing of grout.

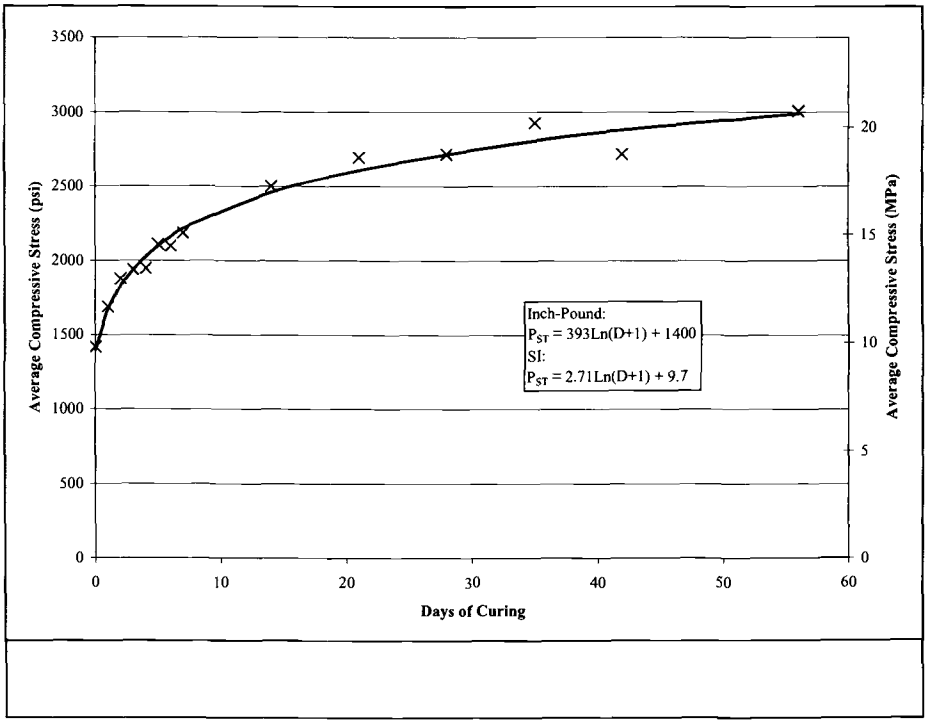

Although Eq. 1 could be used as a means of predicting the compressive strength of concrete masonry prisms constructed with materials similar to those used in this study, a more general form of the equation is sought for more universal application. A generic form of Equation 1 would take into consideration the contribution of the units and the grout on the measured prism compressive strength. Rewriting Eq.1 with this consideration yields the following:

$$P_{ST} = G \ln(D + 1) + U \tag{2}$$

where

G = grout strength coefficient.
U = unit strength influence.

The form of Eq. 2 indicates that the predicted prism compressive strength, P_{ST}, is equal to the contribution of the masonry unit's strength, U, plus a contribution from the grout

equal to $G \ln(D+1)$. This grout contribution is equal to zero at Day 0 and increases as a function of the natural log of time.

Influence of Unit Strength on Prism Strength

The value of U in Eq. 2 can be considered to represent the influence on the measured prism compressive strength provided by the compressive strength of the concrete masonry unit used in constructing the prism. To correlate the contribution of the unit strength, as documented through C 140 testing, to the strength of a unit in a masonry prism, U is multiplied by appropriate factors to account for the volume of the unit to be filled with grout, the type of mortar used in construction, and the impact the aspect ratio has on the measured compressive strength. Further, as discussed above, a moisture factor is included to account for the deleterious impact of increased water content on measured compressive strength. Hence, the value U can be generically expressed as:

$$U = (S_u)(\alpha_u)(\zeta_u)(\omega_u) \tag{3}$$

where

S_u = net area compressive strength of the concrete masonry unit used to construct the prism, lb/in^2 (MPa).
α_u = unit volume proportion factor. This factor is equal to the percent solid of the concrete masonry unit used to construct the prism.
ζ_u = unit construction factor. This factor is a function of the overall dimensions of the prism and the type of mortar used in construction.
ω_u = moisture content factor for the concrete masonry unit.

To understand and determine the unit construction factor, ζ_u, one can start by examining numerous research efforts [3–6] over the past 50 years that have developed a relationship between the measured compressive strength of a unit and the corresponding compressive strength of masonry (as measured through prism testing) constructed with such units. Current practice for determining the compressive strength of masonry based on unit strength and mortar type is documented in ACI 530.1/ASCE 6/TMS 602 [1] and summarized in Table 3. The ratios of the masonry to unit compressive strength are also included in Table 3, although these values are not part of the original ACI 530.1/ASCE 6/TMS 602 table. Inherent in this table is an assumption of at least 28 days of curing for the mortar. Further, this method does not consider the contribution of grout on the measured compressive strength of grouted prisms (although grout could be added, as long as the specified strength is not less than the masonry strength).

Because the unit strength method has known conservatism built into it (since these values are used for design purposes), the original data was analyzed to remove this conservatism for application here. The original results [3–6] are plotted in Figure 2 and a best-fit linear line was determined for each prism set constructed. The coefficient of the best-fit line indicates that for Type M or S mortar the prism strength equals 0.92 times the unit strength. Likewise, for Type N mortar the coefficient of the best-fit line indicates that the prism strength equals 0.86 times the unit strength.

Table 3 – *Unit Strength Method [1].*

Masonry Compressive Strength, lb/in^2 (MPa)	Type M or S Mortar		Type N Mortar	
	Unit Compressive Strength, lb/in^2 (MPa)	Ratio of Masonry Strength to Unit Strength	Unit Compressive Strength, lb/in^2 (MPa)	Ratio of Masonry Strength to Unit Strength
1000 (6.9)	1250 (8.6)	0.80	1300 (9.0)	0.77
1500 (10.3)	1900 (13.1)	0.79	2150 (14.8)	0.70
2000 (13.8)	2800 (19.3)	0.71	3050 (21.0)	0.66
2500 (17.2)	3750 (25.9)	0.67	4050 (27.9)	0.62
3000 (20.7)	4800 (33.1)	0.63	5250 (36.2)	0.57

To determine the factor of conservatism, the coefficient obtained from each of these analyses was divided by the largest ratio of the masonry strength to the unit strength obtained for each mortar type of Table 3. For Type M or S mortar, the maximum ratio is 1000/1250 = 0.80, hence the corresponding factor of conservatism is, 0.92/0.80 = 1.16. Similarly, for Type N mortar, the largest ratio is 1000/1300 = 0.77, hence the ratios from Table 3 are increased by a factor of 0.86/0.77 = 1.12. To determine the corrected unit construction factor, ζ_u, for Equation 3 (thereby removing the conservatism inherent within the unit strength method) for masonry prisms with various masonry compressive strengths and mortar types, the ratios in Table 3 are multiplied by either 1.16 or 1.12 as appropriate depending on mortar type and are shown in Table 4. (For intermediate values of masonry compressive strength, the construction factors may be linearly interpolated.)

Table 4 – *Corrected Ratios of Masonry Strength to Unit Strength*

Type M or S Mortar			Type N Mortar		
Unit Compressive Strength, lb/in^2 (MPa)	Ratio of Masonry Strength to Unit Strength	Unit Construction Factor, ζ_u, [ζ_u = 1.16(Ratio)]	Unit Compressive Strength, lb/in^2 (MPa)	Ratio of Masonry Strength to Unit Strength	Unit Construction Factor, ζ_u, [ζ_u = 1.12(Ratio)]
1250 (8.6)	0.80	0.92	1300 (9.0)	0.77	0.86
1900 (13.1)	0.79	0.91	2150 (14.8)	0.70	0.78
2800 (19.3)	0.71	0.82	3050 (21.0)	0.66	0.73
3750 (25.9)	0.67	0.77	4050 (27.9)	0.62	0.69
4800 (33.1)	0.63	0.72	5250 (36.2)	0.57	0.64

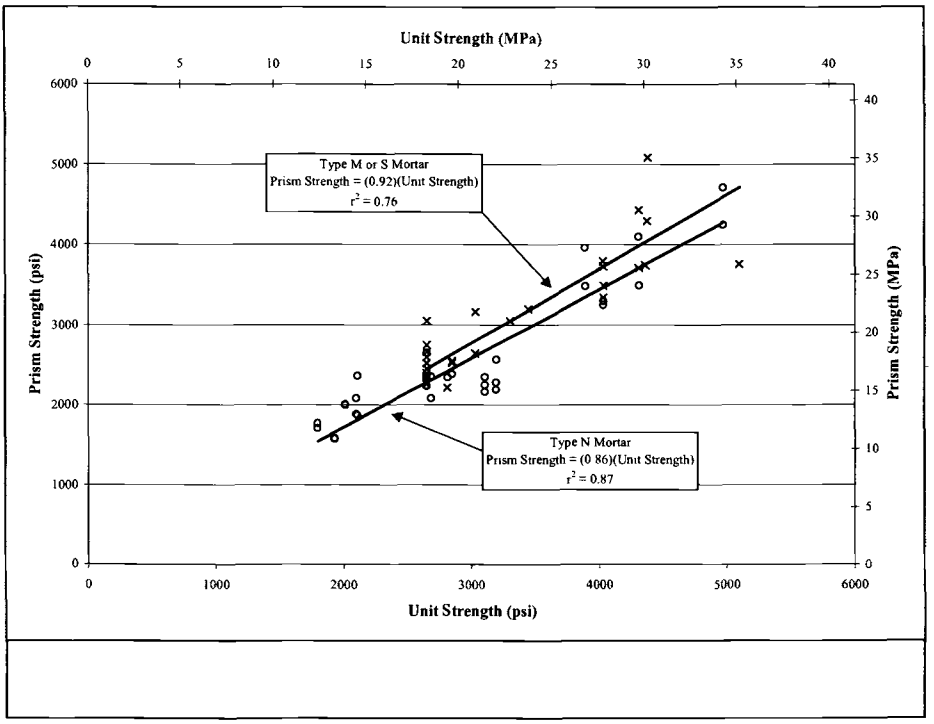

Referring back to the materials properties used in this project, the units had a net area compressive strength of 3630 lb/in^2 (25.0 MPa) and a percent solid of 55.2% (based on the half-length units). Each of the prisms were constructed using Type S mortar. Linearly interpolating the combined mortar and shape factor influence from Table 4 for the material properties used in this study, a value of 0.78 for ζ_u is determined. Therefore, for the specific construction variables of this program, the unit strength influence of the prism strength, U, is calculated as follows (based again on the previous discussion and assumption of a moisture content factor of 0.90):

$$U = (S_u)(\alpha_u)(\zeta_u)(\omega_u) = (3630 \text{ lb/in}^2)(0.55)(0.78)(0.90) = 1402 \text{ lb/in}^2 \text{ (9.7 MPa)}$$

Rounding this value to the nearest 10 lb/in^2 yields 1400 lb/in^2 (9.7 MPa) – a value that happens to equal to the predicted regression constant of 1400 lb/in^2 (9.7 MPa), and is very close to the measured moisture corrected Day 0 prism strength of 1420 lb/in^2 (9.8 MPa) reported in Table 2. Therefore, Eq. 3 appears to be a good predictor of a unit's contribution to the overall compressive strength of a prism. Combining Eqs. 2 and 3 yields:

$$P_{ST} = G \ln(D + 1) + (S_u)(\alpha_u)(\zeta_u)(\omega_u) \quad (4)$$

Therefore, knowing the net area compressive strength of a unit, the percent solid of the unit to be used in prism construction, and the type of mortar used in constructing the prism, the prism compressive strength can be estimated using Equation 4 for grout properties similar to those used in this study. (Alternatively, the gross area unit compressive strength could be used in Eq. 4 instead of S_u by setting α_u equal to 1.0.)

Influence of Grout Strength on Prism Strength

One aspect not yet taken under consideration is the influence the compressive strength of the grout has on the measured prism strength. This influence is equal to G multiplied by the natural log of $D + 1$, as expressed in Eqs. 2 and 4. As with U, G is determined by multiplying the 28-day compressive strength of the grout by similar correction factors to account for the volume of the unit to be filled with grout, the influence of aspect ratio, and adjustments to account for differences in the moisture content of the grout at the time of testing – expressed generically in Eq. 5. In addition, the expression for G as shown in Equation 5 is inversely proportional to the natural log of 29 (28 + 1 days). This term in the denominator normalizes the grout strength to accurately account for strength gain when the expression for G is substituted into Eq. 2. As a result, at an age of 28 days, the ln (28 + 1) terms will cancel each other out and the grout contribution is the 28-day compressive strength multiplied by the various correction factors. At an age of 0 days, the grout contribution will be zero. At other ages, the expression will reflect the contribution of the grout to the prism strength as it increases relative to the natural log of time.

$$G = (S_g / \ln (28+1))(\alpha_g)(\zeta_g)(\omega_g) \tag{5}$$

where

S_g = 28 day net area compressive strength of grout used in prism construction, lb/in^2 (MPa).

α_g = grout volume proportion factor. This factor is taken to be equal to 1- α_u.

ζ_g = grout construction factor, dependent upon the overall dimensions of the prism and the dimensions of the hollow cores of the concrete masonry unit.

ω_g = moisture content factor for the grout.

As a requirement of C 1019, compression specimens are constructed with an aspect ratio of 2 to 1 (height to thickness). However, the aspect ratio of the column of grout within the prism may differ from that of a C 1019 specimen and thus, the grout construction factor, ζ_g, is introduced in Eq. 5. The dimension of the column of grout within the 8-inch (203 mm) masonry prisms used in this investigation is approximately 5 inches (127 mm) in width (using the interior cell dimensions) by 15 5/8 inches (397 mm) in height, yielding an aspect ratio of 3.1 to 1. To account for differences in varying aspect ratios on the measured compressive strength of masonry prisms, C 1314 contains a table of correction factors, shown below in Table 5, to increase or decrease the measured compressive strength accordingly. Interpolating between the values in Table 5 for an aspect ratio of 3.1 provides a correction factor 1.08. This correction factor is employed

here to adjust the strength of grout (through the term ζ_g) that would be expected if the grout column within the prism had an aspect ratio of 2.0.

TABLE 5 — *Grout Construction Factor, ζ_g (Equal to the Height to Thickness Correction Factors for Masonry Prism Compressive Strength from C 1314).*

h_p / t_p	1.3	1.5	2.0	2.5	3.0	4.0	5.0
Grout Construction Factor, ζ_g	0.75	0.86	1.00	1.04	1.07	1.15	1.22

where

h_p = height of masonry prism, in. (mm)
t_p = least lateral dimension of masonry prism, in. (mm)

When grout specimens are tested in compression in accordance with ASTM C 1019, they are tested in a damp condition after they are removed from their moist curing environment. This moisture content is greater than is typical for grout within a masonry prism. Therefore, using a similar analogy as previously discussed, it is necessary to increase the 28-day C 1019 strengths by a factor of 1.11 (ω_g = 1/0.90) to represent the grout's moisture content characteristics within the prism.

Applying these terms into Eq. 5, G can be calculated for the specimens used in this research as follows:

$$G = (S_g / \ln(28+1))(\alpha_g)(\zeta_g)(\omega_g) = ((2300 \text{ lb/in}^2)/(\ln(29))\ (0.45)(1.08)(1/0.90) = 368$$

The calculated constant for G of 368 using this proposed model is within 7% of the coefficient of 393 that was obtained by the regression analysis applied to the data set of 14 prisms tested at different ages.

Combining Eqs. 2, 3, and 5 yields the following general equation that can be used to predict the prism strength from any combination of grout and unit properties:

$$P_{ST} = [(S_g / \ln(28+1))(\alpha_g)(\zeta_g)(\omega_g)]\ln(D+1) + (S_u)(\alpha_u)(\zeta_u)(\omega_u) \quad (6)$$

The metric equivalent of Eq. 6 is the same. A plot of the measured versus predicted prism strength as given by equation 6 is provided in Figure 3. The predicted versus measured compressive strengths illustrated in Figure 3 show good correlation with r^2 = 0.98, with the predicted strengths being a little less (approximately 3% on average) than the measured prism strengths.

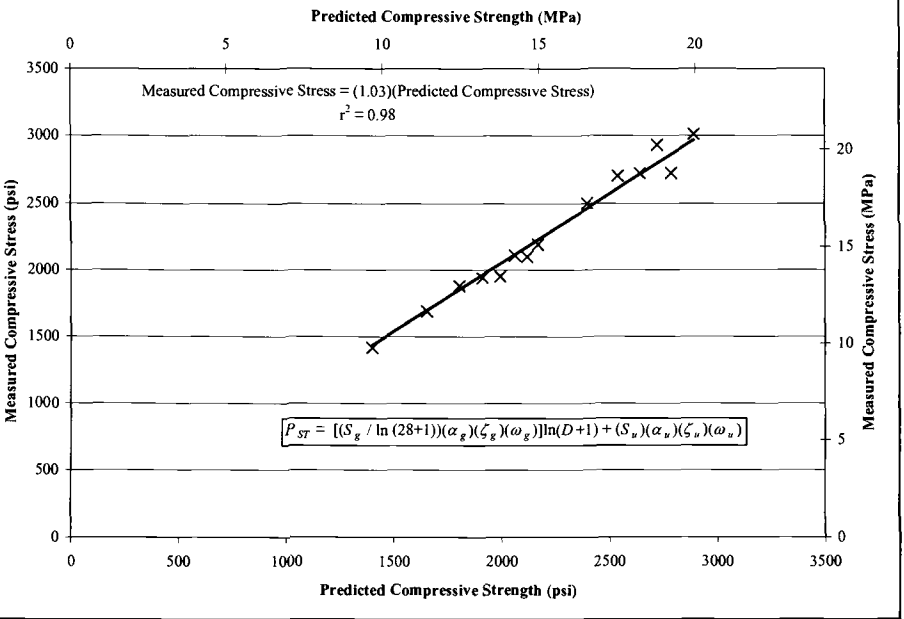

Figure 3 – *Predicted Compressive Strength*

Comparison of Predicted 28-Day Prism Strengths Using Other Test Results

At 28 days, Eq. 6 reduces to a simplified form that represents the sum of the measured 28-day grout strength modified by its volume proportion, construction and moisture factors plus the measured 28-day unit strength modified by its corresponding volume proportion, construction, and moisture factors:

$$P_{ST28} = (S_g)(\alpha_g)(\zeta_g)(\omega_g) + (S_u)(\alpha_u)(\zeta_u)(\omega_u) \quad (7)$$

where

P_{ST28} = predicted 28-day prism compressive strength, lb/in^2 (MPa)

Although Eq. 6 indicates good correlation using the data of this research project, it has not been checked relative to other sources of prism test data. Because unit and grout strengths vary, several independent sources [9, 10] of unit, grout, and 28-day prism strength data were analyzed. A summary of these results (which include the 28-day strengths of this project) is shown in Table 6. Prism test results from each of these research projects were determined in accordance with C 1314. (As a note, prior to 1999 the majority of prism test data available were based on tests conducted in accordance with the discontinued testing procedures of ASTM Test Methods for Compressive Strength of Masonry Prisms (E 447) or by building code modified procedures. As such,

other testing variables such as face shell versus full mortar bedding and method of curing were introduced. Therefore, prism test results obtained by methods other than C 1314 are not included herein.)

Using Eq. 7 to predict prism strengths reported in Table 6, and employing the appropriate construction variables demonstrates that this method provides estimated strengths that range from 90% to 120% of actual strengths and on average overestimate actual strengths by 5% as shown in Figure 5. The r^2 correlation for prediction compared to actual for this data was a reasonable 0.83, considering all of the variables involved.

TABLE 6 — *Compilation of Test Results.*

Unit Strength, lb/in^2 (MPa)	Grout Strength, lb/in^2 (MPa)	Prism Strength, lb/in^2 (MPa)	Equation 7 Predicted Strength, lb/in^2 (MPa)	Ratio of Predicted to Measured Prism Strengths
2640 (18.2)	3560 (24.5)	2850 (19.7)	2950 (20.3)	1.03
2670 (18.4)	4680 (32.3)	3180 (21.9)	3490 (24.0)	1.10
2670 (18.4)	5530 (38.1)	3290 (22.7)	3950 (27.2)	1.20
2170 (15.0)	2050 (14.1)	1700 (11.7)	1920 (13.3)	1.13
3070 (21.2)	5130 (35.4)	4070 (28.1)	3820 (26.3)	0.94
3630 (25.0)	2300 (15.9)	2720 (18.8)	2450 (16.9)	0.90
3070 (21.2)	2634 (18.2)	2320 (16.0)	2480 (17.1)	1.07
3070 (21.2)	2470 (17.7)	2430 (16.8)	2450 (16.9)	1.01
			Average =	1.05

As a means to further simplify the application of this recommended procedure for predicting an estimated prism strength, common values for the construction and testing variables could be introduced into Eq. 7. Assuming $\alpha_g = 0.45$ (applicable for half-length 8-inch (203 mm) units), $\zeta_g = 1.08$ (applicable for 8-inch (203 mm) units and 16 inch (406 mm) prism heights), $\omega_g = 1/0.90$ (assumes a 70% grout moisture content at the time of testing the grout and a 40% prism moisture content at the time of testing), $\alpha_u = 0.55$ (applicable for half-length 8-inch (203 mm) units), $\zeta_u = 0.85$ (assumes Type M or S mortar and a unit strength of approximately 2500 lb/in^2 (17.2 MPa), and $\omega_u = 0.90$ (assumes a 70% prism moisture content at the time of testing and a 40% equilibrium prism moisture content), Equation 7 reduces to:

$$P_{ST28} = (0.54)(S_g) + (0.42)(S_u) \tag{8}$$

Conversely, for applications whereby compression strength results are needed at intermediate days, Equation 8 could be revised as shown in Eq. 9 while employing the values for the natural log of common curing periods given in Table 7.

$$P_{ST} = (0.16)(S_g)\ln(D + 1) + (0.42)(S_u) \tag{9}$$

TABLE 7 – *Natural Log Calculations.*

Day (D)	1	3	7	14	21
ln(D + 1)	0.7	1.4	2.1	2.7	3.1

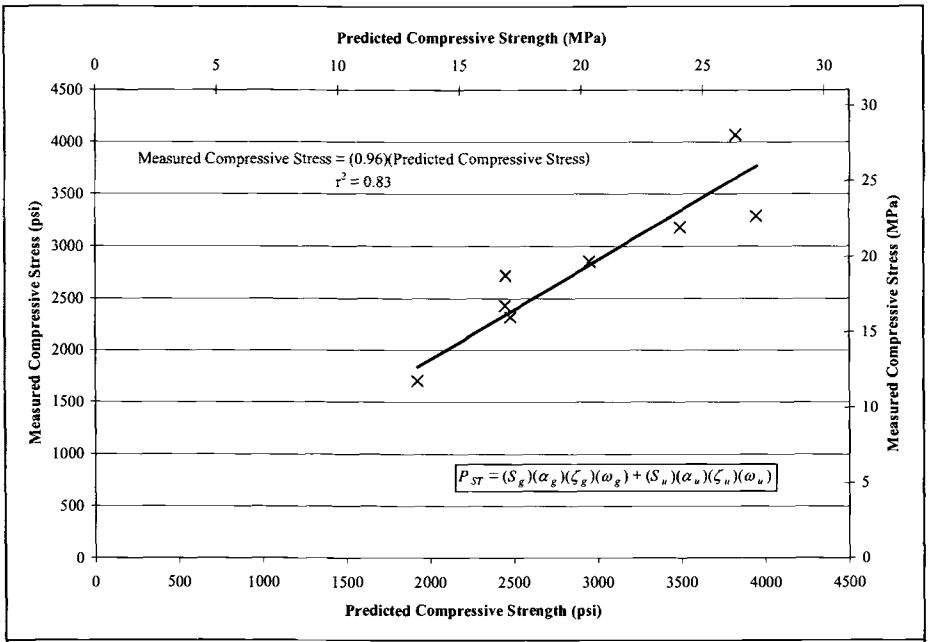

Figure 4 – *Prediction of 28-Day Prism Compressive Strength*

Conclusions

There currently exist scarce resources for those wishing to predict the strength gain of grouted masonry prisms and to predict the 28-day strength of a grouted masonry prism given the characteristics of the materials used to construct the prism. This paper proposes a theoretical approach to accomplish both of these objectives. The theoretical approach was verified by comparison to actual data and appears to provide reasonable estimates.

As discussed herein, the gain in prism strength can be expressed as a function of the natural log of time. Further, predicted strengths at any age must consider the influence of the strength and properties of the concrete masonry unit and grout. This paper proposes that the strength of the grouted masonry prism can be estimated at any age by the following formula:

$$P_{ST} = [(S_g / \ln(28+1))(\alpha_g)(\zeta_g)(\omega_g)]\ln(D+1) + (S_u)(\alpha_u)(\zeta_u)(\omega_u) \quad (6)$$

where

P_{ST} = predicted prism compressive strength, lb/in^2 (MPa).
S_g = 28 day net area compressive strength of grout, lb/in^2 (MPa).
α_g = grout volume proportion factor. This factor is equal to 1- α_u.

ζ_g = grout construction factor, dependent upon the overall dimensions of the prism and the dimensions of the hollow cores of the concrete masonry unit.
ω_g = moisture content factor for the grout.
S_u = net area compressive strength of the concrete masonry unit, lb/in^2 (MPa).
α_u = unit volume proportion factor. This factor is equal to the percent solid of the concrete masonry unit used to construct the prism and is also equal to 1- α_g.
ζ_u = unit construction factor. This factor is a function of the overall dimensions of the prism and the type of mortar used in construction.
ω_u = moisture content factor for the concrete masonry unit.

In its simplest form, Eq. 6 tells us that the strength of a grouted prism is a function of:

- The strength of the concrete masonry unit (which is a relative constant since it is typically cured before the prism is constructed), and
- The strength gain and ultimate strength of the grout (with the strength of the grout being negligible at Day 0 and increasing as the natural log of time).

The equation becomes a little more complex as these contributions are factored to permit them to be used together and to account for contributing variables. Mortar strength has some influence on prism strengths, but this influence is minor in comparison to that of the units and grout and is accommodated for in Eq. 6 in the selection of the appropriate shape factor, ζ_u.

Although this brief analysis of results indicates strong correlation between the individual component properties and the measured prism strength, it should be stressed that this analysis is based on only a limited number of variables and results. As such, users should carefully consider the application of these recommendations for material strengths that are outside the approximate following boundaries not considering in this analysis:

- Grout: Compressive strength below 2,000 lb/in^2 (13.8 MPa) or above 5,500 lb/in^2 (37.9 MPa).
- Units: Compressive strength below 2,100 lb/in^2 (14.5 MPa) or above 3,600 lb/in^2 (24.8 MPa).
- Prisms: Compressive strength below 1,700 lb/in^2 (11.7 MPa) or above 4,000 lb/in^2 (27.6 MPa).

In addition, since the database of prism tests did not contain any results using Type N mortar, units sizes other than 8 or 12 inch (203 or 305 mm), or prisms constructed using full-size units, the application of such should be subjected to further verification.

References

[1] ACI 530.1/ASCE 6/TMS 602, *Specification for Masonry Structures*, reported by the Masonry Standards Joint Committee, 1999.
[2] *Compressive Strength Testing Variables for Concrete Masonry Units* TEK 18-7, National Concrete Masonry Association, Herndon, VA, 1997.
[3] Redmond, T.B., "Compressive Strength of Load Bearing Concrete Masonry Prisms," National Concrete Masonry Association Laboratory Tests, Herndon, VA, 1970, Unpublished.

[4] Nacos, C. J., "Comparison of Fully Bedded and Face-Shell Bedded Concrete Block," Report No. CE-495, Colorado State University, Fort Collins, CO, 1980, Appendix p. A-3.

[5] Baussan, R., and Meyer, C., "Concrete Block Masonry Test Program," Columbia University, New York, NY, 1985.

[6] Hamid, A. A., Drysdale, R. G., and Heidebrecht, A. C., "Effect of Grouting on the Strength Characteristics of Concrete Block Masonry," *Proceedings, North American Masonry Conference*, University of Colorado, Boulder, CO, 1978.

[7] *Evaluation of Minimum Reinforcing Bar Splice Criteria for Hollow Clay Brick and Hollow Concrete Block Masonry*, Council for Masonry Research, Herndon, VA, July, 1999.

[8] *Research Evaluation on the Effects of Concrete Masonry Structural Cover Over Continuous Reinforcing Bars*, National Concrete Masonry Association, Herndon, VA, January, 1996.

Peter J. Holser[1], Richard E. Klingner[2] and John M. Melander[3]

Inter-Laboratory Study to Establish the Precision and Bias of Bond-Wrench Testing under ASTM C 1329 and C 1357

REFERENCE: Holser, P. J., Klingner, R. E., and Melander, J. M., "**Inter-laboratory Study to Establish Precision and Bias of Bond-Wrench Testing Under ASTM C 1329 and C 1357,**" *Masonry: Opportunities for the 21st Century, ASTM STP 1432*, D. Throop and R. E. Klingner, Eds., ASTM International, West Conshohocken, PA, 2002.

Abstract

Under the auspices of ASTM Committee C-01, an inter-laboratory study (ILS) was conducted to determine precision and bias for bond-wrench testing carried out under the requirements of ASTM C 1329-98 ("Standard Specification for Mortar Cement") and ASTM C 1357-98a ("Standard Test Methods for Evaluating Masonry Bond Strength"). The study involved 3 mortars, 15 laboratories and 17 sets of data. Using the statistical analysis procedures of ASTM E 691-99 ("Standard Practice for Conducting an Interlaboratory Study to Determine the Precision of a Test Method") and the computer software developed to carry out those procedures, values of intra-laboratory repeatability, r, and inter-laboratory reproducibility, R, were developed. Normalized repeatability decreases from about 30% of the mean tensile bond strength with the least restricted data subsets, to about 20% of the mean tensile bond strength with the most restricted data subsets. Normalized reproducibility decreases from about 60% of the mean tensile bond strength with the least restricted data subsets, to about 40% of the mean tensile bond strength with the most restricted data subsets. Potential factors contributing to repeatability and reproducibility are discussed.

Keywords: bond-wrench testing, masonry, precision and bias, tensile bond strength

Introduction

Under the auspices of ASTM Committee C-01, an inter-laboratory study (ILS) was conducted, whose purpose was to determine precision and bias for bond-wrench testing carried

[1] former Graduate Research Assistant, The University of Texas, Austin, TX 78712
[2] L. P. Gilvin Professor in Civil Engineering, The University of Texas, Austin, TX 78712
[3] Director, Product Standards and Technology, The Portland Cement Association, Skokie, IL 60077

out under the requirements of ASTM C 1329-98 and ASTM C 1357-98a. The purpose of this paper is threefold:

1) to describe the background of the ILS;
2) to describe how test data were generated and evaluated; and
3) to report the results of the data evaluation, and the corresponding conclusions.

ASTM E 691-99 Requirements

ASTM E 691-99 defines specific requirements for performing an ILS:

- Conduct the ILS using no fewer than 6 laboratories;
- Conduct pilot runs to ensure that each laboratory is familiar with the procedure required for the study; and
- Before conducting the ILS, carry out a "ruggedness study" to determine the specific variables that should be varied or held constant in the ILS. Specific details on how to use a ruggedness study to design an ILS are given in Appendix A of ASTM E 691-99. Before this ILS was carried out, such a ruggedness study was conducted (Ponce et al. 1999).

Background of Inter-Laboratory Study

Fifteen laboratories volunteered to participate in this study, and contributed 17 sets of data. There are two more data sets than laboratories because two of the laboratories first conducted bond-wrench tests using older machines, and then using new machines, and submitted both data sets. In this paper, the data sets are identified as Data Set A through Data Set Q. Table A1 of Appendix A lists reported data for these 17 sets.

The testing protocol for this ILS involved the following basic steps:

- Mix mortar to a flow of 127 ±3 determined in accordance with ASTM C 109.
- Following the requirements of ASTM C 1329-98, construct six, 6-high masonry prisms using standard concrete masonry research units;
- After curing the prisms for 28 days, perform bond-wrench testing in accordance with ASTM C 1072-97a.

This ILS used three different single-bag cements for mortar, distributed to each laboratory by the Cement and Concrete Reference Laboratory (CCRL). Each laboratory was instructed to build six masonry prisms using mortar prepared from the cements and standard silica sand. Since the masonry prisms were 6 units high, 5 joints were available in each prism. Thus, 30 joints each would be generated for each mortar from each laboratory and reported as a test of that mortar. Three replicates of each mortar test were to be conducted, yielding a total of 270 joints from each laboratory. When the ILS was conducted, however, not all laboratories actually followed this protocol. Some laboratories prepared and tested fewer than 3 replicates. One laboratory prepared and tested 4 replicates for two samples. Each laboratory reported data on standard spreadsheets distributed as part of the protocol.

Statistical Analysis of Data for ILS

The basic procedure for the statistical analysis of data from the ILS is outlined in ASTM E 691-99. That standard first prescribes how to determine which data should not be included in the data analysis, and then prescribes how to conduct the actual data analysis.

ASTM has developed special Windows-based software (ASTM Program 1996) for performing the statistical analysis of inter-laboratory data in accordance with ASTM E 691-99. Using the software involves two steps: entering the data, and using the software to generate results.

The first task of data entry was determining how to organize the data. Data from each participating laboratory were arranged by mortars, prisms, and individual joints. The ASTM E 691-99 software allows three sets of entries: number of laboratories, number of materials, and analysis type. In the ASTM E 691-99 software, the analysis type is entered in an "Analysis" field. For purposes of this study, the ASTM E 691-99 software was used as shown in Table 1, by entering the average tensile bond strength from each set of mortar joints in the "Analysis" field.

Table 1 - Arrangements of data in ILS and in ASTM E 691-99 software

ILS Data	E 691-99 Software	E 691-99 Software as Used
Laboratories	Laboratories	Laboratories
Mortars	Materials	Materials
Prisms	Analysis	Average tensile bond strength of each set of 30 joints
Joints		

The ASTM E 691-99 software quickly produces three basic types of results:

- overall averages and standard deviations of tensile bond strengths for each replicate of each mortar, obtained using the average values submitted by each laboratory;
- intermediate statistical values that can be used to evaluate the statistical reliability of results obtained by each laboratory, and the statistical consistency of results obtained for each mortar type; and
- statistics for repeatability and reproducibility of values.

In May 2000, before results had been received from all laboratories, one preliminary subset of data, comprising 13 data sets, was analyzed. Because the corresponding results were reported orally to ILS participants and others in June 2000, and are likely to be compared with other results presented in this paper, that preliminary example is reported here as well. Using the same identifiers noted above, this preliminary subset included Data Sets B, C, D, E, F, G, I, J, K, M, N, O and P.

For each mortar and each set of replicates, each laboratory reported the average and coefficient of variation of the strengths of 30 joints. The averages and coefficients of variation of those average values are given in Table 2.

Table 2 - Averages, standard deviations and coefficients of variation obtained from average values of 13 data sets (preliminary evaluation)

Mortar	Average Tensile Bond Strength, lb/in.^{2} (kPa)	Standard Deviation of Averages, lb/in.^{2} (kPa)	Coefficient of Variation of Averages
1	153.7 (1060)	30.36 (209.4)	19.75%
2	102.9 (709.2)	14.18 (97.78)	13.79%
3	135.9 (936.8)	19.86 (136.9)	14.61%

Results of the ASTM E691 program are expressed in terms of a "repeatability limit," r, and a "reproducibility," R. In the rest of this paper, these are termed simply the repeatability and the reproducibility.

- The repeatability r is 2.8 times the within-laboratory standard deviation. If the repeatability within a laboratory is r, there is a 95% confidence that any two pieces of data from a single laboratory for that mortar, will be within r of each other.
- The reproducibility R is 2.8 times the between-laboratory standard deviation. If the reproducibility from laboratory to laboratory is R, there is a 95% confidence that any two pieces of data from two different laboratories will be within R of each other.

Smaller values of r and R indicate increasing reliability of results.

For this preliminary subset of data, and for each of the three mortars, values of r (repeatability) and R (reproducibility) are given in Table 3.

Table 3 - 95% confidence limits for repeatability (r) and reproducibility (R), obtained using 13 data sets (preliminary evaluation)

Mortar	Average Tensile Bond Strength, lb/in.^{2} (kPa)	95% Confidence Limits			
		Repeatability (r) lb/in.^{2} (kPa)	Repeatability standard deviation (Sr) lb/in.^{2} (kPa)	Reproducibility (R) lb/in.^{2} (kPa)	Reproducibility standard deviation (SR) lb/in.^{2} (kPa)
1	153.7 (1060)	41.47 (285.9)	14.81 (102.1)	86.80 (589.5)	31.00 (213.8)
2	102.9 (709.5)	23.45 (161.7)	8.374 (57.74)	40.42 (278.7)	14.44 (99.56)
3	135.9 (937.0)	36.15 (249.3)	12.91 (89.01)	56.48 (389.4)	20.17 (139.1)

It is useful to discuss the significance of these preliminary results. As reported orally to a group of participants and others in June 2000, although the coefficients of variation of the average values reported by each lab are generally between 15% and 20%, repeatability and reproducibility values are much higher, indicating higher variability.

For Mortar 1, for example, the repeatability value, r, of 41.47 lb/in.^{2} means that if a large number of test series (6 prisms each) were conducted in one laboratory using Mortar 1, then the averages from randomly selected pairs of those test series would be within 41.47 lb/in.^{2} of each other 95% of the time.

In other words, the averages of two test series from a single laboratory would have to differ by more than 41.47 lb/in.^{2} before one could say with 95% confidence that there was a statistically significant difference between the mortars represented in those two test series. This required difference is a significant portion (27%) of the average bond strength of 153.7 lb/in.^{2} for Mortar 1.

For Mortar 1, again, the reproducibility value, R, of 86.80 lb/in.^{2} means that if a large number of test series (6 prisms each) were conducted in a group of laboratories using Mortar 1, the averages from randomly selected pairs of those test series (comparing a test series from one laboratory with a test series from another laboratory) would be within 86.80 lb/in.^{2} of each other 95% of the time.

In other words, the averages from two test series at different laboratories would have to differ by more than 86.80 lb/in.^{2} before one could say with 95% confidence that there was a statistically significant difference between the mortars represented in those two test series. This required difference is a very significant portion (56%) of the average bond strength of 153.7 lb/in.^{2} for Mortar 1.

Evaluation of Statistical Analyses

Based on the preliminary evaluation of data conducted in May 2000 and reported in June 2000, it was agreed to evaluate the repeatability and reproducibility using several subsets of data:

Subset 1: all data sets that conformed to the assigned protocol;

Subset 2: all data sets that conformed to the assigned protocol, removing data sets with poor individual reliability;

Subset 3: all data sets that conformed to the assigned protocol, removing individual data points that appeared invalid;

Subset 4: all data sets that conformed to the assigned protocol, removing data sets with poor individual reliability, and also individual data points that appeared invalid; and

Subset 5: data sets from only NCMA, CTL, and UT Austin, the three laboratories that had participated in two previous bond-wrench studies using controlled conditions similar to those used in this study (Hedstrom et *al.* 1991, Melander *et al.* 1993).

In the remaining sections of this chapter, results are presented from the statistical analysis of each subset. Finally, their significance is discussed.

Statistical Evaluation of Subset 1

When all laboratories had completed their testing, 17 sets of data were received from 15 laboratories. Two of those data sets (Data Sets H and Q) were immediately removed from consideration because the numbers of replicates did not conform to the assigned protocol. In Data Set K, Replicate D of Mortars 2 and 3 was removed from consideration for the same reason. The remaining 15 data sets of 3 replicates comprised Subset 1 (Data Sets A, B, C, D, E, F, G, I, J, K, L, M, N, O and P).

For each mortar and each set of replicates, each laboratory reported the average and coefficient of variation of the strengths of 30 joints. For Subset 1, the averages and coefficients of variation of those average values are given in Table 4.

Table 4 - Averages, standard deviations and coefficients of variation obtained from average values of Subset 1

Mortar	Average Tensile Bond Strength, lb/in.^{2} (kPa)	Standard Deviation of Averages, lb/in.^{2} (kPa)	Coefficient of Variation of Averages
1	152.3 (1050)	35.02 (241.5)	23.00%
2	98.43 (678.7)	19.35 (133.4)	19.65%
3	132.8 (915.7)	24.92 (171.8)	18.76%

Using the data of Subset 1, values of r (repeatability) and R (reproducibility) for those 15 data sets are presented in Table 5. The results are comparable to the preliminary results that were presented and briefly discussed in the previous chapter.

Table 5 - 95% confidence limits for repeatability (r) and reproducibility (R),obtained using Subset 1 (all data sets conforming to the assigned protocol)

Mortar	Average Tensile Bond Strength, lb/in.^{2} (kPa)	95% Confidence Limits			
		Repeata-bility (r) lb/in.^{2} (kPa)	Repeatability standard deviation (Sr) lb/in.^{2} (kPa)	Reproducibility (R) lb/in.^{2} (kPa)	Reproducibility standard deviation (SR) lb/in.^{2} (kPa)
1	152.3 (1050)	41.07 (283.2)	14.67 (101.1)	99.97 (689.3)	35.70 (246.2)
2	98.43 (678.7)	23.39 (161.3)	8.354 (57.60)	55.21 (380.7)	19.72 (136.0)
3	132.8 (915.7)	42.03 (289.8)	15.01 (103.5)	70.82 (488.3)	25.29 (174.4)

Statistical Evaluation of Subset 2

The 15 data sets comprising Subset 1 were now examined for individual reliability. Using the data of Subset 1, the ASTM E 691 software was used to produce plots of h and k, two intermediate statistical parameters indicating the consistency of data within each lab, and the consistency of data from lab to lab, respectively. Laboratories whose value of h exceeds a critical value (calculated using all data) have an undesirably high internal variability of results. Laboratories whose value of k exceeds another critical value (calculated using all data) have an undesirably high variability of results with respect to the other laboratories. The critical values of h and k depend on the data.

According to the reliability analysis, the critical value of h was 2.47. Most laboratories had h-values less than 1.0. Laboratory L had h-values of 1.89, 2.73 and 2.47 for Mortars 1, 2 and 3 respectively. On that basis, Laboratory L was removed from the data set.

According to the reliability analysis, the critical value of k was 2.17. Most laboratories had k-values less than 1.0. Laboratory A had a k-value of 2.25 for Mortar 3. On that basis, Laboratory A was removed from the data set. The remaining 13 data sets (B, C, D, E, F, G, I, J, K, M, N, O, and P) comprised Subset 2. These data sets are the same ones used for the preliminary analysis, so the results are the same also.

For each mortar and each set of replicates, each laboratory reported the average and coefficient of variation of the strengths of 30 joints. For Subset 2, the averages and coefficients of variation of those average values are given in Table 6.

Table 6 - Averages, standard deviations and coefficients of variation obtained from average values of Subset 2

Mortar	Average Tensile Bond Strength, lb/in.^{2} (kPa)	Standard Deviation of Averages, lb/in.^{2} (kPa)	Coefficient of Variation of Averages
1	153.7 (1060)	30.36 (209.4)	19.75%
2	102.9 (709.2)	14.18 (97.78)	13.79%
3	135.9 (936.8)	19.86 (136.9)	14.61%

Using the data of Subset 2, values of *r* (repeatability) and *R* (reproducibility) for those 13 data sets are presented in Table 7. These values are clearly an improvement over the corresponding values for Subset 1. This difference is discussed later in this paper.

Table 7 - 95% confidence limits for repeatability (r) and reproducibility (R),obtained using Subset 2 (all data sets conforming to the assigned protocol, and removing laboratories with high h and/or k values)

Mortar	Average Tensile Bond Strength, lb/in.^{2} (kPa)	95% Confidence Limits			
		Repeatability (r) lb/in.^{2} (kPa)	Repeatability standard deviation (Sr) lb/in.^{2} (kPa)	Reproducibility (R) lb/in.^{2} (kPa)	Reproducibility standard deviation (SR) lb/in.^{2} (kPa)
1	153.7 (1060)	41.47 (285.9)	14.81 (102.1)	86.80 (589.5)	31.00 (213.8)
2	102.9 (709.5)	23.45 (161.7)	8.374 (57.74)	40.42 (278.7)	14.44 (99.56)
3	135.9 (937.0)	36.15 (249.3)	12.91 (89.01)	56.48 (389.4)	20.17 (139.1)

Statistical Evaluation of Subset 3

The 15 data sets comprising Subset 1 were now examined for individual data points that appeared invalid. This criterion could be subjective, and if applied indiscriminately, could distort the results. Because of these concerns, only those individual data points with values equal to zero, or very close to zero, were removed. Individual data points were identified first according to the mortar that they represent (1, 2 or 3); then by the replicate number for that mortar (A, B or C); next by the prism from which they came (1 through 6); and finally by the joint in that prism (1 through 5, counting down from the top).

Using this criterion, the following individual data points were removed from Data Set A:

- Replicate 2C (Joint 1/2) (Prism 1, Joint 2 from the top)

Again using this criterion, the following individual data points were removed from Data Set L:

- Replicate 1A (Joints 1/1, 3/1)
- Replicate 1B (Joint 6/3)
- Replicate 2A (Joints 1/1, 1/3, 1/4, 2/2, 2/5, 3/2, 4/1, 4/2, 4/4, 4/5, 5/1, 5/2, 5/3, 6/1, 6/5)
- Replicate 2B (Joints 2/1, 4/1, 4/3, 5/1, 6/1, 6/2, 6/4)
- Replicate 2C (Joints 3/1, 4/1, 4/2, 4/5, 5/5, 6/2, 6/3)
- Replicate 3C (Joints 2/1, 4/3)

Clearly, there is a strong correspondence between those data sets with poor statistical reliability indices h and k, and those data sets with large numbers of apparently invalid values. The same data sets that were omitted from Subset 2 because of poor statistical reliability, also figure prominently in Subset 3.

For each mortar and each set of replicates, each laboratory reported the average and coefficient of variation of the strengths of 30 joints. For Subset 3, the averages and coefficients of variation of those average values are given in Table 8.

Table 8 - Averages, standard deviations and coefficients of variation obtained from average values of Subset 3

Mortar	Average Tensile Bond Strength, lb/in.^{2} (kPa)	Standard Deviation of Averages, lb/in.^{2} (kPa)	Coefficient of Variation of Averages
1	152.3 (1049)	35.02 (231)	23.00%
2	98.50 (678)	19.32 (127)	19.61%
3	132.8 (904)	24.78 (142)	18.65%

Using the data of Subset 3, values of r (repeatability) and R (reproducibility) are presented in Table 9. The results differ very little from those of Subset 1. This is because zero values entered by the participating laboratories were changed by the authors to the text "xx" in the Excel™ standard spreadsheet that all participating laboratories were asked to use in reporting their results. This practice amounts to ignoring those tests initially reported with zero values. As a result, some of the laboratories had average entries (for a particular mortar and replicate) representing slightly fewer than 30 joints. This difference was not considered significant. The spreadsheets automatically eliminated the "xx" entries when computing averages of groups of numbers. Most of the individual data points in Data Sets A and L that were identified as questionable were equal to zero, and therefore had already been ignored in the original data spreadsheets comprising Subset 1.

Table 9 - 95% confidence limits for repeatability (r) and reproducibility (R),obtained using Subset 3 (all data sets that conformed to the assigned protocol, removing individual data points that appeared invalid)

Mortar	Average Tensile Bond Strength, lb/in.^{2} (kPa)	95% Confidence Limits			
		Repeata-bility (r) lb/in.^{2} (kPa)	Repeata-bility standard deviation (Sr) lb/in.^{2} (kPa)	Reproducibility (R) lb/in.^{2} (kPa)	Reproducibility standard deviation (SR) lb/in.^{2} (kPa)
1	152.3 (1050)	41.07 (283.2)	14.67 (101.2)	99.97 (689.3)	35.70 (246.2)
2	98.49 (679.1)	23.31 (160.7)	8.325 (57.40)	55.12 (380.1)	19.69 (135.8)
3	132.8 (915.7)	41.96 (289.3)	14.99 (103.4)	70.41 (485.5)	25.15 (173.4)

Statistical Evaluation of Subset 4

To obtain the data sets of Subset 4, the two criteria used to obtain Subsets 2 and 3 were applied together. Because the only data sets with apparently invalid individual values (Subset 3) had also been identified as having poor individual reliability (Subset 2), Subset 4 comprised the same 13 data sets (B, C, D, E, F, G, I, J, K, M, N, O, and P) that had comprised Subset 2. The results were therefore identical to those of Subset 2, and are not discussed further.

Statistical Evaluation of Subset 5

Subset 5 comprised three data sets, obtained from the three laboratories that had participated in the original bond-wrench studies reported by Hedstrom *et al.* (1991) and Melander *et al.* (1993) (NCMA, CTL, and UT Austin). All data sets followed the assigned protocol; all were obtained using the same type of bond-wrench machine; all showed acceptable individual reliability in terms of h- and k-values; and none had apparently invalid individual values.

For each mortar and each set of replicates, each laboratory reported the average and coefficient of variation of the strengths of 30 joints. For Subset 5, the averages and coefficients of variation of those average values are given in Table 10.

Table 10 - Averages, standard deviations and coefficients of variation obtained from average values of Subset 5

Mortar	Average Tensile Bond Strength, lb/in.^{2} (kPa)	Standard Deviation of Averages, lb/in.^{2} (kPa)	Coefficient of Variation of Averages
1	168.0 (1158)	23.97 (165.3)	14.26%
2	109.2 (752.9)	11.01 (75.91)	10.08%
3	136.2 (939.1)	22.37 (154.2)	16.42%

For the 3 data sets of Subset 5, values of r (repeatability) and R (reproducibility) are presented in Table 11.

Table 11 - 95% confidence limits for repeatability (r) and reproducibility (R),obtained using Subset 5 (data sets from NCMA, CTL and UT Austin only)

Mortar	Average Tensile Bond Strength, lb/in.^{2} (kPa)	95% Confidence Limits			
		Repeatability (r) lb/in.^{2} (kPa)	Repeatability standard deviation (Sr) lb/in.^{2} (kPa)	Reproducibility (R) lb/in.^{2} (kPa)	Reproducibility standard deviation (SR) lb/in.^{2} (kPa)
1	168.0 (1158)	28.68 (197.8)	10.24 (70.60)	75.70 (522.0)	27.04 (186.4)
2	109.2 (752.9)	18.77 (129.4)	6.704 (46.22)	33.90 (233.7)	12.11 (83.50)
3	136.2 (939.1)	39.49 (272.3)	14.10 (97.22)	68.63 (473.2)	24.51 (169.00)

Significance of Results for Subsets 1 through 5

In Figure 1 and Figure 2 are shown the repeatability, r, and the reproducibility, R, for each of the data subsets discussed previously.

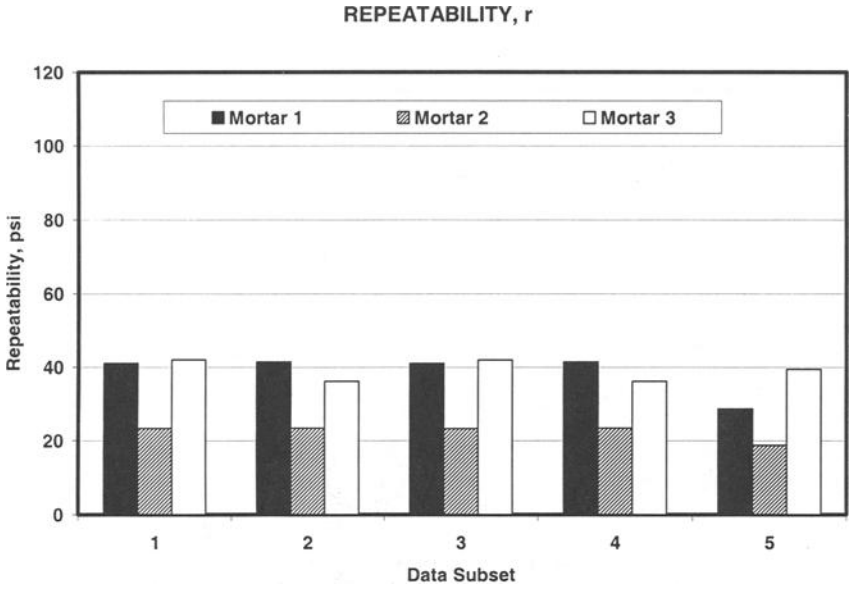

Figure 1 - Summary of repeatability results, r, for each data subset

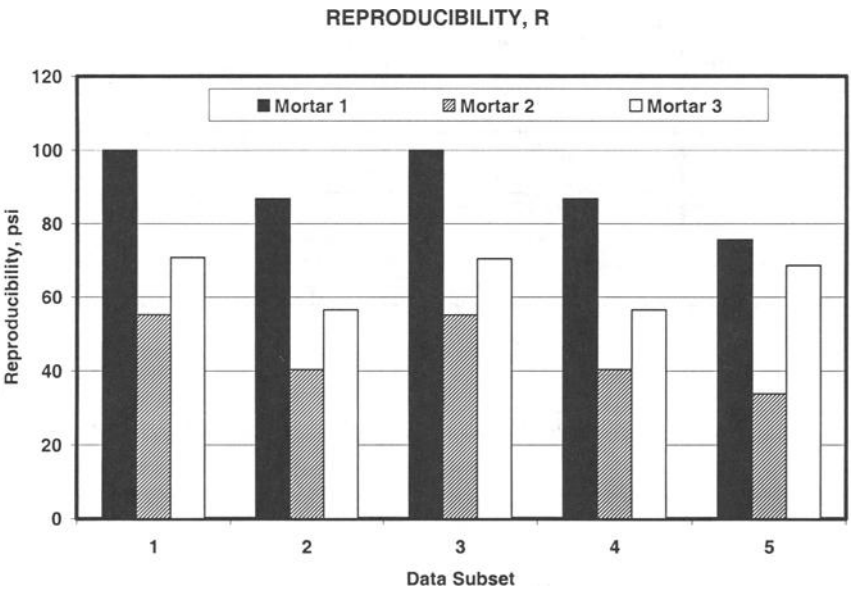

Figure 2 - Summary of reproducibility results, R, for each data subset

The following characteristics of the charts are noted:

1) As suggested in the evaluation of the significance of preliminary data, values of repeatability and reproducibility are higher than the within-laboratory coefficients of variation would suggest.
2) To reduce the effects of differences among the tensile bond strengths of the three mortars tested in this study, the values of repeatability and reproducibility for each mortar were normalized by the average tensile bond strength of that mortar. Normalized values of repeatability and reproducibility are shown in Figure 3 and Figure 4. Clearly, normalization significantly reduces the differences in repeatability and reproducibility from mortar to mortar, implying that for bond-wrench testing, the coefficient of variation is a better measure of precision than the standard deviation.
3) For all data subsets, some mortars have consistently higher or consistently lower repeatability and reproducibility values than other mortars, even when the value for each mortar is normalized by the average tensile bond strength for that mortar. Mortar 2 consistently has the lowest normalized values of repeatability, and often the lowest value of repeatability, across all data subsets. This implies that repeatability and reproducibility are related to the performance of the mortar, as well as the test method itself.
4) For all mortars, as the data subsets become generally more restricted (moving from left to right on the figures, from Data Set 1 to Data Set 5), normalized repeatability stays almost constant, except for Data Set 5, for which it is slightly lower. This implies that the use of stringent criteria to eliminate questionable data sets and apparently invalid individual data points, does not have a significant effect on the computed value of repeatability, r.
5) For all mortars, as the data subsets become generally more restricted (moving from left to right on the figures, from Data Set 1 to Data Set 5), normalized reproducibility decreases, particularly for Data Subset 5, the most restricted. This implies that the use of stringent criteria to remove questionable data sets and apparently invalid individual data points, can significantly decrease the computed value of reproducibility, R.
6) The fact that generally more stringent criteria do not significantly decrease normalized repeatability (within-lab variation), but do significantly decrease normalized reproducibility (variation from lab to lab), has interesting implications:
    a) Suppose that a stringently restricted subset of data has a significantly lower reproducibility value, R, than the entire data set, but about the same repeatability value, r. It can be assumed that the laboratories in the stringently restricted subset construct and test bond-wrench specimens more consistently among themselves, than the other laboratories.
    b) Nevertheless, because the in-laboratory repeatability, r, from those more consistent laboratories is not significantly smaller than that achieved by the other laboratories, one can conclude that each laboratory (the more consistent laboratories as well as the others) achieves a similar internal consistency. This is also suggested from the coefficients of variation of individual data points from each laboratory – most vary from 15% to 20%.
    c) Given (a) and (b) above, it can be concluded that each of the laboratories in the most restrictive subset, with the lowest reproducibility value, R, is doing things differently than the other laboratories. In examining the data from individual laboratories, one fact that stands out is the large variation in elapsed time for mixing mortar and constructing each set of 6 prisms. The laboratories in the most restricted subset (NCMA, CTL and UT Austin) consistently did this in 45 minutes or less. Other laboratories, in contrast, took almost twice as long (Figure 5). This could be a significant source of inter-laboratory variation, because

tensile bond strength depends strongly on flow (Ponce 1999), and flow decreases rapidly as the mortar sets.

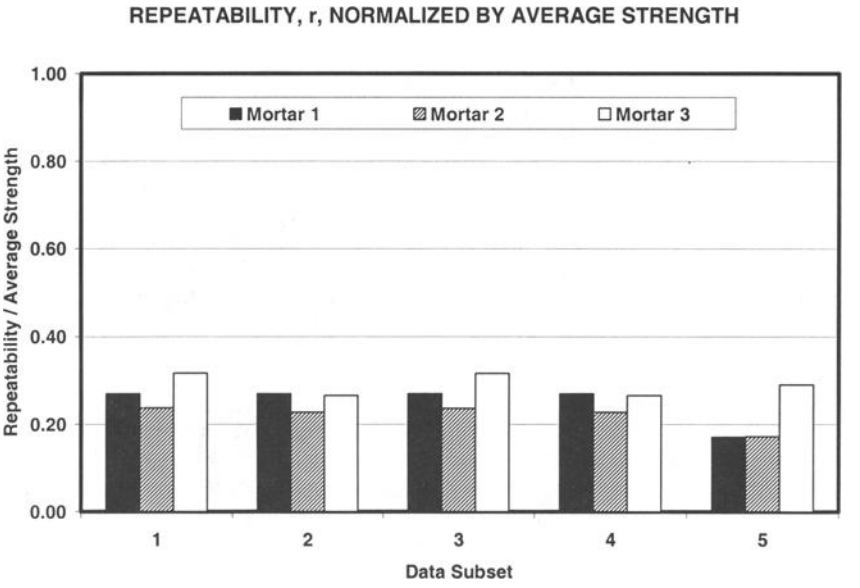

Figure 3 - Repeatability results for each data subset, normalized by average strength

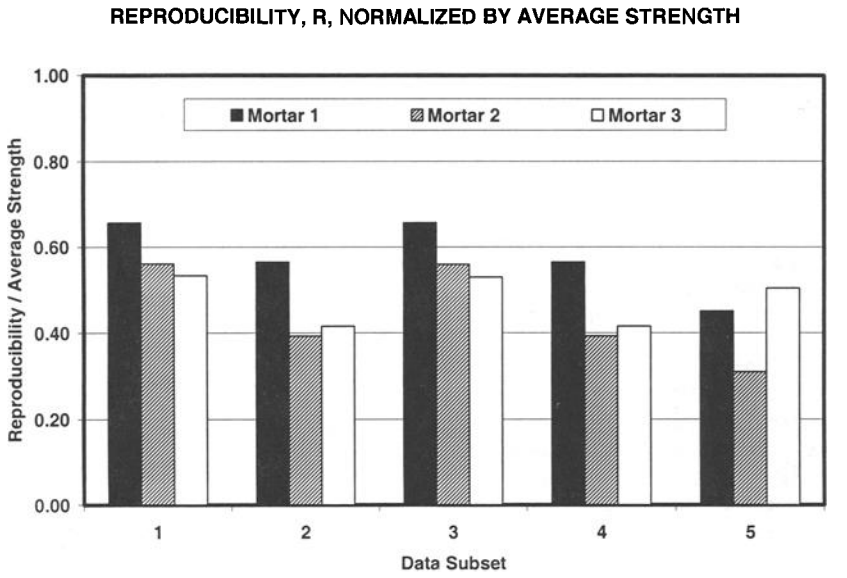

Figure 4 - Reproducibility values for each data subset, normalized by average strength

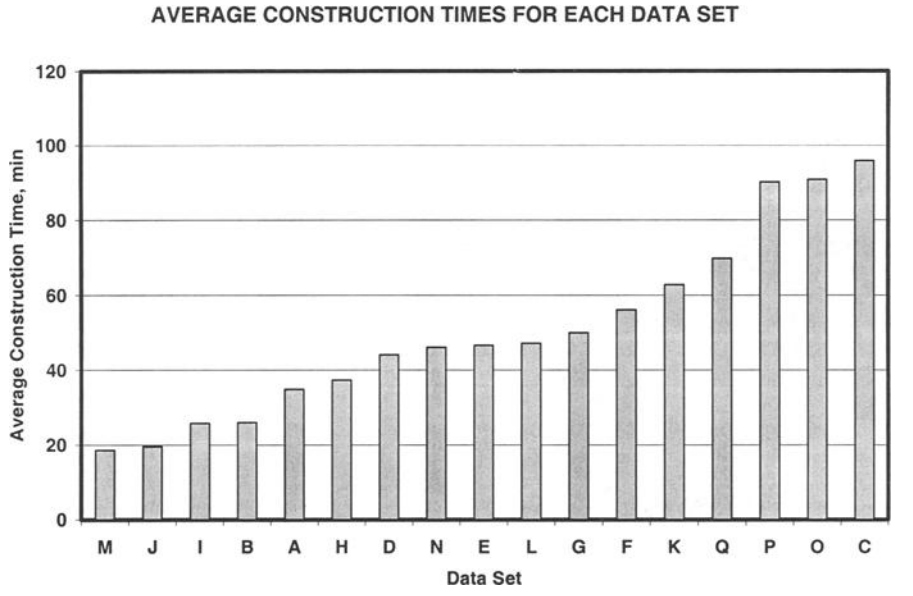

Figure 5 - Average construction times for each data set

Summary, Conclusions and Recommendations

Summary

Under the auspices of ASTM Committee C-01, an inter-laboratory study (ILS) was conducted to determine precision and bias for bond-wrench testing carried out under the requirements of ASTM C 1329-98 and ASTM C 1357-98a. The study involved 3 mortars, prepared and distributed by CCRL, and designated Mortar 1, Mortar 2 and Mortar 3. The study involved 15 laboratories and 17 sets of data.

Using the statistical analysis procedures of ASTM E 691-99 and the computer software developed to carry out those procedures, values of intra-laboratory repeatability, r, and inter-laboratory reproducibility, R, were developed.

Conclusions

Using 5 subsets of data, obtained using increasingly restrictive criteria, values of in-laboratory repeatability, r, and inter-laboratory reproducibility, R, were obtained (Figure 1 and Figure 2). As shown in those figures, values obtained using all data sets are higher than the within-laboratory coefficients of variation would suggest.

To evaluate the results further, those repeatability and reproducibility values were normalized by average tensile bond strength (Figure 3 and Figure 4). As data subsets become more restricted (moving from left to right on the figures, from Data Set 1 to Data Set 5), normalized repeatability (r) does not change much, except for Data Subset 5, the most restricted. Normalized reproducibility (R) does decrease, particularly for Data Subset 5, the most restricted.

Normalized repeatability is approximately constant at about 30% of the mean tensile bond strength with the least restricted data subsets, and decreases to about 20% of the mean tensile bond strength with the most restricted data subset. Normalized reproducibility is about 60% of the mean tensile bond strength with the least restricted data subset, and decreases progressively to about 40% of the mean tensile bond strength as the data subsets are increasingly restricted. The decrease in normalized repeatability and normalized reproducibility with the most restricted subset is inherently related to the laboratories in that subset, and not merely to the reduction in size of the subset. Other three-laboratory groups, selected at random, do not produce similar reductions in repeatability and reproducibility.

The fact that increasingly more restrictive criteria do not significantly decrease normalized repeatability (within-lab variation), but do significantly decrease normalized reproducibility (variation from lab to lab), implies that each of the laboratories in the more stringently restricted subsets is independently obtaining data in a more consistent manner, and their construction and testing techniques are more similar to each other than those of the other laboratories.

One example of such a similarity may be the elapsed time for mixing mortar and constructing each set of 6 prisms. The most restrictive data set (from only NCMA, CTL and UT Austin) consistently involved construction times of 45 minutes or less. Other data sets, in contrast, involved construction times almost twice as long (Figure 5). This could be a significant source of inter-laboratory variation, because tensile bond strength depends strongly on flow (Ponce 1999), which decreases rapidly as the mortar sets.

Recommendations

For tensile bond-strength testing by ASTM C 1329 and C 1357, within-laboratory repeatability, *r*, evaluated as prescribed by ASTM E 691-99, is about 30% of the average tensile bond strength, and can be decreased to about 20% of the average tensile bond strength if data sets are stringently restricted. Reproducibility among laboratories, *R*, is about 60% of the average tensile bond strength, and can be as low as 40% of the average tensile bond strength if data sets are stringently restricted.

Acknowledgments

The research reported in this paper (PCA R&D Serial No. 2144b) was conducted in the laboratories of the following participants: Blue Circle Atlanta, Blue Circle St. Marys, California Portland Cement, Construction Technology Laboratories, Hercules, Holnam Inc., Monarch Cement, National Concrete Masonry Association, North Carolina State A&T University, R. L Nelson & Assoc., Texas Industries Cement Division, University of Texas at Arlington, University of Texas at Austin, W. R. Grace, and Westvaco. The Cement and Concrete Reference Laboratory at the National Institute of Standards distributed cementitious materials to participating laboratories. The Portland Cement Association sponsored (PCA Project Index No. 95-06) distribution of the cementitious materials and analysis of data. The contents of this paper reflect the views of the authors, who are responsible for the facts and accuracy of the analysis of data reported.

References

ASTM Program 1996: "Inter-laboratory Study of Precision Program, version 2, prepared by the E11 Quality and Statistical Committee of ASTM, September 1996.

Hedstrom *et al.* 1991: Hedstrom, E. G., Tarhini, K. M., Thomas, R. D., Dubovoy, V. S., Klingner, R. E., and Cook, R. A., "Flexural Bond Strength of Concrete Masonry Prisms Using Portland Cement and Hydrated Lime Mortars," *The Masonry Society Journal*, Vol. 9, No. 2, February 1991.

Melander *et al.* 1993: Melander, J. M., Ghosh, S. K., Dubovoy, V. S., Hedstrom, E. G., and Klingner, R. E., "Flexural Bond Strength of Concrete Masonry Prisms Using Masonry Cement Mortars," *Masonry: Design and Construction, Problems and Repair*, ASTM STP 1180, J. M. Melander and L. R. Lauersdorf, Eds., American Society for Testing and Materials, Philadelphia, PA, 1993.

Ponce *et al.* 1999: Ponce, L. G., Klingner, R. E. and Melander, J., "Use of Ruggedness Testing to Develop an Inter-Laboratory Testing Protocol for Mortar-Cement Mortar," *Masonry: Materials, Testing and Applications*, ASTM STP 1356, J. H. Brisch, R. L. Nelson and H. L. Francis, Eds., American Society for Testing and Materials, West Conshohocken, PA, 1999.

APPENDIX A – Interlaboratory Study Data

Table A1 Bond Strength Test Results for all Data Sets

Data Set	Mortar	Replicate	Number of Joints	Mean, psi	Mean, kPa	Std Dev, psi	Std Dev, kPa	COV, %
A	1	A	30	177.91	1227	35.8	246.8	20.12
A	1	B	30	205.72	1418	38.14	263.0	18.54
A	1	C	30	206.59	1424	42.93	296.0	20.78
A	2	A	30	82.89	572	27.58	190.2	33.27
A	2	B	30	103.44	713	22.96	158.3	22.20
A	2	C	30	87.92	606	23.36	161.1	26.57
A	3	A	30	179.00	1234	41.53	286.3	23.20
A	3	B	30	150.52	1038	33.5	231.0	22.26
A	3	C	30	111.72	770	28.96	199.7	25.92
B	1	A	30	156.69	1080	22.78	157.1	14.54
B	1	B	30	172.09	1187	49.62	342.1	28.83
B	1	C	30	149.13	1028	33.58	231.5	22.52
B	2	A	30	112.96	779	26.18	180.5	23.17
B	2	B	30	110.43	761	23.86	164.5	21.61
B	2	C	30	106.87	737	19.64	135.4	18.38
B	3	A	30	145.93	1006	39.13	269.8	26.81
B	3	B	30	129.80	895	32.55	224.4	25.08
B	3	C	30	158.72	1094	35.94	247.8	22.64
C	1	A	30	121.00	834	35.24	243.0	29.12
C	1	B	30	100.51	693	28.93	199.5	28.78
C	1	C	30	100.59	694	19.61	135.2	19.49
C	2	A	30	108.24	746	16.77	115.6	15.49
C	2	B	30	80.10	552	16.37	112.9	20.44
C	2	C	30	85.27	588	15.48	106.7	18.15
C	3	A	30	90.87	627	13.78	95.0	15.16
C	3	B	30	110.30	761	22.79	157.1	20.66
C	3	C	30	118.65	818	14.34	98.9	12.09
D	1	A	30	156.02	1076	23.86	164.5	15.29
D	1	B	30	194.00	1338	33.17	228.7	17.10
D	1	C	30	179.07	1235	39.03	269.1	21.80
D	2	A	30	111.19	767	29.3	202.0	26.35
D	2	B	30	102.50	707	15.91	109.7	15.52
D	2	C	30	102.40	706	19.7	135.8	19.24
D	3	A	30	146.17	1008	26.51	182.8	18.14
D	3	B	30	150.98	1041	26.31	181.4	17.43
D	3	C	30	177.40	1223	38.53	265.7	21.72
E	1	A	30	143.02	986	18.79	129.6	13.14
E	1	B	30	137.15	946	16.4	113.1	11.96
E	1	C	30	139.22	960	14.37	99.1	10.32

Data Set	Mortar	Replicate	Number of Joints	Mean, psi	Mean, kPa	Std Dev, psi	Std Dev, kPa	COV, %
E	2	A	30	103.08	711	12.67	87.4	12.29
E	2	B	30	99.62	687	15.15	104.5	15.21
E	2	C	30	98.93	682	15.85	109.3	16.02
E	3	A	30	119.32	823	14.49	99.9	12.14
E	3	B	30	114.52	790	10.8	74.5	9.43
E	3	C	30	121.65	839	11.49	79.2	9.45
F	1	A	30	117.44	810	20.73	142.9	17.65
F	1	B	30	91.45	631	23.81	164.2	26.04
F	1	C	30	82.74	570	15.39	106.1	18.60
F	2	A	30	89.93	620	17.67	121.8	19.65
F	2	B	30	78.23	539	18.55	127.9	23.71
F	2	C	30	67.13	463	15.28	105.4	22.76
F	3	A	30	136.09	938	29.04	200.2	21.34
F	3	B	30	125.54	866	26.14	180.2	20.82
F	3	C	30	120.93	834	25.33	174.7	20.95
G	1	A	30	170.06	1173	35.54	245.0	20.90
G	1	B	30	145.35	1002	20.31	140.0	13.97
G	1	C	30	149.40	1030	20.16	139.0	13.49
G	2	A	30	119.43	823	20.57	141.8	17.22
G	2	B	30	120.27	829	15.72	108.4	13.07
G	2	C	30	130.02	896	14.61	100.7	11.24
G	3	A	30	119.20	822	24.44	168.5	20.50
G	3	B	30	113.55	783	13.1	90.3	11.54
G	3	C	30	120.63	832	12.42	85.6	10.30
H	1	A	30	216.42	1492	41.88	288.8	19.35
H	2	A	30	147.13	1014	24.99	172.3	16.98
H	3	A	28	197.48	1362	31.01	213.8	15.70
I	1	A	30	172.32	1188	23.27	160.4	13.50
I	1	B	30	180.14	1242	34.44	237.5	19.12
I	1	C	30	170.08	1173	22.35	154.1	13.14
I	2	A	30	99.01	683	14.56	100.4	14.71
I	2	B	30	101.68	701	18.35	126.5	18.05
I	2	C	30	116.31	802	15.45	106.5	13.28
I	3	A	30	122.77	846	15.73	108.5	12.81
I	3	B	30	127.29	878	19.62	135.3	15.41
I	3	C	30	139.33	961	26.6	183.4	19.09
J	1	A	30	128.65	887	30.25	208.6	23.51
J	1	B	30	162.00	1117	19.32	133.2	11.93
J	1	C	30	144.76	998	21.47	148.0	14.83
J	2	A	30	90.91	627	17.31	119.4	19.04
J	2	B	30	95.54	659	16.17	111.5	16.92
J	2	C	30	92.92	641	14.58	100.5	15.69

Data Set	Mortar	Replicate	Number of Joints	Mean, psi	Mean, kPa	Std Dev, psi	Std Dev, kPa	COV, %
J	3	A	30	131.14	904	18.36	126.6	14.00
J	3	B	30	131.48	907	20.39	140.6	15.51
J	3	C	30	161.45	1113	22.78	157.1	14.11
K	1	A	30	205.61	1418	27.48	189.5	13.37
K	1	B	30	190.58	1314	24.92	171.8	13.08
K	1	C	30	192.99	1331	32.92	227.0	17.06
K	2	A	30	122.59	845	16.69	115.1	13.61
K	2	B	30	104.82	723	14.17	97.7	13.52
K	2	C	30	104.88	723	19.37	133.6	18.47
K	2	D	30	105.87	730	18.11	124.9	17.10
K	3	A	30	149.07	1028	19.58	135.0	13.13
K	3	B	30	151.69	1046	30.45	210.0	20.07
K	3	C	30	174.68	1204	28.61	197.3	16.38
K	3	D	30	176.00	1214	33.50	231.0	19.03
L	1	A	28	100.44	693	16.3	112.4	16.23
L	1	B	29	80.72	557	23.02	158.7	28.52
L	1	C	30	84.63	584	19.86	136.9	23.47
L	2	A	15	42.74	295	12.81	88.3	29.97
L	2	B	23	50.36	347	11.89	82.0	23.61
L	2	C	23	50.75	350	8.15	56.2	16.06
L	3	A	30	88.01	607	18.01	124.2	20.46
L	3	B	30	73.06	504	14.28	98.5	19.55
L	3	C	30	73.64	508	17.8	122.7	24.17
M	1	A	30	180.84	1247	25.86	178.3	14.30
M	1	B	30	209.35	1443	29.06	200.4	13.88
M	1	C	30	180.11	1242	22.91	158.0	12.72
M	2	A	30	125.39	865	19	131.0	15.15
M	2	B	30	124.73	860	21.96	151.4	17.61
M	2	C	30	113.70	784	20.2	139.3	17.77
M	3	A	30	141.28	974	22.11	152.4	15.65
M	3	B	30	154.41	1065	30.74	212.0	19.91
M	3	C	30	185.28	1278	42.81	295.2	23.11
N	1	A	30	151.97	1055	27.79	191.6	18.17
N	1	B	30	146.72	1012	22.7	156.5	15.47
N	1	C	30	144.54	997	21.2	146.2	14.67
N	2	A	30	81.55	562	12.93	89.2	15.86
N	2	B	30	110.23	760	20.54	141.6	18.63
N	2	C	30	103.42	713	20.48	141.2	19.80
N	3	A	30	142.93	986	27.05	186.5	18.93

Data Set	Mortar	Replicate	Number of Joints	Mean, psi	Mean, kPa	Std Dev, psi	Std Dev, kPa	COV, %
N	3	B	30	143.06	986	28.14	194.0	19.67
N	3	C	30	147.48	1017	34.45	237.5	23.36
O	1	A	30	137.14	946	23.09	159.2	16.84
O	1	B	30	173.24	1194	29.44	203.0	16.99
O	1	C	30	164.21	1132	43.89	302.6	26.73
O	2	A	30	85.18	587	9.02	62.2	10.59
O	2	B	30	91.87	633	14.5	100.0	15.78
O	2	C	30	92.97	641	13.72	94.6	14.76
O	3	A	30	125.94	868	16.71	115.2	13.27
O	3	B	30	132.12	911	19.55	134.8	14.80
O	3	C	30	148.30	1023	27.54	189.9	18.57
P	1	A	30	164.99	1138	39.36	271.4	23.86
P	1	B	30	121.78	840	44.13	304.3	36.24
P	1	C	30	168.81	1164	38.77	267.3	22.97
P	2	A	30	108.75	750	29.81	205.5	27.41
P	2	B	30	108.59	749	26.62	183.5	24.51
P	2	C	30	109.79	757	19.15	132.0	17.44
P	3	A	30	108.91	751	31.46	216.9	28.89
P	3	B	30	133.23	919	24.13	166.4	18.11
P	3	C	30	126.83	874	25.74	177.5	20.29
Q	1	A	30	186.51	1286	24.42	168.4	13.09
Q	1	B	30	188.04	1297	22.13	152.6	11.77
Q	2	A	30	96.90	668	12.15	83.8	12.54
Q	2	B	30	112.98	779	19.81	136.6	17.53
Q	3	A	30	182.86	1261	24.54	169.2	13.42
Q	3	B	30	196.73	1356	31.93	220.2	16.23

Table A12 Averages, standard deviations and coefficients of variation obtained from average values of all 17 data sets

Mortar	Average Tensile Bond Strength, lb/in.^{2} (kPa)	Standard Deviation of Averages, lb/in.^{2} (kPa)	Coefficient of Variation of Averages
1	155.1 (1069)	35.78 (246.7)	23.08
2	99.7 (688)	20.09 (138.5)	20.15
3	137.3 (947)	28.49 (196.5)	20.75

Craig T. Walloch,[1] Philip J. Press,[2] Richard E. Klingner,[3] and Robert D. Thomas[4]

Increasing the Cost-Effectiveness of Interlaboratory Studies and Routine Comparative Testing: A Practical Example Involving Masonry Bond Strength

REFERENCE: Walloch, C. T., Press, P. J., Klingner, R. E., and Thomas, R. D., **"Increasing the Cost-Effectiveness of Interlaboratory Studies and Routine Comparative Testing: A Practical Example Involving Masonry Bond Strength,"** *Masonry: Opportunities for the 21st Century, ASTM STP 1432*, D. Throop and R. E. Klingner, Eds., ASTM International, West Conshohocken, PA, 2003.

ABSTRACT: Under the auspices of ASTM Committee C01 on Cement, an interlaboratory study was conducted to determine precision and bias for bond-wrench testing carried out under the requirements of ASTM Specification for Mortar Cement (C 1329-98) and ASTM Test Methods for Evaluating Masonry Bond Strength (C1357-98a). Another paper at this symposium [1] describes in detail that interlaboratory study and the results of the corresponding analysis for precision and bias. One objective of that analysis is to determine a "repeatability limit," r, and a "reproducibility limit," R. The repeatability limit quantifies what is commonly called the "within-lab variability," whereas the reproducibility limit quantifies what is commonly called the "lab-to-lab variability." The goal of this paper is to take the data from that interlaboratory study and analyze in more detail the possible sources of within-lab variability, including batch-to-batch, prism-to-prism, and bond-to-bond variability. This detailed analysis enables the prediction of variability for different test protocols (that is, with different numbers of batches, prisms and bonds). It also enables the prediction of how much time each test protocol would take to complete, which is directly related to the cost of testing. Finally, by comparing the probable variability and probable cost of each test protocol, it is possible to identify those test protocols that are most cost-effective for routine comparison of two mortars. This type of analysis is also useful in setting up other interlaboratory studies and interpreting their results.

[1] Technical Services Manager - Masonry Products, W. R. Grace & Co. – Conn., 62 Whittemore Avenue, Cambridge, MA, 02140.

[2] President, Philip Press, Inc., Statistical Consulting, 9489 Battler Court, Columbia, MD, 21045.

[3] L. P. Gilvin Professor in Civil Engineering, The University of Texas, Austin, TX, 78712.

[4] Vice President of Engineering & Research, National Concrete Masonry Association, 13750 Sunrise Valley Drive, Herndon, VA, 20171.

KEYWORDS: analysis of variance, bond-wrench testing, components of variance, flexural bond strength, interlaboratory study, masonry, mortar, precision and bias, tensile bond strength

Background and Results of Interlaboratory Study

The interlaboratory study described in Ref.1 involved three cements. From each cement, three replicate batches of mortar were made by each laboratory participating in the study. From each batch, 30 mortar joints were made and their flexural bond strengths determined and averaged. These batch averages were analyzed in Ref. 1.

For that interlaboratory study, 17 data sets were generated at 15 laboratories. The original paper reporting that interlaboratory study [1] looked at various subsets of this group of 17 data sets. One of those subsets, designated "Subset 2," contained 13 data sets. To generate Subset 2, two sets of data were removed from the original 17 because the reporting laboratories did not produce the prescribed number of replicate batches, and hence did not conform to the assigned testing protocol. Two other sets were removed because they had poor individual reliability. This current paper focuses exclusively on Subset 2.

The three replicate batch averages reported for each mortar were analyzed in Ref. 1 in accordance with ASTM Practice for Conducting an Interlaboratory Study to Determine the Precision of a Test Method (E691-99). One result of this analysis is the "repeatability limit," r. If the repeatability limit within a laboratory is r, there is a 95% confidence that any two results from a single laboratory for that mortar will be within r of each other. By definition, r is 2.8 (an approximation to $2\sqrt{2}$, or 2.828) times Sr, the repeatability standard deviation. Sr is the "pooled standard deviation[5]," and represents the best estimate of the standard deviation of the three replicate batch averages within a lab.

The repeatability standard deviations, Sr, for each of the three mortars used in the interlaboratory study, are shown in Table 1. Also shown are the coefficients of variation (COV) for the corresponding Sr values. The COV is equal to the standard deviation divided by the average bond strength and multiplied by 100 to give a percentage. The values of Sr for the three mortars ranged from 8.4 to 14.8 psi (0.058 to 0.102 MPa), with an overall value of 12.3 psi (0.085 MPa). The overall value, a composite of the results for the three mortars, is designated as "All" in Table 1. Interestingly, the COV values are more tightly grouped than the Sr values, ranging from 8.2– 9.6% with an overall value of 9.4%. This tight grouping suggests that within-lab variability is more uniform as a percentage of the average bond strength than as an absolute bond strength.

[5] Pooled standard deviation is the square root of the average of the individual variances, where variance is the square of the standard deviation.

TABLE 1 — *Within-Lab Standard Deviation and COV from Interlaboratory Study [1].*

Mortar	Average Bond Strength, Psi (MPa)	Repeatability Standard Deviation *Sr*, psi (MPa)	Coefficient of Variation COV %
A	153.7 (1.060)	14.8 (0.102)	9.6
B	102.9 (0.709)	8.4 (0.058)	8.2
C	135.9 (0.937)	12.9 (0.089)	9.5
All	130.8 (0.902)	12.3 (0.085)	9.4

Preliminary Evaluation of Results

The results of the interlaboratory study raise three questions: (i) What do these results mean?; (ii) Are these results expected?; and (iii) Why does it matter?

Meaning of E 691 Results

What do the results mean? ASTM E 691 indicates that if the COV is 9.4%, then 95% of all pairs of test results for a specified mortar mix design from a laboratory similar to those in the interlaboratory study can be expected to differ by no more than 2.8 times the COV, or about 26% of the average bond strength. That seems like a pretty wide range, considering that each test result is the average of 30 bond strengths from a single batch of mortar.

Expected Results from C 1329 and C 1357 Bond Testing

Are these results expected? To answer this question, let's review how each test result is determined. Each result is the average of 30 bond strengths from a single batch of mortar. For the 13 data sets in the interlaboratory study, the COV for each individual set of 30 bond strengths ranged from about 9% to 36%, and averaged about 18%. Assuming that bond strengths are approximately normally distributed, and if the COV for the individual bond strengths is 18%, statistics tell us that if we averaged each of many sets of 30 bond strengths, we would expect the distribution of 30-bond averages to have a COV of 18% divided by the square root of 30, or about only 3.3%. C 1329 and C 1357 require 30 joints for flexural bond testing because with a property as variable as mortar

bond strength, 30 joints are needed to provide confidence that the average reflects the true bond strength of the tested mortar.

But another question now arises. If statistics predicts that the test results obtained by averaging the bond strengths of multiple 30 joint tests should result in a distribution with a COV of 3.3%, why did the interlaboratory study find the within-lab COV of the test results to be 9.4%, or three times as high as expected? The answer is that the above calculation assumes no batch-to-batch variability in the results. Obviously, this is not the case with the interlaboratory data.

The higher-than-expected COV for the test results indicates significant batch-to-batch variability, which must be accounted for. Figure 1 shows the distribution for the individual bonds (COV of 18%), the expected distribution of 30-bond averages assuming no batch-to-batch variability, and the expected distribution of 30-bond averages from the interlaboratory study with the actual batch-to-batch variability included.

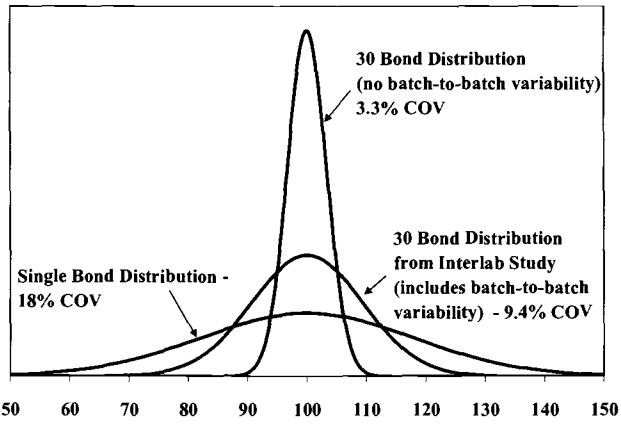

Figure 1 – *Distribution of Bond Values*

Why it Matters — Comparing Two Mortars

So why does it matter if there is significant batch-to-batch variability and the test results have a distribution with a COV that is three times what was expected assuming no batch-to-batch variability? It matters if we want to have a high degree of confidence in our conclusion about whether or not two mortars being compared are truly different. For example, assume that we want to compare two mortars, A and B, both of which have a standard deviation of 18 (units are irrelevant here) for individual bond-strength measurements. Further assume that Mortar A has a "true" average bond strength of 80 and Mortar B has a "true" average of 100 [6]. If we were to measure just a single bond

[6] For illustration purposes, the bond strengths and standard deviations for Mortar A and B have been left dimensionless, with Mortar B having a nominal value of 100. Therefore, since the standard deviation of Mortar B is 18, the COV for Mortar B is 18%. Because we are assuming for simplicity that the standard deviations of the

strength each for A and B and compare them, we would have a very difficult time telling if A was truly less than B or not. This can be seen in Figure 2, in which the distributions of bond strengths for Mortars A and B are shown on the same graph[7]. The region of overlap between the curves is quite substantial, and represents an "area of ambiguity" in which we would not be sure if A was weaker than B. In fact, a significant portion of trials would show that Mortar A was stronger than Mortar B!

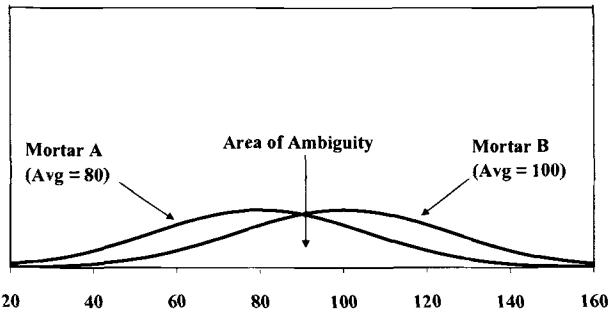

Figure 2 — *Comparison of Single Bond-Strength Values for Mortars A & B (COV - 18%)*

To help solve this problem we could make single batches of Mortar A and of Mortar B, test 30 bonds from each batch, and then compare the average bond strengths. With no batch-to-batch variability, as implicitly assumed in C 1329 and C 1357, we would expect the distribution of the average bond strength to have a COV of 3.3%. In this case, the "area of ambiguity" would be very small (Figure 3) and we could say with a high degree of confidence that Mortars A and B were indeed different.

---

two mortars are the same, the actual COV for Mortar A will be somewhat higher ($80/18 \times 100\% = 22.5\%$).

[7] For a statistical test of the difference between the averages of two normal distributions with the same standard deviation and equal sample sizes, the standard deviation of the difference is $\sqrt{2}$ times the common standard deviation [2]. This $\sqrt{2}$ factor has been included in the graphical representations shown in this paper.

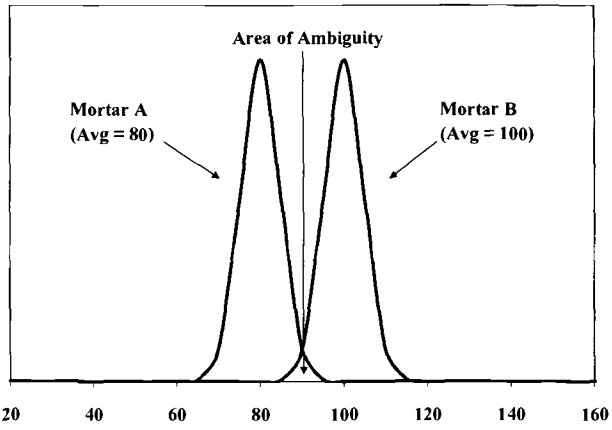

Figure 3 — *Comparison of Averages of Multiple 30 Bond Tests for Mortars A & B (Assuming no Batch-to Batch Variability – COV = 3.3%).*

Unfortunately, however, there is significant batch-to-batch variability in flexural bond strengths, and the actual COV (as determined in the interlaboratory study) is 9.4% for the average of 30 bonds. In this case, the "area of ambiguity" is still rather large (Figure 4). Again, in many cases, it is difficult to determine if Mortar A is really different from Mortar B.

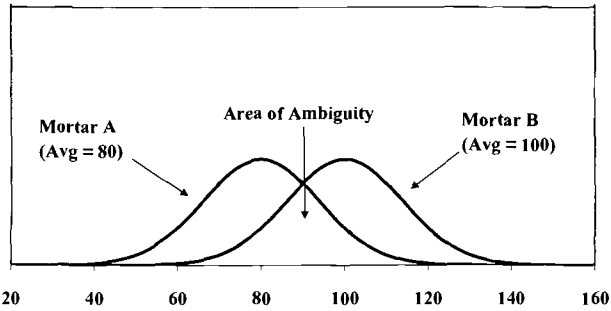

Figure 4 — *Comparison of Averages of a Single 30 Bond Test for Mortars A & B (from Interlaboratory Study – Includes Batch-to-Batch Variability – COV = 9.4%).*

One way to reduce the uncertainty in comparing Mortars A and B would be to follow the testing protocol and data-evaluation procedures used for the interlaboratory study referenced here [1]. In that case, we would make three batches each of Mortars A and B, and test 30 bonds from each batch. We would then average the bond strengths for all three batches of Mortar A and compare it to the average of all three batches of Mortar B. The COV would now be equal to 9.4% divided by the square root of 3, or about 5.4%. This helps reduce the "area of ambiguity," but it is still not as low as we might like

(Figure 5). To explore the sources of error further, we must use another statistical tool: components-of-variance analysis.

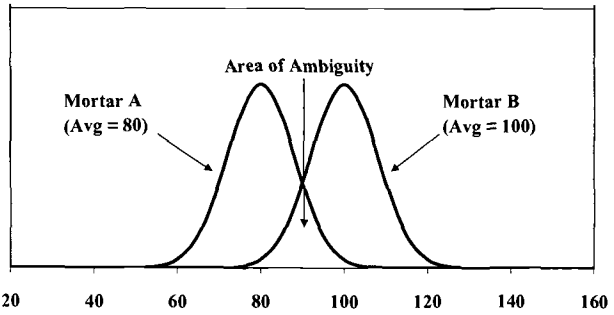

Figure 5 —*Comparison of Averages of Three Sets of 30 Bond Tests for Mortars A & B (from Interlaboratory Study – Includes Batch-to Batch Variability – COV = 5.4%).*

Further Evaluation Involving Components of Variance

The E 691 analysis of interlaboratory data, while valid, has limitations. One limitation is that because the test results were entered as the average of 30 bonds rather than individual bond strengths, we can estimate within-lab variability only for the protocol that was tested (30 bonds from each batch of mortar). The analysis does indicate that with the given interlaboratory test protocol (3 batches with 6 prisms per batch and 5 joints per prism, for a total of 90 bonds), we can expect the resulting averages to have a COV of 5.4%. Given large batch-to-batch variability, however, how do we know that this is the most efficient testing protocol? Would we be better off testing more batches with fewer bonds per batch? What would the estimated COV be for these other testing protocols? How much time would it take to undertake the other possible protocols, and how would this compare with the protocol used in the interlaboratory study referenced here?

Components-of-Variance Analysis

To answer these questions, we can again use statistical tools to examine the data more closely. We must now look at each individual bond value, and not just the average of each set of 30 bonds. Using each bond value, we can perform a statistical analysis of variance to estimate components of variance [3]. This analysis will let us estimate how much of the variability in the data is due to batch-to-batch, prism-to-prism, and joint-to-joint variability. From these estimates we can predict what COV would be obtained for other hypothetical testing protocols.

Batch-to-batch variability within a testing laboratory can occur because of such factors as small differences in weights of ingredients (especially water) added to each batch, operator procedural differences, changes in flow (consistency) or air content of the mortar, change in laboratory ambient conditions, and many other small differences.

Prism-to-prism variability within a batch can be caused by change in mortar workability over time, operator differences when mounting the prisms in the test jigs, possible segregation of material within a batch, etc. Joint-to-joint variability within a prism can occur because of lack of microscopic homogeneity of the mortar and bricks, differences in dead load experienced at different joint positions, small misalignments of the bricks within a prism, inherent variability in the tensile performance of portland cement based mortars, etc.

To estimate the magnitudes of these sources of variability, an analysis of variance was performed on the raw data produced by the interlaboratory study referenced here [1]. A key assumption for analysis of variance is that the precision of each data point is the same. This assumption is violated if, for example, there are large differences in within-batch standard deviation or COV. As part of the analysis of variance, a check is made for uniform precision and, if necessary, weights are applied to the data to reflect differences in precision. Weighted analysis of variance is a standard statistical technique for dealing with unequal variances [4, 5].

Weighting By Batch

For the interlaboratory study data used here, the analysis of variance identified significant variation in the "within-batch" standard deviation from lab-to-lab and mortar-to-mortar. For the 117 batches in the 13 data sets, the "within-batch" standard deviation ranged from 9 to 50 psi^2 (0.4 to 2.4 $MPa^2 \cdot 10^{-3}$) (Figure 6). One-quarter of the batches had within-batch standard deviations lower than 15 psi^2 (0.7 $MPa^2 \cdot 10^{-3}$) or higher than 34 psi^2 (1.6 $MPa^2 \cdot 10^{-3}$). Approximately one-half of the batches had within-batch standard deviations lower than 17 psi^2 (0.8 $MPa^2 \cdot 10^{-3}$) or higher than 29 psi^2 (1.4 $MPa^2 \cdot 10^{-3}$). The "within-batch" COV values show a similar range of variability (Figure 6). To compensate for this variation in "within-batch" standard deviations, the statistical analysis was repeated, weighting the analysis by batch using weighting factors proportional to the reciprocal of the variance of each batch, where variance is the square of the standard deviation. Weighting by batch assigns more weight to sets of data with lower within-batch variance, and less weight to those with higher within-batch variance. The logic behind this weighting is that data sets with lower variability are more "reliable" (contain better information) than those with higher variability.

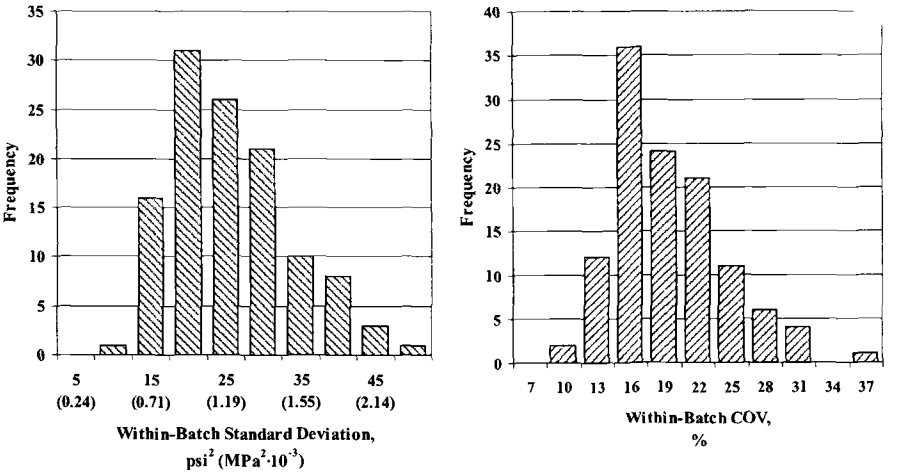

Figure 6 —*Histograms for Within-Batch Standard Deviation and COV for Referenced Interlaboratory Study.*

Results of Components-of-Variance Analysis

Table 2 shows the results of these analyses, in terms of the components of variance for each separate mortar and for all of the mortars combined. The latter results are not the same as the average of the results for each individual mortar, because of the weighting process. Figure 7 also graphically displays the percent of total variance of the various components for all the mortars combined.

Several observations can be made. The first is that the individual components of variance (batch, prism, joint) differ in absolute magnitude for each mortar but are strikingly similar when expressed as a percent of total variance. The batch-to-batch component of variance is about 17% of the total variance. Likewise, the prism-to-prism component of variance is 11% overall, and ranges from about 5% to 14% of the total variance. Finally, the joint-to-joint component of variance is about 72% overall, and ranges from 70% to 78% of total variance. This consistency in the percentages of each component of variance suggests that this analysis of variance reflects the underlying variability in bond-wrench testing and is valid across all mortars tested here.

TABLE 2 — *Estimated Components of Variance for Bond Strength by Mortar Type Estimated by Method of Moments, Variance Weighted by Batch.*

Mortar	Avg Bond Strength psi (MPa)	Variance, psi^2 ($MPa^2 \cdot 10^{-3}$) Batch	Prism	Joint	% of Total Variance Batch	Prism	Joint
1	153.7 (1.060)	154.8 (7.36)	108.2 (5.14)	611.4 (29.07)	17.7%	12.4%	69.9%
2	102.9 (0.709)	59.3 (2.82)	18.7 (0.89)	274.3 (13.04)	16.8%	5.3%	77.9%
3	135.9 (0.937)	108.8 (5.17)	90.4 (4.30)	453.0 (21.54)	16.7%	13.9%	69.5%
All	130.8 (0.902)	102.2 (4.86)	65.3 (3.10)	418.8 (19.91)	17.4%	11.1%	71.5%

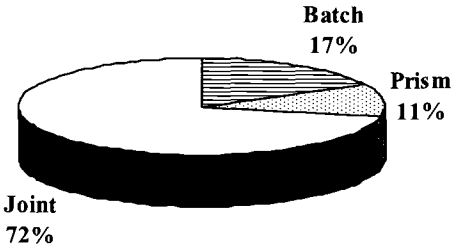

FIGURE 7 — *Estimated Components of Variance for Bond Strength – All Mortars Combined.*
Estimated by Method of Moments, Variance Weighted by Batch

The above components of variance can also be examined in terms of the square root of variance (standard deviation) (Table 3). This allows examination of the relative error of each source of variance. Relative error is similar in concept to COV, and is simply the standard deviation of each component of variance divided by the average bond strength and multiplied by 100 to give a percentage. Components of relative error are also consistent across all three mortars. The batch-to-batch component is approximately 8% of the average bond strength; the prism-to-prism component is about 6%; and the joint-to-joint component is about 16% of the average bond strength. This consistency again suggests that this analysis is valid across mortars, and probably reflects the inherent bond-strength information obtained from this type of bond testing.

Table 3- *Estimated Standard Deviation and Relative Error Components for Bond Strength.*

	Avg Bond Strength	Standard Deviation, psi (MPa)			Relative Error (% of Avg Bond)		
Mortar	psi (MPa)	Batch	Prism	Joint	Batch	Prism	Joint
1	153.7 (1.060)	12.4 (0.085)	10.4 (0.072)	24.7 (0.170)	8.1%	6.8%	16.1%
2	102.9 (0.709)	7.7 (0.053)	4.3 (0.030)	16.6 (0.114)	7.5%	4.2%	16.1%
3	135.9 (0.937)	10.4 (0.072)	9.5 (0.066)	21.3 (0.147)	7.7%	7.0%	15.7%
All	130.8 (0.902)	10.1 (0.070)	8.1 (0.056)	20.5 (0.141)	7.7%	6.2%	15.6%

Significance of Components-of-Variance Analysis

Now let's examine the significance of these components of variance. At first glance (Figure 7), the joint-to-joint component of variance might seem to be the most important source of variability, because it accounts for about 71% of the total variance, while the batch-to-batch and prism-to-prism components account for only about 17% and 11%, respectively. It is not surprising that joint-to-joint variance is by far the largest component, because the bond-wrench test measures the resistance of a non-homogeneous material to fracture, and bond strength is the result of the propagation of small random failures. While this statement is true, it does not tell the whole story.

To calculate the variance of the average bond strength for a particular test protocol, each component of variance is divided by the number of observations of that component. For example, for the testing protocol used in the referenced interlaboratory study, the total number of batches was 3, the total number of prisms was 3 times 6, or 18, and the total number of bonds was 3 times 6 times 5, or 90. Thus, for that protocol the batch-to-batch contribution to the variance of the average for all mortars combined is equal to the value in Table 2 (102.2 psi^2), divided by the number of batches (3) or 34.1 psi^2. Likewise, the prism-to-prism contribution is 65.3 psi^2 divided by 18, or 3.6 psi^2. Finally, the joint-to-joint contribution is 418.8 psi^2 divided by 90, or 4.7 psi^2. The batch, prism and joint portions of the variance of the average strength for the individual mortars can be calculated similarly (Table 4).

Table 4 also shows the total variance of average strength, which is simply the sum of the contributions from batch-to-batch, prism-to-prism and joint-to-joint variance. Now a different picture emerges regarding the most important sources of variance (Figure 8). For the interlaboratory test protocol referenced here, batch-to-batch variance accounts for about 80% of the total variance of average strength; prism-to-prism variance is only about 9% of the total; and joint-to-joint variance is only about 11% of the total. Thus, the batch-to-batch variance is by far the biggest contributor to the total variance of average strength. This is precisely because there are so few batches compared to the number of

prisms or joints, and suggests that we may be able to reduce the overall testing variability by making more batches while testing fewer bonds per batch.

TABLE 4 – *Estimated Contribution to Variance of Average Bond Strength by Mortar Type for the Referenced Interlaboratory Test Protocol (3 Batches, 6 Prisms/Batch, 5 Joints/Prism).*

	Avg Bond Strength	Variance, psi^2 (MPa^2· 10^{-3})				% of Total Variance			
Mortar	psi (MPa)	Batch	Prism	Joint	Total	Batch	Prism	Joint	Total
1	153.7 (1.060)	51.6 (2.45)	6.0 (0.29)	6.8 (0.32)	64.4 (3.06)	80.1%	9.3%	10.5%	100%
2	102.9 (0.709)	19.8 (0.94)	1.0 (0.05)	3.0 (0.14)	23.9 (1.14)	82.9%	4.4%	12.8%	100%
3	135.9 (0.937)	36.3 (1.73)	5.0 (0.24)	5.0 (0.24)	46.3 (2.20)	78.3%	10.8%	10.9%	100%
All	130.8 (0.902)	34.1 (1.62)	3.6 (0.17)	4.7 (0.22)	42.3 (2.01)	80.4%	8.6%	11.0%	100%

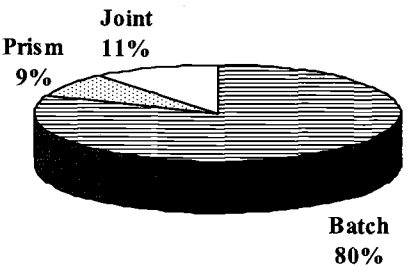

FIGURE 8 — *Estimated Contribution to Variance of Average Bond Strength – All Mortars Combined for the Referenced Interlaboratory Test Protocol (3 Batches, 6 Prisms/Batch, 5 Joints/Prism).*

Table 5 shows the standard deviation (square root of the variance) and COV of average bond strength for the protocol used in the referenced interlaboratory study. For this test protocol (3 batches, 6 prisms/batch, 5 bonds/prism, 90 total bonds), the total combined COV values are very consistent, averaging about 5% for all mortars.

TABLE 5 —*Estimated Variance, Standard Deviation and COV of Average Bond Strength by Mortar Type for Referenced Interlaboratory Test Protocol (3 Batches, 6 Prisms/Batch, 5 Joints/Prism).*

		Estimated Total Combined		
Mortar	Avg Bond Strength psi (MPa)	Variance, psi^2 ($MPa^2 \cdot 10^{-3}$)	Standard Deviation, psi (MPa)	COV
1	153.7 (1.060)	64.4 (3.06)	8.0 (0.055)	5.2%
2	102.9 (0.709)	23.9 (1.14)	4.9 (0.034)	4.7%
3	135.9 (0.937)	46.3 (2.20)	6.8 (0.047)	5.0%
All	130.8 (0.902)	42.3 (2.01)	6.5 (0.045)	5.0%

Comparison of Components-of-Variance Analysis and E 691 Analysis

After examining the components of variance for the interlaboratory study data, we can compare the predictions from this analysis with the results from the E 691 analysis in Reference [1]. The E 691 analysis predicted that the COV for the interlaboratory study test protocol (3 batches, 6 prisms/batch, 5 bonds/prism, 90 total bonds) would be about 5.4% and the COV for the average of a single set of 30 bonds (1 batch, 6 prisms/batch, 5 bonds/prism) would be about 9.4%. The components-of-variance analysis predicts that the COV for the interlaboratory study test protocol would be about 5.0% and the COV for the average of a single set of 30 bonds would be about 8.6% (see Line 1 in Table 6.) Agreement between the two analyses is quite reasonable, considering that the E 691 analysis depends solely on comparing three data points per laboratory for each mortar (each data point being the average of 30 bonds for one batch of mortar), whereas the analysis of components of variance uses all 90 individual bond values for each laboratory. The COV values predicted by analysis of components of variance are slightly lower than the values predicted by the analysis by E 691, most likely because of the batch weighting, which assigned more weight to batches with lower standard deviations and less weight to batches with higher standard deviations.

Predicted Variability of Other Test Protocols

Results of the components-of-variance analysis can be used to explore the expected variability for a variety of possible test protocols. For this analysis we will concentrate on results for the combined mortars. The estimated COV values for several test protocols are shown in Table 6. That table also shows the "Relative COV," which compares the various protocols normalized to the current C 1329 and C 1357 requirement of 30 bonds from a single batch of mortar. Increasing the number of batches lowers the COV of the

average bond strength substantially. We can achieve a 23% reduction in the COV of the average strength by increasing the number of mortar batches from 1 to 2, and we can achieve an almost 40% reduction by making 4 batches, all while keeping the total number of bonds tested at about 30. In fact, testing 4 batches of mortar with 2 prisms per batch and 4 joints per prism, for a total of 32 bonds, gives a 5.2% COV of the average strength, only slightly higher than the 5.0% given by the interlaboratory study test protocol that had a total of 90 bonds (3 batches, 6 prisms/batch, 5 joints/prism). It is also apparent that some protocols with 60 total bonds have an even lower COV of average strength than the 90-bond protocol used in the referenced interlaboratory study.

Time Estimates for Other Test Protocols

When choosing a test protocol, one should consider, in addition to the reliability of the results, the time required to prepare and test the samples. Estimated times for each protocol are shown in Table 6. That table also shows the "Relative Total Time," which compares the various protocols normalized to the current C 1329 and C 1357 protocol of 30 bonds from a single batch of mortar. The estimated total time for testing is split into two parts: the time to make the prisms, and the time to test (or break) the prisms.

The estimated time to make prisms assumes that 40 minutes are required to make each batch of mortar, and that 10 minutes are required to make each prism. The per-batch time includes setup, cleanup and the required testing for each batch (flow, initial penetrometer, and final penetrometer). The per-prism time assumes 7.5 minutes to actually make each prism (the approximate average for the referenced interlaboratory study), plus 2.5 minutes for setup and cleanup. The estimated time to break prisms assumes 3 minutes per bond or about 1.5 hours for a set of 30 bonds.

TABLE 6 —*COV Values and Time Estimates for Various Bond Test Protocols*

	No. of Batches	Prisms per Batch	Joints per Prism	Total Bonds	COV of Avg	Relative COV	Time Required, h Make	Break	Total	Relative Total Time
Current C 1329	1	6	5	30	8.6	100%	1.7	1.5	3.2	100%
Inter-lab Study	3	6	5	90	5.0	58%	5.0	4.5	9.5	300%
30-Bond Protocols	2	3	5	30	6.7	77%	2.3	1.5	3.8	121%
	3	2	5	30	5.9	68%	3.0	1.5	4.5	142%
	4	2	4	32	5.2	61%	4.0	1.6	5.6	177%
	6	1	5	30	4.9	57%	5.0	1.5	6.5	205%
60-Bond Protocols	2	6	5	60	6.1	71%	3.3	3.0	6.3	200%
	3	4	5	60	5.2	60%	4.0	3.0	7.0	221%
	4	3	5	60	4.7	55%	4.7	3.0	7.7	242%
	6	2	5	60	4.1	48%	6.0	3.0	9.0	284%
90-Bond Protocols	6	3	5	90	3.8	45%	7.0	4.5	11.5	363%
	9	2	5	90	3.4	39%	9.0	4.5	13.5	426%

By factoring in the time estimates for each test protocol, it is apparent that the lower COV of average strength for some protocols does come at the price of more testing time than is currently required by C 1329 and C 1357 (single batch and 30 total bonds tested). Many of the hypothetical test protocols, however, require less time than the protocol of the referenced interlaboratory study which required 3 batches with a total of 90 bonds tested.

Choosing A Specific Test Protocol — The True-Cost Index

To help determine relatively efficient test protocols, we have constructed an index that combines the inherent reliability of results from a given protocol with the cost of that protocol. This True-Cost Index is the square of ("Relative COV"/100), for each protocol, multiplied by the "Relative Total Time" for that protocol. The COV is squared to give it extra weight because it is important to reduce the variability as much as possible to reduce the "area of ambiguity" between two mortars. The lower the True-Cost Index, the better the protocol. Calculated True-Cost Indices for several test protocols are shown in Table 7.

In terms of the True-Cost Index, the requirement of C 1329 and C 1357 (30 bonds from one batch) is equivalent in efficiency to the interlaboratory test protocol of 30 bonds from each of 3 batches of mortar (90 bonds total). The other 30-, 60- and 90-bond protocols shown in Table 7 are at least as efficient as those two standard protocols. Relatively efficient testing protocols are highlighted in the table.

Which protocol to use depends on how much we want to reduce the "area of ambiguity" when comparing two mortars, versus the amount of time we can afford for testing. For an investment of only 42% more time than the current C 1329 protocol (1 batch, 6 prisms/batch, 5 joints/prism, 30 total bonds) we can reduce the COV of average strengths by almost one-third (from 8.6% to 5.9%), by making 3 batches of mortar and only 2 prisms per batch, while maintaining the same 30 total bonds. To reduce the COV of average strengths to about the same 5% level as in the 90-bond interlaboratory study referenced here, one could test only 32 bonds (4 batches, 2 prisms per batch and 4 bonds per prism), thus reducing the required time by over 40%.

To reduce the COV of average strength to 4.1%, we could choose a 60-bond protocol (6 batches, 2 prisms per batch, 5 joints per prism) and still spend less effort than for the 90-bond protocol used in the referenced interlaboratory study. Finally, to approach the 3.3% COV of average strengths that we first expected from a 30-bond testing protocol (assuming no batch-to-batch variability), we could choose a 90-bond protocol (9 batches, 2 prisms per batch, 5 joints per prism); this, however, would require four times the effort of the current 30-bond C 1329 protocol or almost 1.5 times the effort of the 90-bond protocol of the interlaboratory study referenced here.

TABLE 7 — *True-Cost Index for Various Bond-Test Protocols.*

	No. of Batches	Prisms per Batch	Joints per Prism	Total Bonds	COV of Avg.	Relative COV	Total Time h	Total Time Relative	True-Cost Index
Current C 1329	1	6	5	30	8.6	100%	3.2	100%	100%
Inter-lab Study	3	6	5	90	5.0	58%	9.5	300%	100%
30-Bond Protocols	2	3	5	30	6.7	77%	3.8	121%	72%
	3	**2**	**5**	**30**	**5.9**	**68%**	**4.5**	**142%**	**66%**
	4	**2**	**4**	**32**	**5.2**	**61%**	**5.6**	**177%**	**65%**
	6	1	5	30	4.9	57%	6.5	205%	68%
60-Bond Protocols	2	6	5	60	6.1	71%	6.3	200%	100%
	3	4	5	60	5.2	60%	7.0	221%	81%
	4	3	5	60	4.7	55%	7.7	242%	72%
	6	**2**	**5**	**60**	**4.1**	**48%**	**9.0**	**284%**	**66%**
90-Bond Protocols	6	3	5	90	3.8	45%	11.5	363%	72%
	9	**2**	**5**	**90**	**3.4**	**39%**	**13.5**	**426%**	**66%**

Conclusions

The data used for the basis of this paper was an interlaboratory study [1] conducted to determine precision and bias for flexural bond strength testing of masonry mortars. This paper details additional statistical analyses that were performed using components-of-variance techniques to document the contributions that different mortar batches, different masonry prisms, and different mortar joints have on the resulting overall variability that is inherent in masonry bond strength testing.

Based on these statistical analyses, the following conclusions can be drawn:

- Variability is inherent in bond wrench testing because the method measures the resistance of a non-homogeneous material to fracture, and bond strength is the propagation of small random failures. The coefficient of variation for single sets of 30-bond tests in the interlaboratory study averaged 18%. When many sets of 30-bond tests are performed, the coefficient of variation of the 30-bond averages would theoretically drop to 3.3%, if there were no batch-to-batch variability. This is the underlying assumption behind the 30-bond protocols required by C 1329 and C1357.
- Due to substantial batch-to-batch variability in the interlaboratory results, however (each lab prepared and tested three replicates of each mortar batch), the actual COV for 30-bond averages was about 9%, or nearly three times that theoretically predicted.
- A components-of-variance analysis was used to quantify the amount of variability due to batch-to-batch, prism-to-prism and joint-to-joint variability. For the particular

protocol used in the interlaboratory study (3 batches, 6 prisms per batch, and 5 joints per prism), the analysis indicates that batch-to-batch variability accounts for about 80% of the total variance of average bond strength. The remaining variability was split evenly between prism-to-prism variability and joint-to-joint variability.

- The large contribution to total variance from batch-to-batch variability occurs because the number of total batches (3) is small compared to the total number of prisms (18) and joints (90). This suggests that testing protocols with more mortar batches and fewer joints per batch will be more efficient in reducing total variability while limiting the amount of testing effort.
- The components-of-variance analysis allowed the development of a "True-Cost Index" to compare the cost of achieving a particular reliability of results from testing protocols with differing numbers of batches, prisms and bonds. Because batch-to-batch variability is such a substantial component of the variability in flexural bond test results, the True-Cost Index indicates that the most efficient test protocols involve multiple batches of mortar with only two prisms, and thus 8–10 bonds, per batch.
- One efficient 32-bond testing scheme (4 batches, 2 prisms per batch, 4 joints per prism) is nearly as reliable as the 90-bond interlaboratory protocol, and reduces the required preparation and testing time by 40%.
- Other efficient 60- and 90-bond protocols were also identified that could reduce the variability to levels close to the 3.3% COV theoretically achievable from a single batch of 30 bonds assuming no batch-to-batch variability.
- To compare the bond strengths of two mortars, choosing an appropriate test protocol depends on the desired size of the "area of ambiguity" between the statistical distributions of the two mortar strengths. This in turn depends on the relative difference between the average bond strengths of the two mortars, and on the COV of the average strengths for the chosen test protocol.

Recommendations for Changes to ASTM Procedures

- Non-mandatory guidance should be added to ASTM C 1357 regarding the statistical influence that the number of batches, prisms per batch, and joints per prism has on total variability of results.
- For ASTM testing standards in general, guidance should be prepared regarding the number of batches, specimens per batch, and tests per specimen, to achieve the desired level of confidence of compliance with performance criteria.

Recommendations for Further Study

- Based on conclusions presented in Reference 1 that the time required to construct masonry prisms may be a significant influence on the variability of bond-strength results, a new subset of data should be generated using a smaller subset of labs who completed prism fabrication in 45 minutes or less. That data set should be subjected to the same type of components-of-variance analysis presented here.
- The tools presented here should be used to develop relatively efficient test protocols for determining if two mortars are statistically equivalent or if a modified mortar is not statistically different from a reference mortar.

Acknowledgments

We would like to thank J. M. Melander for supplying us with the raw data from the interlaboratory study in a way that made it easy to use while preserving the confidentiality of the laboratories that participated in the study.

References

[1] Hosler, P. J., Klingner, R. E. and Melander, J. M., "Interlaboratory Study to Establish the Precision and Bias of Bond-Wrench Testing Under ASTM C 1329 and C 1357," *Masonry: Opportunities for the 21st Century, ASTM STP 1432*, D. Throop and R. E. Klingner, Eds., ASTM International, West Conshohocken, PA, 2003.

[2] Brownlee, K. A. "Statistical Theory and Methodology in Science and Engineering," 2nd ed., John Wiley & Sons Inc., New York, 1965, p. 119.

[3] *Ibid.*, pp. 482–489.

[4] Draper, N. and Smith, H., "Applied Regression Analysis," 2nd ed., John Wiley & Sons Inc., New York, 1981, p.108.

[5] "RS/Explore Release 4, Statistical Appendices," RS/Series Software, Brooks Automation, Chelmsford, MA, 1995.

Edward A. Gerns,[1] and Anthony D. Cinnamon[2]

Inspection and Evaluation of Masonry Facades

REFERENCE: Gerns, E. A., Cinnamon, A. D., **"Inspection and Evaluation of Masonry Facades,"** *Masonry: Opportunities for the 21st Century, ASTM STP 1432*, D. Throop and R. E. Klingner, Eds., ASTM International, West Conshohocken, PA, 2002.

Abstract:

With the recent passage and enforcement of facade inspection ordinances in cities throughout the United States, including Chicago, New York, Boston, and Detroit, the need for proper and effective evaluation of building facades has become increasingly important. A proper understanding of the facade system being evaluated, as well as the mechanisms of deterioration, is critical to an effective and accurate evaluation.

As cladding systems age, damage resulting from environment forces can compromise both the structural and performance characteristics of the cladding system. A lack of proper maintenance or inappropriate maintenance can result in a failure of the cladding, posing a threat to both public safety and the building integrity.

This paper will provide a brief overview of the historical development of cladding systems. A discussion of failure mechanisms and representative examples will also be included. Finally, a systematic approach for the evaluation of facades will be given.

Keywords: Masonry Facades, Inspection, Evaluation

Evolution of the Facade

Historically facades can generally be categorized in one of two ways—monolithic or composite. Prior to the 1850s, the majority of the larger civic building facades were of monolithic masonry construction. The walls were typically load bearing masonry systems consisting almost exclusively of masonry materials and mortar. These systems were constructed and intended to work as a monolithic entity. Other less important buildings combined various combinations of timber and other organic materials as well as masonry to create the building envelope. During this time period, economics and the cultural significance of a particular structure determined the system.

[1] Consultant, [2] Senior Architect/Engineer, Wiss, Janney, Elstner Associates, Inc., 120 North LaSalle, Suite 2000 Chicago, IL 60602

With the onset of the Industrial Revolution and the increased availability and affordability of iron and steel, the development of an alternate construction system was inevitable. In addition, today's skyscrapers would not have been possible without the invention of the elevator. The idea of separating the exterior skin of the building from the structural system was the logical evolution of the necessity to reduce the weight of the exterior cladding so that the height of buildings could continue to increase (Figure 1).

The development of the modern skyscraper and the skeleton frame system resulted in the exterior façade of buildings becoming an increasingly complex assemblage of various materials, each with its own physical and mechanical characteristics. Generically referred to as a curtainwall, cladding systems of the past 100 years are composed of a relatively thin exterior decorative layer tied to a backup system which protects the building's structural system or the structural system itself. The relationship between the outer skin and the backup or structure is hard to characterize. It is even more difficult to predict the life cycle behavior of this assemblage. Typically, modern cladding systems do not possess significant redundancies. Therefore, as the system ages and deteriorates, the margin between stability and failure is reduced. Further, continued evolution of the curtainwall and inevitable experimentation has resulted in minor and major failures. Each failure has led to a greater understanding of the behavior of the systems and its failure mechanisms.

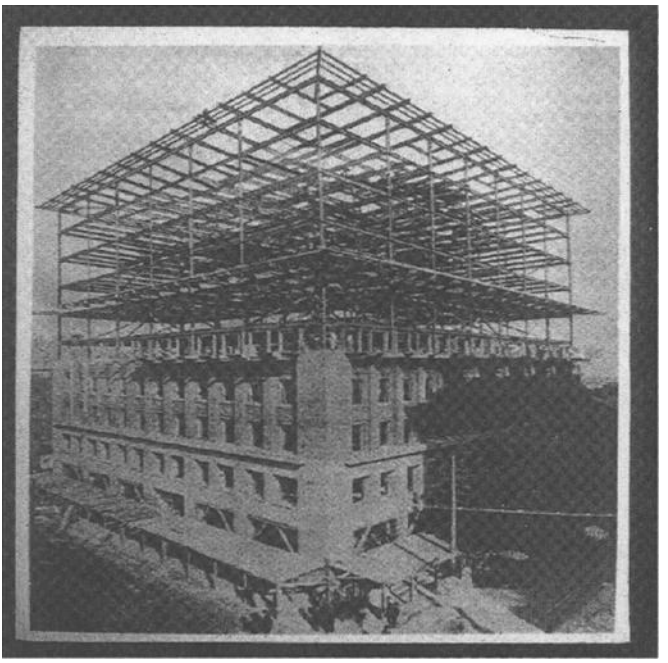

Figure 1 – *Skeleton Frame Structural System*

The structural systems of almost all high-rise structures built in the past 100 years are concrete or steel systems. Each system offers advantages and disadvantages. In general, the steel system has the advantages of material consistency, repeatability and relative ease of fabrication. Concrete allows for geometric flexibility and inherent fire protection. Each of these systems present different issues related to the exterior cladding systems. Steel frames are usually much more flexible than concrete. Erection tolerances of both systems vary, and the cladding systems must accommodate these variations. In addition, the frames will compress to varying degrees as the dead load is applied to the building and concrete frames also undergo creep over time.

The exposed portion of the curtainwall system can be comprised of a variety of materials. Early curtainwalls through the 1920s were typically of brick, terra cotta and stone. This material was generally at least 4 inch (10 cm) thick with at least an 8-inch (20 cm) backup wall system comprised of brick or terra cotta. In the 1920s cast stone was introduced as a replacement facing material for both terra cotta and stone. Between the 1930s and the 1950s stone continued to be used on the lower floors of buildings, but the pieces were being cut as thin as 1 ½ inches (4 cm) [*1*]. In the 1940s precast concrete systems were introduced. In the 1940s and 1950s the glass and metal curtainwall system became popular, with various materials such as stone, metal and glass, being glazed directly into the curtainwall framing. The 1960s brought the introduction of composite systems. Stone faced precast and various laminated combinations of materials were being introduced in an attempt to reduce costs and speed construction.

The various mechanisms of decay vary between materials and systems, but in general can be reduced to a few simple concepts.

Decay Mechanisms

Moisture Infiltration and Weathering

Infiltration of moisture is an inevitable reality of all cladding systems. Monolithic systems relied on the mass of the brick masonry to absorb the moisture until it evaporated. Composite curtainwall systems typically rely on a secondary system to collect and divert water out of the cladding system. Moisture within a composite system is a much more complex issue than in monolithic systems if the water management system is nonexistent, has failed or was improperly installed.

Moisture absorbed by new masonry results in expansion of the masonry. Generally, initial expansion ranges between 0.02 and 0.07 percent of the wall area [*2*]. Moisture expansion in combination with the frame shrinkage can range between 0.07 and 0.15 percent of the height of the wall [*3*]. Therefore, depending on the structural system, the combination of material expansion and frame shrinkage can result in significant accumulation of internal compressive stresses. If properly designed relief joint details are not incorporated into the cladding design and properly installed, significant distress can result. These internal stresses have the potential to fracture masonry or displace material.

Moisture in the cladding systems of older buildings is a common problem. Absorptive, permeable and porous materials will absorb and hold water within the material itself. If water remains within the material and the exterior temperature drops

below freezing, the water within the material will freeze, expand, and degrade the material if the pore structure cannot accommodate or resist the forces of the expanding water. As temperatures increase, the water returns to a liquid state. This is known as freeze-thaw cycling [*4*]. Freeze-thaw damage in masonry materials is characterized by a crumbled appearance of the units themselves, as well as the mortar (Figure 2).

Figure 2 – *Severe freeze-thaw damage of brickwork*

Efflorescence, the accumulation of salt deposits on the exterior surface of a material, is an indication of moisture within the wall system. Water moving through a wall system will suspend salts in the mortar and masonry. As the water evaporates from the exterior surface, the salt deposits remain. New walls sometimes exhibit a type of efflorescence known as "new bloom" resulting from the drying out of the new wall following construction. Generally, new building bloom does not present a problem. It is easily removed or will be washed away over time.

Exfoliation or flaking of some sedimentary stones is a natural weathering characteristic of many sandstones and some limestones (Figure 3). Depending on the orientation of the bedding planes and the exposure of the stone and protection of the pieces, the exfoliation may not manifest itself.

Figure 3 – *Exfoliation of windowsill*

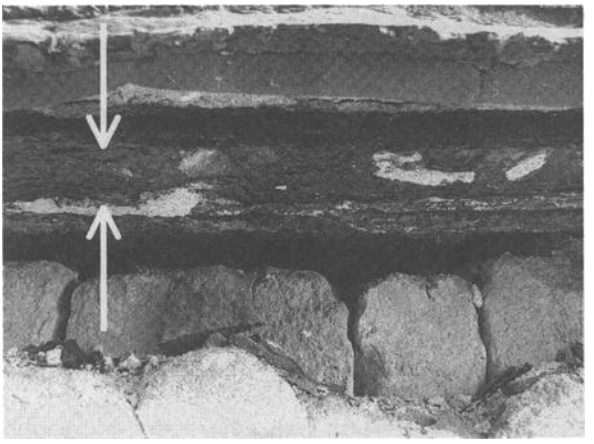

Figure 4 – *Accumulation of corrosive scale at shelf angle*

Water that bypasses the outer layer of material in a composite cladding system has the potential to degrade the wall from within the layer between the cladding and backup material. The most common manifestation of this is corrosion of embedded steel elements. The by-product of corrosion of steel is corrosive scale that can occupy a volume between four and ten times the volume of the original uncorroded steel (Figure 4). The forces resulting from the confined corrosion of the embedded steel elements can cause distress in the cladding. Localized failures can include spalling and cracking of individual units (Figures 5 and 6) as well as displacement of larger areas (Figure 7).

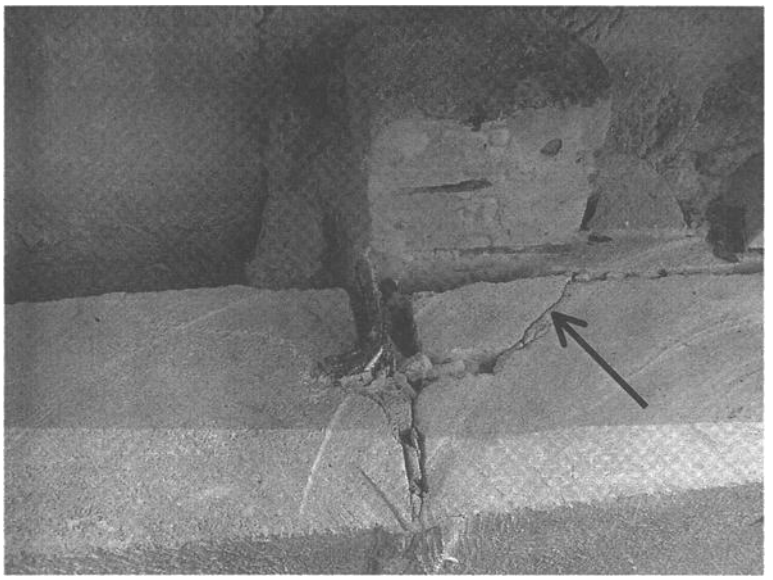

Figure 5 – *Inside spall of stone panel*

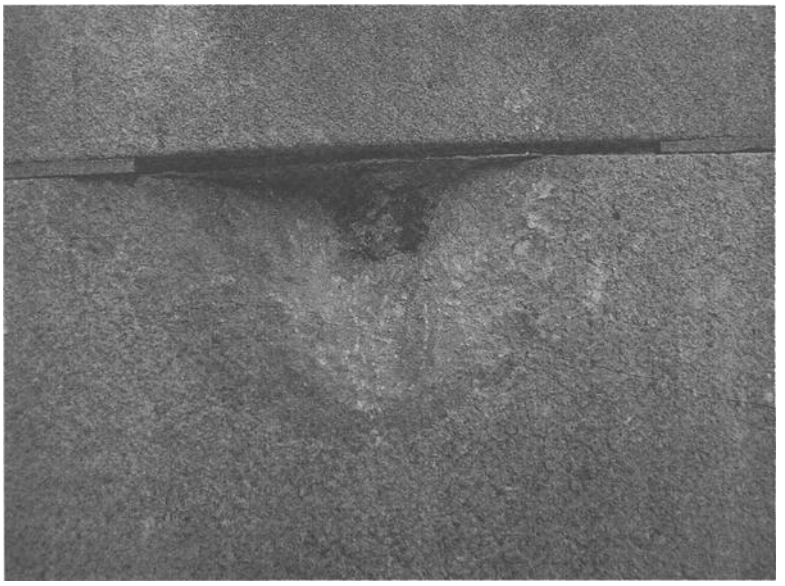

Figure 6 – *Localized spalling caused by corrosion of embedded anchor*

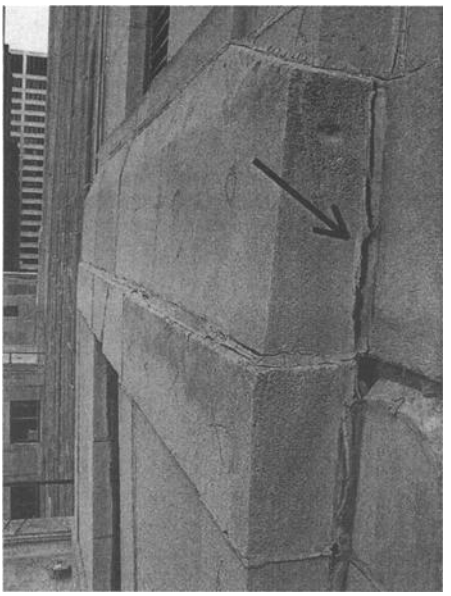

Figure 7 – *Displacement resulting from corrosion of support angle*

In some instances, the corrosion does not manifest itself in externally visible distress. Complete disintegration is not uncommon in thinner embedded steel elements such as lateral anchors in masonry construction (Figure 8) or spalling of the back face or non-visible portion of materials such as stone panels (Figure 5) and terra cotta.

Figure 8 – *Corroded lateral strap anchors*

Another unique problem related to moisture infiltration is the introduction of gypsum products into a wall system which are then exposed to moisture. Gypsum has been used by masons when setting stone, because it allowed the mortar to set up quickly, thus speeding the installation. Gypsum plaster was also used to resist inward loads in thin stone systems by placing discrete spots of plaster on the back face of the panel. When gypsum gets wet however, a chemical reaction occurs that results in dramatic expansion of the mortar or plaster. If the expansion cannot be accommodated, localized spalling or displacements of panels can result.

Unaccommodated Movements:

Prior to the 1950s accommodation of thermal cycling was generally not considered in the design of exterior cladding systems. Depending on the material and the range of potential temperatures, significant stresses can develop if the expansion or contraction is not properly accommodated. Physical properties of materials, color and exposure all affect the interaction between adjacent materials. Because modern wall systems are a complex assemblage of various materials, the effects of thermal cycling on the wall systems are difficult to predict.

In masonry construction, unaccommodated thermal cycles result in cracking and displacement in long expanses of masonry. Buildings constructed without vertical expansion joints to accommodate horizontal expansion usually create joints in the form of vertical or step cracking near corners. Parapets are typically the most susceptible to horizontal expansion. Outward displacements and cracking are not uncommon near corners of parapets. When longer expanses of walls are restrained by stiffer elements, the wall may tend to snake between the restraint points.

Unaccommodated vertical expansion results in localized crushing at restraint points such as shelf angle or outward displacements, if the wall is not properly tied to the backup system. Unaccommodated vertical expansion is also exacerbated as a result of frame shrinkage. Both vertical and horizontal cracking may result, depending on the cladding system.

One unique thermal cycling issue related to thin marble panels is hysterisis. Because marble is a metamorphic stone, its microstructure consists of elongated particles held within the surrounding matrix. As the marble panel is exposed to the sun, the exterior surface tends to grow more than the inside surface of the panel. When the exterior surface cools, the geometry of the particles do not return to their original position, but are slightly displaced. As the panel continues to cycle, the separation between particles continues to increase. Depending on the degree of restraint created by the panel anchorage, different distress will result. If the panel is supported along the top and bottom edge, the panel may bow outward between the restraint of the edge supports (Figure 9). If the main body of the panel is restrained, cracking may result in a variety of patterns.

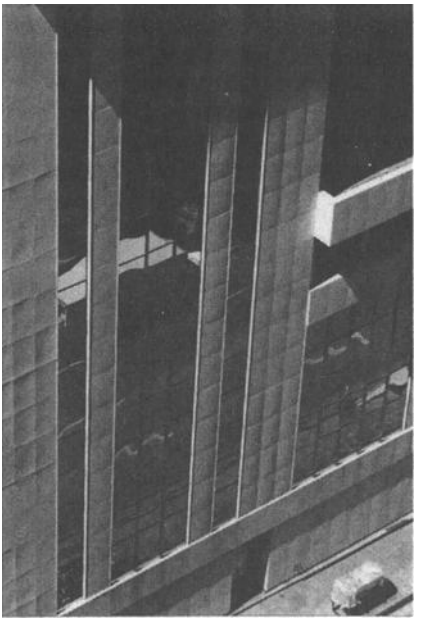

Figure 9 – *Hysterisis of marble panels*

Differential coefficients of thermal expansion is a phenomena that became more common with the introduction of many of the new composite panel systems that rely on bonding different materials together, using adhesives. If the materials being bonded have significantly differing coefficients of thermal expansion, the different layers of the panel can actually delaminate from each other, resulting in a significant loss of structural strength.

In addition to movements of materials within a façade system, the entire building or portions of the building may move as a result of settlement, differential settlement or soil subsidence. All of these movements can result in distress in the exterior façade, but masonry buildings are particularly susceptible as a result of the brittle nature of masonry materials. Generally, distress resulting from such movements causes cracks to develop at openings, offsets, where the building massing changes or the point where the subsurface conditions change.

Original Installation Deficiencies:

Accommodation of tolerances are a critical component in the detailing of new cladding systems as well as understanding how improper accommodation of tolerances can result in failures. Obviously, no building has ever been constructed exactly as shown in contract documents. Materials used in construction have variations resulting from manufacturing process. Natural variations at a global scale of a building layout are an inevitable result of human error. The construction of a structural frame will vary both in

plan and elevation from its theoretical position. Connections for the cladding material that are to be attached to the frame must be able to accommodate these frame variations as well as the fabrication variations so that the cladding system will be installed essentially plumb and true. Typically, the allowable and acceptable tolerance of the cladding system installation is much tighter than the supporting frame. When connections do not properly accommodate tolerances, the contractor will frequently attempt to modify the connection to maintain the finish tolerances of the cladding. These modifications vary widely, and frequently are executed to achieve the desired end without a full appreciation of the required design or code issues to be addressed.

Still another issue related to installation of a cladding system is how the last piece of a system or portion of the system is installed. In many instances, the final piece must be installed with special details to maintain the structural and performance integrity of the system. If the systems are connected from the interior of the building such as a panelized system, the issue is not as critical as when the backup wall is constructed at the same time as the cladding. In this instance, the last piece is frequently installed using a blind anchorage system, or it is not addressed in the contract documents, and left to the discretion of the installation contractor.

Evaluation Techniques

A systematic approach for the evaluation of facades is critical to achieve economical and accurate results. Perhaps the most important component of the evaluation is familiarity with the cladding system used on the building. With newer buildings, review of the original architectural and structural drawings and specifications can be invaluable. Finding a complete set of drawings for older buildings is usually more challenging. Thus, the inspector should be familiar with the system employed and potential issues based on past experience or precedent. In both instances, however, a review of past maintenance records and informal interviews with building maintenance and management can provide valuable insight into the performance of the building and potential issues to be addressed.

Following a review of documentation related to the building, a visual survey from grade and adjacent areas should be performed, using binoculars or a spotter scope. With taller buildings it is usually very difficult to properly inspect the building only from grade. Whenever possible, access to adjacent buildings can be very helpful in developing a more comprehensive evaluation of the façade. While the entire façade should be observed, particular attention should be given to the corners and top of the building as well as windows and other openings. Though not always the case, frequently the most severe problems develop in these areas. Vertical surfaces of the building should be inspected by sighting up and/or down columns, piers and other flat wall areas. Horizontal areas should be sighted from the roof or grade if applicable.

If possible, the façade should be viewed in a variety of lighting. Obviously, the most advantageous situation is when the sun is shining parallel to the face of the façade being viewed. Variations in surface position, displacements and other imperfections of the plane of the wall are much more evident when the sun is in such a position that the imperfections cast a shadow.

Close-up Inspections

There are numerous shortcomings to inspecting a building from some distance. Small imperfections in the façade are often difficult to detect and are sometimes an indication of a much larger problem. Small cracks or slight displacements are difficult if not impossible to identify using binoculars and spotter scopes. Therefore, the need to include close-up inspections, of at least representative areas, is critical to properly evaluate most facades.

A variety of techniques are available to perform close-up inspections. The initial visual inspection should be used to determine the most appropriate locations for the close-up inspection. If the number of inspections will be limited, it is usually most advantageous to select corners if no significant distress is observed from afar.

If a building is less than 120 feet tall (37 m), a personnel lift can enable large areas of the façade to be inspected relatively quickly. These machines generally have a maximum working platform range between 40 and 120 feet (12 and 36 m). The area adjacent to the building should be fully evaluated prior to using a personnel lift to ensure that the weight of the machine can be properly supported and that it can be maneuvered to gain access to the desired areas. Personnel lifts are also a very effective method for inspecting soffit areas when the first floor of a building is inset from the main façade.

Another common technique for access to buildings of any height is a swingstage. A swingstage is a cable-supported motorized platform that can be assembled in a variety of lengths and configurations. Rope scaffolds are an older system used for smaller areas that rely on a pulley system to raise and lower a platform. All swingstage systems and related components should comply with all OSHA requirements and should be installed and operated only by properly trained personnel.

Another procedure that can be used when appropriate is rappelling. This system offers the advantage of speed of set-up and inspection, but there are some limitations if further investigations of a particular area are required. In many instances rappelling may be the only realistic technique available to access certain portions of the buildings for close-up inspection (Figure 10). Again, all staging should comply with applicable standards and only qualified, properly trained, personnel should perform inspections using rappelling techniques.

Figure 10 – *Inspection being performed by rappelling techniques*

Regardless of the technique used to access the facade close-up, the inspection methodology should be similar. Obviously, a thorough visual inspection should be made of the area. Any evidence of distress, displacements, discoloration or deterioration should be documented. The documentation should include photographs, sketches and notations on building elevations.

In most instances the pattern of distress provides a clear indication of the cause or potential cause of distress observed. The patterns of distress must be studied with an understanding of the building cladding system and building structure to determine an interrelationship between the two. Distress should be evaluated relative to zones of the building. The patterns should be evaluated from the global to the micro level. The most obvious first step is the distress by the building elevations. This is then followed by an evaluation of vertical and horizontal zones of building. Vertical zones may include corners of the building and the field between the corner areas. In addition, cladding systems may change around the perimeter of a building; thus these areas may need to be considered separately. Horizontal zones of a building could include parapets, entrance floors or changes in building articulation between lower areas and the upper portions of the building. The evaluation by zone should also be considered as it relates to the building elevations. Finally, individual components should also be evaluated as they relate to the cladding system. For example, corrosion of supporting shelf angle within a terra cotta facade could result in distress that may not be directly related to a zone of a building, but rather the original installation techniques or subsequent maintenance. This condition may also exist relative to fabrication and installation tolerances. Statistically, localized distress related to tolerances will not necessarily correspond to a specific zone.

Often the full extent of distress of older buildings is difficult to ascertain if the building facade is dirty. The dirt will frequently fill cracks or create a crust over the surface making detection of cracks and other deterioration very difficult. When developing repairs, the extent of repairs and potentially the scope of repairs may change dramatically once the building is cleaned and all distress is visible. The accumulation of dirt will also contribute to the deterioration of the facade if the dirt forms an impervious layer on the exposed surface. Selection of an appropriate cleaning technique as well as the timing of the cleaning must be considered to achieve the desired information and not damaging the masonry or collateral damage associated with excessive water infiltration.

The actual inspection should include some level of non-destructive evaluation. The extent and scope will depend on the professional's discretion, based on the facade system and the level of distress observed. Simple non-destructive techniques can include sounding with a hammer. Sounding is an effective technique for determining delaminated areas of materials such as concrete, masonry, terra cotta and stone. Delaminated areas will create a dull thud sound when struck with a hammer while non-delaminated areas will create a ringing sound. The type of hammer used should be carefully considered to achieve the desired intent, while not damaging facade materials. Steel masons' hammers are very effective in evaluating concrete and some masonry facades, but can be damaging if fragile materials are hit too hard. Acrylic and leather hammers can also be an effective alternative to steel hammers if the material being sounded is susceptible to damage. Rubber mallets are effective for larger thin panels. The rubber mallet can be used to cause entire panels to oscillate or move without damage.

Checking the plumbness of portions of a facade is another effective method of evaluating the condition of a facade. Localized displacements can be easily determined using a 4-foot (1.2 m) or shorter level if appropriate (Figure 11). Modifications can be made to a level or other straight edge to determine localized bowing of a panel. By raising the ends of straight edge a fixed distance, the displacement between the raised ends can be determined by measuring the difference between the ends and the midpoint. Alternatively, displacements of panels can be determined using a straight edge set on the joint between panels. For larger areas of walls, a plumb-bob can be used. Horizontal displacements can be determined by using a string line.

Since corrosion of embedded steel is perhaps the most common cause of distress in masonry cladding systems, the specific location of steel can be determined using a metal detector. Typically, gravity support in masonry systems is provided by a continuous shelf angle that is anchored to the perimeter spandrel beams. Examination of the facade will usually provide an indication of the location of the shelf angle if drawings are not available. A metal detector can be very useful in finding discrete anchors, such as lateral anchorage within a masonry system (Figure 12). Care should be taken, however in the interpretation of metal detector readings since extraneous positive readings can be quite common, depending on the sensitivity of the equipment, experience of the user, and the facade and related components of the system.

Other more sophisticated techniques such as thermography, nuclear moisture and x-ray inspections can also be used to determine potential areas of distress. Impact-echo can find voids and discontinuities at specific areas of a wall system. The skill of the data interpreter, as well as verification of the findings, are critical to attaining useful data.

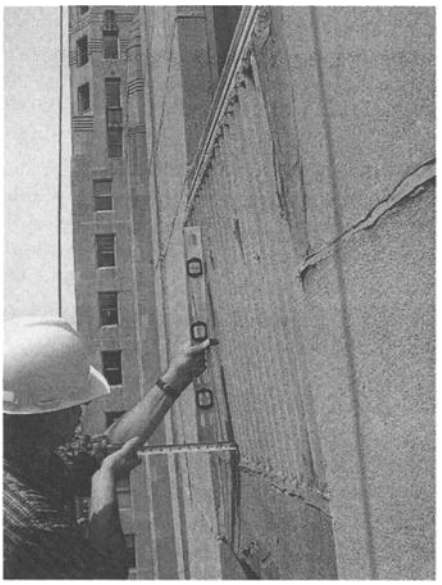

Figure 11 – *Checking plumbness of limestone panel*

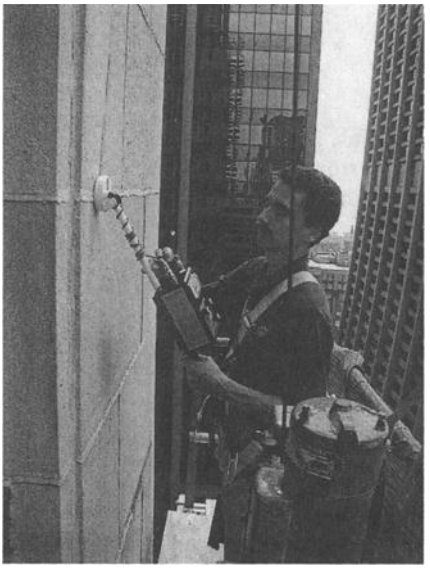

Figure 12 – *Using a metal detector to find embedded steel*

An alternative method of evaluating the underlying conditions of a facade is through inspection probes. The size of the opening can vary depending on the goal of the probe. Drilling a small diameter hole and inserting a fiber optic boroscope can be an effective method of evaluating facades that incorporate a cavity. Inspection of the cavity can provide an indication of the condition of the visible portions of lateral anchors, flashings and mortar bridging and other conditions within the cavity.

For many systems, such as solid masonry walls, larger openings are required to evaluate concealed conditions. The location and extent of the opening should be carefully considered to maximize potential information without creating excessively large openings. Material removed should be saved for physical and compositional testing that may be necessary to perform effective subsequent repairs.

Conclusion

At the most basic level, facade deterioration is the result of moisture, temperature fluctuation and gravity. Knowledge of facade systems is critical to understanding how the systems may fail, but it must also be recognized that a building's history and context can also provide valuable insight.

Even with a very thorough inspection of a facade system, all defects may not be detected. Hidden conditions cannot always be found even with extreme diligence on the part of the inspector. Given the restraints of cost, time, and practicality, it is unreasonable to expect all hidden conditions to be detected. Generally, serious conditions will manifest themselves prior to failure, but unforeseen occurrences and circumstances both natural and human remain a factor.

References

[1] Scheffler, M. J. and Gerns, E. A. "**Thin Stone Veneer; Twentieth-Century Building Materials; History and Conservation**," edited by Thomas Jester, National Park Service, McGraw-Hill, Inc. New York, NY, 1995, pp. 170-171.

[2] Beall, C., "**Masonry Design and Detailing for Architects, Engineers, and Contractors**," McGraw-Hill, Inc. New York, NY, 1993, p. 225.

[3] Schueller, W., "**The Vertical Building Structure**," Van Nostrand Reinhold, New York, NY, 1990, p. 219.

[4] Harris, S., "**Building Pathology; Deterioration, Diagnostics and Intervention**," John Wiley and Sons, Inc. New York, NY, 2001, pp. 285-286.

Into the 21st Century

Clayford T. Grimm, P. E.[1]

Air Barriers for Masonry Walls

REFERENCE: Grimm, C. T., **"Air Barriers for Masonry Walls,"** *Masonry Opportunities for the 21st Century, ASTM STP 1432*, D. Throop and R. E. Klingner, Eds., ASTM International, West Conshohocken, PA 2002.

ABSTRACT: This paper discusses prevention of interstitial condensation in masonry walls due to infiltration of warm moist air into air-conditioned buildings in summer and exfiltration of warm moist air in winter. The following aspects of the problem are discussed: air pressure differentials due to wind, stack effect, and mechanical ventilation; air leakage, modes, and test methods; climate effects; air barriers, insulation materials, and their placement in cavity walls, veneer walls, and single wythe walls; methods for sealing cracks and joints; and building code requirements. Thirty-one references are cited.

KEYWORDS: adhesive, air barrier, air leakage, air pressure, building code, cavity wall, climate, condensation, crack, exfiltration, infiltration, insulation, joint, masonry, mold, moisture, screw anchor, sealant, sealing tape, single wythe wall, stack effect, testing, vapor retarder, veneer wall

Introduction

Leaky walls admit wind driven rain, but they also transmit warm moist air from the exterior or interior. Condensation of that moisture can be just as damaging as wind driven rain. When water permeates a wall, freeze-thaw fractures, cracks occurs, efflorescence blooms, walls stain, insulation fails, materials swell, wood warps, gypsum decays, metals corrode, paint peels, mold grows, mildew forms, and odors reek. More importantly, mold and mildew can impair human health.

Water enters masonry walls due to wind driven rain, rising damp, and condensation. Grimm [1] provides a review of the literature with 282 citations on water permeance in masonry due to wind driven rain. Several authors discuss prevention of rising damp [2,3].

[1] Clayford T. Grimm, PE, Consulting Architectural Engineer, 1904 Wooten Drive, Austin, TX 78757-7702, ctgpeinc@uts.cc.utexas.edu

Condensation may result from air transmission through walls by diffusion or convection. The design of vapor retarders to limit diffusion is well described in the literature [4, 5]. However, without effective control of airflow, vapor retarders are completely ineffective [6].

Air barriers can prevent convection and damage due to condensation of air born water vapor. Air barriers can also substantially reduce heating and air-conditioning costs. Walls may account for as much as 50% of air leakage in residential buildings [6]. In an improperly designed or constructed building, air leakage can account for as much as 80% of the total energy load [7]. Although infiltration can account for a large portion of heating and cooling costs, those costs are beyond the scope of this paper. This discussion focuses on air barriers to prevent interstitial condensation of water vapor transmission through masonry walls by convection.

In 1990 alone interstitial condensation caused $68 million in mold and mildew damage in hotel-motel buildings [8]. In 1991 all the brick veneer was removed from a hotel in Charleston, SC, due to mold growth caused by condensation of infiltrating warm moist air. In 1982 all brick masonry was removed from the façade of a large hospital in Sioux City, IA, because warm moist interior air condensed in the masonry and froze [9]. Quirouette reports spalling of concrete masonry caused by freezing of moist air from the interior [10].

In winter as warm moist air moves outward through the wall, it becomes colder, and its humidity rises. In summer as warm moist air moves inward toward air-conditioned space, it becomes cooler, and its humidity rises. If air becomes cold enough to raise the humidity to 100%, condensation occurs. An air barrier placed on the warm side of the wall can prevent air from reaching a point cold enough to cause condensation.

Air Pressure Differential

Wind, stack effect, and mechanical ventilation can create a difference in air pressure to force moist air through a wall by convection.

Exterior air pressure is increased on the windward side of a building and reduced on the leeward side and the sides parallel to wind [11]. Wind pressure or suction may be well over 30 psf (1.44 kPa). In winter warm air rises in tall buildings, creating a stack effect that causes decompression of air in the lower stories and compression in the upper stories [12]. Pressure difference due to stack effect in tall buildings may be about 3 psf (144 Pa).

Interior air pressure may be increased by mechanical ventilation or reduced by exhaust fans. In a home when bedroom doors are closed, mechanical air supply pressurizes the room, especially with a minimum return air system. That condition can lead to significant decompression in other areas of a house. In hot-humid climates, mechanically induced positive air pressure should be maintained on the interior by air supply 10 to 20 % in excess of exhaust. Even with positive interior air pressure, wind can induce air from the exterior. Pressure differences due to mechanical equipment are small, highly variable, and unpredictable

In tall buildings the phenomena of wind, mechanical draft, and stack effect may combine to create a significant pressure differential across exterior walls, perhaps as much as 40-psf (2 kPa) acting inward or outward.

Air Leakage

Air under pressure passes readily through cracks in masonry caused by: changes in temperature, moisture, or stress, incompatibility of materials, vibration, metal corrosion, deflection of supporting structure, void mortar joints, or unsealed construction joints. Table 1 provides a list of common thermal defects in exterior walls. Figures 1, 2, and 3 illustrate some typical air leakage paths.

Air barrier membranes are available in sheet form in a variety of materials: liquid applied rubber copolymers; "peal-and-stick" self-adhesive rubberized asphalt, EPDM, ethylene-propylene diene monomer, and elastomeric bitumen. Hildebrand [13] reports on a battery of tests conducted for the Canadian Mortgage and Housing Corporation to evaluate the performance of seventeen commercially available, air barrier membranes applied to concrete masonry walls. Table 2 provides air and vapor permeance data for some common building materials.

Quirouette [14] provides a steady state example to demonstrate that air leakage by convection transfers more than 200 times the amount of water transferred by vapor diffusion. However, traditional calculation methods cannot predict the amount of condensation, because exterior and interior air and vapor pressures are constantly changing. The problem becomes so complex as to make a solution impractical [15]. Yet, the Building Technology Center at the Oak Ridge National Laboratory has developed a computer program that can assess:

- drying time of masonry with trapped construction moisture,
- danger of interstitial condensation,
- influence of driving rain on exterior building components,
- effect of repair and retrofit measures, and
- hygrothermal performance of roof and wall assemblies under unanticipated use or in different climatic regions.

For a complete description of the computer program go to:
http://www.ornl.gov/ornl/btc/moisture/index.html

Climatic Effects

In winter when interior air at 70°F (21.1°C) and 50% RH (relative humidity) is cooled to 50°F (10°C), its RH increases to 100%, and condensation occurs. During summer in many parts of the United States the climate is hot and humid. In summer when the sun drives water vapor inward by diffusion or warm moist air is forced inward by convection

toward an air-conditioned space, its ability to hold water diminishes and its RH increases. If air at 85°F (29.4°C) and 90% RH is cooled just three degrees to 82°F (27.8°C), its RH increases to 100% and condensation occurs. The purpose of an air barrier is to prevent the air from reaching a point in the wall cool enough to cause precipitation.

Table 1 - *Summary of thermal defect* [16].

Thermal Bridges	Structural elements, component connections, envelope penetrations
Insulation Defects	Discontinuity in insulation system design, voids and gaps, unsupported insulation, compression by fasteners and other elements, fibrous insulation exposed to air spaces, poorly fitted batt insulation
Wall Assemblies	Airflow passages within the envelope and poor material selection or attachment. See Figs. 1, 2, and 3.
Concrete Masonry	Air leakage through blocks and mortar joints, air seal to spandrel beams and columns, and upward air movement through concrete masonry units
Air Barriers and Sealants	Discontinuity of air barriers, use of insulation or insulation adhesives as air barriers, punctured or displaced air barriers, inadequate support and lack of continuity for polyethylene, and sealant failure due to differential movement
Unsealed Component Interfaces	Floor/wall, window/wall, wall/roof, wall/wall, wall/ceiling, and column/wall
Other Assemblies	Overhangs, soffits, stairwells, and interior partitions

Masonry is hygroscopic. That is, its moisture content varies widely with environmental humidity. For example, a standard modular brick measuring 3.63 x 2.25 x 7.63 in. (92.2 x 57.2 x 193.7 mm) having a density of 105 lb/ft^3 (1680 kg/m^3) at 100% RH may contain 0.6 oz (18 cc) of water. When saturated that brick may contain 3.5 oz (108 cc) of water.

In a hot-humid climate in an air-conditioned building, if a vapor retarder is placed on or near the interior wall surface and there is no air barrier to prevent inward air movement, condensate may form immediately behind the vapor retarder. If wallboard behind interior vinyl wall covering becomes moist, mold growth may flourish. The smell may make human occupancy intolerable, causing evacuation of property. If interior vinyl wall covering is used in warm climates, an air barrier should be placed on the outside of the insulation.

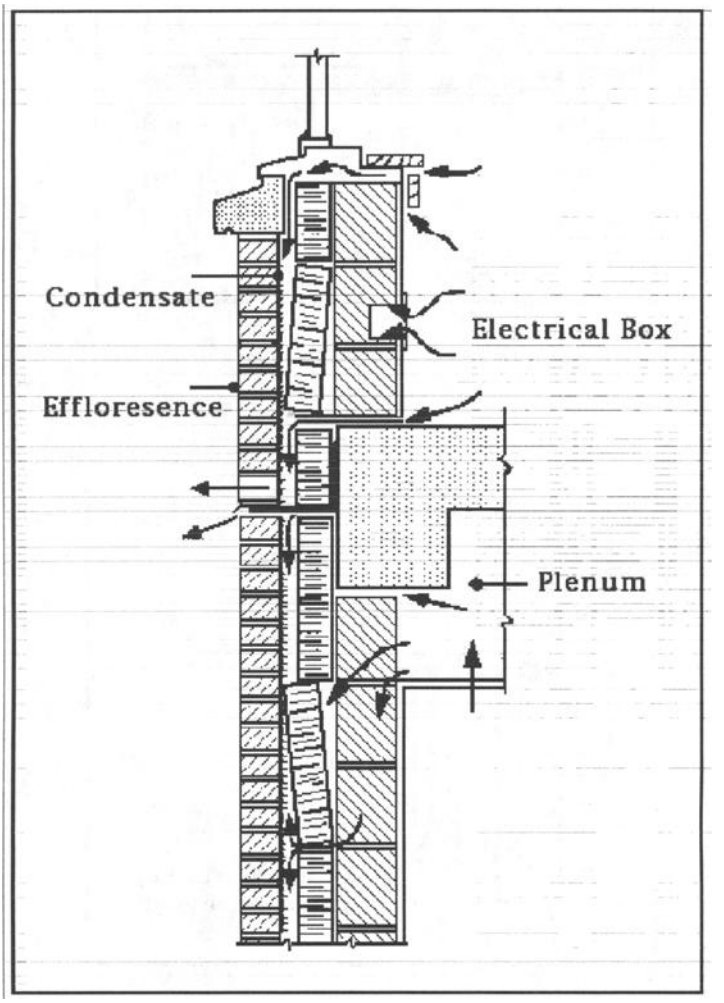

Figure 1 - *Air exfiltration through exterior wall [17].*

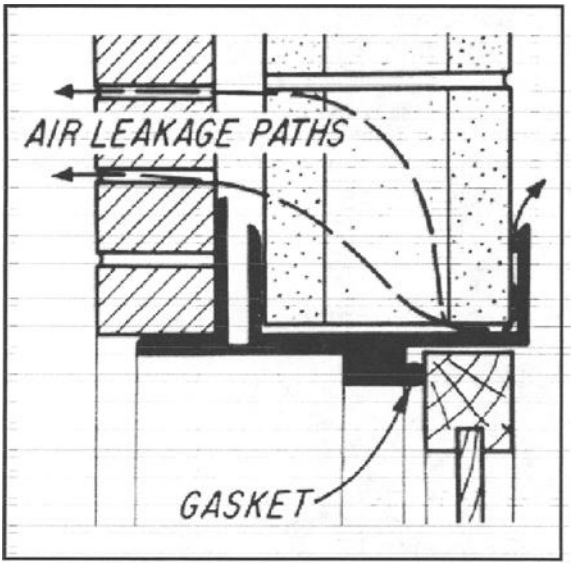

Figure 2 - *Air leakage at lintels [18].*

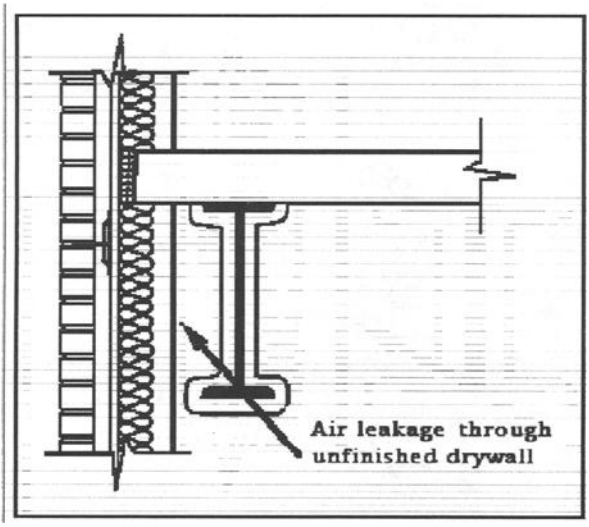

Figure 3 - *Air leakage through unfinished drywall [19].*

Table 2 - *Air and vapor permeance data for some common building materials* [20].

Material	Air Permeance at 1.57 lb/ft^2, ft^3/hr-ft^2	Vapor Permeance Perm gr/h-ft^2-in. Hg
4-in. (102-mm) brick masonry	18.9 [21].	0.8 [6].
8-in. (203-mm) hollow concrete masonry	24.8 [21].	2.4 [6].
1/2-in. (12.7-mm) gypsum board	0.107	24
3/32-in. (2.70-mm) modified bituminous torch on grade membrane (polyester reinforced mat)	0	0.07
3/32-in. (2.70-mm) modified bituminous torch on grade membrane (glass fiber mat)	0	0.07
1/16-in. (1.50-mm) modified bituminous sell adhesive membrane	0	0.03
15-1b. (6.8-kg) non-perforated asphalt felt	3.19	5.57
1.5-in. (38.0-mm) extruded polystyrene	0	0.26-1.04
1-in. (25.4-mm) phenolic insulation board	0	2.31
2-in. (50.8-mm) phenolic insulation board	0	1.17
Glass fiber rigid insulation board with spunbonded polyolefin film on one face	5.76	19.9
6-in. (152-min) glass fiber wool insulation	433	19.3
Vermiculite insulation	832	29

1 Pa = 0.0209 lb/sq ft
1 lb/ft^2 = 47.8803 Pa
1 L/(s – m^2) = 11.8 ft^3/hr-ft^2
1 ft^3/hr-ft^2 = 0.0847 L/(s – m^2)
1 ng/(Pa - s – m^2) = 0.0174 gr/h-ft^2-in. Hg
1 gr/h-ft^2-in. Hg = 1 perm = 57.4525 ng/(Pa s – m^2)

Achenbach provides an example of interstitial condensation [22].

> "Air-conditioned buildings constructed of masonry blocks and finished with furring strips, insulation, vapor retarder between furring strips, and plasterboard interior frequently experience condensation on the back of the vapor retarder and softening of the plasterboard interior in humid and rainy climates. Even though the masonry block is painted, expansion and contraction can cause many hairline cracks in the painted surface. During heavy rains, water is absorbed into the cracks and is stored in the masonry block. Subsequent solar radiation drives the water vapor inward to condense on the vapor retarder and to be transferred through the furring strips to the plasterboard, causing it to soften and discolor. Enough solar heat can be stored in the masonry blocks during the day to continue vapor

transfer to the vapor retarder and the plasterboard throughout the night. A surface coating on the masonry block that retains sufficient elasticity to avoid cracking under the temperature changes to which it is exposed would alleviate this problem. A saturated sheathing paper installed between the masonry block and the insulation would also protect the insulation and the interior plasterboard."

Air Barrier Systems

An air barrier system is a continuous and durable network of materials and joints providing air tightness with adequate strength and stiffness to prevent excessive deflection under air pressure differences. An air barrier system requires continuity at connections: 1. joints between sheets of the air barrier membrane; 2. interfaces between walls and wall openings; 3. intersections between exterior walls and interior walls and floors; and 4. cracks at wall penetrations.

A correctly installed air barrier membrane of low vapor permeance may serve both as a vapor retarder and an air barrier, giving rise to the term "air/vapor barrier". Although a material may serve both functions, the two are quite different and should not be confused. The Construction Science Research Foundation, Inc. in Baltimore, MD, provides architectural guide specifications for Air Barriers in Section 7270 and Vapor Retarders in Section 07260 (http://www.spectext.com). The National Technical Information Service in Springfield, VA lists eight references on air barriers published since 1989 (http://neptune.fedworld.gov/cgi-bin/waisgate).

Air Barrier Placement

Air barriers must be continuous, durable, impermeable, and structurally capable of sustaining the anticipated air pressure differential. Every effort should be made to ensure as tight an enclosure as possible. However, it is practically impossible to seal completely the entire building envelope, although every effort should be made to do so. Not all cracks can be sealed to insure absolute air tightness. Specifications that simply require a continuous air barrier are not likely to achieve that effect in actual construction. Because it may be impossible to anticipate every airflow path, craftsmen should be encouraged to understand the importance of the problem and to make on site suggestions for practical sealing solutions [23].

The three primary types of masonry walls in which air barriers are placed include cavity walls, masonry veneer walls, and single wythe walls. All of those have metal anchors, ties, and fasteners that cause thermal bridges. In winter connectors provide cool interior surfaces on which exfiltrating warm moist air can condense. In summer infiltrating warm moist air can condense on metal ties cooled by interior air-conditioning [24]. For that reason and because of the permeance of masonry to wind driven rain,

corrosion protection for metal connectors in masonry often necessitates use of stainless steel connectors [25].

Table 3 provides recommendations for the position of air/vapor barriers and insulation in masonry cavity, veneer, and single wythe walls in hot and cold climates. Those recommendations depend on climatic regions. (See Figure 4).

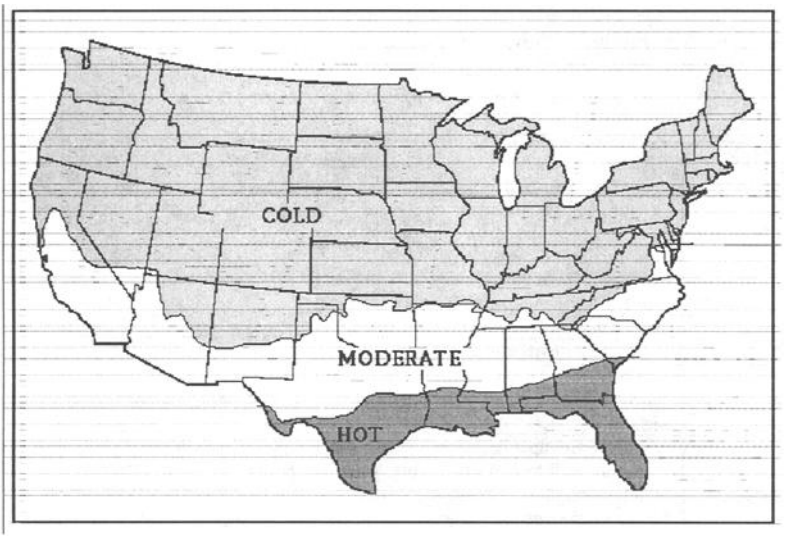

Figure 4 –*Recommended United States climatic regions*

Cold climates are here defined as having more than 4000 annual heating degree-days. Hot climates are here defined as having less than 2200 annual heating degree-days. Moderate climates are here defined as having more than 2200 annual heating degree-days but fewer than 4000. Air/vapor barriers are not usually necessary in moderate climates with two exceptions. They are recommended on the warm side of the wall in air-conditioned buildings within 50 mi. (80.5 km) of the Atlantic coast south of Cape Hatteras and in buildings with refrigeration or other cold occupancies.

For any one 24-hour day, the number of heating degree-days is the difference between 65°F (18.3°C) and the mean outdoor temperature for that day. The number of annual heating degree-days is the sum of those values for a year. The number of annual heating degree-days can be found for each of 284 United States cities in *Local Climatological Data – Annual Summary with Comparative Data*, National Climatic Data Center, Ashville, NC.

In cavity walls location of the air barrier as indicated in Table 3 should prevent exfiltration or infiltration of warm moist air from reaching a point in the wall cold enough to cause condensation. However, location of the air barrier on the exterior face of the interior wythe has the disadvantage of perforation by wall ties and inability of inspection to ensure that all holes are sealed. Harper and Colonna describe the design and construction of continuous air barriers in a building with masonry cavity walls [26].

In veneer and single wythe walls in cold climates an air barrier may be located on the interior face of the wall where it can serve also as a vapor retarder. That location facilitates inspection. However, care must be taken to ensure proper installation behind cabinets, pipes, and equipment; in plenum spaces; and at intersecting partitions.

Care must be taken to ensure that materials to be joined as part of the air barrier system are compatible. Asphalt-based materials are incompatible with polyvinyl chloride, polyethylene, and polystyrene. Manufacturers should be consulted regarding compatibility of their products with other materials.

Table 3 - *Recommended position of air/vapor barriers and insulation.*[a]

Wall Type	Climatic Region	
	Hot	Cold
Cavity	Place air/vapor barrier on exterior face of interior masonry wythe. Place insulation in the core/cells of hollow masonry units in the interior wythe and/or between furring on the interior face of the interior masonry wythe.	Place air/vapor barrier behind board insulation on exterior face of interior masonry wythe. See Figure 5.
Veneer	Place air barrier on exterior face of sheathing, Place insulation between studs, and vapor retarder at or near the interior surface.	Place insulation between studs, and place air/vapor barrier at or near the interior surface.
Single wythe	Place air/vapor barrier behind stucco at exterior wall face. Insulate cores/cells of hollow masonry units and/or between furring on the interior surface.	Insulate cores/cells of hollow masonry units and/or between furring on the interior surface. Place air/vapor barrier on the interior surface.

a Note: In all buildings with low interior design temperatures, for example cold storage or ice rinks, place the air barrier and vapor retarder on the exterior side of the insulation.

Seals

Four types of joint seals are necessary in an air barrier system:

a joints in air barrier sheets applied to the exterior face of the interior masonry wythe or to sheathing over a frame structure;
a. joints between air barrier sheets and other construction elements;
b. joints between insulation boards; and
c. joints in the wall interior surface.

Some have said that one should to able to trace a line of air tightness completely around a building drawing in plan or section without lifting the pencil. Exterior walls with no interior finish above suspended ceilings offer an opportunity for increased exfiltration, especially when that plenum space is used for air supply. See Figure 3. Points of air leakage in and around exterior walls include:

- Σ joints at intersections of interior and exterior walls,
- Σ joints at the top of walls,
- Σ joints between ceiling and wall,
- Σ interior cracks between walls and windows or doors,
- Σ unsealed electrical outlets, pipe sleeves and ducts,
- Σ cracks at pluming fixtures, and
- Σ cracks at recessed light fixtures in ceilings.

Holes, open joints, and other voids should be filled with mortar. The substrate for air barrier sheets, tapes, and sealants should be free of surface dirt, irregularities, holes, and joints that cannot be bridged. Air barrier penetrations by wall ties should be sealed with mastic. Practical details should be developed that recognize the location of leakage paths.

Joints between peal-and-stick air barrier sheets are usually lapped and self sealed. Elastic peal-and-stick tapes seal joints between air barrier sheets and other construction elements such a windows and doors. The tapes are air and moisture resistant and measure 4 in. (101.6 mm) to 12 in. (304.8 mm) in width. Concealed air seals between masonry walls and structural frames must be sufficiently durable to accommodate differential movement over the life of the building.

Joints in board insulation are typically sealed with tape about 2 in. (51 mm) wide formed of acrylic adhesive with polypropylene backing. Tapes act as a vapor retarder and air barrier. Both tapes and sealants seal joints and cracks on the wall interior. Fire stop materials at wall perforations can also provide an air barrier. The web site http://www.oikos.com/library/airsealing/materials.html lists the relative merits of: sealants, adhesives, foams, gaskets, and sheets.

The materials, design, construction, specifications, and maintenance of sealant joints are well described in *Sealants: The Professionals' Guide* [27]. ASTM Specification for Elastomeric Sealants (C 920) provides classifications for various properties of joint sealants and identifies the relevant ASTM test methods. ASTM Guide for Use of Joint Sealants (C 1193) provides design criteria. Guide specifications for joint sealants are provided by the Construction Sciences Research Foundation in *Spectext* Section 7900 (http://www.spectext.com) and the United Facilities Guide Specifications 07920 (http://www.ccb.org/html/home.html).

Insulation

Foamed-in-place plastic, plastic inserts, and loose fill insulations are used to fill cells in single wythe walls of hollow masonry units. Rigid boards insulation is placed in wall cavities and on interior wall surfaces. A drainage mat on the cavity face of board insulation can drain mortar-clogged cavities.

Board insulations may be extruded or molded polystyrene (ASTM Specification for Rigid, Cellular Polystyrene Thermal Insulation (C578)) or polyisocyanurate (ASTM Specification for Faced Rigid Cellular Polyisocyanurate Thermal Insulation Board (C 1289)). Boards are usually 1 in. (25.4 mm) to 2 in. (50.8 mm) thick and are cut or kerfed to fit between metal ties in cavity walls. In those walls in cold climates boards are

attached to the air barrier on the exterior face of the interior wythe. In single wythe walls insulation boards may be attached to a wall's interior surface. The boards may be held in place by stainless steel screws with large plastic washers.

When adhesives are used to attach board insulation to masonry walls, the masonry should be pargeted to provide a smooth surface. A full bed of adhesive, conforming to ASTM Specification for Adhesives for Fastening Gypsum Wallboard to Wood Framing (C 557), should be fully troweled to within 1 in. (25 mm) of each edge on clean and dry boards using a 1/4 in. (6 mm) deep, notched trowel. Other methods such as spot daubs or beads should not be used, because they allow air to circulate behind the insulation, reducing insulation effectiveness. Insure that the adhesive is compatible with the air barrier. Synthetic rubber adhesives may not be compatible with EPDM (ethylene-propylene diene monomer) flashing. Some adhesives are highly flammable and give off noxious vapor. Following instructions on the Material Safety Data Sheet is especially important. After adhesive application, the board is positioned on the wall and pressed firmly over the entire surface. Joints between boards should be staggered and tightly butted.

When board insulation has a reflective foil surface facing an air space in a well-insulated wall, the foil may have very little effect on the wall thermal resistance [28]. Furthermore, the corrosive effects of mortar on aluminum are well known. For these reasons reflective foil on board insulation is of dubious value.

The air space between board insulation and the exterior wythe in a cavity wall, as shown in Figure 5, can be vented to provide a rain screen to reduce penetration of wind driven rain [29]. A vented air space should not be continuous from floor to floor to avoid excessive vertical air currents. Venting of the cavity causes air suction that tends to dislodge insulation from the interior wythe. Displacement permits air currents behind the insulation that increase heat transmission and may damage the air barrier.

Batt insulation with vapor retarder is placed between studs in masonry veneer walls and may be placed between interior furring strips in single wythe walls.

Testing Air Leakage

ASTM Practices for Air Leakage Site Detection in Building Envelopes and Air Retarder Systems (E 1186) describes standardized techniques for locating air leakage and offers a choice of methods with each method offering certain advantages. Some of the techniques require knowledge of infrared scanning, building pressurization or depressurization; smoke generation techniques, sound generation and detection, and tracer gas concentration measurement techniques. The methods described are of a qualitative nature rather than determining quantitative leakage rates.

ASTM Test Method for Determining Air Leakage Rate by Fan Pressurization (E779) describes a standardized technique for measuring air-leakage rates through a building envelope under controlled pressurization and de-pressurization.

ASTM Test Methods for Determining Air Tightness of Buildings Using an Orifice Blower Door (E1827) describes two techniques for measuring air leakage rates through a building envelope in buildings that may be configured to a single zone. Both techniques

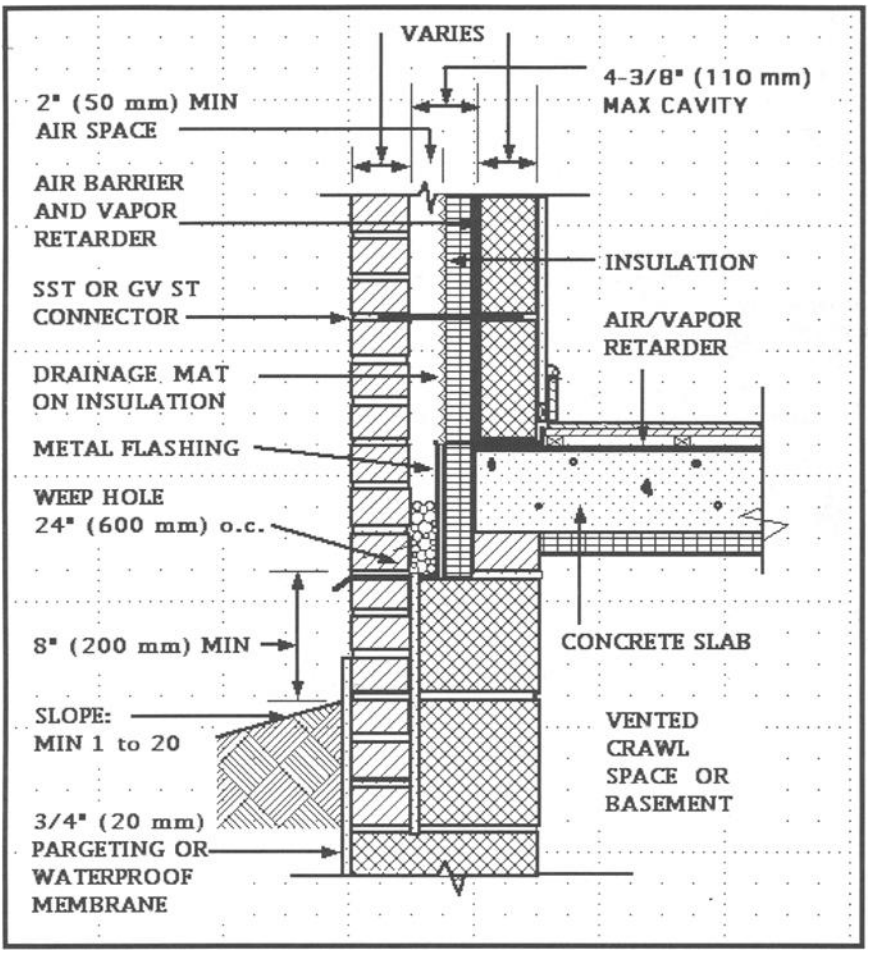

Figure 5 - *Vapor/air barrier in masonry cavity wall*

use an orifice blower door to induce pressure differences across the building envelope and to measure those pressure differences and the resulting airflows. The measurements of pressure differences and airflows are used to determine air tightness and other leakage characteristics of the envelope.

Those test methods are applicable to small indoor-outdoor temperature differentials and low wind pressure conditions.

Building Code Requirements

Section 1403.3 of the *International Building Code* [30] requires an interior vapor retarder in exterior walls, but specifically excludes masonry single wythe walls, composite walls, and cavity walls designed in accordance with Chapter 21. However, that code does not exclude and, therefore, can be interpreted as requiring a vapor retarder for veneer walls designed in accordance with Section 1505.5. This potential inconsistency should be resolved.

Occupants and buildings can be adversely affected by the absence of a vapor retarder and an air barrier in building walls in many parts of the United States, whether or not the exterior masonry wythe is in a cavity wall or a veneer wall. More over a vapor retarded in the interior of a veneer wall in a hot-humid climate can be damaging.

The National Building Code of Canada requires both a vapor retarder and an air barrier in all walls, except where an analysis shows that safety of building and health of its occupants will not be adversely affected [31].

Conclusions

In winter, as warm moist air moves outward through walls, it becomes colder, and its humidity rises. In summer, as warm moist air moves inward toward air-conditioned space, it becomes cooler, and its humidity rises. Frequently air becomes cold enough to raise the humidity to 100% and condensation occurs. Free water in the wall can cause efflorescence, stains, corrosion, cracks, warps, decay, rot, insulation inefficiency, mold, odor, loss of rental income, and health hazard. An air barrier placed on the warm side of the wall can prevent air from reaching a point cold enough to cause interstitial condensation that causes millions of dollars of damage each year in the United States.

References:

[1]. Grimm, Clayford T.: "Water Permeance of Masonry Walls: A Review of the Literature," *Masonry: Materials, Properties, and Performance*, ASTM STP 778, ASTM International, West Conshohocken, PA, 1982, pp. 178-199.

[2]. Heiman, J. L.: "An Evaluation of Methods of Treating Rising Damp," *Moisture Mitigation in Buildings*, ASTM STP 779, ASTM International, West Conshohocken, PA, 1982, pp. 121-137.

[3]. Ashurst, John and Nicola Ashurst: *Practical Building Conservation-Brick, Terracotta, and Earth*, Halsted Press, New York, NY, 1988, pp. 2-9.

[4]. "Condensation Control in Concrete Masonry Walls," *NCMA TEK*, No. 6-17A, National Concrete Masonry Association, Herndon, VA, 2000.

[5]. "Moisture Resistance in Brick Masonry Walls – Condensation Analysis," *Technical Notes on Brick Construction*, No. 7D, Brick Institute of America, Reston, VA, May 1988.
[6]. *ASHRAE Handbook of Fundamentals*, American Society of Heating, Refrigerating, and Air Conditioning Engineers, Inc., Atlanta, GA, 2001, pp. 23.15 and 26.13.
[7]. Diuigi, James A.: "Architectural Design," *Mold and Mildew in Hotel and Motel Guest Rooms in Hot and Humid Climates*, The Hospitality Lodging & Travel Research Foundation, Washington, DC, 1991, pp. 32.
[8]. Boelens, Theodore: "Introduction," *Mold and Mildew in Hotel and Motel Guestrooms in Hot and Humid Climates*, The Hospitality Lodging & Travel Research Roundation, Washington, DC, 1991, pp. 1-4.
[9]. Lotz, William A.: "Vapor Barriers in Masonry Construction", *Masonry Construction*, Addison, IL, October 1991, pp. 403-404.
[10]. Quirouette, Richard L.: "Technics: Air and Vapor Barriers," *Progressive Architecture*, New York, NY, September 1991, pp. 45-51.
[11]. *Minimum Design Loads for Buildings and Other Structures*, ASCE 7-98, American Society of Civil Engineers, Reston, VA, 1998.
[12]. Wilson, A. G. and G. T. Tamura: "Stack Effect in Buildings", *Canadian Building Digest*, National Research Council of Canada, Ottawa, Ontario, CBD-104, 1968.
[13]. Hildebrand, G.: *Development of Test Procedures and Methods to Evaluate Air Barrier Membranes for Masonry Walls*, Canada Mortgage and Housing Corporation, Ottawa, Ontario, Nov. 2, 1990.
[14]. Quirouette, Richard L.: "Difference between a Vapor Barrier and an Air Barrier," *Building Practice Note*, No. 54, National Research Council of Canada, Ottawa, Ontario, 1985.
[15]. Kudder, Robert J. and Kurt R. Hoigard: "Vapor Control and Psychrometric Monitoring in Exterior Walls," *Water in Exterior Building Walls: Problems and Solutions*, ASTM STP 1107, ASTM International, West Conshohocken, PA, 1991, pp. 124-137.
[16]. Persily, Andrew K.: *Development of Thermal Envelope Design Guidelines for Federal Office Buildings*, National Institute of Standards and Technology, Gaithgersburg, MD, October 1990, pp. 9.
[17]. Drysdale, R. G. and G. T. Suter: *Exterior Wall Construction in High-Rise Buildings*, Canadian Mortgage and Housing Corporation, Ottawa, Ontario, 1991.
[18]. Garden, G. K.: "Control of Air Leakage Is Important," *Canadian Building Digest*, National Research Council of Canada, Ottawa, Ontario, CBC-72, December 1965.
[19]. Kudder, Robert J. and Kurt R. Hoigard: "Construction Details Affecting Wall Condensation," *Symposium on Air Infiltration, Ventilation and Moisture Transfer*, Building Thermal Envelope Coordinating Council, Washington, DC, 1988.
[20]. Hershfield, Morrison: *Air Barrier Systems for Walls of Low-Rise Buildings: Performance and Assessment*, Institute for Research in Construction, National Research Council of Canada, Ottawa, Ontario, March 1997, pp. 20.
[21]. Lux, M. E. and W., C. Brown: "Air Leakage Control", *Building Science Insight*, National Research Council of Canada, Ottawa, Ontario, 1986.
[22]. Achenbach, Paul R. "General Construction Principles," *Moisture Control in Buildings*, ASTM International, West Conshohocken, PA, 1994, pp. 285.

[23]. Handegord, G. O.: "Air Leakage, Ventilation, and Moisture Control in Buildings," *Moisture Mitigation in Buildings*, ASTM STP 779, ASTM International, West Conshohocken, PA, 1982, pp. 223-233.
[24]. Tuluca, Adrian: "Thermal Bridges in Buildings," *The Construction Specifier*, Construction Specifications Institute, Alexandria, VA, October 1996, pp. 38-46.
[25]. Grimm, Clayford T.: *Recommended Metal Connectors for Clay Brick and Concrete Masonry: Anchors, Ties, and Fasteners*, The Masonry Society, Boulder, CO, in publication
[26]. Harper, R. J. and J. A. Colonna: "Design and Construction of a Continuous Air Barrier in Masonry Cavity Wall Construction," *Proceedings of the 4th Canadian Masonry Symposium*, University of New Brunswick, Fredericton, NB, Vol. 1,1986. pp. 188-202.
[27]. *Sealants: The Professionals' Guide*, Sealant, Waterproofing & Restoration Institute, Kansas City, MO, 1995.
[28]. Contreras, A. G. and A. J. Palfey: "Thermal Resistance of Insulated Brick Veneer Walls with Reflective and Non-reflective Air Spaces," *Thermal Insulation, Materials, and Systems for Energy Conservation in the '80s*, ASTM STP 789, ASTM International, West Conshohocken, PA, 1983, pp. 373-383.
[29]. "Brick Masonry Rain Screen Walls," *Technical Notes on Brick Construction*, No. 27, Brick Institute of America, Reston, VA, May 1994.
[30]. "Vapor Retarder", *International Building Code*, Section 1403.3, International Code Council, Inc., International Conference of Building Officials, Whittier, CA, 2000, pp. 266.
[31]. *National Building Code of Canada*, National Research Council of Canada, Ottawa, Ontario, Sections 5.4, 5.5, 9.25.3, and 9.25.4, 1995.

DISCUSSION

Lynn R. Lauersdorf[1] *(written discussion)*—(1) The vast difference between a barrier to air leakage and a barrier to vapor diffusion should not lead to "vapor confusion." Leakage of warm, moisture-laden air is usually much more destructive to the integrity of an exterior wall system than is vapor transmission. In fact, leakage of interior air into exterior walls in northern climates during the winter is a leading cause of exterior wall problems.

The amount of interior moisture passing through a typical square foot of finished exterior wall is insignificant when compared with the moisture passing through minor penetrations, separations or even hairline cracks in the primary air barrier for the exterior wall. The amount of moisture passing through one square unit of foil-backed gypsum board was calculated. When the foil backing from that one square unit was removed, the calculated moisture passing through by vapor diffusion increased by a factor of 15 to 500, depending upon the type and number of paint coats applied. When the gypsum board, paper facing and applied paint were removed from that same one square unit, the calculated moisture (worst case) now passing through by air leakage increased by a factor of 5,000,000 over what originally passed through by vapor diffusion. This equates to 40 gallons of water transmitted by air leakage for every drop of water diffusing a given unit area over time.

Development of practical details is essential. Quite commonly, the devil is in the details. An example of this is the use of fiberglass shown in drawing details as the termination for an air barrier.

The *International Building Code* (IBC) does not currently address air leakage or the real problems that may be created from it. Because of this, the Wisconsin State Building Code, which just recently adopted most of the IBC, included a "Wisconsinism" to the code. That modification incorporates the following:

> **ADD TO IBC 202.1 DEFINITIONS**:
>
> **Air Retarder**: A material or combination of materials collectively having maximum air leakage rates of 0.06 cfm/ft.^{2} at 0.30 in. H_2O, when tested in accordance with ASTM E 783, installed to resist air leakage into the exterior envelope.
>
> **ADD TO IBC 1403 EXTERIOR WALL PERFORMANCE REQUIREMENTS**:
>
> **Air Retarder**. An approved durable air retarder shall be provided when a building component or assembly separates interior conditioned space from the exterior. Air retarders shall be located on the interior side of the wall insulation.

[1] State of Wisconsin, P.O. Box 7866, Madison, WI 53707-7866.

Exceptions:

1. Where other approved means to avoid condensation and frost within the wall assembly are provided.
2. Plain and reinforced concrete exterior walls designed and constructed in accordance with Chapter 19.

Note: Although air retarders are to reduce transmission of water vapor by convection (air movement) and vapor retarders are to reduce transmission of water vapor by diffusion, these functions may be combined in a single membrane. In practice, considerably more moisture is transported by convection than by diffusion.

It is extremely important to have this air retarder topic properly addressed and included in the next revision to the IBC.

C. Grimm (author's closure)—(1)Lynn's comments are correct. I have no closure.

Michel Küntz ,[1] Paul Lavallée ,[2] Jean Chevalier, [3] Pierre Riopelle, [4] Martin Goyer[5]

Confirmation of Anomalous Diffusion in Non-saturated Porous Building Materials by a New Capillary Rise Absorption Test

Reference: Küntz, M., Lavallée, P., Chevalier, J., Riopelle, P. and Goyer, M., **"Confirmation of anomalous diffusion in non saturated porous building materials by a new capillary rise absorption test,"** *Masonry: Opportunities for the 21st Century, ASTM STP 1432*, D. Throop and R. E. Klingner, Eds, ASTM International, West Conshohocken, PA, 2003.

Abstract: A new one-dimensional capillary rise absorption test by direct weighing is presented in this note. The motivation is to obtain more accurate cumulative infiltration measurements in order to test the validity of a new theoretical description of the absorption process recently introduced in [1]. While in most of the technical specifications, weighing is generally carried out manually and requires to remove the specimen from water at intervals, the new apparatus allows a continuous automatic weighing of the specimen during water absorption. The typical performance of the experimental set-up is one measure per second with an accuracy of 0.01 g. Preliminary tests were conducted on four specimens of common red fired-clay bricks. The adjacent sides of the specimens were previously sealed with paraffin to prevent water infiltration from lateral faces of the material: this guarantees that the absorption process actually remains unidirectional. Whereas the amount of absorbed water is expected to increase as $t^{1/2}$ (with t the elapsed wetting time) according to the standard unsaturated flow theory, the cumulative infiltration (I) was found to systematically deviate from the simple $t^{1/2}$ relation. It is shown that absorption in brick scales as t^{α} with $0.57 \leq \alpha \leq 0.59$ (i.e. larger than ½), as previously predicted in [1]. This implies that the long-time predictions of both the amount and the penetration depth of absorbed water based on the classical $t^{1/2}$ relation are generally underestimated. Because this may also apply to the many deleterious chemical agents mediated by water, the consequences of water infiltration on the durability of building materials may also be dramatically underestimated. We suggest that the ASTM technical specifications for water absorption measurements should be reexamined at the light of these new results. The experimental procedure should be

[1] Research associate, Department of Physics, UQAM, C.P. 8888 Downtown, Montréal H3C 3P8, Canada.
[2] Professor, Department of Physics, UQAM.
[3] Technical staff, Department of Physics, UQAM.
[4] Technical staff, Department of Physics, UQAM.
[5] MSc student, Department of Physics, UQAM.

improved to increase the number and accuracy of cumulative infiltration data, especially at short times, to allow more reliable estimates of the absorption properties of porous building materials.

Key words: Porous building materials, water absorption, anomalous diffusion, sorptivity.

Introduction

The role of water in the mechanisms of deterioration of porous building materials has been recognized for a long time. Freeze/thaw cycles, leaching and transport of deleterious chemical agents are a few of the many damage processes directly or indirectly mediated by water. Understanding the physical processes which control water movements in porous materials remains a critical issue to get more reliable predictions of the long time behavior of building structures and to eventually improve their durability. Theoretical analysis of water infiltration and propagation of moisture front is based on the standard diffusion equation, derived by application of Fick's law and mass conservation to the invading fluid [2–10]. Application of the diffusion equation to one-dimensional absorption in rigid, macroscopically homogeneous and isotropic materials predicts that the moisture front progresses as $t^{1/2}$, i.e., that the successive moisture fronts scaled to the variable $x/t^{1/2}$ (where t is the elapsed wetting time and x is the direction of propagation) should coincide [6, 8]. A corollary is that the cumulative water absorption (I) is proportional to $t^{1/2}$, i.e., (I) plotted against $t^{1/2}$ should result in a straight line passing through the origin. The constant of proportionality, referred to as the sorptivity (S), is an important derived quantity which reflects the capacity of a given porous material to absorb and transmit water by capillarity [6-7]. Sorptivity is a physically well-defined material property [6, 11] and can be easily measured through capillary rise absorption tests, for instance. It has therefore been systematically used in studies of the absorption properties of porous building materials in the last two decades.

A number of inconsistencies were recently reported in [1] between the predictions of the standard theoretical model of capillary absorption and several available published data, including Nuclear Magnetic Resonance (NMR) data, of one-dimensional infiltration in different common building materials. Evidence that the absorption process actually does not follow the expected $t^{1/2}$ scaling was directly inferred from the cumulative infiltration data: although a plot of (I) as a function of $t^{1/2}$ was generally well fitted by a straight line, this line did not go through the origin and resulted in a negative, meaningless, intercept at t=0. This led us to propose a new diffusion equation for infiltration, based on a modified Fick's law, that predicts a scaling law of the type x/t^{α} in one dimension, with α any real number [1]. The reader is referred to [1] for additional details. Absorption was found to be compatible with the so-called non-Fickian or anomalous diffusion model in the different building materials analysed. The scaling exponent α was systematically larger than ½ and ranged from 0.55 to 0.63, depending on the nature of the material [1]. It must be realised that anomalous diffusion leads to much larger volume of water and much deeper front penetrations and thus may have important implications for assessing the durability of porous materials.

Deviation from the $t^{1/2}$ scaling is expected to be the rule for all porous building materials [1]. However, the standard experimental procedure generally used to measure capillary rise absorption (as defined in references [12-13] and in ASTM Test Method for Absorption of Architectural Cast Stone (C1195), and ASTM Specification for Concrete Brick (C55)) are not sufficiently rigorous to confirm the general occurrence of anomalous diffusion during water infiltration in porous media. Weighing is carried out manually and requires that the specimen be removed at intervals from the water container. This drastically limits the number and accuracy of measurements. Furthermore, penetration of water through the side faces of the specimens induces a systematic bias [6, 14] which may represent a large fraction of the total weight gain in the firsts minutes of the test. The consequence is that the point of origin and the early readings are thus omitted in practice when interpreting the cumulative infiltration data in the numerous absorption measurements reported in the litterature.

Our objective in this work was to design and build an absorption apparatus that overcomes the main limitations of the standard procedures, in order to confirm the systematic deviation from the standard diffusion of the absorption process for different common building materials. To get more reliable measurements of the water absorption rate requires that we increase the number and accuracy of cumulative infiltration measurements points, especially at the beginning of the test, where deviation from the $t^{1/2}$ behavior is expected to be the most important [1] and that we limit water absorption as much as possible along the adjacent faces of the specimens. The experimental set-up is decribed in section 2. Preparation of the specimens is sketched in section 3. For this preliminary set of tests, red fired-clay brick was used. Experimental results are reported in section 4. The experimental evidence of the deviation of the absorption process from the $t^{1/2}$ relation is reviewed. The anomalous diffusion model introduced in [1] is then applied to the absorption data in section 5. It is shown that infiltration in common fired-clay brick is compatible with an anomalous diffusion mechanism scaling as $\approx t^{0.58}$. Several recommendations to improve the technical specifications for the absorption test by capillary rise are formulated in the conclusion.

Experimental Set-up

We used the capillary rise absorption test in this study. In this method, absorption is controled by two opposing forces: the moisture flow is driven upwards by capillarity, whereas gravity pulls the fluid downwards. In general, the capillary forces are dominant and gravity effects can be neglected to a first approximation, except for some materials with extremely coarse pore structure [6, 14]. The new absorption apparatus [15] is based on the principle of a continuous automatic weighing of the porous specimen during absorption. The specimen is hung to a 20N load cell connected to a calibrated analog-digital meter (Figure 1). The weighing system has an accuracy of 0.01g. A data acquisition system on a PC automatically records the digital signal at specified time intervals which can be as small as 1 second. Accurate high-rate measurements of the weight gain arising from capillary suction are thus obtained without removing the specimen from the water source. The concept of continuous weighing was already proposed by [16] but our set-up differ from theirs in many aspects. Note that the column that supports the load cell and the specimen can be moved up and down (Figure 1):

specimens ranging from a few cm up to 30 cm in length can thus be tested, provided that their weight does not exceed the capacity of the load cell.

To maintain a constant level in the source reservoir while water is continuously absorbed by the porous specimen, a continuous circulation of water is established in the container during the test. The reservoir, 14 cm wide and 17 cm long, is connected to the building's water supply. The pressure is controlled to ensure steady-state flow at the entry of the container (Figure 1). A flow-meter, set downstream of the pressure regulator, allows precise tuning of the flow rate. It was fixed to 600 cm^3 mn^{-1} for this set of experiments: this is far beyond the absorption rate of porous materials. The water in excess continuously runs over one side of the reservoir and is evacuated (Figure 1). Because the water level is dynamically maintained, specimens with up to 70 cm^2 in cross-section can be tested with a limited water surface. Furthermore, the bias that may result from evaporation and water temperature changes for long-time experiments are avoided because of the continuous flow. The reservoir is supported by a platform that can be translated vertically when establishing the contact between the absorption face of the specimen and the water surface of the container.

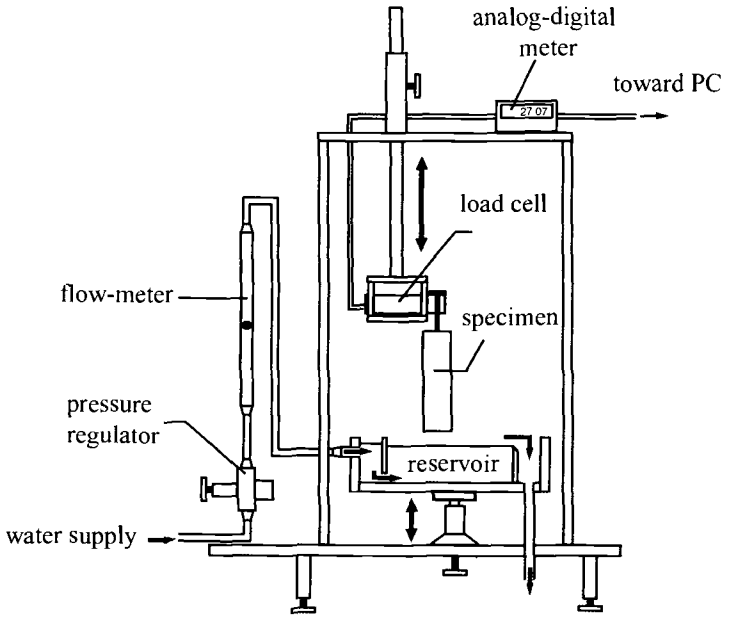

Figure 1- *Schematic view of the experimental apparatus.*

Sample Preparation

As specified in the introduction, non-reactive, macroscopically-homogeneous isotropic materials were required to test the respective merits of the two theoretical models of absorption in competition. Fired-clay bricks appear as a suitable material for

this purpose (see for example [8, 17]). Two common red fired-clay Glen-Gery[6] molded bricks 5.7 cm deep 9.5 cm wide and 19 cm long were used for this set of experiments. The material looks quite homogeneous to the naked eye with a fine-grained texture free of any fracture or discontinuity. A complete characterization, including composition, porosity and pore size distribution measurements, is currently being carried out but is not yet available. Each brick was first (wet) sawed longitudinally in two equal-size specimens: this is especially useful to test the repeatability of the experiments. A slice of about 1cm was also removed along the absorption face to have a fresh, unaltered section. The four pieces of bricks referred to as br09, and br10 (brick 1) and br11 and br12 (brick 2) were dried at 105°C in an oven for 24 hours. The material was then stored in our laboratory at constant room temperature of 23°C and relative humidity of about 25%. Before testing, an impermeable layer of paraffin was applied on the adjacent sides of each specimen. Preliminary tests confirmed that water absorbed along the unprotected sides of the samples is the principal source of error when determining the capillary absorption rate in unsaturated porous materials. Paraffin was first heated up to the melting point and painted liquid over a band about 2 cm wide along the sides adjacent to the absorption surface. To ensure a close contact between the coating and the brick, the paraffin layer was reheated by pulsing hot air on the surface of the specimen to allow the wax to completely fill the surface pores of the specimen. Note that this did not change the effective absorption section of the specimen since the penetration depth was very small and systematically less than one mm.

Experimental Procedure and Results

Before the test, the specimen was hung about 5 mm above the water surface at the center of the reservoir. The reservoir was then translated upwards until the surface of the specimen was just in contact with the water surface. Due to surface tension, the absorption face is almost instantaneously wetted and a sudden increase of the apparent weight of the specimen is observed. This point is taken as the time origin $t = 0$ for the test. Since the specimen is just at the surface of water, no buoyancy forces apply. The absorption face of the specimen was visually examined to ensure that no air was trapped under the absorption side. For each experiment reported in this note, no air bubbles were detected. It must be mentioned however that small bubbles progressively formed during the tests. We believe that the air dissolved in water is progressively released at the specimen interface which acts as a nucleation surface. Simple tests have shown that the disturbance induced by bubbles on the apparent weight of the specimen is below the accuracy of the weighing system. However, the formation of bubbles may eventually reduce the effective surface of absorption of the specimen as time elapses. This problem will be corrected in the next version of the experimental set-up by using de-aerated water.

The interval between two measurements was fixed at 1 second for all tests and experiments were conducted over a period of at least two hours. Since the wet portion of the brick is a bit darker than the dry one, it was possible to see the progression of the moisture front inside the sample during the test. For each experiment, the wetting front was sharp and almost horizontal. The weight gained by each sample was normalized to its cross-section (in cm^2) to make the results comparable. The results are reported in Figure 2

[6] Glen-Gery Corporation, PO Box 7001, 1166 Spring Street, Wyomissing, PA 19610-6001

as a function of time for the different specimens. As expected, the water absorption rate is initially high and progressively decreases as time elapses. As can be seen, the water cumulative infiltration data on the two specimens of a same brick are nearly identical: this provides a direct measure of the quality and repeatability of the experiments. Note also that the absorption capacity differs significantly between the two bricks, although they are supposed to be the same material (and actually they can not be distinguished by eye). The origin of such a discrepancy is attributable to the manufacturing process which may induce variations in the microstructure (such as porosity and/or mean pore size for instance) from one brick to another. The structural study in progress will hopefully confirm this assumption.

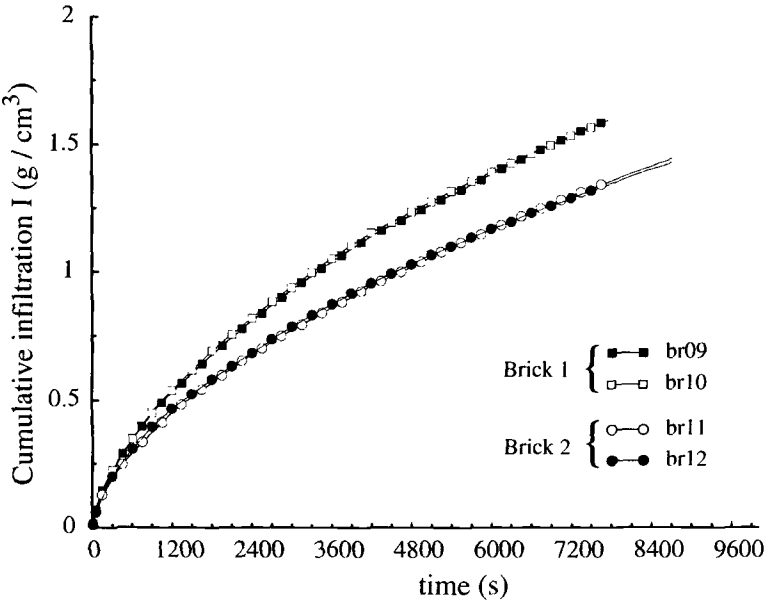

Figure 2 - *Cumulative infiltration I as a function of time in the four fired-clay brick specimens tested. The symbols are only given as an aid to distinguish the different curves.*

Assuming that absorption in brick is driven by normal diffusion, the four cumulative infiltration data sets were plotted as a function of $t^{1/2}$ in Figure 3 and Figure 4. While the unsaturated flow theory predicts that (I) is proportional to $t^{1/2}$, data are shown to differ significantly from the $t^{1/2}$ relation. This is especially evident during the first 10 min of the test where all the curves exhibit a clear upward curvature (Figure 3 and 4). As a consequence, least squares linear regression of the data points exhibit a negative intercept at $t = 0$: this is not physical because the moisture content cannot be less than 0 at $t = 0$. It must be stressed that the slope of the cumulative infiltration curve does not become constant after 10 min but continues to increase with time. The main consequence is that

although the data are well approximated by a straight line, the value of the slope strongly depends on the time interval on which the linear approximation is calculated (Figure 5). The apparent absorption capacity of the brick thus increases with time. The sorptivity (S) which is assumed to be a constant material parameter according to the unsaturated flow theory, is then clearly time dependent. This was already noted in [1] from the analysis of one-dimensional NMR absorption profiles measured in a brick by [8–9], but could not be confirmed from the cumulative infiltration data because the data points were too scarce. The high rate weighing measurements provided by the new absorption apparatus allow unambiguous confirmation of the increase of (S) with time directly from the cumulative infiltration curves. Although the variation of the apparent sorptivity decreases as time elapses (Figure 5), there is no evidence of an asymptotic behavior, i.e., the apparent sorptivity is expected to continuously increase with time. It is interesting to note that the variations of the apparent sorptivity with time shown in Figure 5 for the different samples define quite noisy curves. In our opinion, this reflects the short wavelength variations of the absorption rate due to local inhomogeneities in the structure inside each specimen. The use of high precision cumulative infiltration data (as those obtained with the new absorption apparatus) as an indirect "scanning probe" may be an interesting avenue to characterize the internal structure of porous building materials.

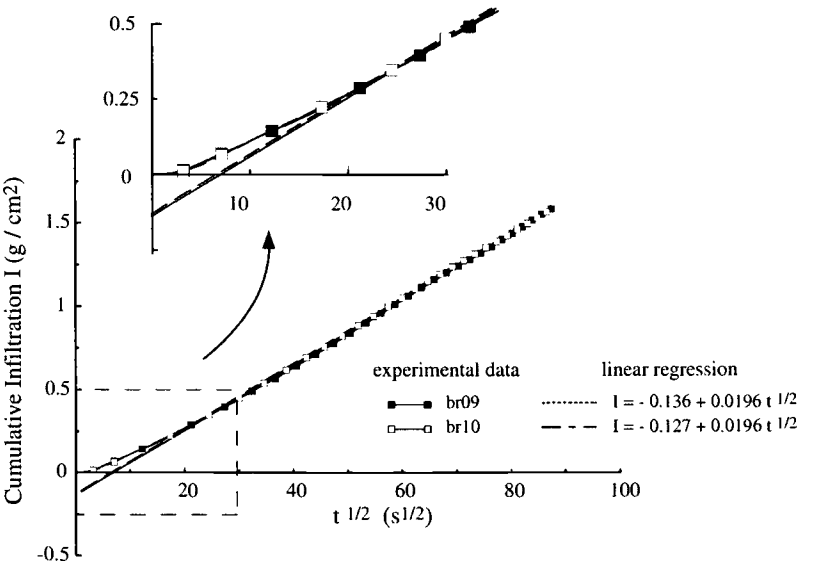

Figure 3 — *Cumulative water absorption (I) as a function of* $t^{1/2}$ *for the specimens br09 and br10 (brick 1). Note the upward curvature of the infiltration curve and the resulting negative intercept at* $t = 0$ *of the best least-squares linear fit (the symbols represent only 1/300th of the data points).*

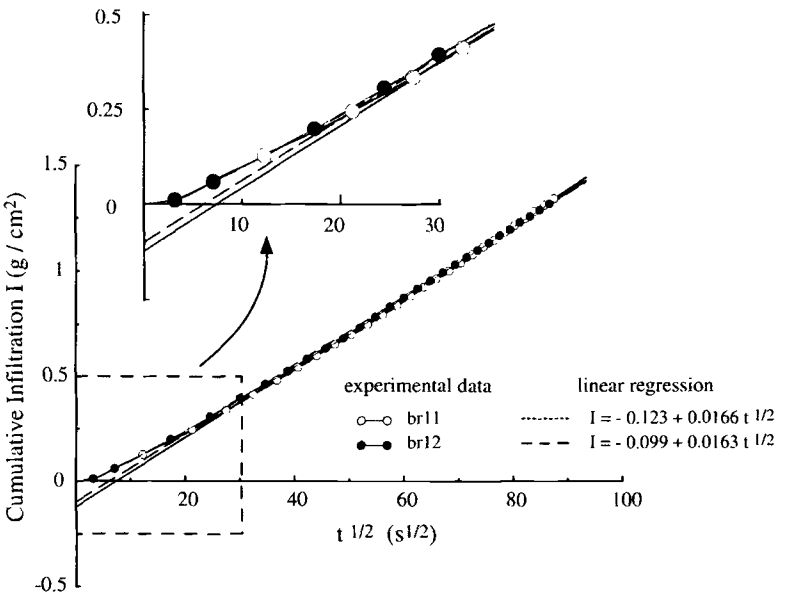

Figure 4 — *Cumulative water absorption I as a function of $t^{1/2}$ for the specimens br11 and br12 (brick 2). Note the upward curvature of the infiltration curve and the resulting negative intercept at t=0 of the best least-squares linear fit (the symbols represent only 1/300 th of the data points).*

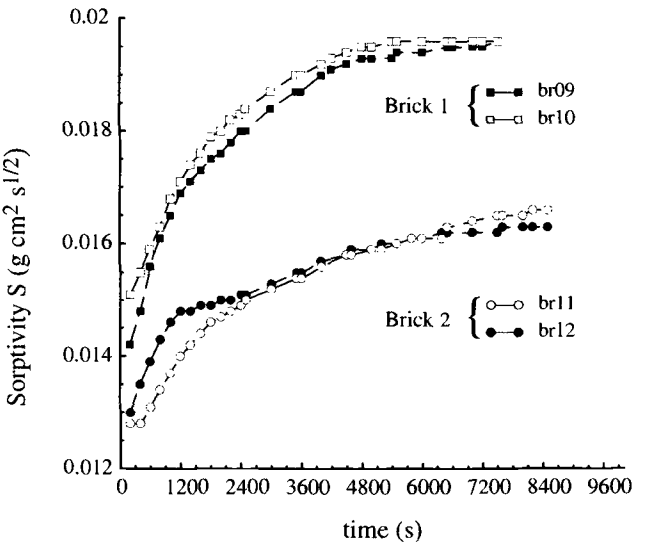

Figure 5 – *Evolution with time of the apparent sorptivity for the different brick specimens.*

Discussion

The experimental results reported in the previous section show that one-directional water infiltration as measured in a common fired-clay brick does not scale as $t^{1/2}$, i.e., the absorption process actually does not conform to the predictions of the unsaturated flow theory. Besides the upward curvature of the cumulative infiltration curve with respect to the expected $t^{1/2}$ linear trend, an additional evidence of the departure from the $t^{1/2}$ scaling of the absorption process is given by the negative intercept that systematically arises from least square linear fitting of the data points. Several examples of absorption tests exhibiting such negative intercepts have in fact already been found in the literature, as pointed out in [1]. It must be mentioned however that this anomaly was usually ignored in the interpretation of the cumulative infiltration data (see for instance [16]). For the few cases where the occurrence of a negative intercept was explicitly reported, this was attributed to experimental problems such as the presence of a "dense layer" at the surface of the specimens [14, 17]. These data, obtained on a variety of common building materials including mortars and limestone, corroborate our own results. This suggests that deviation from the $t^{1/2}$ scaling of the absorption process is the rule rather than an exception. One of the most important consequences is that the sorptivity, determined as the slope of the best least-squares linear fit of the cumulative infiltration *vs* $t^{1/2}$ curve, varies in time, whereas it is expected to be constant. The concept of sorptivity is thus highly questionable. It is obvious that any extrapolation of the amount of absorbed water to long times based on the application of the unsaturated flow theory will be biased. Furthermore, the error will critically depend on the time interval on which the apparent sorptivity is evaluated. Most absorption tests are conducted over periods less than one hour. This correspond to the time interval for which the variation of the apparent sorptivity is the most important (Figure 5). The error can thus actually be very important.

The cumulative infiltration data that we have measured on the four brick specimens were interpreted by assuming that the absorption process is driven by anomalous diffusion [1]. Each data set of Figure 2 was first approximated by power law regression to estimate the value of the anomalous scaling exponent α which arises from the application of the anomalous diffusion equation to one-dimensional absorption (see [1] for further details). We found a mean value $\langle\alpha\rangle = 0.59$ for br09 and br10 and $\langle\alpha\rangle = 0.57$ for br11 and br12. The absorption is thus expected to scale as $t^{0.59}$ and $t^{0.57}$ in bricks 1 and 2 respectively. The cumulative infiltration data measured on the specimens br09 and br11 were plotted as a function of the new time scaling in Figure 6 and Figure 7 respectively. It can be shown that, in both cases, the data points now align along a straight line, even at short times. The best least-squares linear fits calculated on the two data sets pass now through the origin at $t = 0$, i.e., all the data including the initial moisture content and early readings are well accounted for by the new time scaling. The dimension of the constant of proportionality, referred to as S* in [1], is g cm^{-2} $t^{-\alpha}$. Although S* has evident similarities with sorptivity, it does not have the same dimension as S (g cm^{-2} $t^{-1/2}$). Furthermore, assessing the absorption properties of porous materials now requires evaluation of both S* and α. It must be noted that the scaling exponent is not exactly the same in brick 1 and 2. Besides any imprecision that may eventually result from the experimental measurements, this may reflect the differences of the porous microstructure between the two bricks, which has already been pointed out.

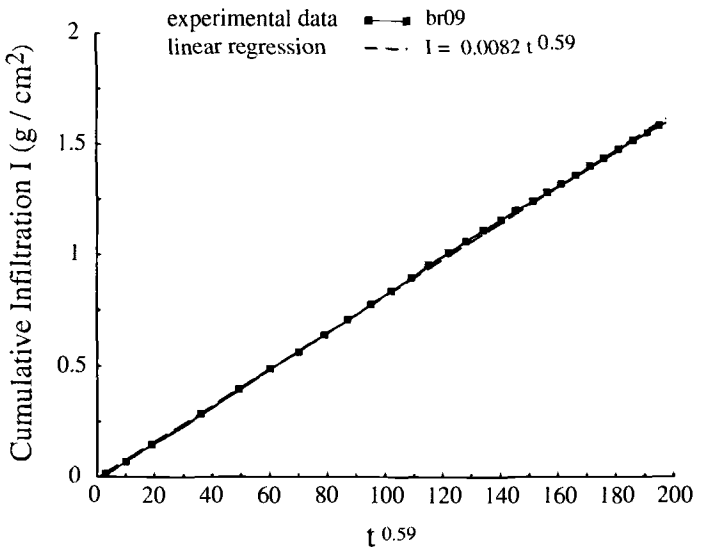

Figure 6 - *Cumulative water absorption I against $t^{0.59}$ for the brick specimen br09 (time is in seconds).*

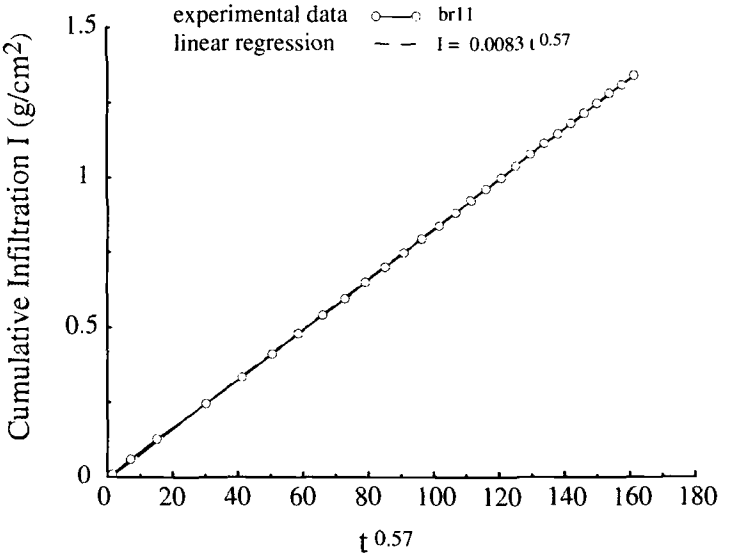

Figure 7 - *Cumulative water absorption I as a function of $t^{0.57}$ for the brick specimen br11 (time is in seconds).*

A time scaling exponent greater than ½ implies that the wetting front progresses much faster than expected in the brick specimens, i.e., both the penetration depth and the volume of absorbed water are larger than predicted from the application of the standard unsaturated flow theory. To illustrate this, we extrapolated up to 100 hours the evolution of the cumulative water infiltration in the specimen br09 from the standard unsaturated flow theory and the anomalous diffusion model respectively. We used the relations $I = 0.0196\ t^{0.5}$ of Figure 3 and $I = 0.0083\ t^{0.59}$ of Figure 5 for that comparison. Note that the negative constant found from least squares linear regression in $t^{1/2}$ (Figure 3) was not taken into account because the relation between (I) and $t^{1/2}$ does not include any extra term according to the unsaturated flow theory. The results are plotted against (t) in Figure 8. The two theoretical curves are initially close (the two relations were fitted to the same experimental data). It can be seen, however, that the anomalous diffusion model predicts a larger volume of absorbed water after ≈10 hours (Figure 8). The difference between the two estimates increases continuously as time elapses and reaches about 25% after 100h. Although not shown, similar results are obtained with the three other specimens br10, br11 and br12. This comparison suggests that application of the standard unsaturated flow theory leads to underestimating the capacity of water absorption of porous materials: this may have important implications when assessing the durability of building materials.

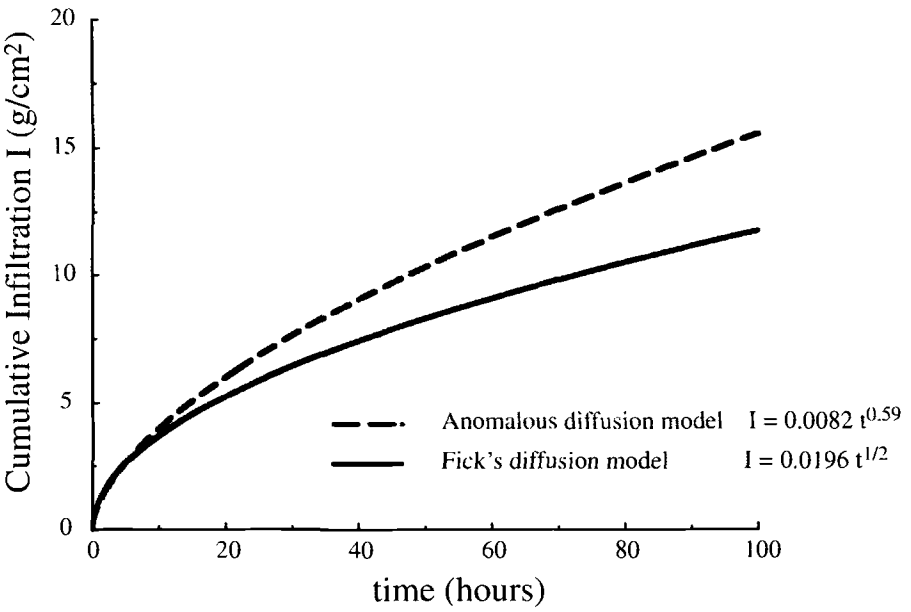

Figure 8 – *Comparison of the one-dimensional cumulative water infiltration (I) in the specimen br09 as predicted from the application of the standard unsaturated flow theory and from the anomalous diffusion model respectively. The evolution of (I) is plotted as a function of time.*

The long-lasting misinterpretation of cumulative absorption tests clearly points out that the standard absorption procedures are too imprecise. The consequence has been a dramatic under-estimate of the actual absorption properties of porous media, that still precludes any reasonable prediction of the long-term behavior of building materials. We suggest that the standard method should be changed to get more rigorous estimate of the capacity of water absorption by porous building materials. Continuous automatic weighing and application of a impermeable sealant along the adjacent faces of the specimens have been proved to significantly improve the quality and reliability of the cumulative infiltration measurements. This should be urgently included in the technical capillary rise absorption test specifications. The procedure we used in this test should also be improved to prevent the formation of bubbles below the absorption surface during the test. Although their effect remains small as indicated by preliminary tests, they may i) artificially lighten the specimen, and ii) progressively shorten the effective absorption area of the specimens. The absorption capacity of the different brick specimens could be actually a bit larger than given here, i.e., deviation from the $t^{1/2}$ relation could be even larger than reported. A supply system using de-aerated water will be implemented on the experimental set-up in the near future to overcome this problem. Other porous building materials are currently being tested using the new absorption apparatus. The aim is now to establish the relations which may exist between the exponent α of the anomalous diffusion model and the geometric pore structure and physical properties of the materials tested to hopefully constrain the absorption mechanisms in porous media.

Conclusion

Several one-dimensional absorption experiments were carried out in a common red fired-clay brick with a new absorption apparatus. The experimental results demonstrate that:

1) The standard unsaturated flow theory which predicts a time scaling in $t^{1/2}$ of the cumulative infiltration for one-dimensional absorption does not hold, and

2) The evolution of the cumulative infiltration data in the brick is best accounted for by a time scaling in t^{α}, with $0.57 \leq \alpha \leq 0.59$, in agreement with the predictions of the anomalous diffusion infiltration model recently introduced in [1].

The $t^{1/2}$ scaling therefore underestimates the volume of water that can be actually absorbed by porous materials. This result has particular relevance for evaluating the durability of porous building materials.

This work clearly shows that determination of the absorption properties of porous materials requires much more rigorous measurements than those allowed by the application of the standard specifications. The new procedure and results presented in this note should be taken into account to change the technical standards for the one-dimensional absorption measurements in porous media. We strongly suggest that:

1) Weighing should be automatized to significantly increase the number and accuracy of the cumulative absorption measurements,

2) The adjacent sides of the specimen should be systematically sealed with an impermeable coating to prevent water from being absorbed through the surface pores of the material, and

3) Absorption tests should be conducted over periods typically longer than one hour.

Such modifications should lead to more accurate estimates of the absorption properties of porous building materials and thus improve our capacity to predict the durability of building structures.

Acknowledgments

This work was supported in part by the Natural Sciences and Engineering Research Council of Canada (NSERC) through a rearch grant to PL. MK also gratefully acknowledges FV Donzé for financial support.

References

[1] Küntz, M. and Lavallée, P., "Experimental evidence and theoretical analysis of anomalous diffusion during water infiltration in porous building materials, "*J. Phys. D: Appl. Phys.*, Vol. 34, , 2001, pp. 2547–2554.

[2] Philip, J. R., "The theory of infiltration: 1. The infiltration equation and its solution," *Soil Sci.*,Vol. 83, 1957a, 345–357.

[3] Philip, J. R., "Theory of infiltration, " *Adv. Hydrosci.*,Vol. 5, , 1969, pp. 215-296.

[4] Hall, C., "Water movements in porous building materials –I. Unsaturated flow theory and its application," *Bldg. Env.*, Vol. 12, 1977, pp. 117–125.

[5] Ho, D. W. S., and Lewis, R. K., "The water sorptivity of concretes: the influence of constituents under continuous curing," *Durab. Bldg. Mater.*,Vol. 4, 1987, pp. 241–252.

[6] Hall, C., "Water sorptivity of mortars and concretes: a review," *Mag. Concrete Res.*, Vol. 41, 1989, pp. 51–61.

[7] Hall, C., "Barrier performance of concrete: a review of fluid transport theory, " *Materials and Structures*, Vol. 27,1994, pp. 291–306.

[8] Pel, L., *Moisture transport in porous building materials*, PhD thesis, Eindhoven Technical University, The Netherlands, 1995.

[9] Pel, L., Kopinga, K., and Brocken, H., "Moisture transport in building materials," *Heron*, Vol. 41, 1996, pp. 95–105.

[10] Lockington, D., Parlange, J. Y., and Dux, P., "Sorptivity and the estimation of water penetration into unsaturated concrete," *Mat. Struct.*, Vol. 32, 1999, pp. 342–347.

[11] Philip, J. R., "The theory of infiltration: 4. Sorptivity and algebraic infiltration equations, "*Soil Sci.*, Vol. 84, 1957b, pp. 257–264.

[12] RILEM, "Testing methods for natural stones," *Mat. Struct.*, Vol. 5, 1972, pp. 231-245.

[13] British Ceramic Research Association, "Model specification for load-bearing clay brickwork, "BCRA, Stoke on Trent, Special Publication 56, 1967.

[14] Hall, C., and Kam Min Tse, T., "Water movement in porous building materials: VII. The sorptivity of mortars", *Bldg. Env.*,Vol. 21, 1986, pp. 113–118.

[15] Küntz, M., and Lavallée, P., Canada Patent Copyright N_0 2342119, March 2001.

[16] Sabir, B. B., Wild, S., and O'Farell, M., "A water sorptivity test for mortar and concrete", *Materials and Structures*, Vol. 31, 1988, pp. 568–574.

[17] Gummerson, R. J., Hall, C., and Hoff, W. D., "The suction rate and the sorptivity of brick," *Trans. and J. of Br. Ceram. Soc.*,Vol. 80, 1981, pp. 150–152.

Bernhard Middendorf,[1, 3] Jana Mickley,[2] Fernando Martirena[3] and Robert L. Day[4]

Masonry Wall Materials Prepared by Using Agriculture Waste, Lime, and Burnt Clay

---

Reference: Middendorf, B., Mickley, J., Martirena, F., and Day R. L., "**Masonry Wall Materials prepared by Using Agriculture Waste, Lime and Burnt Clay,**" *Masonry: Opportunities for the 21st Century, ASTM STP 1432*, D. Throop and R. E. Klingner, Eds., ASTM International, West Conshohocken, PA, 2003.

Abstract: Low cost building materials prepared with ash of burnt agriculture waste and lime represent an alternative binder/construction system. Pure lime and Portland cement (OPC) are energy intensive to manufacture, and are expensive and scarce in developing countries. However, pozzolanic binders prepared by burning agriculture waste can be used as partial or complete substitutes for pure lime or OPC. These agricultural wastes, such as rice husks, wheat straw, sugar cane bagasse and sugar cane straw are widely available in many developing countries. Some types of clay are also pozzolanic after thermal treatment. The reactivity of the ash depends on its composition and on several factors involved in the burning process such as temperature, time, environment and cooling rate as well as chemical activation. This paper presents research focused on building materials produced by using lime combined with a pozzolanic mixture of thermally treated clay and ash from agricultural wastes. The study assesses the accelerating effect of sodium sulfate in strength development of building materials.

Keywords: Pozzolana, lime, mortars, building materials, ashes, agriculture waste

Nomenclature

SCSA	Sugar Cane Straw Ash	CH	Calcium Hydroxide ($Ca(OH)_2$)
XRD	X-ray diffraction	SEM	Scanning electron microscopy
C-S-H / C-A-H	Calcium Silicate Hydrate / Calcium Aluminate Hydrate		

[1] Senior Researcher, Faculty of Civil Engineering, Department of Structural Materials, University of Kassel, Moenchebergstr. 7, D-34125 Kassel, Germany.

[2] Graduate Student, Faculty of Civil Engineering, Department of Structural Materials, University of Kassel, Moenchebergstr. 7, D-34125 Kassel, Germany.

[3] Professor, Faculty of Constructions, Central University of Las Villas, Carretera Camajuani km 5, 54830 Santa Clara, Cuba.

[4] Professor, Associate Dean, Faculty of Engineering, University of Calgary, 2500 University Drive NW, Calgary, Alberta, Canada T2N 1N4.

Introduction

The critical housing situation in many third world and developing countries demands appropriate low-cost building materials. Building materials such as pure lime and OPC are energy intensive and therefore expensive. However, pozzolanic materials obtained from burning agriculture waste can be used as partial or complete substitutes for OPC. Agricultural wastes, such as rice husks, wheat straw, sugar cane bagasse and sugar cane straw are available in huge amounts in many developing countries.

An interesting process has been developed as part of this study: calcined clay can be combined with ash from agricultural waste to provide a reactive pozzolana; the interaction between both materials produces an improved pozzolana. A combination of lime and the above mentioned reactive pozzolana can act as a pozzolanic binder, suitable to be used in masonry construction [1].

Thermally treated kaolinite and Ca-montmorillonite have been found to be the most suitable clay minerals to use as pozzolana. The temperature range of kaolinite to activate the pozzolanic reactivity is relatively wide (500°C to 900°C). In contrast, the temperature range of Ca-montmorillonite is more restricted (800°C ± 50°C) [2]. According to He et al. [3], at a temperature of 550°C most of the kaolinite structure is destroyed; from an economic viewpoint they recommend a calcination régime of 550°C for 110 minutes.

Agricultural waste shows pozzolanic properties after pyroprocessing at temperatures between 500°C and 600°C. Both the calcination temperature and the calcination time have an influence on pozzolanic reactivity [4,5]. Combustion in a carbon dioxide environment produces a higher specific surface area than combustion in an oxidizing environment because in a carbon dioxide environment a lower heat of reaction occurs and the pore structure is less damaged [6,7]. In addition, breaking down the cellulose with zinc chloride instead of the grinding the ash before burning increases the specific surface area [5].

In presence of water the amorphous silica and alumina react with calcium hydroxide at room temperatures. The most important reaction products are calcium silicate- and calcium aluminate hydrates (C-S-H and C-A-H phases), which account for the strength. The mix proportion of 70 wt.% pozzolana to 30 wt.% lime gives an optimum in reference to the compressive strength [8].

The reaction process of lime-pozzolana is slow in comparison to the hydration of OPC. There are several treatment methods that improve the initial and/or the final strengths [9-13]: (a) grinding of the pozzolana to increase specific surface; (b) thermal treatment enhances pozzolanic activity, (c) an elevated curing temperature accelerates strength development, and (d) chemical additions to mortars enhances both initial and final strength. Chemical additions of sodium sulfate, for example, has been found to be more effective in improving strength gain and lowering cost than prolonged grinding and elevation of the curing [12,13].

Experimental Program

The experimental program involves the preparation of mortars made with combinations of calcined kaolinite and Ca-montmorillonite, SCSA (Sugar Cane Straw Ash), and a mixture of SCSA and calcined clay. In a second part of the experimental program, sodium

sulfate was added to investigate the acceleration of the reaction rate and enhancement of strength development.

The clay minerals kaolinite and Ca-montmorillonite, supplied by the German company "Bassermann Minerals" were calcined in thin layers for 2 hours at 540°C for kaolinite and 800°C for Ca-Montmorillonite. The SCSA was obtained from a special incinerator designed to produce an amorphous ash – the incinerator is situated near a sugar factory in Santa Clara, Cuba. The ash was burnt for 1-2 hours at temperatures between 400-500°C. The SCSA was ground in a ball mill for one hour.

The density, specific surface area and the chemical composition of the pozzolana mixture is shown in Table 1. The Ca-montmorillonite and the SCSA have the highest silica content. However, the kaolinite has the highest alumina content and also the sum of silica and alumina (85 wt.-%) is higher than in the other examined pozzolanas.

Table 1-*Density, surface area and chemical composition of pozzolanas.*

		kaolinite	Ca-mont.	SCSA
density [g/cm^3]		2.50	2.51	2.36
specific surface area (acc. BLAINE) [cm^2/g]		13,320	3,700	11,340
SiO_2	[wt.-%]	52.0	58.7	58.2
Al_2O_3	[wt.-%]	33.1	19.3	2.5
Fe_2O_3	[wt.-%]	0.7	7.2	1.7
MgO	[wt.-%]	0.3	2.3	2.5
K_2O	[wt.-%]	3.7	1.7	5.7
Na_2O	[wt.-%]	0.1	0.1	0.6
CaO	[wt.-%]		1.5	8.4
BaO	[wt.-%]		-	0.04
TiO_2	[wt.-%]	0.05	0.51	-
SrO	[wt.-%]			0.02
Mn_2O_3	[wt.-%]			0.27
SO_3	[wt.-%]			0.77

The hydrated lime used in these experiments was commercial grade with a density of 2.25 g/cm^3 and a Blaine specific surface of 11,940 cm^2/g.

The amorphous nature of the pozzolanas was measured by using X-ray diffraction methods. Both clay minerals were investigated untreated and after calcination (Figures 1 and 2).

All mortars were prepared with sand from the Eder Lake, Germany with a defined particle size distribution which corresponds the European Standard DIN EN 196-1. The proportions of pozzolana to lime (70 to 30 wt.-%) are typically reported in the literature where an optimum for burned agricultural waste was investigated [8]. A water binder ratio of 0.8 for all samples was used. For some mixes, 4 wt.-% sodium sulfate was added based on the mixture of pozzolana and lime. The fresh mortar was cast in 40 x 40 x 160 mm prismatic molds. After two days storing in water saturated environment (20°C, 100% rela-

tive humidity) the samples were demolded and cured in a climatic chamber at constant temperature and humidity (20°C, 65% relative humidity).

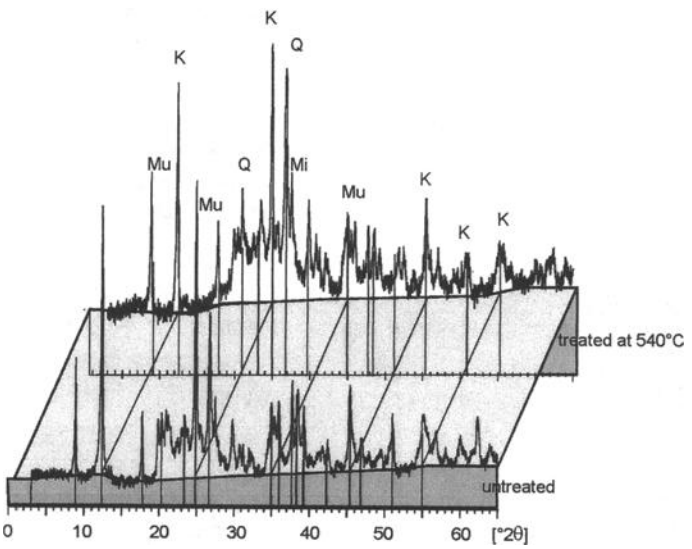

Figure 1-*XRD pattern of clay: K-kaolinite, Mu-muscovite, Q-quartz, Mi-microcline.*

Table 2-*Mortar proportions.*

Pozzolana		lime/pozzolana ratio	pozzolana+ lime/sand ratio	water / pozzo-lana + lime ratio
kaolinite / SCSA ratio	1/2.33	1/2.33	1/3	0.8
Ca-montmorillonite / SCSA ratio	1/2.33			

Compressive strength tests and lime consumption were measured after 7 and 28 days. Lime consumption was measured by titration. The identification of reaction products by using XRD and SEM was done at the age of 28 days.

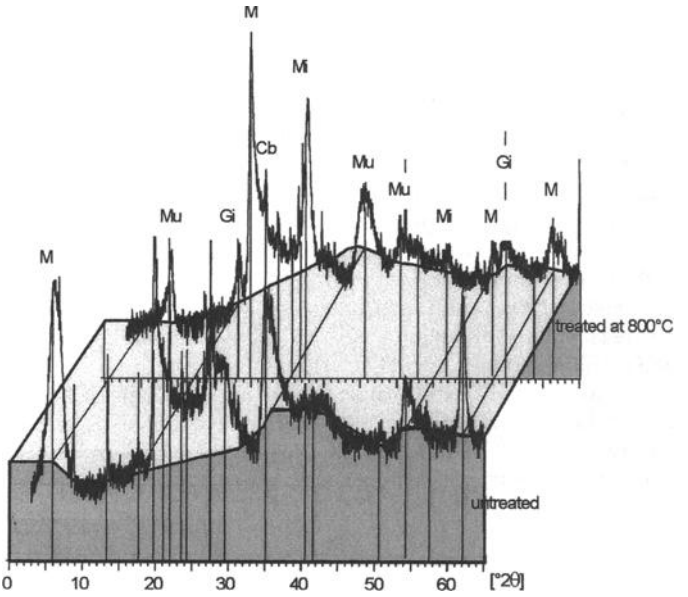

Figure 2-*XRD pattern of clay: M-Ca-montmorillonite, Mu-muscovite, Q-quartz, Mi-microcline, Gi-gibbsite, Cb-cristobalite.*

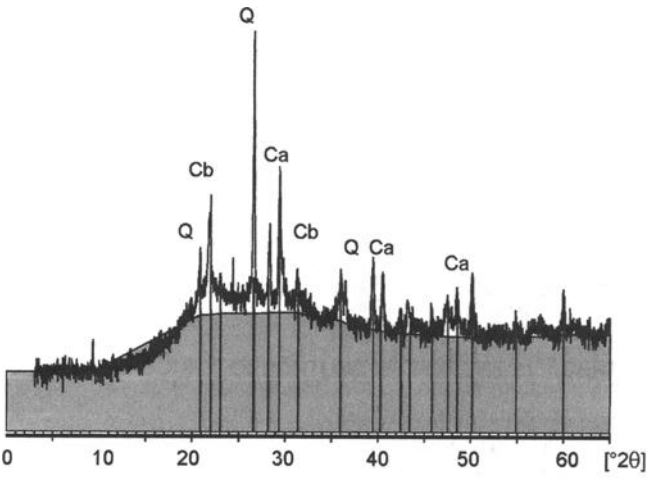

Figure 3-*XRD pattern of SCSA: Q-quartz, Cb-cristobalite, Ca-calcite.*

Results and Discussion

Kaolinite shows an increase in the amorphous background, or hump, after calcination at a temperature of 540°C (Figures 1, 2). However, the clay mineral Ca-montmorillonite shows not such a significant increase in amorphous content. Therefore it can be concluded that untreated Ca-montmorillonite also contains less crystalline material. Because of heat treatment the clay mineral montmorillonite was transformed to gibbsite [2].

The XRD-pattern of the SCSA (Figure 3) shows a considerable amount of cristobalite which is an indicator of crystalline phases caused by temperature higher than 800°C during the burning process [8].

Pozzolanic reactivity was confirmed in all cases by measuring the lime consumption (Figure 4) and the compressive strength after 7 and 28 days (Figure 5). Mortars prepared with SCSA and calcined kaolinite proved to be highly reactive. The compressive strength after 28 days was around 8 MPa. However, the compressive strength of the separate components was lower (kaolinite 7.6 MPa, SCSA 5.2 MPa), this apparently is caused by the higher workability in mortars where mixed pozzolana was used, which reflects in better compaction. That indicates that not only chemical influences but also physical influences play an important part.

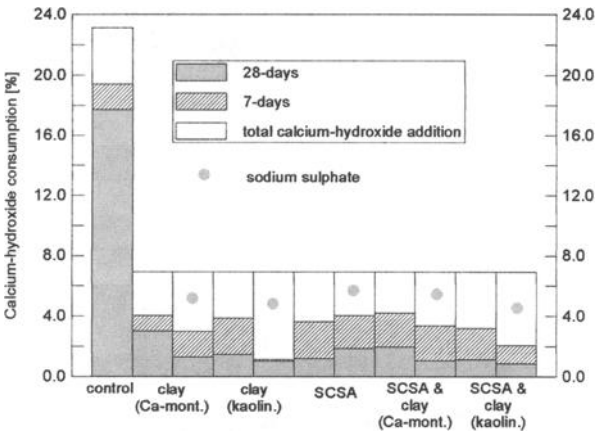

Figure 4-*Lime consumption after 7 and 28 days.*

In the presence of sodium sulfate the compressive strengths were increased in mortars that were prepared with clay, but decreased in mortars that were prepared with SCSA. All mortar mixtures prepared with both SCSA and clay showed improved strengths when sodium sulfate was used, in spite of the fact that the weight proportion of SCSA was higher than of clay (SCSA :clay 70 : 30 wt.-%). The most significant strength improvement is achieved with kaolinite. In particular, the compressive strength after seven days in

the presence of sodium-sulfate activator was eight times higher than without activator. Kaolinite consists of a high content of alumina, which increases the dissolution of pozzolana in high alkaline solution because of the lower bonding energy of Al-O than Si-O.

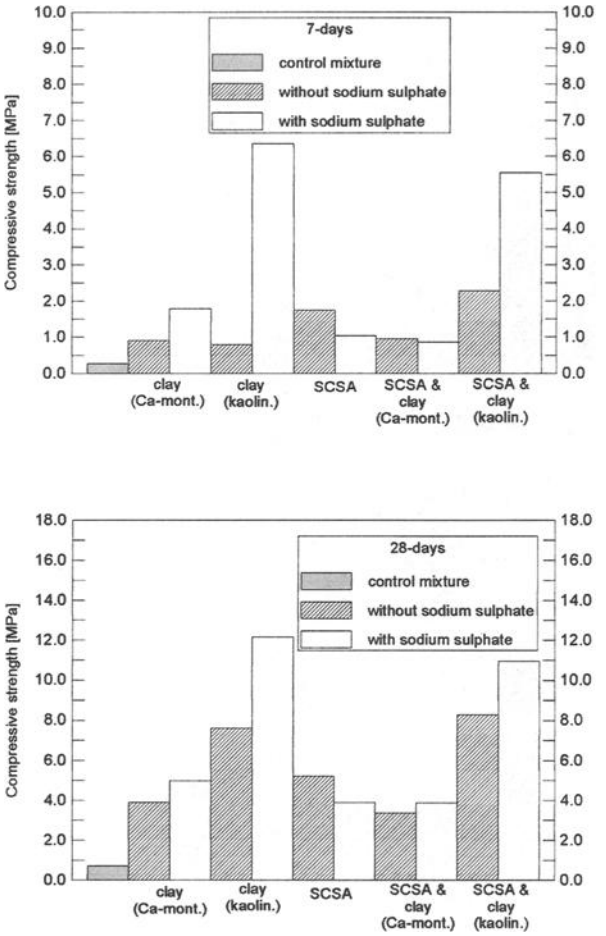

Figure 5-*Compressive strength after 7 and 28 days.*

The lime consumption after 7 and 28 days (Figure 4) shows a good correlation to the compressive strength. Most of the calcium hydroxide was consumed in all cases after seven days. Higher CH consumption was also observed in all clay-based mortar samples where sodium sulfate enhances the compressive strength. Of particular interest is the rapid

lime consumption of the mortar prepared with kaolinite and sodium sulfate. Most of the lime was consumed after seven days.

Reaction products such as C-S-H and C-A-H phases were identified by using XRD and SEM. C-S-H and C-A-H phases in mortar prepared with kaolinite with and without sodium sulfate showed a different structure. In sodium sulfate activated mortars, the phases were larger and thicker (Figures 6 and 7). The difference is also assessed from the results of compressive strength testing (mortar with sodium sulfate achieved 7.6 MPa , while without sulfate they achieved 12.2 MPa).

C-S-H as well as C-A-H phases were identified by using energy disperse X-ray analysis (EDX). The amount of C-S-H and C-A-H phases formation of the Ca-montmorillonite mortars was smaller than in kaolinite mortars.

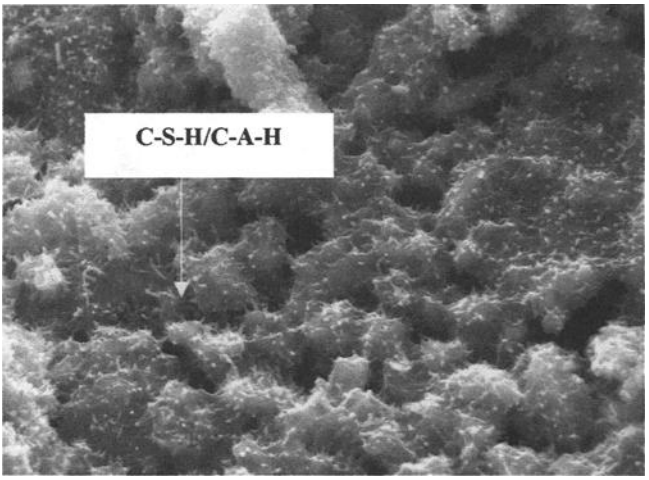

Figure 6-*SEM observation of kaolinite mortar sample (width 46 μm).*

SEM observation of the mortar prepared with SCSA (Figure 8) shows thin C-S-H phases. In contrast, C-S-H phases in mortar prepared with SCSA and sodium sulfate showed a more bulky morphology and also a smaller amount was detected. In general it can be said that the morphology of C-S-H and C-A-H phases in the SCSA and kaolinite mortars with sodium sulfate (Figure 9) is different.

Compressive strength test results show that all mortar mixtures prepared with waste-materials fulfill the German standard specification for masonry mortar (DIN 1053-1 mortar Group II). According to DIN 1053 at least a compressive strength of 3.5 MPa for mortars of Group II is required.

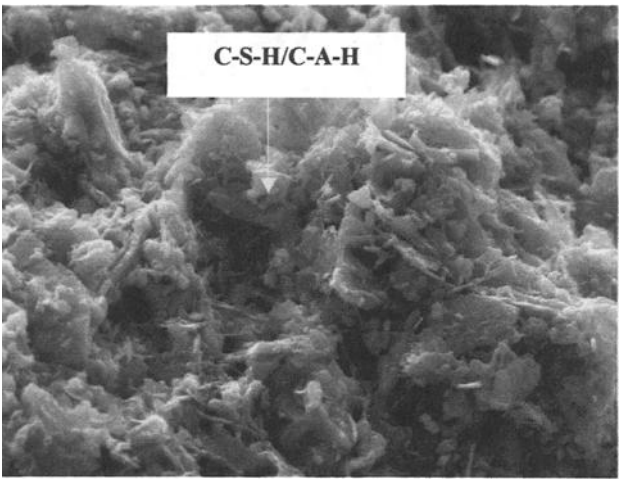

Figure 7-*SEM observation of kaolinite mortar sample and sodium sulfate (width 46 μm).*

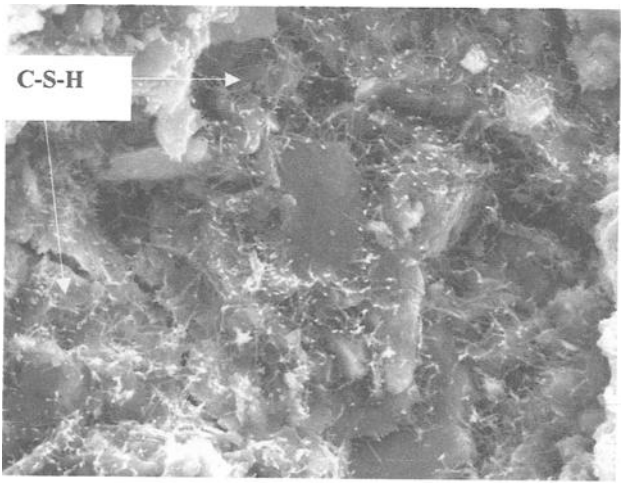

Figure 8-*SEM observation of SCSA mortar sample (width 46 μm).*

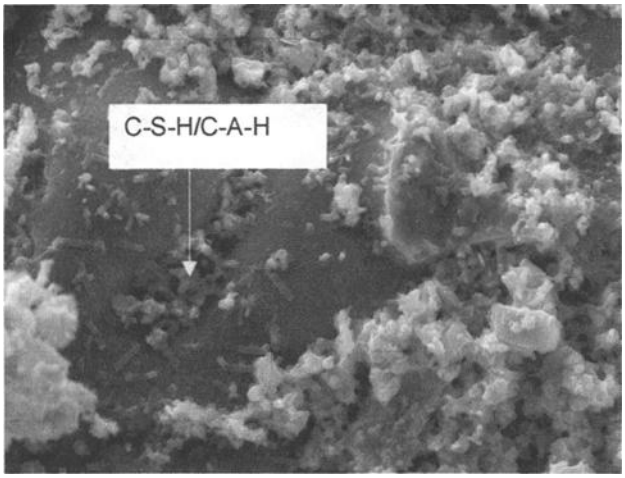

Figure 9-*SEM observation of SCSA and kaolinite mortar sample with sodium sulfate (width 46 μm).*

Conclusions

The combination of the calcined clay minerals kaolinite (540°C) and Ca-montmorillonite (800°C) with the ash of agricultural waste burned at temperatures between 500°C and 700°C results into an enhanced pozzolana. Combined with lime it has substantial promise to be used in masonry construction. Pozzolanic reactivity was assessed by measuring the compressive strength, lime consumption and by identification of reaction products by using XRD and SEM. In particular, the mixture of SCSA and kaolinite gave relatively high compressive strengths (around 8 MPa).

Sodium sulfate admixture in the range of 4 wt.-% enhances the pozzolanic reactivity of clay-based mortars, but decreases the pozzolanic reactivity of mortars prepared with only SCSA. Mortars prepared with kaolinite clay and SCSA and sodium sulfate activator show the best structural performance (comp. strength: 12 MPa for kaolinite; 11 MPa for kaolinite with SCSA). Such mortars meet international standards for masonry wall applications.

References

[1] Massazza, F.," Pozzolana and Pozzolanic Cements", *Lea's Chemistry of Cement and Concrete*, P.C. Hewlett, Ed., 4th Edition, London: Arnold, 1998, pp. 471-632.

[2] Liebig, E. and Althaus E., "Kaolinit und Montmorillonit als puzzolanische Komponenten in Kalkmörteln unbehandelt und nach thermischer Aktivierung," *ZKG International*, 50. Jahrg., No.5, 1997, pp. 282-290.

[3] He, Ch., Makovicky, E. and Osback, B., "Thermal stability and pozzolanic activity of calcined kaolin," *Applied Clay Science*, Vol. 9 , 1994, pp. 165-187.

[4] Forester, J.A., "Burnt Clay Pozzolana," R. Spence, Ed., *Proc. of a one-day seminar on small scale manufacturing of cementitious materials*, Intermediate technology development group, London, England, 1974.

[5] Cook, D.J., "Rice husk ash," *Cement Replacement Materials*, R.N. Swanny, Ed., Vol. 3, Concrete Technology & Design, Surrey University Press, 1986, pp. 171-196.

[6] Martirena, F., "The development of pozzolanic cement in Cuba," *Appropriate Technology*, Vol. 21, No.2, 1994, pp.25-27.

[7] Hara, N., Yamada, H., Inoue, K., Inoue, N, Tsunematsu, S. and Noma, H., "Hydrothermal reactivity of rice husk ash and its use for calcium silicate products," *Proceedings of the 3rd International Conference, American Concrete Inst., Special Publication SP-114*, 1989, pp.499-516.

[8] Martirena, F., Middendorf, B., Gehrke, M. and Budelmann H., "Use of wastes of the sugar industry as pozzolana in lime-pozzolana binders: Study of the reaction," *Cement & Concrete Research*, Vol. 28, No.11, 1998, pp.1525-1536.

[9] Shi, C. and Day, R. L, "Acceleration of strength gain of lime-pozzolan cements by thermal activation," *Cement & Concrete Research*, Vol. 23, 1993, pp. 824-832.

[10] Shi, C. and Day, R.L., "Chemical activation of blended cements made with lime and natural pozzolans," *Cement & Concrete Research*, Vol. 23, 1993, pp.1389-1396.

[11] Cook, D.J., "Calcined clay, shale and other soils," *Cement Replacement Materials*, R.N. Swanny, Ed., Vol. 3, Concrete Technology & Design, Surrey University Press, 1986, pp. 40-72.

[12] Shi, C. and Day, R.L., "Pozzolanic reaction in the presence of the chemical activators, Part II. Reaction products and mechanism," *Cement and Concrete Research*, Vol. 30, 2000, pp. 607-613.

[13] Shi, C. and Day, R.L., "Pozzolanic reaction in the presence of the chemical activators, Part I. Reaction kinetics," *Cement and Concrete Research*, Vol. 30, 2000, pp. 51-58.

MASONRY: OPPORTUNITIES FOR THE 21ST CENTURY

AUTHOR INDEX

SUBJECT INDEX